Performance of Spent Mushroom Compost Biochar as Filter Media in Metal Retention Pond Systems for Heavy Metal Removal in Abandoned Mine Water

Zafira Madzin

MSc Environmental Pollution Control and Technology

A thesis submitted for the degree of Doctor of Philosophy at

Monash University in 2023

School of Engineering

Copyright notice

© Zafira Madzin (*2023*).

I certify that I have made all reasonable efforts to secure copyright permissions for third-party content included in this thesis and have not knowingly added copyright content to my work without the owner's permission.

Abstract

Overpopulation and rapid development have strained the environment, resulting in widespread water crises. To address global water scarcity, the utilization of water from abandoned mines as an alternative raw water source has emerged as a potential solution. However, the high concentration of heavy metals in abandoned mine water necessitates an economical and effective method for their removal before reuse. This study aims to address this challenge by employing Spent Mushroom Compost (SMC) biochar, derived from biomass waste, as a novel filter media to selectively remove copper, manganese, iron and lead from abandoned mine water. Additionally, the study incorporates biochar modeling using machine learning techniques to predict the adsorption capacities of SMC biochar. The research unfolds in multiple stages. The first stage of the research assessed the preliminary characterization of SMC biochar as raw material (RS) and its variations when produced at different pyrolysis temperatures (300^{o}C, 500^{o}C, and 700^{o}C, denoted as B300, B500, and B700, respectively). Subsequent batch studies as the second stage of research evaluated the adsorption performance of the pyrolytic SMC biochars under diverse environmental conditions. The results revealed that SMC biochar effectively removes heavy metals from abandoned mine water, with varying adsorption performance depending on the pyrolysis temperature. The highest to lowest order was B700 > B500 > B300 > RS with percentage removal performance of 98.38 %, 97.43 %, 87.11 % and 66.33 % respectively. The best adsorption capacity was achieved by SMC biochar at 500°C (B500) that showed the highest maximum adsorption capacity of Cu (2.573 mg/g), Mn (1.522 mg/g) and Pb (2.491 mg/g). The third stage of the research was a lab-scale metal retention column study using B500 biochar as filter media. Seventeen sets (B500A – B500Q) of different initial metal concentrations and pH, from lowest to highest concentrations based on actual mine concentrations, were chosen. The column study was interpreted through breakthrough analysis. All sets showed significant S-shaped breakthrough plots, and Cu showed the highest adsorption capacity of 49.833 mg/g, followed by Fe at 33.186 mg/g, Pb at 16.218 mg/g, and Mn at 6.665 mg/g. The final stage of the research investigated the performance of biochar modelling to predict adsorption capacities to remove heavy metals using machine learning. Machine learning chosen in this study was the adaptive network-based fuzzy inference system (ANFIS) and multilinear regression (MLR) models. Overall, both models show high evaluation performance with R^2 > 0.9, proving the feasibility of both models. Notably, the ANFIS model outperformed the MLR model in terms of prediction accuracy. Consequently, detailed design charts for each heavy metal were developed based on the prediction model, providing valuable insights for researchers, professionals, and decision-makers seeking to achieve predictive adsorption performance for abandoned mine water. In summary, this study presents the novel application of SMC biochar as a promising filter media for efficient removal of heavy metals from mine-related water. The development of design charts using machine learning techniques adds a novel perspective to the research, offering valuable guidance for future endeavors related to abandoned mine water treatment.

Declaration

This thesis is an original work of my research and contains no material which has been accepted for the award of any other degree or diploma at any university or equivalent institution and that, to the best of my knowledge and belief, this thesis contains no material previously published or written by another person, except where due reference is made in the text of the thesis.

Signature: ……..

Print Name: …Zafira Madzin…….

Date: ……March 2023…….

Publications during enrolment

Published

1. Potential application of spent mushroom compost biochar as low-cost filtration media in heavy metal removal from abandoned mining water: a review. International journal of environmental science and technology. http://doi.org/10.1007/s13762-022-04617-7

Submitted

1. Biochar from spent mushroom compost for heavy metal removal in synthetic mine water: characterization and influence of pyrolysis temperature

Undergoing

1. Characterization, application and mechanism of biochar as low-cost adsorbent for heavy metal removal in wastewater: a review

2. Feasibility of spent mushroom compost biochar in removing heavy metals from synthetic mine water in continuous fixed bed column study: effect of initial metal concentrations and pH

3. The application of machine learning for predictive modelling using spent mushroom compost biochar in removing heavy metals from abandoned mining water.

Acknowledgements

In the name of Allah, the most Merciful and Compassionate,

I want to give my highest gratitude to Monash University Malaysia for providing this golden opportunity for me to pursue my Ph.D. I am grateful to be chosen as one of the Graduate Merit Scholarship receivers that provides full tuition fee waiver and stipend. It has been such a great memory studying here with all the conducive environments, full equipped laboratories and supportive administrations that I received throughout the journey. It is such an honor to receive my Ph.D scroll from this prestigious institution.

I want to express my most profound appreciation to my main supervisor, Ir. Dr. Izni Mohd Zahidi, and my co-supervisors, Dr. Mavinakere Eshwaraiah Raghunandan and Assoc. Prof. Amin Talei. Thank you for your endless guidance and support these past years and staying besides me giving full emotional supports throughout my ups and downs. To Dr Izni, who knows starting from a job application, we crossed path as your first Ph.D student. These amazing people inspired me and shaped me to be the person I am today. Next, I want to acknowledge my two mentors, Dr Andreas Aditya Hermawan and Dr. Chang Tak Kwin for providing me assistances and guidance on my research. Not forgetting all the valuable assistance from all the lab technicians that give nothing but great corporations to ensure my smooth laboratory experiments.

This paragraph is specially made for my colleagues cum friends that I met during my study. Special thanks to Dr. Lee Li Yong for always being there for me. She always makes time for me and assist me during my hard times and with that I am truly thankful for you. To my FYP students, Ryan, Kevin, Koon Yong, Gowineish, and Sean, thank you for helping out and this achievement would not have accomplished without them. Not forgetting my Geng Tekun Thesis and Geng Bini Haru, thank you for your endless moral support and encouragement.

Next, I am foremost grateful to the most incredible backbone, my biggest support system which are my family. I am forever thankful to have such supportive parents, Hj Madzin Majid & Hjh Halimah

Ahmad throughout this journey. I will not receive this outstanding achievement without their endless prayers and motivations for me. Not forgetting to my siblings, my sisters and brothers, Heliziana, Hizmawati, Haziq, and Hazwan, thank you so much for your physical and emotional support that got me through this journey. You guys were always there when I needed you the most and only God be able to repay for everything. And to my extended family and friends, thank you for the endless supports and motivations. May Allah SWT repay you with an abundance of rezq and happiness dunya akhirah.

I would like to dedicate this section for my heart and soul, my partner in crime, the cheese to my crust, my two-favorite person in the whole wide world, my husband, Muhammad Azril Izwan and my daughter, Naadine Azril. No words could describe how thankful I am for having you two in my life. My dearest husband, thank you for being there through my ups and downs. Thank you for being my shoulder to lean on. Thank you for your understanding and your sacrifices in everything. Thank you for being a kind, loving and gentle husband. I am so lucky to have you as both bestfriend and life partner. We did it sayang! And my dearest Naadine, you have changed my life completely. You have shaped me into the strongest person I've known and made me realize my true capabilities. Throughout this PhD journey, I have carried you, delivered you and watch you grow gracefully. Having you as my daughter is my more remarkable achievement than this scroll. From delivering you at 29 weeks, to watching you fighting in NICU for 96 days. From a premature baby with a chronic lung disease to the 3 years old you now, you are the best thing ever happened to me. We both have been through a lot and we both deserved this accomplishment! Watching you fight for your life strengthened me, encouraged me to keep swimming and helped me to achieve my goals. You are my inspiration and together, we will rock this world.

Finally, a special section to the author, congratulations dear self. You are the toughest person we have ever known. You persevered, you endured and you survived! You have gone through so much and yet here we are at the finish line. Thank you for always giving your best and keep pushing the limits. Thank you for getting up everytime we fall. Thank you for not giving up whenever we face challenges. Most importantly, thank you for believing in yourself while others don't. Let strive for more success and contributions in near future.

I want to dedicate this achievement to a dearest friend who pursued PhD while fought cancer. You taught me the true meaning of courage. This is for you Nur Tsiqah Mohd Nasir. Alfatihah.

Zafira Madzin
March 2023

List of Abbreviation

AC	Activated carbon
AMD	Acid mine drainage
AN	Ammonia nitrogen
ANFIS	Adaptive network-based fuzzy inference system
ANN	Artificial neural network
As	Arsenic
ASTM	American society testing method
ATM	Americam testing method
BET	Brunauer-Emmett-Teller
B_L	Temkin constant
BOD	Biological oxygen demand
COD	Chemical oxygen demand
CTAB	Cetyltrimethylammonium bromide
Cu	Copper
$Cu(Cl)_2$	Copper chloride
DO	Dissolved oxygen
DOE	Department of environment
EDS	Energy dispersive spectrometer
Fe	Iron
$FeSO_4$	Iron sulphate
FESEM	Field emission scanning electron microscopy
FTIR	Fourier transform infrared
GSD	Grain size distrubution
H	Hydrogen
H_2O	Water

HRT	Hydraulic retention time
IBI	International biochar initiative
ICP	Inductively coupled plasma
K	Potassium
K_2	Pseudo second order constant
K_F	Freundlich constant
K_L	Langmuir constant
KT	Temkin constant
L	Liter
MAE	Mean absolute error
MCH	Metal-methylidyne
MCH_3	Methyl-metal
MF	Membership function
MLR	Multilinear regression
Mn	Manganese
$MnSO_4$	Manganese sulphate
MOH	Ministry of health
MSE	Mean square error
MSMA	Stormwater management manual
MTZ	Mass transfer zone
ND	Non detected
NO_3	Nitrite
NWQS	National water quality standard
OES	Optical emission spectroscopy
OH	Hydroxide
Pb	Lead
PFO	Pseudo first order
PSO	Pseudo second order constant
PV	Pore volume

PVC	Polyvinyl chloride
R^2	The coefficient correlation
RL	Separation factor
RMSE	Root mean square error
RS	Raw spent mushroom compost
S_{BET}	Surface area
SMC	Spent mushroom compost
SO_4	Sulphate
SS	Suspended solids
WHO	World health organization
WQI	Water quality index
Zn	Zinc

Table of contents

List of Figures

List of Tables

Chapter 1 Introduction

1.1. Overview

Water scarcity poses a significant challenge to urbanization, with the rapid growth of industries and population being key factors. By 2050, the global population is projected to reach 70%, as reported by the United Nations in 2014. The availability of clean drinking water is crucial for maintaining a healthy life, but these factors contribute to an increased global water demand, leading to pollution and compromised water sources. Climate change exacerbates the issue by causing floods and droughts, which intensify the toxicity of chemical contaminants in the environment (Joseph et al., 2019). To address the imminent water shortage in densely populated areas, state water authorities in Malaysia have proposed utilising abandoned mining ponds as alternative raw water sources. This approach has been successfully implemented in other countries such as Australia (Dein 1974; Prosser et al., 2011) and South Africa (Winde, 2020), where mining ponds have been converted into reservoirs to serve as alternative water resources during dry seasons.

Kusin et al. (2016) reported that Selangor state water authority has proposed pumping water from abandoned mining ponds in Bestari Jaya into Sungai Selangor to meet the Wilayah Persekutuan Kuala Lumpur's 2670 million liters per day water demand. Correspondingly, the government authorities in Melaka utilised abandoned mining ponds of Tasik Biru Chin Chin to supply 500 million liters raw water daily in 2017 (Koki et al., 2018a). However, these operations don't involve removal of heavy metal contaminants especially in abandoned mining ponds that have certain levels of heavy metals exceeding the raw water standard limit by the Ministry of Health (MOH, 2009).

Additionally, surface runoff in paved urban areas often contains various pollutants, including heavy metals from different types of land use in highly populated areas. Heavy metals, especially copper (Cu), manganese (Mn), iron (Fe), and lead (Pb), are present in abandoned mining ponds (Sun et al., 2020). These pollutants are of particular concern as they are highly toxic, bioaccumulating in the environment, and non-biodegradable. Hence, there is an urgency to develop a practical, cost-effective, potent and sustainable solution in removing these low concentrations of heavy metals from stormwater before discharging it for alternative use.

There are several technologies in removal of heavy metals in water presented in literature (Hanandeh et al., 2021; Luo et al., 2018a; Yang et al., 2019), however adsorption is one of the most utilized method due to its cost-effective and practical technology (Pal et al., 2021). The search of the most effective adsorbents are currently being explored as the conventional adsorbents such as activated carbons are costly and ineffective (Joseph et al., 2019). Biochar, on the other hand, is a promising green material that has been proven to achieve high removal efficiencies for heavy metals (Tsang et al., 2019). Biochar is a carbon-rich product made from biomass waste materials produced through simple thermo-chemical conversion. This low cost, often locally available material has caught a lot of attention in exploring its properties as well as its adsorption performance in removing heavy metals (Wu et al., 2019a). Among the raw materials that have been explored as biochar are wood biochars, carbon shell biochars, poultry litter biochars, biomass waste biochars and lignocellulosic biochars (Gai et al., 2014; Giachini et al., 2018; Niazi et al., 2016; Shaheen et al., 2018). Nevertheless, limited studies were reported on feasibility of mushroom compost as biochar and its application as potential filter media in mine-related water.

This study explores the potential use of biomass biochar as a filter media in metal retention pond systems. Spent mushroom compost (SMC) biochar has been extensively studied and proven to be an excellent adsorbent, particularly for removing heavy metals, thanks to its large surface area and multiple functional groups that facilitate strong binding with metals. However, no previous studies have investigated the application of SMC biochar as a filter media in metal retention pond systems specifically for abandoned mining ponds. Therefore, this proposed research aims to assess the viability of using SMC biochar as a filter media in heavy metal retention systems. Additionally, machine learning techniques are employed to predict the adsorption capacities of heavy metal removal, and the results are presented through design charts that consider environmental factors such as pH and initial metal concentrations. The study will also generate a design chart illustrating the efficiency of metals removal based on pH variations. By utilising locally abundant and cost-effective biomass material, this study offers a sustainable and environmentally friendly approach to remove heavy metals from abandoned mining ponds effectively

1.2 Research gap and contribution

The performance of biochar as adsorbent using various feedstock materials in a batch and column test has been thoroughly explored, and its effectiveness in removing heavy metals has been proven. Biochar has a vast surface area, comparable to activated carbon (AC), but with a much lower cost, approximately $2000/tonne for granulated activated carbon and below $250/tonne for biochar (Ulrich et al., 2017).

Introducing biochar as filter media in metal retention cells is a promising application as these adsorbents have active chemisorption mechanisms to effectively adsorp heavy metals. Biochar has unique physicochemical properties where its porous structure has abundant functional groups, large surface area, and is readily available as it is the byproduct from feedstock process. Furthermore, biochar has irregular circular plates that contain high concentrations of pi-pi electrons that cause unsaturated capacities, unpaired electrons, and active sites that contribute to proper adsorption of polar molecules (Foroutan et al., 2019). Moreover, removal performance is highly dependent on the pyrolysis temperature of biochar. Low temperature biochar contains oxygen functional groups to aid surface complexation removal while high temperature biochar contains aromatic functional groups that enable binding solid affinity toward the metal (Tsang et al., 2019). In addition to heavy metals, biochar can also effectively remove other contaminants such as nitrate since biochar provides carbon substrates as electron donors and promotes denitrification (Ahmad & Danish, 2018).

Water supply shortages necessitates use of abandoned mining ponds as raw water source alternative (Kusin et al., 2016). However, abandoned mining ponds often contain various heavy metals that requires treatment to ensure their concentrations do not exceed the allowable raw water standard limit by the

Ministry of Health before releasing to the users. Hence, an environmentally friendly and sustainable approach that is practical and require minimal cost to remove these heavy metals is proposed in this study; the application of biochar as filter media in a metal retention system to remove heavy metals from mine-impacted water. By proposing a metal retention pond system with novel SMC biochar as filter media, this research has produced detailed design charts that predicts the adsorption capacity of SMC biochar at given initial metal concentrations and pH. These design charts were validated with a real case study to compare the efficiency for real applications in the future.

This research is crucial as it assesses the potential of SMC biochar in removing heavy metals from abandoned mining ponds where the ponded water may be an alternative for raw water resources. This will be a novel approach as no study has been done in utilizing SMC biochar in abandoned mine water before. Moreover, another point of view is the use of machine learning to provide design charts that can predict the adsorption capacity of heavy metals at given initial metal concentrations and pH. This can be a novel perspective in incorporating computational approach for prediction of metals sorptions using the SMC biochar which can be a great reference for potential real-life applications in the future. This research is a plan of action towards sustainability and to reduce waste build up in this country. Furthermore, it is a call of action towards United Nation's Sustainable Development Goals (SDGs) of goal 6, to ensure availability and sustainable management of water and sanitation for all.

1.3 Research questions

Among the research questions are as follows,

1. What is the relationship between the production of SMC biochar in different pyrolytic temperature conditions and its performance characterisations in removing proposed heavy metals using batch study, and which of the pyrolytic temperature produces the highest efficiency in removing heavy metals?

2. How is the performance of SMC biochar as a filter media in removing heavy metals in a lab scale metal retention column involving abandoned mine water, and how is it affected by the pH and initial metal concentration to model the optimum adsorption capacity?

3. How does the biochar modeling using machine learning for predictive heavy metals adsorption capacities be useful for real application in actual abandoned mining ponds?

1.4 Research aim and objectives

The main aim of this research is to evaluate the performance of SMC biochar as a sustainable filter media in a metal retention pond system to ensure effective removal of heavy metals in abandoned mine water using a series of laboratory investigations followed by the development of design charts for potential application of this technology infield.

1. To determine the most promising pyrolytic temperature of SMC biochar that gives the highest performance in heavy metal removal in a batch study

2. To evaluate the adsorption performance of SMC biochar as filter media in a lab-scale metal retention column study with effect of pH and initial metal concentration

3. To develop detailed design charts for optimal adsorption capacities of SMC biochar using machine learning with influence of initial metal concentrations and pH and validate the chart with actual case studies.

1.5 Research hypotheses

These hypotheses will be tested during the research to validate the effectiveness and feasibility of using SMC biochar as a sustainable filter media in a metal retention pond system for removing heavy metals from abandoned mine water. The result of the study will help support or reject the stated hypotheses and provide valuable insights for the development of this technology in real-world applications

1. SMC biochar is an effective adsorbent for removing heavy metals. However, the performance of removal is influenced by the production of biochar at different pyrolytic temperatures, and there may be an optimal temperature of SMC biochar that yields the highest performance in heavy metal removal during a batch study.

2. The adsorption performance of SMC biochar as filter media can be conducted in lab scale metal retention column study to study the influence of environmental condition factors such pH and initial metal concentrations. These factors are expected to cause variations in heavy metal removal efficiency.

3. The development of detailed design charts for optimal adsorption capacities of SMC biochar using machine learning, incorporating the influence of initial metal concentrations and pH levels, will result in accurate predictions of heavy metal removal. Furthermore, validating these design charts through actual mine site studies will demonstrate their effectiveness in practical applications.

1.6 Scope of study

This study focuses on applying SMC biochar as filter media to remove heavy metals in a proposed metal retention pond system before supplying abandoned mine water as raw water alternative sources. In this study, the proposed metals to remove in this research are Cu, Mn, Pb, and Fe. These heavy metals were selected in this study as these are the highly concentrated common metals found in mining water.

The first step of the study is the production of SMC biochar using slow pyrolysis thermal processes. It is important to note that different pyrolytic temperatures ranging from 300^{o}C, 500^{o}C and 700^{o}C were produced in this study to see the effect of pyrolysis temperature and the heavy metals adsorption performance. Accordingly, characterization of biochar at different pyrolysis was explored to assess the physico chemical characteristics and its potential as filter media in removing heavy metals.

Correspondingly, the second stage of research is a series of batch adsorption study to assess the performance of SMC biochar with multiple pyrolytic temperatures in removing heavy metals. The batch study came with a parametric study of pH, time and initial metal concentrations. Therefore, the batch study performance was discussed in terms of characterization improvement, heavy metal removal efficiencies, adsorption capacities, adsorption isotherms, and adsorption kinetic analysis corresponding to the parametric studies. As a result, SMC biochar temperature that reflects the highest overall heavy metals adsorption capacity from the batch study was chosen as the filter media for the lab scale metal retention column study.

Notably, the third stage of research consists of a lab-scale metal retention column study with SMC biochar as filter media with influence of pH and initial metal concentration to imitate the actual condition for potential real-life application. Correspondingly, a continuous system is adopted to investigate the performance of SMC biochar when the solution of adsorbate continuously passed through a column and consistently have interaction with SMC biochar as filter media. This method is a crucial step to perform continuous adsorption and to imitate pH and initial metal concentration from real abandoned mining water concentrations before releasing it to the river for an alternative raw water source. In this continuous system, a lab scale metal column was developed consisting of a mixture of soil and SMC biochar as filter media. A series of synthetic mine water with different initial metal concentrations from low to high concentrations based on literature passed through the downward flow column and the water was sampled at different time intervals for data analysis. Then, the adsorption capacity and metal retention behavior were discussed through the breakthrough curve analysis and adsorption isotherm through a mathematical model approach.

In the final stage of research, biochar modeling was applied to predict the adsorption capacity of SMC biochar with influence of pH and initial metal concentrations through machine learning. In this study, the machine learning technique chosen was the adaptive neuro-fuzzy inference system (ANFIS) and multilinear regression (MLR). The ANFIS model simulated the column study experimental data and model the adsorption capacities. Subsequently, design charts comprising optimal adsorption capacities of each of the heavy metals at different initial metal concentrations and pH using the SMC biochar were presented. Finally, these design chart simulations were validated with actual case studies to verify its efficiencies.

1.7 Thesis outline

Chapter 1 provides the introduction of research, which consist of problem statement, research gap and contributions, research questions, research aim and objectives and scope of study.

Chapter 2 describes the literature reviews relating to the research topic and provides overviews of topics covered throughout the study. This study includes the overview on abandoned mining ponds as alternative raw water source, applications of biochar as filter media, heavy metal removal mechanisms of biochar and biochar modeling using machine learning.

Chapter 3 focuses on the materials and research design of the study, which includes the production and characterisation parameters for the mushroom biochar and production of synthetic mine water. In overall, three stages were defined to achieve research aim and objectives. Stage 1 is production and characterisation of biochar; stage 2 is batch adsorption study, stage 3 is lab scale metal retention column study, and stage 4 is the biochar modelling and prediction using machine learning.

Chapter 4 discusses the results obtained from from first and second stage of research and satisfies research objective 1 of study. This chapter discusses the physicochemical characteristics of SMC biochar and batch adsorption study. Three different pyrolysis temperature biochar were produced and batch study was done to assess the heavy metal removal performance with influence of environmental conditions of pH, time and initial metal concentrations. The removal efficiency was further elaborated in terms of adsorption kinetics, isotherms and removal mechanism of SMC biochar.

Chapter 5 discusses the results obtained from third stage of research which satisfies research objective 2 of study. The lab scale metal retention column study was conducted using SMC biochar pyrolysis temperature that gave the highest removal performance form batch study. Removal efficiency and adsorption capacities are discussed through breakthrough curves and mathematical modeling approach.

Chapter 6 covers the final stage of research and satisfies research objective 3 of study. This chapter discusses the biochar modeling using machine learning to come out with design charts that predicts adsorption capacities of biochar to remove heavy metals with influence of pH and initial metal concentrations.

Chapter 7 summarized major findings of this study in fulfilling the research objectives. Limitation of study and recommendations for future studies are also included in this study.

Chapter 2 Literature review

2.1 Introduction

Chapter 2 is structured into the following main sections:

- Section 2.2 provides information on abandoned mine water, its role as an alternative water source, heavy metal contaminations, and conventional methods to remove heavy metals and its limitations.
- Section 2.3 describes the role of raw adsorbents in removing heavy metals in water treatment and what is biochar. Next, the process advancement of converting adsorbents into biochars. This includes the role of SMC as adsorbent and biochar in removing heavy metals.
- Section 2.4 introduces the application of biochar as filter media to remove heavy metals. Subsequently, biochar characterisation from surface morphological structure, chemical and physical composition are discussed. Removal of heavy metals using biochar in batch and study are provided and well discussed.
- Section 2.5 provides an overview of heavy metal removal mechanisms using biochar and the influences of pH, initial metal concentrations, time and adsorbent dosage.
- Section 2.6 discusses the biochar removal prediction in data modeling and optimisation using machine learning.
- Section 2.7 describes the summary of literature review for this study

Part of the content of this chapter appears as, Madzin, Z., Zahidi, I., Talei, A. & Raghunandan, M. E. (2022). *Potential application of spent mushroom compost (SMC) biochar as low - cost filtration media in heavy metal removal from abandoned mining water : a review*. International Journal of Environmental Science and Technology. Nov. 2022. http://doi.org/10.1007/s13762-022-04617-7

2.2 Abandoned mine water as an alternative water source and heavy metal contaminations

River is the primary raw water source in Malaysia, fulfilling almost 97% of the demand, unlike countries that depend on groundwater and seawater (Koki et al., 2018a). However, due to severe water pollution in rivers caused by rapid industrialisation and urbanisation in Malaysia, water scarcity has become an increasing concern. According to an assessment on lake water to meet the water needs and demands in Malaysia, most lakes are polluted with its crucial water quality parameters way higher than the permitted levels set by the Department of Environment (DOE) Malaysia (Koki et al., 2018). Consequently, a significant project for alternative water sources has been implemented since 2007, where rainwater harvesting systems have been implemented in Selangor and Sarawak while other states like Kelantan, Perlis, Pahang and Terengganu use surface water and groundwater (Hamid, 2015). Nevertheless, the water demand in Malaysia is on an increasing trend and so does the water scarcity problem. To address this issue, the Selangor state authority has utilised water from abandoned mining ponds as raw water resources (Kusin et al., 2016). However, this approach resulted in some disagreement among researchers on the water quality as abandoned mining ponds contain high concentrations of heavy metals (Lau et al., 2017). Heavy metal contamination is a rising concern due to its toxic and carcinogenic feature and current water treatment methods are ineffective at removing heavy metals (Joseph et al., 2019).

Kusin et al. (2016) reported that the Selangor state water authority in Malaysia has proposed to pump water from abandoned mining ponds in Bestari Jaya catchments into Sungai Selangor to fulfil water demand of 2670 million liters per day in Wilayah Persekutuan Kuala Lumpur. Correspondingly, the government authorities in Melaka are utilising abandoned mining ponds of Tasik Biru Chin Chin to supply 500 million liters raw water daily in 2017 (Koki et al., 2018a). However, these operations are not designed

to remove heavy metals contaminants especially in abandoned mining ponds with certain levels of heavy metals that exceeded the raw water standard limit by the Ministry of Health (MOH, 2009).

Water quality is assessed using many chemicals, physical and biological parameters set by authorities. In Malaysia, the National Water Quality Standards (NWQS) are formally used to develop the water quality index (WQI) and represent the overall status of a water source. The WQI uses the assessment recommended by the DOE in 1974 to evaluate the pollution levels in Malaysian rivers. In this process, six important water quality parameters including pH, ammoniacal nitrogen (AN), biological oxygen demand (BOD), chemical oxygen demand (COD), suspended solids (SS), and dissolved oxygen (DO) are determined to classify the water into five classes starting from Class I (practically no treatment necessary) to Class V (not meant to be used at all) (Kura et al., 2015). The details of these five classes are provided in Table 2.1. Consequently, due to the increasing speculations on the water quality status, numerous studies have contributed to the evaluation of the water quality in abandoned mining ponds throughout Malaysia.

Table 2.1. WQI classification for Malaysia (DOE, 2006)

Parameter	Unit	Class				
		I	II	III	IV	V
pH	-	>7	6-7	5-6	<5	<5
Dissolved oxygen (DO)	mg/L	>7	5-7	3-5	1-3	<1
Biochemical Oxygen Demand (BOD)	mg/L	<1	1-3	3-6	6-12	>12
Chemical Oxygen Demand (COD)	mg/L	<10	10-25	25-50	50-100	>100
Suspended Solids (SS)	mg/L	<25	25-50	50-150	150-300	>300
Ammoniacal Nitrogen (AN)	mg/L	<0.1	0.1-0.3	0.3-0.9	0.9-2.7	>2.7
Water Quality Index (WQI)	-	<92.7	76.5-92.7	51.9-76.5	31.0-51.9	>31.0

Table 2.2 shows the heavy metals analyses in water from abandoned mines in Malaysia. Based on the data, a few abandoned mining sites have high heavy metals concentrations that exceeded the standard limits for raw water quality by the Ministry of Health (MOH). Other than high concentrations of heavy metals, studies also have detected low pH in the abandoned mining ponds, indicating high level of heavy metals present in the abandoned mine ponds, which was possibly related to acid mine drainage (AMD). AMD occurs due to the weathering of sulphide minerals, resulting in very acidic water and increased concentrations of heavy metals (Kefeni et al., 2017). Hence, these studies concluded that there is an urgent need for appropriate water treatment before using the water as alternative raw water source.

Table 2.2. Heavy metal analysis in water from abandoned mining ponds in Malaysia

Location	State	pH	Heavy metals (mg/L)						Reference
			Cu	Mn	Pb	Zn	As	Fe	
Serendah and Tasik Biru Kundang	Selangor	5.7	0.06-0.10	ND	1.84	ND	ND	ND	(Hamzah et al., 2018)
Lembah Klang	Selangor	3.4 – 5.0	ND	0.03	6.00	ND	56.00	ND	(Koki et al., 2018)
Melaka	Melaka	3.4 – 5.0	ND	ND	6.00	ND	10.00	ND	(Koki et al., 2018)
Sungai Lembing	Pahang	2.6	279	115	256	208	179	251	(Hatar et al., 2013; Wan Yaacob et al., 2009)
Lombong Barit	Pahang	3.1	11.06	3.30	0.45	1.58	0.01	7.14	(Hatar et al., 2013)
Lubuk Mandi	Terengganu	3.2	0.17	1.12	0.01	0.62	ND	2.15	(Hatar et al., 2013)
Bestari Jaya	Selangor	3.2-7.2	9.5-95	48	69.46	87.8	66	14	(Ashraf et al., 2011)
Bukit Besi	Terengganu	2.5-6.5	0.001-0.19	2.03-7.82	ND	0.02-0.17	ND	45.60	(Kusin et al., 2021)
Mamut Copper mine	Sabah	2.9-3.4	154-238	104	ND	177	ND	6.2-58.8	(Jopony & Tongkul, 2009)
MOH untreated raw water		5.5-9.0	1.0	0.20	0.10	5.00	0.05	1.00	Ministry of health

ND= none detected*

2.2.1 Heavy metals contamination and its impact on the ecosystem and human health

Anthropogenic and natural sources can contribute to high level of heavy metals, but researchers found that most water pollution cases are linked to human activities from rapid industrialisation (Koki et al., 2018). The environmental impacts from pollution especially heavy metal contamination, and their impacts on human have been discussed in many studies as presented in Table 2.3. This table shows that lead (Pb), manganese (Mn), iron (Fe) and copper (Cu) are the most common heavy metals found in the abandoned mine water and have impacts on human bodies from long term of exposure.

Apart from the impact of heavy metals on human health, excess or uncontrolled exposure of heavy metals in the environment has shown disturbing impacts on the ecosystem as well. Figure 2.1 collates selected impacts of heavy metals contamination on the aquatic systems, ecology, and soil from the literature. The alarming impact from the environmental viewpoint is the accumulation of these contaminants in plants and aquatic species, which persists for an extended period once it occurs (Chowdhury et al., 2016). Such uptake and accumulation of heavy metals in plants and aquatic life will eventually end up in human tissues, thereby posing a serious health hazard to humans due to the fact that they are part of the food chain as well.

Table 2.3. Commonly observed heavy metals and their impacts on human bodies due to long term exposure

Heavy metals	Sources	Symptoms	Health effects	References
Lead (Pb)	Application of lead in gasoline, drinking water, fuel combustion, paint industry, ceramic and dishware industry, PVC-mini blinds, solid waste combustion	Nausea, vomiting, thirst, diarrhoea/constipation, abdominal pain, load colic, lead palsy and lead encephalopathy	Anaemia, hypertension, kidney damage, miscarriage, disruption of the nervous system, irreversible learning impairment in infants and children, infertility, intellectual disorders, renal and hemopoietic system	(Jan et al., 2015; Lim et al., 2012)
Copper (Cu)	Mining, smelting, agricultural activities	Gastrointestinal distress	Anaemia, encephalopathy, hepatitis and nephritic syndrome, liver or kidney damage	(Xu et al., 2019)
Manganese (Mn)	Paint industry, plane industry, mining, smelting	Short term memory and vision, depression, and anxiety	Pheumonia, circulatory collapse, parkinson disease, edema of respiratory system	(Fseha et al., 2022; Kulkarni et al., 2022)
Iron (Fe)	Mining, smelting and manufactural activities	Dementia, nausea, vomiting, and abdominal pain	Hemochromatosis, heart failure, diabetes, Alzheimer	(Brewer, 2010; Fernández-Real & Manco, 2014; Fishbane et al., 2014; Walker & Walker, 2000)

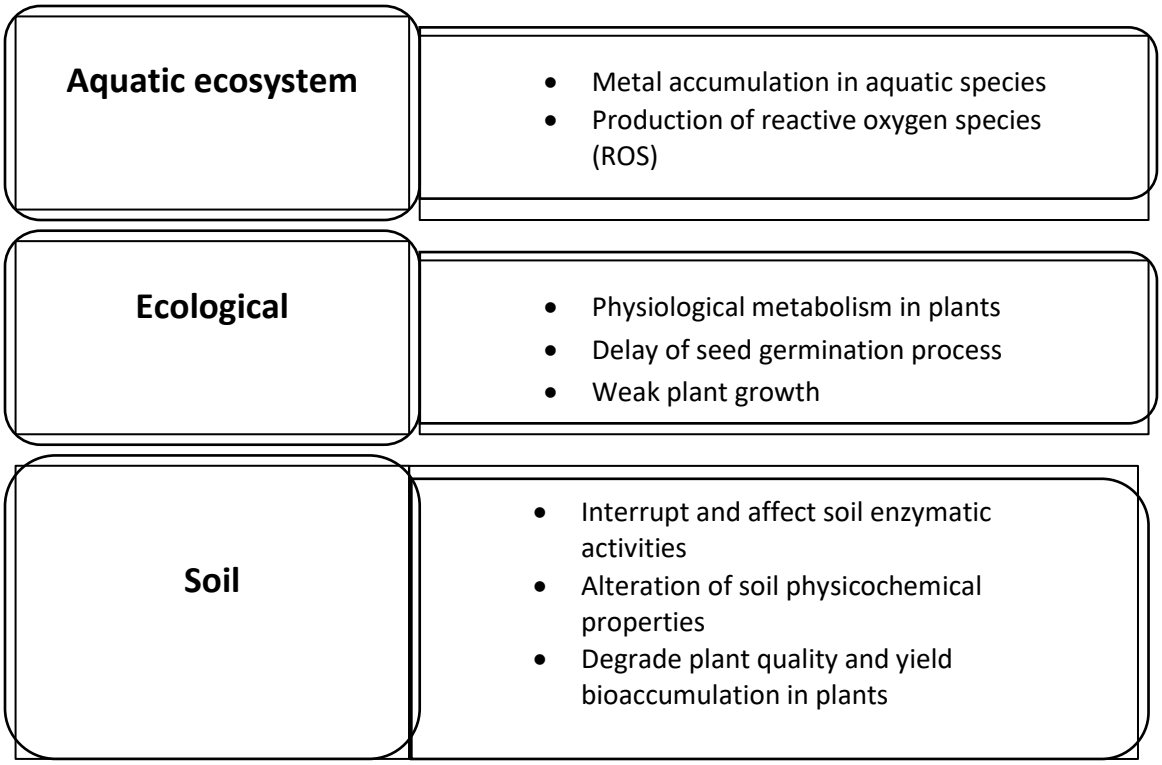

Figure 2.1. Impact of heavy metals to aquatic system, ecological and soil (adapted from Elmorsi et al., 2019)

2.2.2 Conventional treatment methods to remove heavy metals and its limitations

Generally, the water of abandoned mining ponds mostly contains heavy metal contaminants, leading to a great concern among researchers. Most researchers suggested that further treatment is required before releasing the raw water into river streams for water supply (Anticó et al., 2017; Cheng et al., 2020; Joseph et al., 2019). However, there is no specific approach to treat heavy metals prior to release into water bodies. Table 2.4 summarizes the conventional methods of heavy metal removals with respective

advantages and limitations. The most appropriate and employed method among water treatment technologies is adsorption. Only certain heavy metals are successfully removed in the tertiary treatment, except for adsorption, which is known to remove high concentrations of heavy metals (Alias et al., 2020). Adsorption has already been applied as a supplementary treatment to remove organic and inorganic contaminants in wastewater (Vareda et al., 2019). The method is cheap, easily operable, and offers flexibility in design and operation (Nasir et al., 2019). The most common adsorbent used is activated carbon (Yang et al., 2019) due to its well-developed porous structure, high surface area, and multi-functional groups. However, activated carbon is expensive and the recovery of heavy metals is a tedious process (Burakov et al., 2018). Therefore, more research and alternative technologies are required to remove heavy metal contamination in wastewater.

Table 2.4. Conventional methods in heavy metals removal from wastewater

Technology	Properties description	Advantages	Limitations	Effect on pH	Removal efficiency (%)	References
Chemical precipitation	Chemical reagent reacts with metal ions and precipitates as insoluble solid particles	Low capital cost Simple operation Safe operations	Sludge generation Slow metal precipitation Require massive chemicals to reduce metal ions	Optimal removal rate at pH 9-11. pH> 11 will cause dissolution of heavy metal compounds in precipitates and promotes the growth of metal hydroxyl complexes	80-99.7	(Aziz et al., 2008; Barakat, 2011; Lu & Chen, 2018)
Ion exchange	Reversible interchange whereby insoluble substance (resin) removes ions from electrolytic solution and releases other ions of similar charge without any structural change in the resin	High treatment capacity High removal efficiency Fast kinetics	Not applicable in high metals concentrations Highly sensitive to pH Fouling of metal ions	Heavy metal removal works efficiently with pH	64-90	(Abdullah, Tajuddin, & Yusof, 2019; Agustiono et al., 2006; Fu & Wang, 2011)

Coagulation-flocculation	Destabilization of cataloids (coagulation) Agglomeration of destabilized particles (flocculation)	Simple design; Low energy consumption High versatility	Toxicity of alum/polymeric coagulants; Sludge production Enable to remove heavy metals effectively	Optimal removal efficiency at pH 8-10 depending on the type of heavy metals; Zn^{2+} (pH=8-10), Cu^{2+} (pH=10)	95-99.9	(Bora & Dutta, 2019; Yongjun et al., 2019)
Membrane technology	Separation of substances across a semi-permeable material to pass through and excrete undesired substances	Small space requirement; Low pressure; High separation; Zero sludge production	Large capital investments Irreversible Membrane fouling Anti-hydrophobicity	Highest removal efficiency is obtained at pH ranging from 8-10	95-100	(Abdullah et al., 2019; Agustiono et al., 2006; Fu & Wang, 2011; O'Connor et al., 2018)
Adsorption	Flexible, simple and easy method where physical and chemical adsorption takes place	Low cost and maintenance Easy operation and handling Can be used to remove high concentrations of heavy metals	Production of waste products Performance and efficiency depend on the type of adsorbent Poor tolerant of different pH range	Very much dependent on the type of adsorbent	85-100	(Abu et al., 2020; Alias et al., 2020)

2.3 Converting adsorbents to biochar for heavy metals removal

Adsorbents are the most popular alternative adsorbents to replace costlier activated carbon as adsorption media. Adsorbents from biomass had drawn much attention due to its biosorption mechanisms that can immobilise metals from industrial effluents (Niazi et al., 2016). Various biomass have been identified to produce low-cost adsorbents for water and wastewater treatments due to the ability in immobilising heavy metals and feasibility to store more carbon, increase crop yields, and enhance adsorption mechanisms (Li et al., 2017; Pan et al., 2019; Wang et al., 2019b).

2.3.1 SMC as adsorbents

Producing low-cost adsorbents from agricultural wastes for removing organic and inorganic contaminants (including heavy metals), have previously been studied on various biomass materials such as sugarcane bagasse (Hussain & Qazi, 2016; Mattos et al., 2015; Mohamed et al., 2017; Sarker et al*.,* 2017), rice husk (Noor Syuhadah & Rohasliney, 2012), and oil palm (Daneshfozoun et al., 2016; Mohd Salleh et al., 2018; Montoya-Suarez et al*.,* 2016). Although these adsorbents showed satisfactory results in removing heavy metals through adsorption, these adsorbents have lower sorption capacity than other sorbents, such as activated carbon and ion-exchange resins. Hence, research has focused on enhancing the sorption capacity of adsorbents through chemical and physical modifications.

Mushroom production and demand in Malaysia have been steadily increasing, and mushroom is identified as one of the high-value commodities under the National Agro-food Policy (2011−2020). As the demand for mushrooms increases yearly, improper handling of SMC may result in environmental pollution. SMC contains a mix of cellulose, hemicellulose and lignin, which is high in the amount of hydroxyl, carboxyl, carbonyl, amino and phosphate that act as active functional groups on the surface of this material. These active functional groups favour metallic ion adsorption to achieve high adsorption capacity (Xiao-jing et al., 2014).

SMC has been applied extensively in environmental remediation treatments. In many studies, SMC have been used as adsorbents to remove organic and inorganic pollutants. Applications of SMC as adsorbent to remove heavy metals are presented in Table 2.5. Generally, SMC have shown great adsorption capacity in removing single and multiple metal ions and is an excellent adsorbent as it minimizes the plugging in bioreactors and has large pore spaces and small void volume (Muhammad et al., 2017). On the other hand, SMC contain different types of polymers such as lignin, cellulose and hemicellulos which are degraded into numerous pores that are suitable for metal adsorption (Kulshreshtha, 2019).

However, one of the limitations in utilising SMC is the compost can easily get exhausted, affecting its long-term performance (Roychowdhury et al., 2015). Thus, to improve the adsorption capacity of SMC, chemical or physical modification is introduced to pre-treat SMC adsorbents. However, very limited studies have been done. For example, the co-pyrolysis of SMC and macroalgae improved the cationic dye adsorption capacity by 2.2 times higher than raw SMC (Sewu et al., 2017). The study added that more oxygen-containing groups, exchangeable cations, and coarser surface morphology were obtained through this technique, thus improving adsorption synergism. Meanwhile, SMC adsorbent was modified using

cationic surfactants (Zang et al., 2017) and the uptake capacity of Cr (VI) improved to 21.44%–27.34% using chemically-modified SMC with cetyltrimethylammonium bromide (CTAB). These studies showed that modifying SMC is effective in enhancing the adsorption capacity. However, further studies on SMC modification need to be conducted, specifically on physical modifications where simpler operation, easy handling, and minimal investment are required.

Table 2.5. Application of SMC as biosorbent to remove heavy metals from literature

Biosorbent	Heavy metals	Adsorption capacity (mg/g)	Removal efficiency (%)	Reference
Spent Mushroom Compost (SMC)	Cr (VII)	9.327		(Dong et al., 2018)
	Pb (II)	149.1		(Liu et al., 2018)
	Mn (II)	17.25		(Kamarudzaman et al., 2015)
	Cu (II)	50		(Xiao-jing et al., 2014)
	Cd (II) Pb (II) Fe (II) Co (II) Mn (II) Zn (II) Cu (II)		80-98	(Corral-Bobadilla et al., 2019)
	Pb (II)		60-97.87	(Molahid et al., 2018)
	Mn (II)	3.341		(Kamarudzaman et al., 2015)
	Cd (II) Pb (II) Cu (II)	40.43 15.16 36.2		(Frutos et al., 2016)
	Ni (II)	3.04		(Tay et al., 2011)

2.3.2 Application of SMC as biochar

Biochar is the carbonaceous material obtained from raw biomass through thermochemical processes with limited oxygen. These processes enhance the overall surface area of the biochar and generate active sites that facilitate adsorption (Mohanty et al., 2018; Phing et al., 2014). Biochar is a porous solid composed of carbon produced via thermochemical procedures, converting organic materials in an oxygen-restricted environment. It serves as a stable and long-lasting carbon storage medium in the environment (Shackley, et al., 2012). Biochar is made from a multifunctional material high in carbon content, which is produced from thermal decomposition under a limited supply of oxygen (Ahmad et al., 2014). However, according to the International Biochar Initiative (IBI), "Biochar is a solid material obtained from the thermochemical conversion of biomass in an oxygen-limited environment" (IBI, 2012). Thermochemical processes involve conventional slow pyrolysis, fast pyrolysis, gasification, torrefaction, and hydrothermal conversion (Shaheen et al., 2018). Biomass pyrolysis is the most common technique to produce biochar.

This process is low-cost and achievable, which results in thermochemical decomposition of biomass by heating it in elevated temperature under oxygen-limited condition (Lee et al., 2018; Niazi et al., 2016; Shaheen et al., 2018). Pyrolysis is generally divided into fast to slow process, and the characteristics of the products depend on the residence time, heating rate, and the operating temperature. Fast pyrolysis with a very brief residence time will give approximate 15 - 35 % biochar yield and is often used to produce bio-oil. On the other hand, the slow pyrolysis process with its longer residence time is generally the most considered process for biochar production, which gives the highest yield (Ahmad et al., 2014). Alternatively, torrefaction and gasification are not favourable in producing biochar due to the production of highly volatile organic compounds and their very low yield compared to other processes.

The entire process is similar to the production process for activated carbon, but activated carbon requires additional processes that need costly oxygen and strong acids for char activation (Mohanty et al., 2018). Biochars have received increasing attention due to their economic production and unique features, such as high carbon content, cation exchange capacity, and large activation sites for metal binding (Wang and Wang, 2019). Various biomass materials have been transformed into biochars and critically investigated. The overall adsorption capacities in removing heavy metals are tabulated in Table 2.6, including SMC. The adsorption performance and efficiency of biochars are highly dependent on the biochar properties.

Table 2.6. Biochar from various feedstock materials and the adsorption capacities in removing Cu (II), Zn(II) and Pb(II).

Biochar	Pyrolysis temperature (°C)	Residence time	Heavy metals	Adsorption capacity (mg/g)	Reference
Agricultural and forest residues					
Palm oil	700	12h	Cu (II)	49.4	(Samsuri et al., 2014)
			Pb (II)	58.8	
			Zn (II)	45.7	
Rice husk	700	12h	Cu (II)	37.5	(Samsuri et al., 2014)
			Pb (II)	43.9	
			Zn (II)	34.3	
Peat moss	800	90 min	Cu (II)	39.8	(Lee et al., 2015)
			Pb (II)	81.3	
Pistachio shell	550	1hr	Cu (II)	1.17	(Komnitsas et al., 2015)
			Pb (II)	1.22	
Peeled pine wood	700	3h	Pb (II)	91.98	(Komnitsas et al., 2015)

Hickory chips	600	2h	Zn (II)	0.71	(Ding et al., 2016)
Phyllostachys pubescens	450	3h	Pb (II)	67.4	(Zhang et al., 2017)
Mushroom stick	800	90 min	Cu (II) Pb (II)	2.43 4.9	(Chen et al., 2019)
Spartina alterniflora	500	2h	Cu (II)	48.49	(Li et al., 2013)
Nut shield	600	1h	Pb (II)	4.61	(Vítková et al., 2016)
Sugarcane bagasse	500	3h	Cu (II)	86.96	(Abdelhafez & Li, 2016)
Orange peel	500	3h	Cu (II)	27.86	(Abdelhafez & Li, 2016)
Cactus fibres	600	1h	Cu (II)	3.5	(Hadjittofi et al., 2014)
Porplyra tenera	500	1h	Cu (II)	75.1	(Kim et al., 2016)
E. Compresa (microalgae)	500	1h	Cu (II)	137	(Cho et al., 2015)
Colocasia esculenta	600	1h	Cu (II)	2.31	(Banerjee et al., 2016)
Swine and goat manure	800	1h	Cu (II)	40.64	(Zeng et al., 2018)
Pinewood	600	2h	Pb (II)	4.91	(Wang et al., 2015)
Plum stone	600	2h	Pb (II)	47.05	(Vítková et al., 2016)
Marine macro-algae	600	1h	Cu (II) Zn (II)	23.16 22.22	(Bakshi et al., 2018)
Sugarcane leaf	550	1h	Pb (II)	103	(Li et al., 2018)

Rice hull	400	2h	Pb (II)	367.65	(Han et al., 2016)
Hickory wood	600	1h	Pb (II) Cu (II)	22.82 15.7	(Wang et al., 2019)
Banana peels	230	1h	Pb (II)	241	(Zhou et al., 2017)
SMC	500	3h	Cu (II) Zn (II) Pb (II)	364.2 333.2 564	(Abdallah et al., 2019)
SMC	300-600	4h	Cu (II)	65.6	(Jin et al., 2020)
Industrial by-products					
Sewage sludge	900	20 min	Cu (II) Pb (II) Zn (II)	0.19 0.926 0.2	(Yuancheng et al., 2014)
Dried sewage sludge	650	30min	Pb (II) Cu (II)	40.30 6.70	(Otero et al., 2009)
Anaerobically digested sugarcane bagasse	600		Pb (II)	135.5	(Inyang et al., 2011)
Anaerobically digested whole sugar beet	600		Pb (II)	40.8	
Anaerobically digested animal waste	600		Pb (II)	51.4	(Inyang et al., 2012)

The application of SMC as biochar is still relatively new in the research field. Therefore, the knowledge on SMC as biochar is limited and needs to be thoroughly explored. Most studies of SMC biochar are pioneered by mushrooms producing countries on a large scale, where the waste produced has become a waste management problem and adequate management is required to turn the waste into a potential feedstock especially for biochar. Table 2.7 lists the applications of SMC biochar to remove heavy metals from previous literatures. Abdallah et al. (2019) studied the role of SMC biochar in removing heavy metals (Zn, Cu, and Pb) from wastewater in both batch and continuous systems.

Table 2.7. Application of SMC biochar in removing heavy metals from aqueous solution to date

Biochar	Heavy metals	system	Initial concentration (mg/L)	Adsorption capacity (mg/g)	Description	Reference
Spent mushroom compost	Pb Cu Zn	Batch and column	30	Pb 564 Cu 364 Zn 332	Biochar was prepared by carbonisation and evaluated by several lab factors including initial pH, contact time, temperature and competitive adsorption in removing mixed metals	(Abdallah et al., 2019)
Spent *P.ostreatus* substrate	Pb	Batch	1000	326	Two types of SMC were chosen as biochar raw materials to investigate	(Wu et al., 2019b)
Spent shiitake substrate	Pb	Batch	1000	398	Pb adsorption performance and study the physicochemical properties	(Wu et al., 2019b)

Spent mushroom compost	Cu	Batch and column	50	52.6 – 65.6	16 biochars were produced from four types of SMC to study the effect of pyrolysis temperature and characterisation in removing Cu (II) in batch and continuous system	(Jin et al., 2020)
Spent mushroom compost	Cu Zn Cd	batch	100	68.1 55.2 64.8	Novel application of mineral-rich biochar from SMC with various pyrolysis temperature (350-750°C) to remove mixed metals.	(Agaricus, 2021)
Spent mushroom compost	Pb Cd	batch	700	262.75 75.82	SMC biochar to remove Pb and Cd from water with effect of pyrolysis temperature.	(Chang et al., 2020a)

Jin et al. (2020) conducted an advanced study on the characterisation of various SMC types and evaluated the adsorption performance in removing Cu (II) from aqueous solution. A total of 16 biochars from four types of SMC were utilised and produced at different pyrolysis temperatures. All SMC biochars showed significantly different properties and were markedly affected by the pyrolysis temperatures. Furthermore, all four SMC biochars showed effective Cu (II) removal with the maximum adsorption capacities between 52.6 and 65.6 mg/g for biochars pyrolyzed at 600°C. These properties define each unique condition. Different materials show different performances and efficiencies, depending on their physical properties (i.e., surface morphology and pore size), chemical composition, and materials. The performance of biochars as adsorbents is also influenced by pH, initial metal concentration that involves adsorption isotherms, contact time (adsorption kinetics), and adsorbent dosage.

Other than that, the production of biochar using different pyrolysis temperature affects the overall removal performance of SMC biochar. Chang et al. (2020) and Agaricus (2021) studied the effect of pyrolysis temperature on the adsorption capacities and revealed SMC had the most removal ability at high pyrolysis temperature (> 650°C) due to rapid increase in surface area and well developed mesoporous structure resulting in effective adsorption of heavy metals.

2.4 Biochar characteristics as filter media to remove heavy metals

As the exploitation of SMC as biochar is relatively new, there is no study yet on incorporating SMC biochar as a filter media to treat heavy metals related to mining water. The adsorbents' characteristics are crucial in determining their performance in different field applications. The physical and chemical characteristics vary significantly depending on the raw material and the production processes (Spokas et al., 2014). In order to evaluate the performance of biochar, it is crucial to identify the relationship between biochar properties, the production conditions, and material formation. Thus, these exclusive aspects allow different materials to be derived from biochar. Factors that need to be considered are morphological structure, pore size and chemical compositions.

2.4.1 Physical characteristics

Two types of characterisation are further discussed in this topic which are physical characteristics, including surface morphological structure and pore size as well as chemical compositions of the biochar. Physical characteristic such as surface morphologic and pore size is a crucial property to measure adsorption efficiency. Table 2.8 shows the comparison of physicochemical properties of SMC as biosorbent and biochar at multiple pyrolysis (300^{o}C, 500^{o}C, and 700^{o}C) as compared to activated carbon from previous literatures. This compilation of information provides a comprehensive explanation of how SMC biochar represents a significant advancement over its raw material, displaying comparable or even superior performance to activated carbon. The surface area and pore volume of biochars are critical characteristics that greatly influence the adsorption and retention properties. Masebinu (2019) found that the uptake of adsorbate into biochar relies on the accessible volume of micropores and surface area of the biochar. Based on the radius of the openings, three types of pores can be defined: (1) micropores, which are responsible for the surface area and immersive adsorption capacity factor of biochar; (2) mesopores, which are critical for liquid-solid adsorption processes; and (3) macropores, which are responsible for aeration, hydrology and bulk soil structure (Qambrani et al., 2017).

Table 2.8. Comparison of physicochemical properties of SMC adsorbent and SMC biochar

Media	pH	BET surface area (m^3/g)	Pore volume (cm^3/g)	Pore size (nm) _	Elemental analysis				Reference
					C	H	N	O	
Raw SMC	7.2	0.32	0.003	30.73	54.3	3.45	2.16	24.9	(Corral-Bobadilla et al., 2019)
SMC biochar at 300°C*	10.22	12.97	0.028	8.77	46.78	2.84	2.71	19.65	(Wu et al., 2019a)
SMC biochar at 500°C*	10.64	47.07	0.070	5.97	45.92	1.94	2.11	12.36	(Wu et al., 2019a)
SMC biochar at 700°C*	12.07	218.70	0.138	2.52	44.85	1.23	1.09	9.55	(Wu et al., 2019)
Activated carbon	5.84	1162	0.6193	10.6	41.59	6.18	1.67	45.98	(Tsai et al., 2020)

As stated by Chen et al. (2019), greater pore volume and Brunauer-Emmett-Teller (BET) analysis grants stronger physical adsorption capacity, whereby BET is a method to calculate the surface area involving nitrogen adsorption (Shaheen et al., 2018). From the table, the BET surface area of biochar with pyrolysis temperature at 700°C is 200 times higher than the SMC as raw materials. The pyrolysis process decomposed the lignin material, released the volatile substance, and enhanced the surface area of biochar. High surface area contains more micropores which are responsible for adsorbing heavy metals.

Hence, higher pore volume of SMC biochar compared to biosorbent aids in adsorption and increases the adsorption performance. Although high surface area gives excellent adsorption performance, smaller pore size is needed to increase the adsorption rate and this is shown with the smaller size distribution of SMC biochar compared to biosorbent. Kizito et al. (2015) concluded that smaller particle size increases the adsorption rate due to shorter diffusion path and causes higher penetration of adsorbates into the pores of the adsorbent, increasing adsorption performance. Further statement on the porosity can be supported by the surface morphological images using Scanning Electron Microscope (SEM) as shown in Figure 2.2. From the SEM images, it is observed that the porous image of SMC biosorbent is enhanced by the pyrolysis process which promotes the formation of micropores in SMC biochar.

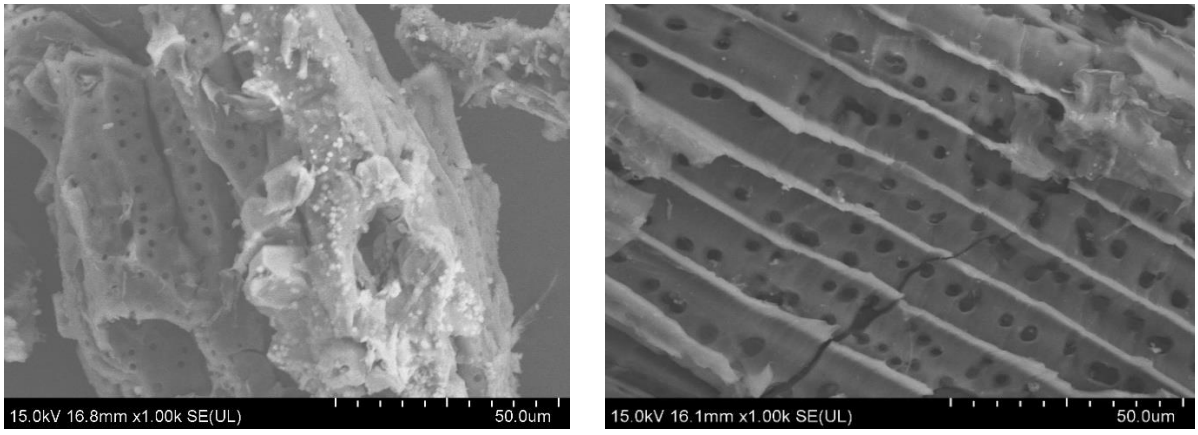

(a) (b)

Figure 2.2. SEM images of (a) SMC adsorbent and (b) SMC biochar at 700^{o}C

2.4.2 Chemical characteristics

Chemical properties such as pH and elemental analysis play significant roles in the adsorption of heavy metals. Based on Table 2.8, SMC biochar has slightly higher pH than SMC adsorbent and this favors the adsorption of heavy metals. High pH contributes to better heavy metals adsorption by biochar (Mohan et al., 2019). Samsuri et al. (2014) found that low pH creates higher hydrogen ion condition which competes with heavy metals for the sorption sites. High pH adsorbent can also act as alkalinity generator to increase the acidic pH in acid mine drainage, which subsequently facilitates the condition for metal removal (Muhammad et al., 2017). Hence, by increasing pH, more adsorption sites are made available for heavy metals. Additionally, elemental analysis is an important parameter as it exhibits the elemental composition of feedstocks and different materials have different proportions of element composition, thus exhibiting different properties and adsorption capacities.

The percentage of cellulose, hemicellulose, and lignin present in various biomass materials affect the elemental composition of biochar. Generally, biochar consists of carbon, hydrogen, oxygen, nitrogen and other elements. The content of carbon in the biochar is important as it gives idea about the stability of the biochar and the development of functional groups (Qiu et al., 2021). The carbon content in SMC biochar is highly similar to activated carbon hence explaining the stability of the biochar. The H and O contents of feedstocks also strongly influence biochar characteristics, this includes polarity and association/dissociation of hydrogen ions, which influence the biochar interactions with organic and inorganic solutes (Hassan et al., 2020). Surface functional groups such as aromatic structures and alkyl groups composed of these elements are one of the main component of biochar adsorption performance (Li et al., 2019b).

Another vital chemical characteristic shared by all biochars is the rich surface functional groups available after pyrolysis process. The chemical and physical interactions between surface functional groups and heavy metals that aids in the adsorption efficiency of heavy metals (Shan et al., 2020a). Heavy metals removal mechanism that involves surface functional groups are through functional group complexation, and ion exchange where connections between heavy metal ions with various functional groups are available on the surface of adsorbent (Xu et al., 2016). Qambrani (2017) stated that the types and levels of surface chemical functioning group determine the adsorption performance of biochar. Oxygen containing functional groups such as carboxyl and hydroxyl groups are the most common functional groups which have been found to contribute widely to the adsorption of heavy metals (Jin et al., 2021).

Furthermore, these chemical functional groups too are affected by pyrolytic temperature as an experiment conducted by Ahmad and Lee (Ahmad et al., 2012) reported that during FTIR test to measure the chemical functional bond in biochar, strong hydrogen bonding decreased when pyrolytic temperature increased. Nevertheless, this ultimately brings us back to the fundamental point that different feedstock materials will yield distinct conditions, resulting in varying chemical functional groups. In lignocellulosic biochar, hydroxyl, amino and carboxylic functional groups decreased at higher pyrolytic temperature (Rangabhashiyam, 2019) while biochar derived from sewage and poultry manure possess higher amounts of N- and S- functional groups (Masebinu et al., 2019). Conversely, oxygen functional groups are found in lower pyrolysis temperature while aromatic functional groups take over at higher pyrolysis temperature. Consequently, surface functional groups of biochar play a vital role in removal of heavy metals from aqueous solution. Overall, biochar that has unique structures as surface functional groups is a promising adsorbent for various environmental applications especially with respect to the removal of heavy metals.

2.5 Heavy metal removal mechanisms of biochar

There are many mechanisms controlling the removal of heavy metals in aqueous solution. The primary method of removing metal contaminants is commonly attributed to physical adsorption, which is valued for its ability to exhibit a high sorption capacity. Mandu et al. (2015) reported that biochars have an enormous surface area with an astounding pore network, consisting of micropores, mesopores, and macropores. Besides, the biochar removal capacity is influenced by its surface conditions, feedstock materials, and pyrolysis status. Biochars with vast surface areas and pore volume have strong interaction with metallic ions because the ions can be physically adsorbed onto the surface of biochars and remain in the pores. Heavy metal ions in the aqueous solution diffuses from the solution onto the surface of biochars with an opposite surface charge. Hence, the metal ions attached to the surface and are then removed from the solution. This type of adsorption occurring at the surface of biochars is associated with van der Waals forces (Sulyman et al., 2017). This method does not involve any chemical bonds. Therefore, surface area and porosity are essential for biochars.

Apart from adsorption, ion exchange with dissolved metal species is argued as the most dominant mechanism (Fakhre & Ibrahim, 2018). The ion-exchange mechanism involves the exchange of ionizable cations on the surface of biochars with metallic ion contaminants. Several researchers suggested that the abundance of negatively-charged sites on the surface of biochars is provided by multiple functional groups, such as carboxyl, hydroxyl, and phenol ($-COO^-$ and $-OH^-$) bind the metallic ions, such as Cu, Pb, and Zn (Joseph et al., 2019; Shaheen et al., 2018; Shamsollahi & Partovinia, 2019). Dai et al., (2018) explained the ion exchange mechanism and proposed that the removal of heavy metals is accelerated by carboxyl and hydroxyl groups, as well as electron donor functional groups (-C-OH, C-O, and C-O-R) that promote

the chemisorption of Cu^{2+}, Pb^{2+}, and Zn^{2+} on the surface of biochar. The pH of the aqueous solution is vital in this mechanism. Functional groups (phenol) can deprotonate metal ions by a decrease of pH according to the following chemical formula in (1):

$$Me^{2+} + 2(-ROH) = Me(RO)_2 + 2H^{2+} \quad (1)$$

Notably, adsorption of heavy metals through ion exchange mechanism can also involve with other cations including Na, K, Ca, and Mg. This can be proven through elemental analysis to observe the changes in cations available before and after adsorption.

Besides ion exchange, another predominant removal mechanism in adsorption of heavy metals that involves surface functional group is surface complexation mechanism. Heavy metals can be bound effectively by complexation with surface functional groups mostly prepared at lower pyrolysis temperature such as carboxyl, phenolic and lactonic functional groups. Wang et al (2019) reported the removal of Cu (II) by carbon adsorbent pyrolyzed at 550^{o}C containing C-O groups involves surface complexation as the dominant mechanism of removal. In contrast, at higher pyrolysis temperature, more aromatic functional groups are available that aids in heavy metal adsorption (H. S. Lee & Shin, 2021). Jin et al. revealed that strong inner-sphere surface complexation dominate the Pb (II) sorption by biomass biochar at high pH. Complexation with functional groups that were responsible for the adsorption of metals can be confirmed through Fourier Transform Infrared Spectroscopy (FTIR) analysis result where there are changes of the surface functional groups in the peaks area before and after adsorptions. When the functional groups were utilised during the adsorption, most of the peaks were shown weakened or

decreased (Subratti et al., 2021). Most studies suggested surface complexation as a crucial removal mechanism for the adsorption of heavy metals by biochar (Liu et al., 2018; Mahdi, Yu, et al., 2019).

During sorption, the formation of solids in a solution or on the surface of the adsorbent is inevitable due to the binding of metallic ions and the presence of chemical groups, hence creating precipitation. This mechanism is often correlated to the immobilisation of heavy metals by biochars. Moreover, precipitation is favoured with strong interaction between metallic ions and plant biochars. The biochars produced at high temperatures will have high mineral matter content (Ca, Mg, Fe, Cu, and Si). Hence, this mineral matter will come in contact with metallic ions and successfully immobilise the materials through precipitation (Shen et al., 2019).

Many biochar applications have only been conducted in batch and column experiments. In SMC biochar, the alkalinity of the biochar promotes precipitation, which could be proven in the X-ray diffraction patterns where the peak intensities show a crystallisation process in the form of quartz (Agaricus, 2021). Removal mechanisms can be best explained through adsorption kinetics test. For example, in the batch experiment, the high R^2 values in the pseudo-second-order model for the kinetics test indicate the involvement of chemisorption (Abdallah et al., 2019). Jin (2020) determined the dominant adsorption mechanism for four types of SMC biochars through precipitation, followed by π-complexation. The complexation mechanisms involved surface functional groups abundant in SMC biochars, highlighting a promising low-cost adsorbent for heavy metal removal. Therefore, it is crucial to further explore the potential of these biochars and to identify the maximum adsorption efficiencies for an optimum performance of metal removal.

2.5.1 Influence of pH

pH is vital in the adsorption capacity of heavy metals. High pH contributes to better heavy metal adsorption by biochars (Mohan et al., 2014; Rangabhashiyam, 2019; Samsuri et al., 2014). Samsuri et al. (2014) found that low pH creates a higher hydrogen ion condition that competes with heavy metals for the sorption sites. Hence, by increasing the pH, more adsorption sites are made available for heavy metals. Subsequently, the changes in pH can significantly affect the adsorption capacity of biochars due to the oxidation and reduction of functional groups between biochars and heavy metal ions (Masebinu et al., 2019). Furthermore, the ability of these functional groups to disperse adsorption sites depends on the pH of the solution as well. Most functional groups are efficiently available at the pH range of 3.5–5.5, where the functional group is deprotonated and increases the number of negatively-charged sites available for adsorption (Torab-mostaedi et al., 2013). Meanwhile, a study observed that the most optimum deprotonation at higher pH ($3 \leq pH \leq 5$) and an increase in negative charges allow heavy metals to coordinate with the surface functional groups and increase the removal efficiency (Paranavithana et al., 2016). This statement is supported by Kaya & Ozer (2014), where adsorption decreased with a decrease in pH.

The theory is almost similar for SMC biochar. At low pH values, biochar surface is protonated and more positively charged ions are available, decreasing the adsorption capacity of metal ions. As pH increases, deprotonation occurs and initiates more binding sites, thus promoting adsorption (Abdallah et al., 2019). Jin (2020) discovered a similar trend with the four tested biochars. The removal efficiencies decreased with increased pH as ion exchange occurred and reduced the electrostatic repulsion that favored Cu (II) adsorption. However, when pH > 6, the removal mechanism was dominated by the formation of $Cu(OH)_2$

precipitates that should not exist and could complicate the whole reaction (Kim et al., 2016); hence, pH 5 was the optimal condition for Cu (II) removal. At pH > 6, the interaction between cations and the surface of biochars is interrupted by the presence of precipitates, thereby decreasing adsorption. This finding is supported by another study, where Abdallah (2019) adjusted the amount of sodium hydroxide and nitric acid to maintain the pH value at 6 to avoid further precipitation. Another explanation of the influence of pH can be discussed in terms of the zeta potential changes in pH. Chang (2020) observed that the zeta potential of SMC biochar changed significantly from pH 3.0 to 10.0. The zeta potential showed more negative charges with increased pH, promoting deprotonation and adsorption mechanisms through electrostatic interactions on the surface of SMC biochar (Chang et al., 2020).

2.5.2 Influence of initial metal concentration

The effect of initial metal concentration has been discussed in many studies, where it is mostly associated with adsorption isotherms, which have a significant role in the application of biochars as adsorbents. Theoretically, as the initial concentration of heavy metals increased, more sorption sites would be filled until equilibrium is reached (Wang et al., 2018). The isotherms provide further understanding of the interaction between the adsorbent and the adsorbate that varies with different adsorbent properties. Many mathematical models are available to calculate the adsorption isotherms. Two most common mathematical models used to calculate isotherms are the Langmuir and Freundlich isotherms. The Langmuir model assumes monolayer adsorption on the surface of adsorption sites, whereas the Freundlich model represents an empirical model of multilayer adsorption onto a heterogeneous surface with varying affinities (Abdallah et al., 2019). Other models for calculating the adsorption isotherms are the Temkin and Dubinin-Radushkevich (D-R) isotherm models.

The Temkin isotherm describes the adsorption equilibrium between the metal solution and the biochar related to the interaction between adsorbents and metal ions to be adsorbed around the surface coverage (Kiliç et al., 2013; Dawodu and Akpomie, 2014), while the D-R model determines the nature of biosorption as either physical or chemical (Zhou et al., 2017) and finds the isotherm that fits the adsorption data well (Shen et al., 2019). According to Wu (2019), the adsorption capacity of SMC biochar increased rapidly by increasing initial metal concentration and reaching equilibrium at higher concentrations. The highest value of R^2 (the value between $0 < R < 1$) in the linear correlation coefficients of the Langmuir model suggests that the process tends to be monolayer adsorption. The adsorption is irreversible for $R < 0$, linear for $R = 1$, and unfavorable for $R > 1$ (Amosa, 2016). In contrast, Jin (2020) introduced the Harkins-Jura isotherm to evaluate the multilayer adsorption and the existence of heterogeneous distribution on the surface of adsorbents.

The Langmuir model well fitted the data with $R^2 > 0.99$, indicating monolayer adsorption. In contrast, the evaluation of SMC biochar by Abdallah (2019) found that the Freundlich model provided a better fit with higher R^2 values than the Langmuir model and promoted heterogeneous multilayer adsorption. Another study also proved that the Freundlich model provided the best fit to the data, indicating the adsorption was non-uniform and multi-layered (Chang et al., 2020). Meanwhile, the fabrication of Mg-Fe modified SMC biochar considered the Redlich-Peterson model, a combination of the Langmuir and Freundlich models. The Langmuir model showed the best fit with the maximum theoretical monolayer adsorption capacity of 247 mg/g for phosphate (Alhujaily et al., 2020). From these studies, it can be concluded that the difference in the best-fit isotherm models is largely dependent on the adsorbent properties and experiment conditions, and is influenced by solution concentration, characterisation, and pyrolysis temperature.

2.5.3 Influence of time

The influence of contact time on adsorption capacities is best described by kinetic modelling. The analysis of adsorption kinetics explains the overall solute distribution for the solid-liquid interface and describes the adsorption mechanisms. The analysis of dynamic behaviour is essential for the application in water treatment to determine the rate-limiting step and the contact time required for optimal adsorption (Abdallah et al., 2019). The commonly used models in the kinetic analysis are the pseudo-first-order and pseudo-second-order models. The pseudo-first-order model assumes that adsorption is controlled by adsorbate. Meanwhile, the pseudo-second-order model indicates that the rate-limiting step involves chemisorption process from the surface adsorption interactions. The fitting model with the highest R^2 value is the best model.

The influence of contact time is consistent with many kinetic adsorption studies of other biochars. Therefore, for SMC biochars, the overall process can be divided into the rapid initial phase, followed by the slow phase until equilibrium is reached (Joseph et al., 2019; Park et al., 2016; Sulaiman et al., 2010). Initially, rapid adsorption occurs due to massive metal transfer forces from the high concentration of heavy metals towards the available adsorption sites on the surface of SMC biochar. Then, over time, the adsorption sites begin to saturate, slowing down and decreasing the adsorption rate until equilibrium is reached. Temperature plays a vital role during this process. Chang (2020) stated that as the temperature increased, a significant increase in adsorption capacity was observed, and this finding is supported by several studies (Abdallah et al., 2019; Abdolali et al., 2016; Wu et al., 2019). Abdallah (2019) claimed that the R^2 value in the pseudo-second-order model is higher than the pseudo-first-order model, suggesting the involvement of chemisorption, such as ion exchange, surface complexation, and precipitation.

Previous studies found that the pseudo-second-order model was a better model to describe heavy metal sorption on biochars than the pseudo-first-order model, and this observation can also be applied to SMC biochar (Laghari et al., 2016; Pullammanappallil et al., 2015). The Pb (II) adsorption data using SMC biochar are well-described by the pseudo-second-order kinetic model and the Langmuir model (Wu et al., 2019). This is supported by a study mentioning SMC biochar best fitted the pseudo-second-order model, and intraparticle diffusion played a role in the adsorption of Zn and Cu ions, with the Langmuir model as the best-fitting isotherm (Abdallah et al., 2019). Another model was also applied in the kinetic analysis. The Weber-Morris model was studied to identify any intraparticle diffusion domination during the overall adsorption process for removing Cu (II), Zn (II), and Pb (II) using SMC biochar.

Table 2.9 Adsorption kinetic model of different biochars and pollutants.

Biochar	Adsorption kinetics model	Pollutants	Reference
SMC	Pseudo second order	Pb	(Wu et al., 2019b)
SMC	Pseudo second order Intraparticle diffusion	Zn,Cu	(Abdallah et al., 2019)
SMC	Pseudo second order	Cu	(Jin et al., 2021)
Mushroom biochar	Pseudo second order	Pb, Cu, Cd and Ni	(Chen et al., 2019)
Magnetic biochar composite	Pseudo second order	Malachite green dye	(Eltaweil et al., 2020)
Rice husk, cow dung and sludge	Pseudo second order	Methylene blue dye	(Ahmad et al., 2020)
Rice husk	Pseudo second order	Dye	(Ganguly et al., 2020)
Date seed	Pseudo second order	Ni, Cu	(Mahdi et al., 2018)

Ginko leaf and peanut shell	Pseudo second order	Pb, Cu	(Lee et al., 2019)
Date and regia seed	Pseudo second order	As	(Pal et al., 2021)

Abdallah (2019) concluded that the model could be considered because the line representing the intraparticle diffusion was close to the origin but only for Zn (II) and it was impossible to apply the model for Pb (II) and Cu (II). Hence, the pseudo-second-order model is still the best option (Abdallah et al., 2019). Another study implemented the Weber-Morris model to evaluate the performance of an advanced SMC biochar fabricated with Mg-Fe to remove phosphate, and the line failed to pass through the plot's origin point, indicating that intraparticle diffusion was not the only rate-limiting step (Alhujaily et al., 2020). In conclusion, most of the biochars, including SMC biochars, favour the pseudo-second-order model for predicting the adsorption of heavy metal ions on biochar through chemisorption interactions. The process can be divided into two stages: the initial phase, where rapid adsorption takes place due to massive heavy metal ion transfer to available active sites on the surface of biochars, and the second phase, where the adsorption has reached a plateau when saturation is reached.

2.6 Biochar removal prediction in data modelling using machine learning

In order to comprehend the implementation of machine learning, it is helpful to reflect on a few past events. High heavy metals concentrations such as Pb, Mn, Fe and Cu in abandoned mining ponds post significant risks to human health and ecological system as the nature of heavy metals to be non-

biodegradable, highly toxic and bio-accumulation. Adsorption is known to be the most utilized and efficient method to remove heavy metals due to its efficiency, operability and low cost (Rashidi & Yusup, 2019). Numerous adsorbents have been reported to be able to remove heavy metals such as commercial activated carbon (Dimpe et al., 2018), carbon nanotubes (Burakov et al., 2018), natural or modified clay and oxide minerals (Yadav et al., 2019) and natural biomaterials (Molahid et al., 2018). Recently, biochars received tremendous attention as adsorbents due to its porous structures, abundant functional groups and additional organic minerals contained (Wang & Wang, 2019). Moreover, the extensive range of feedstock available to produce biochars from woody and agricultural wastes, manures and sludges which are by products and abundantly available. Thus, the application of biochars as low-cost adsorbents promotes recycling and reusing waste hence can be a great solution in reducing waste buildup.

To this date, numerous studies on the adsorption of heavy metals using lignocellulosic biomass biochars. Lignocellulosic biomass contained high proportioned lignin, cellulose and hemicellulose, which resulted higher surface area and surface functional groups of biochars that aids in heavy metals adsorption. Based on previous study, the removal efficiency of lignocellulosic biomass can reach up to 21,840 mg/kg in the leather tanning wastewater which is comparable to commercial activated carbon (Abdel-Fattah et al., 2015). Adsorption capacities are affected by many factors, including operational conditions such as pH, contact time, initial metal concentrations, and adsorbent dosage. The adsorption removal mechanisms was also summarised as ion exchange with cations, surface complexation, coordination with π electrons, and precipitations (Pan et al., 2021). Many empirical adsorption isotherms and kinetics models were developed to describe the adsorption process. However, these models are usually static models where the given set of operational conditions are fixed. Furthermore, experimental methods such as batch and column study can be time consuming and complex. Thus, the conventional equations-based simulation is limited. Accurate prediction of breakthrough curves is important to the design of metal retention column

operations. However, due to complexity and nonlinearity processes, simple mathematical approach are unable to stimulate the behavior accurately (Chittoo & Sutherland, 2020). Thus, the need to find models that can accommodate the multi-dimensional nature of adsorption.

Machine learning method are capable to resolve the problem through modeling and learning the adsorption behavior of heavy metals on biochars. This method is able to build and train high quality model to accurately predict the adsorption efficiency (Zhu et al., 2019). This method is capable of analysing the complex and highly nonlinear relationship between variables (Blagojev et al., 2019). Although mathematical modelling such as Langmuir and Freundlich were employed to describe the adsorption equilibrium, it is impossible to draw predictive conclusion and the relationship between adsorption results and operation condition was unavailable. Several studies have explored the efficiency of modelling in the removal process of heavy metals. Recently, a study was done by Wong et al. (2020) to examine the effect of experimental conditions like contact time, operating temperature, dosage, and initial concentration on the use of rambutan peel biochar for the adsorption of Cu^{+} using artificial neural network (ANN), adaptive neuro fuzzy inference system (ANFIS) and multilayer regression (MLR). The results show the best performance accuracy of 90.24 %, 88.27 %, and 59.14 % for training and testing datasets, respectively. On the other hand, a study by Ke et al. (2021) successfully performed ANFIS model for estimating the efficiency in removal of Ni^{2+} and Cd^{2+} in wastewater based on pH with $R^2 > 0.98$. They concluded that this model was a promising predicting technique for simulating and predicting heavy metal sorption.

2.6.1 Adaptive neuro fuzzy inference system (ANFIS)

Adaptive network-based fuzzy inference system (ANFIS) is a hybrid intelligent system derived by hybridizing fuzzy theory and neural networks created by Jang (1993). The adaptive network has a multilayer feed forward where the output behaviour is determined by a set of parameters. It can capture nonlinear association between input and output through fuzzy logic by using low level learning capabilities of neural networks (Chang et al., 2017). The common model in this field is the Takagi-Sukeno fuzzy inference system. Following equations demonstrate a Takagi-Sukeno model with two input x and y and one input f for two rules as Equation 2 and 3 below,

$$Rule1 : if\ (x\ is\ A) and\ (y\ is\ B) Then\ (f = px + qy + r) \quad (2)$$

$$Rule\ 2 : if\ (x\ is\ A_2) and\ (y\ is\ B_2)\ Then\ (f_2 = px_2 + qy_2 + r_2) \quad (3)$$

ANFIS model comprised of five-layered network. The first layer is the input layer, In Layer 1, this layer contains the membership functions that convert input variables to corresponding fuzzy membership value. The second layer is fuzzification layer, where this layer has fixed nodes and every node produces one fuzzy output. Every output of the nodes represents the firing strength of each rule. The third layer is logic rule layer where each node executes the needed fuzzy rules matching by computing the activation level of each rule. This layer is non-adaptive where it is computed as ratio of rule's firing strength to the sum of all the firing strength rule. The forth layer is defuzzification layer where this layer defuzzify the

membership function to compute the output. Finally, layer 5 is the output layer which is the sum of all outputs of the nodes in the defuzzification layer.

To achieve effective technique model, it is important to discover these 3 parameters; 1) number of membership function, 2) type of membership function, and 3) epoch number. A series of membership functions will involve in the second layer followed by a logical rule in the third layer to stimulate the output and forth layer is comprised of output membership function to predict the actual output (Hanumanthu et al., 2021) The model is capable of conducting learning through minimization of global error within the model. Several researchers have reported the efficiency of ANFIS to model and predict column adsorption data more accurately than conventional column models (Chittoo & Sutherland, 2020). A study done by Al-Yaari et al. (2022) compared the accuracy of both ANN and ANFIS to simulate breakthrough curve for rhamnolipid adsorption and reported that ANFIS showed better accuracy in representing the curves. Nevertheless, a detailed understanding on the removal mechanisms on the biochar is vital for effective design and optimization of the adsorbents.

These removal effect both adsorption capacities and regeneration efficiency of adsorbents. Generally, removal mechanisms can be proven by adsorption isotherms and kinetics, however the underlying mechanisms that governs adsorption process remains unclear. A study done by Nguyen et al., 2022 to determine the underlying mechanisms using linear regression model and observe the relationships of experimental variables responsible for the adsorption capacity. The initial concentration distinguished to tbe the most influential parameter in adsorption capacity. Other than that, surface area of biochar, pore volume, pyrolysis temperature and pore size presented higher ranks and these foundings are insightful for future reference. To the best of the author's knowledge, there is no published research work on the

data optimisation of biochar filter media in heavy metal removal from an abandoned mine pond system before. Therefore, this study will use the ANFIS model to predict the adsorption performance of SMC biochar as filter media in a metal retention pond system.

2.7 Summary

Although biochars have been applied as sorbents in removing organic and inorganic contaminants, little attempt has been made to employ biochars as a reactive media associated with mining water. Based on a review study on SMC biochar, theoretically, SMC biochar is an economical and effective approach to be used as filtration media to remove heavy metals from mining water. The high pH characteristic of SMC biochar will be a great alkaline generator to treat the low pH mining water. Its many physical and chemical composition features will provide multiple binding sites and enhance the adsorption performance. Therefore, further studies on SMC biochar as a potential filter media in heavy metal retention systems could be essential, specifically for applications such as mining water treatment. Moving from that, prediction of heavy metal adsorption onto SMC biochar can be further explored through machine learnings. This method is able to do biochar modeling to predict the adsorption efficiency on the SMC biochar based on its metal's characteristics, initial metal concentrations as well as environmental conditions such as pH which is essential when it comes to abandoned mine waters.

In this study, SMC biochar was produced via slow pyrolysis and tested to remove heavy metals by considering the effects of several factors including pH, initial solution, contact time, temperature and competitive adsorption. The characterisation of SMC biochar showed the presence of functional groups

and the value of cation exchange capacity which could contribute to high adsorption capacity of heavy metals. Next, a series of experiments were conducted to investigate the adsorption performance of SMC biochar as filter media to remove heavy metals from abandoned mine water. Finally, biochar modeling to predict the adsorption efficiency of SMC biochar using machine learning was explored.

This research is crucial as it assesses the potential of SMC biochar in removing heavy metals from abandoned mining ponds where the ponded water may be an alternative for raw water resources. This will be a novel approach as no study has been done in utilizing SMC biochar in abandoned mine water before. Moreover, another point of view is the use of machine learning to provide design charts that can predict the adsorption capacity of heavy metals at given initial metal concentrations and pH. This can be a novel perspective in incorporating computational approach for prediction of metals sorptions using the SMC biochar which can be a great reference for potential real-life applications in the future.

Chapter 3 Materials and Methodology

3.1 Introduction

This chapter discusses the materials and experiment procedures involved in this research. This study includes laboratory experiments through the production and characterisation of media, batch and column experiments, and modelling using machine learning. The potential filter media is made from organic waste material called spent mushroom compost (SMC) to remove heavy metals in synthetic mine water. The SMC is produced using slow pyrolysis process at multiple temperatures. Both batch adsorption and lab scale metal retention column studies were done for 24 hours as laboratory experiments (Abdolali et al., 2017; Chen et al., 2021; Chittoo & Sutherland, 2020). Data from the treatments were analysed using statistical analyses and mathematical modeling, including adsorption isotherms and kinetic studies to assess the adsorption performance of SMC biochar. Subsequently, machine learning techniques were employed to conduct biochar modeling based on column study data. The objective was to predict the adsorption capacities of SMC biochar for removing heavy metals, and the findings were represented in the form of design charts.

This study was done in four stages to achieve the research aim and three research objectives. As a recap, the main aim of this research is to evaluate the performance of SMC biochar as a sustainable filter media in a metal retention pond system to ensure an effective removal of heavy metals in abandoned mine water using a series of laboratory investigations followed by the development of design charts for potential prediction of heavy metals adsorption capacities for future infield application. Overall, three

research objectives to be accomplished are; Objective 1 - to determine the most promising pyrolytic temperature of SMC biochar that gives the highest performance in heavy metal removal in a batch study, Objective 2 - To evaluate the adsorption performance of SMC biochar as filter media in a lab-scale metal retention column study with the effect of pH and initial metal concentration, and Objective 3 - To develop detailed design charts for optimal adsorption capacities of SMC biochar with the influence of initial metal concentrations and pH from lab-scale metal retention column study.

In order to achieve research objective 1, involved Stages 1 and 2 research, where Stage 1 is the production and characterisation of SMC biochar. SMC biochar is produced through a slow pyrolysis process and is pyrolyzed at three different temperatures; 300^{o}C, 500^{o}C, and 700^{o}C. Next, its physicochemical parameters were analysed to observe the potential characteristics of filter media to remove heavy metals. The physicochemical properties include Fourier Transform Infrared (FTIR), Scanning Electron Microscope (SEM), Energy Dispersive Spectrometer (EDS), and gas adsorption Brunauer-Emmett-Teller (BET). As for the lab column study, hydraulic properties tests were done for the soil biochar mixture in a ratio of 20% biochar and 80% loamy soil. Hydraulic properties measured were grain size distribution (GSD) and infiltration rate measurement.

Stage 2 is the batch adsorption study where 0.2 g of SMC biochar from different pyrolytic temperatures were added into a 50ml synthetic metal solution and shaken for 24 hours. Then the water solution is sampled for inductively coupled plasma/optical emission spectrometry (ICP-OES) analysis. The biochar from the batch study was oven dried and analysed using FTIR and SEM-EDX. Potential adsorption performance was assessed through its adsorption capacity and removal rate. Further adsorption assessments were explored and discussed using mathematical modeling of adsorption isotherms and

kinetics. The batch study was conducted with experimental conditions of pH, initial metal concentrations, adsorbent dosage, and contact time. The pyrolytic temperature SMC biochar that showed the best adsorption performance was used as the lab metal retention column study filter media.

Stage 3 is the lab-scale metal retention column study to achieve objective 2. SMC biochar at 500^{o}C was chosen as the filter media in the column setup with a ratio of 20 % biochar and 80 % soil. Synthetic metal mine water in different initial metal concentrations and pH ranges was injected into the column, and water was sampled at time intervals for 24 hours. The adsorption performance of the metal retention column was assessed through breakthrough curve analysis and adsorption isotherm using the Thomas model.

Finally, Stage 4 of the research satisfies objective 3, which is biochar modeling through machine learning. Further simulation was conducted to predict SMC biochar's adsorption capacity to remove heavy metals with the influence of pH and initial metal concentrations. Biochar modeling of SMC biochar from a lab-scale metal retention column study was done using adaptive neuro fuzzy inference system (ANFIS) machine learning model. The model output is the simulated adsorption capacity. Next, the ANFIS model is compared with the multilinear regression (MLR) model. These prediction results were then presented in design charts to represent the predicted adsorption capacity at different initial metal concentrations to remove heavy metals with different pH. Model validation using real case studies was done to validate the model accuracy, which will then be able to simulate adsorption capacity for future reference. The detailed research framework is shown in Figure 3.1.

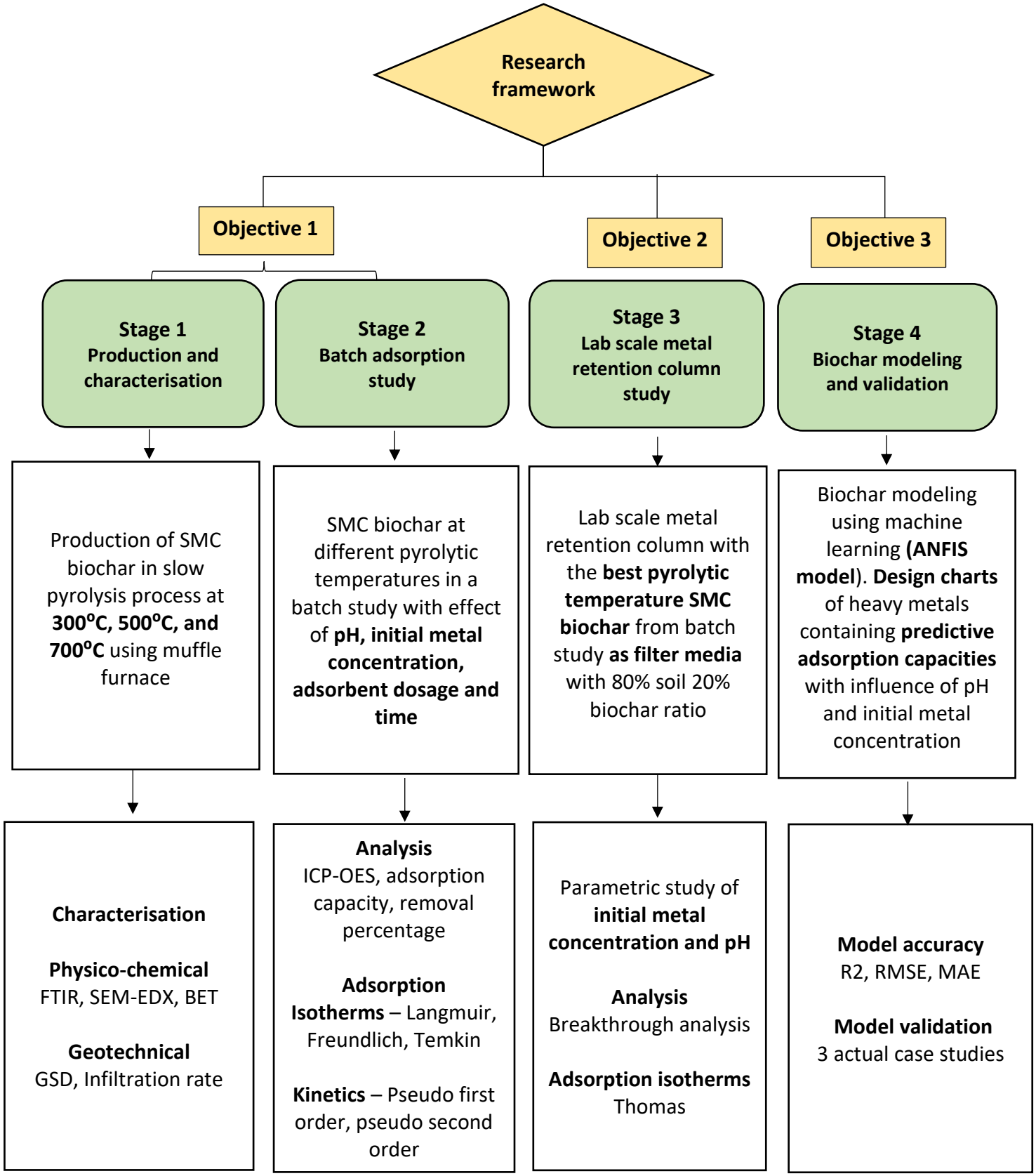

Figure 3.1 Research framework

3.2 Materials

3.2.1 Spent mushroom compost (SMC)

One hundred polybags of raw SMC were collected from 2 mushroom farms located in Selangor and Negeri Sembilan, Malaysia, as illustrated in Figure 3.3. Location 1 is in Kampung Tengah, Puchong, Selangor, with coordinate location of 3°01'11.6" N 101°35'41.5"E, while location 2 is Uwais Cendawan mushroom farm located at Pantai, Negeri Sembilan, with a coordinate of 2°47'25.1"N 101°59'49.5"E. The raw feedstock is mixed, oven dried for 24 hours at 100^{o}C, and stored in air-tight containers. Figure 3.2 showed the image of mushroom compost before and after oven dried.

(a) (b)

Figure 3.2 Image of spent mushroom compost (a) in a compost bag, (b) after oven dried

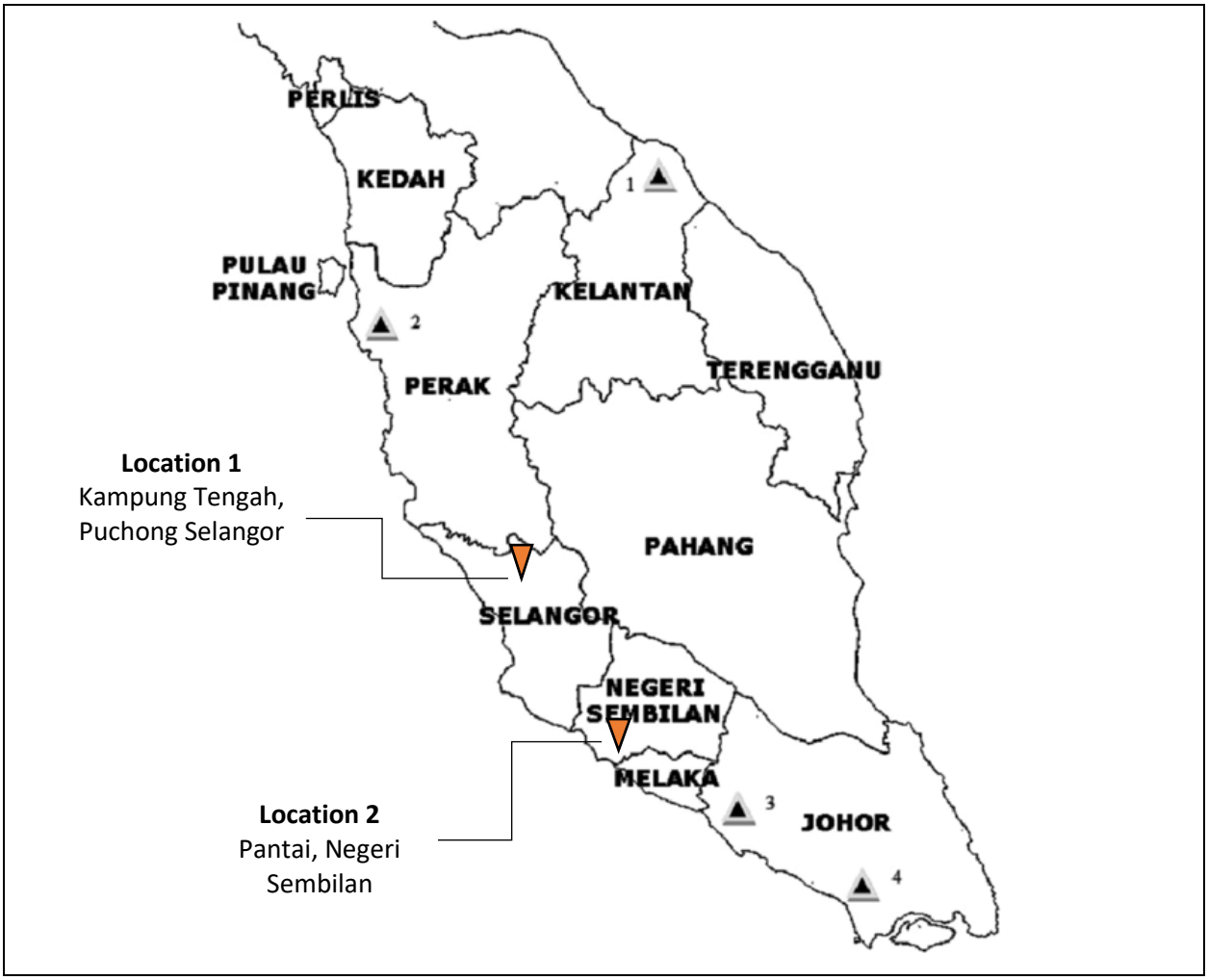

Figure 3.3 The location of raw mushroom composts sampling in Selangor (location 1) and Negeri Sembilan (location 2), Malaysia.

3.2.2 Synthetic mine water

Synthetic mine water was prepared for both batch and column experiments. Synthetic water was used in this study due to the synthetic mine water was made up to contain primary metals of concern (Cu, Mn, Pb, and Fe) commonly found in mine water related pollutions. As this study focused on the heavy metal removing performance of four specific metals, the synthetic solution is proposed to inhibit interruption in the adsorption behavior as actual mine water contains other elements and compositions which might interrupt the actual mechanism happening in the treatment. This also provides treatment consistency and prevents any possible intrusion by conflicting pollutants (Cheong et al., 2010).

The synthetic mine water used in the batch are made up of two types: 1) single metal concentration and 2) mixed metal concentration; both concentrations are in 50 mL solutions. The synthetic mine water solution was simulated by dissolving analytical laboratory salts using ultrapure water. As pH is one of the experimental conditions imparted in both studies, hydrochloric acid and sodium hydroxide was added drop by drop until they reached the desired pH. Table 3.1 shows the composition of synthetic mine water used in the batch adsorption study for both single and mixed solutions. Metal salts of Fe, Mn, Cu and Pb were used to make the desired metal concentrations in the batch study. Low initial metal concentrations ranging from 1 mg/L to 10 mg/L were used in the batch study to imitate the average metal concentrations found in the abandoned mine ponds in Malaysia (Koki et al., 2018b; Wan Yaacob et al., 2009).

Table 3.1. Metal composition of synthetic abandoned mine water for batch study

Component	Salt	Batch concentrations (mg/L)
Fe^{2+}	$FeSO_4.H_2O$	1.0, 3.0, 5.0, 10.0
Mn^{2+}	$MnSO_4.H_2O$	1.0, 3.0, 5.0, 10.0
Pb^{+}	$Pb(NO_3)_2$	1.0, 3.0, 5.0, 10.0
Cu^{2+}	$Cu(Cl)_2$	1.0, 3.0, 5.0, 10.0

Table 3.2 shows the heavy metal concentrations of synthetic mine water in the lab-scale metal column study. It is important to note that the column concentrations were produced based on actual metal concentrations found from various abandoned mine ponds based on literatures. The metal concentrations were prepared from the lowest to the highest metal concentrations and were divided into seventeen different sets of B500A to B500Q. Furthermore, these concentration sets were generated to explore the effect of adsorption competition between these heavy metals on the removal performance.

Table 3.2. Metals' concentration in synthetic mine water for the lab scale metal retention pond column study

Name of set	Initial metal concentrations (mg/l)			
	Pb	Mn	Cu	Fe
B500A	1	5	1	5
B500B	5	7	5	10
B500C	10	10	10	20
B500D	23	12	30	23
B500E	15	13	35	25
B500F	17	14	40	30
B500G	20	15	70	50
B500H	22	16	72	55
B500I	25	18	77	60
B500J	28	19	87	65
B500K	30	20	100	70
B500L	35	25	105	85
B500M	50	30	150	100
B500N	60	33	160	135
B500O	70	40	200	150
B500P	85	45	215	175
B500Q	100	50	300	200

3.3 Stage 1 Production and characterisation of SMC

3.3.1 Production of SMC biochar at different pyrolysis temperature

In order to produce biochar from SMC, oven dried feedstock was placed in ceramic crucibles with lids, and slow pyrolyzed in an oxygen-limited condition using a muffle furnace with a heating rate of 5°C/min. Three different peak temperatures, namely 300°C, 500°C, and 700°C, were adapted to carbonise, which were held for 3 hours, then cooled down to room temperature inside the furnace. These proposed

temperatures were selected to distinguish their different physicochemical properties, as reported by previous research (Luo et al., 2018b; Shi et al., 2019; Zhang et al., 2019). The biochar samples obtained from SMC at different pyrolysis temperatures were labeled as B300, B500, and B700, respectively. After the pyrolysis process, it can be observed that the media is perfectly carbonised and turned from brownish color to black. Figure 3.4 (a) shows the process of slow pyrolysis using a muffle furnace and (b) the image of raw SMC before pyrolysis and SMC as biochar after the pyrolysis process. Following pyrolysis, samples were manually ground by pestle and mortar, sieved to size <500 µm, and stored in airtight plastic bags for further use.

(a) (b)

Figure 3.4 (a) SMC in crucibles before pyrolysis process in muffle furnace and (b) Image of SMC before and SMC as biochar after pyrolysis

3.3.2 Characterisation of SMC biochar

Successful treatment relies on the suitability and effectiveness of a filter media. SMC biochar was characterised by multiple pyrolytic temperatures before and after adsorption to explore the chemical, physical and geotechnical properties at different pyrolysis temperatures. This characterisation procedure will help to better understand the connection between its characteristics and the adsorption performance on heavy metal removal. The chemical properties involved were biochar yield, pH, and redox potential (Eh). Next, the physical properties explored were the surface area of feedstock (BET), the active surface functional group (FTIR), and the surface morphological analyses (FESEM-EDX). Geotechnical properties conducted were the grain size analysis and infiltration rate measurement.

3.3.2.1 Chemical characteristics

The measurement of pH and redox potential (Eh) was done through Myron 6P Ultrameter using ultrapure water based on a solid-to-liquid ratio of 1:2 (Wei et al., 2020). 2 g of SMC biochar was inserted into a beaker before adding 50 ml ultrapure water and mixed in a shaker for 15min. Then, the samples were transferred into centrifuge tubes and inserted into Kubota 2420 high speed centrifuge shaker at 1000 rpm to separate the liquid and solute. Next, water is sampled using an ultrameter for both pH and Eh. As for biochar yield, after the biochar pyrolysis process using a muffle furnace is completed and cooled down, the biochar-containing crucible was weighed to calculate the biochar yield at various pyrolysis temperatures in Equation 1,

$$\text{Biochar yield } (\%) = (m_1/m_0) \text{ X } 100\%, \quad (1)$$

Where m_0 (g) was the weight of dry SMC biochar before pyrolysis and m_1 (g) was the biochar weight of SMC biochar after pyrolysis.

Fourier Transform Infrared (FTIR)

The surface functional group of the biochar before and after adsorption was investigated using Thermo Scientific Nicolet IS10 Fourier Transform Infrared (FTIR) spectroscopy. The FTIR test is crucial to assess the active functional group of each SMC biochar with different pyrolytic temperatures and to understand the adsorption mechanism involving modifications and chemical interactions on the functional groups of SMC biochar before and after adsorption. The biochar samples were analysed at 8 cm^{-1} resolution wavenumbers ranging between 4000-650 cm^{-1}. Surface morphological analyses are essential for a clear view of the successful adsorption of heavy metals on the surface area of feedstock biochar (Joseph et al., 2019).

3.3.2.2 Physical characteristics

Field Emission Scanning Electron Microscope (FESEM) & Energy dispersive spectrometer (EDS)

Field Emission Scanning Electron Microscope (FESEM) analysis was used in microanalysing solid materials. The surface morphology of the biochar (coated with Ag) was tested using FESEM model Hitachi SU8010. The biochar samples were air dried and spread on an equipment stub using carbon tape. Then, the sample was subjected to gold plating for 45 seconds using Qurum/Q150RS Sputter Coater to avoid an electrostatically distorted image. Then the sputtered samples were viewed with a resolution of up to 1 nm. The whole area of biochar was scanned and photographed for further analysis and observation. FESEM, with multiple modifications and resolutions, is equipped with energy dispersive spectrometer (EDS) analysis to identify the elemental composition to establish the correlation with the effects of pyrolysis temperature of the feedstock (Li et al., 2019).

Brunauer-Emmett-Teller (BET)

Brunauer-Emmett-Teller (BET) (Micrometritics ASAP, 2020) analysis was determined to measure the surface area and pore size distribution of the biochar. Before the test, the biochar samples were degassed with nitrogen at 200 °C to remove moisture for a uniform pore size distribution.

3.3.2.3 Geotechnical characteristics

Grain size analysis

Geotechnical properties were studied in lab scale metal retention column using a soil biochar mixture of 20 % biochar and 80 % mixed soil. Mixed soil in this study was a mixture of 60 % medium sand and 20 % topsoil (MSMA, 2012) from an agricultural farm. Geotechnical properties measured were grain size distribution (GSD) to find the distribution of different particle sizes in soil samples. GSD was measured using ATM D6913/D6913M-17. The soil sample is sieved through multiple sieve sizes in the sieve analysis. It is crucial to ensure the sample is dry enough to prevent particles from sticking together due to water moisture.

Infiltration rate measurement

Infiltration rate is one of the soil hydraulic properties describing the average fluid velocity to pass through porous media. Infiltration rate, also known as hydraulic conductivity (K) was measured by the Falling Head Test Method (ASTM D5084-03). The soil samples were compacted using water in a rigid-wall compaction sample tube, a U100 tube 10 cm in diameter and 13 cm high. The compaction mold was then connected to an experiment set-up consisting of a standpipe with an inner diameter of 0.5 cm and a liquid reservoir. In the permeated cell, a wire gauze is placed in contact with each trimmed end of the sample. The samples were permeated until a steady state effluent flow characterised by an inflow/outflow of 0.8 to 1.25 was observed. The length (L) of the sample is determined by measuring the distance to each face of the sample

from each end of the tube. In order to evaluate the value, k_{sat} was determined using Darcy's law, as presented in Equation 4.

$$k_{sat} = \frac{Q}{A.\frac{dH}{dL}} \quad (4)$$

Where k_{sat} is the saturated hydraulic conductivity (m/s), Q is the flow rate (m^3/s), A is the cross-section of the reactor (m^2), and $\frac{dH}{dL}$ is the hydraulic gradient.

3.4 Stage 2 Batch adsorption study

Batch experiments, also known as static systems, are carried out by inserting a potential substrate into the solution containing a concentration of contaminants with a solid/liquid ratio (Wang et al., 2015). This study utilises a batch adsorption study as this process effectively analyses the feasibility of SMC biochar as an adsorbent in removing heavy metals from the mine water system with multiple experimental conditions (Patel, 2022). It is an easy and practical approach to determine which pyrolysis temperature gives the highest adsorption efficiency in removing heavy metals. In this study, the batch test was conducted in individual (single) and mixed solutions (where four proposed metals were mixed in a solution) to establish the effect of competitive adsorption. The batch study was performed using a 50mL centrifuge tube containing 50 ml of desired metal concentrations at ambient temperature (± 25°C).

0.2 g of SMC biochar from B300, B500, and B700 was added to a 50 mL heavy metals solution in individual (Pb, Mn, Fe, and Cu) with an initial concentration of 10 mg/L and mixed metal solution with a 1:1 ratio.

One control setup consisting of metal solution and 0.2 g of raw SMC (RS) was tested. Subsequently, the solid-liquid mixture was shaken on a rotating shaker (Luo et al., 2018b) at 150 rpm for 24 hours (Jin et al., 2018) for homogenous sorption. After the designated shaking time, the mixture was filtered through a 0.45 µm membrane. The metal concentration in the filtrate was measured by inductively coupled plasma/optical emission spectrometry (ICP-OES) (Perkin Elmer, Optisma 8300). All samples were taken in triplicates, and the means were used in data analysis to highlight quality assurance. Next, the batch experiment was carried out to study the effect of solution pH, adsorbent dosage, time, and initial metal ion concentration using the same procedure. Table 3.3 shows the experimental conditions chosen for the batch adsorption study. The pH involved were 2, 4, 6, 8, and 10, adsorbent dosage of 0.05 g, 0.1 g and 0.2 g were chosen and at initial metal concentrations of 1 mg/L, 3 mg/L, 5 mg/L and 5 mg/L. Figure 3.5 shows the batch adsorption study.

Table 3.3 Experimental conditions for batch adsorption study

Filter media	Experimental conditions			
	pH	Time (hour)	Adsorbent dosage (g)	Initial metal concentrations (mg/L)
B300 B500 B700	2 4 6 8 10	0.5 1 3 8 24	0.05 0.1 0.2	1 3 5 10

The percent metal removal (%) was obtained using the following Equation (5):

$$\text{Percentage removal, R (\%)} = \frac{Ci - Co}{Ci} \times 100 \quad (5)$$

And the biosorption capacity (q) of metals (Pb, Cu, Mn, Zn and Fe) in solution was calculated using Equation 6,

Adsorption capacity, $Q = \frac{(C_i - C_o)\,V}{m}$ (mg/g) (6)

Where R is the removal percentage of metal (%); C_0 and C_i denote the final and initial concentration (mg/L), while Q is the adsorption capacity (mg/g) and V is the volume of sample (L) and m is the mass of the biochar in the sample (g). Meanwhile, the SMC biochar from the batch study were sampled for FTIR and FESEM-EDX analysis. From this analysis, the pyrolysis temperature SMC biochar that displays the best adsorption performance will be chosen as the filter media in the column study.

Figure 3.5 Batch adsorption study setup

3.4.1 Adsorption kinetics

Besides adsorption isotherms, the kinetic study is another essential part of a batch study. Adsorption kinetics explains different rate-controlling steps, including the chemical reaction, mass transport processes, and diffusion control. This mathematical model also reveals how the required contact time between the adsorbent and the adsorbate influence the adsorption efficiency where the estimated maximum adsorption capacity can be calculated and modeled (Ahmad et al., 2020; Patel, 2022). The kinetic models adopted in this study included pseudo-first-order and pseudo-second-order. Table 3.4 shows the equation for the kinetic models.

Table 3.4 Adsorption kinetic nonlinear models and parameters

Kinetics	Equation	Parameters	Reference
Pseudo first order	$ln\left(Q_e - Q_t\right) = ln\left(Q_e\right) - K_{1t}$	Q_e = amount adsorbed per kg of adsorbent at equilibrium (mmol/kg) and K_1 = pseudo first order constant (1/min). for initial condition at t = 0 and Q_t = 0	(Paranavithana et al., 2016)
Pseudo second order	$\frac{t}{Q_t} = \frac{1}{K_2 Q_e^2} + \frac{t}{Q_e}$	K_2 = pseudo second order constant (kg/mmol/min). for initial condition at t = 0 and Q_t = 0	(Paranavithana et al., 2016)

3.4.2 Adsorption isotherms

Adsorption isotherms is a mathematical modeling approach using equilibrium isotherms to analyse the adsorption capacity of metals on the biochar. It also plays a vital role in predicting and comparing adsorption performance, explaining the pollutants' interaction with the adsorbent, and evaluating process optimisation and adsorption mechanism (Patel, 2022). Table 3.5 shows the adsorption isotherms and their parameters. The most common well-fitted models are the Langmuir model, which assumes monolayer adsorption on the surface of adsorption sites, and the Freundlich model, which represents an empirical multilayer model adsorption onto a heterogeneous surface with varying affinities (Abdallah et al., 2019). Additionally, the Temkin isotherm was used to describe the adsorption equilibrium between metal solution and biochar related to the interaction between adsorbents and metal ions to be adsorbed around the surface coverage (Dawodu & Akpomie, 2014; Kiliç et al., 2013) and determine which isotherm fits the adsorption data well.

Table 3.5 Adsorption isotherms used in this study and their parameters

Isotherm	Equation	Parameters	Reference
Langmuir	$q_e = \frac{q_m K_L C_e}{1 + K_L C_e}$	q_e (mg/g): the amount of metal ion adsorbed at equilibrium q_m (mg/g): the complete monolayer adsorption capacity C_e(mg/L): the equilibrium concentration K_L(L/mg): the Langmuir adsorption constant	(Abdallah et al., 2019)
Freundlich	$q_e = K_F C_e^{1/n}$	*n:* the empirical parameter relating adsorption intensity, which distinguish with heterogeneity of the material K_F((mg/g) (L/mg)$^{1/n}$): the Freundlich adsorption constant	(Jin et al., 2020)
Temkin	$q_e = B\ ln\ (\ K_T C_{e)}$	b_T (J/mol): the Temkin constant related to the heat of adsorption *KT* (L/mg): the Temkin constant related to the equilibrium binding energy	(Shen et al., 2019)

3.5 Stage 3 Lab scale metal retention column study

Different pyrolytic temperatures of SMC biochar are produced and characterised during the production of biochar to explore its physicochemical properties. Consequently, the adsorption performance of SMC biochar in removing heavy metals was conducted in batch studies. Each pyrolysis temperature produced a different adsorption result, and the pyrolysis temperature that showed the highest removal efficiency was chosen as filter media for further investigation. Although the batch experiment has proven which pyrolysis temperature filter media gave the highest adsorption performance, the study is helpful in a small amount with a lower pollution load; hence, it is not practical for industrial purposes (Patel, 2019). In contrast, column study is a continuous system where the solution of adsorbate continuously passes through a column and consistently interacts with the adsorbent as filter media. This method can remove a higher quantity of polluted solution and imitate the actual industrial conditions (Malik et al., 2018).

Thus, a lab-scale metal retention column was constructed to investigate the performance of SMC biochar in removing heavy metals in abandoned mine water and establish its optimal removal efficiency for real-life applications. This laboratory study was conducted to determine optimal design parameters such as its composition, physico-chemical characteristics, and system configuration (Neculita et al., 2007). The column is a crucial step in performing continuous adsorption to imitate pH and initial metal concentration for abandoned mining water before releasing it to the river as an alternative raw water source (Abdallah et al., 2019; Mohanty et al., 2018b).

A metal retention column study was conducted in a continuous column adsorption experiment to stimulate a metal retention system with SMC biochar as filter media and remove heavy metals, namely Fe, Mn, Cu, and Pb. Figure 3.6 (a) shows the schematic column setup, while 3.5 (b) shows the image of the column setup. In all, four columns have been set up where three columns were set as triplicate and another as control (filter media is 100% soil) in a downward flow where the adsorbate is passed at the same direction of gravity. SMC biochar was mixed in soil at a ratio of 20% biochar to 80% soil (20% compost, 20% topsoil, and 60% medium soil) according to the Urban Stormwater Management Manual for Malaysia (MSMA) to improve infiltration and metal removal (Goh et al., 2019).

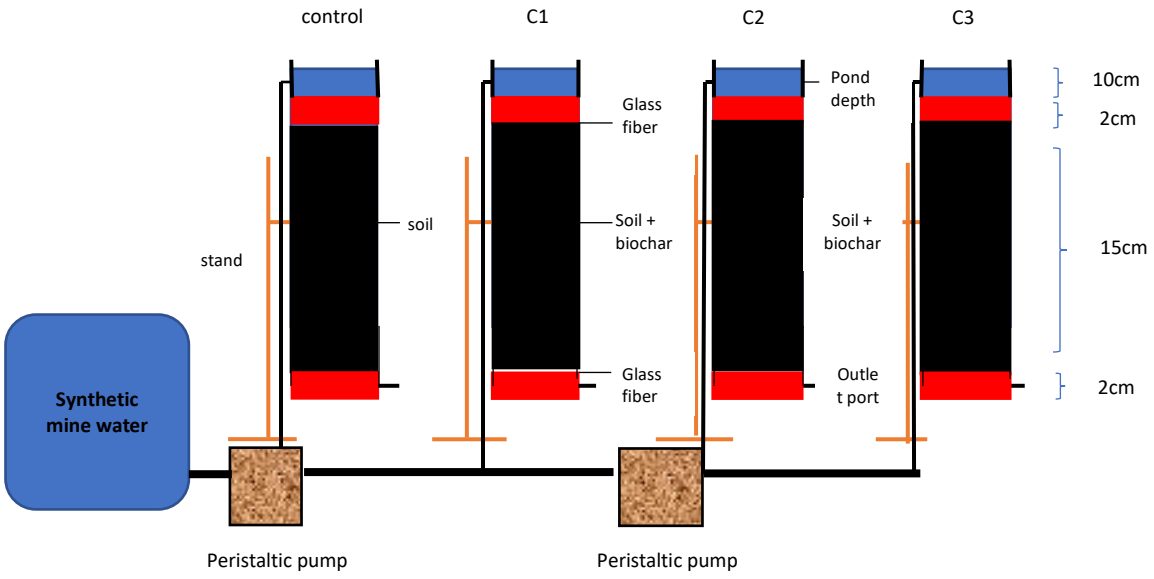

(a)

(b)

Figure 3.6 (a) Schematic column setup (b) Figure of column setup

Table 3.6 shows the particle size distribution of the filter media, and Figure 3.7 is the grain size analysis for the filter media. The biochar chosen as the column filter media is SMC biochar pyrolyzed at 500^{o}C (B500) based on the result of adsorption performance from the batch study. An influent distributor was placed at the top side to ensure uniform inlet flow of the mixed metal solution into the column. Column setup was done in a Pyrex column with a 5 cm inner diameter and 30cm in length. 2 cm of gravel and geotextiles were constructed on the bottom of the column to prevent any loss. The mixture of soil and biochar was uniformly packed into the column with a fixed 15 cm bed height, assuming adsorption capacity was not affected by bed depth (Chittoo & Sutherland, 2020).

Table 3.6. particle size distribution of filter media

Particle diameter (mm)	Percentage finer (%)	
2.36	23..4	Coarse Sand
1.18	8.6	Medium Sand
0.6	5.4	Medium Sand
0.425	7.3	Medium Sand
0.075	20	Clay + silt + biochar

Once the columns were filled, the media were fully immersed in ultra-pure water and left to swell to ensure an equilibrium state and complete air bubbles expulsion (Evans & Ko, 2013). Following this, the column was compacted by gravity. 20 L synthetic metal concentration of different sets were injected using a peristaltic pump with varying influent concentrations of 1- 300 mg/L at different pH of 2, 5, 7, and 10, respectively. A 10cm pond depth was set up to maintain a constant flow rate of 10ml/min. Infiltration rate of these biochar columns were k = 1.64 m/day. This rate was close to the recommended infiltration rate provided by the MSMA guideline for soil columns (1.2 – 1.5 m/day). Water samples were collected from the effluent point at a designated interval (every 15 min for the first 2 hours and 60 min until finish) to measure heavy metal concentrations.

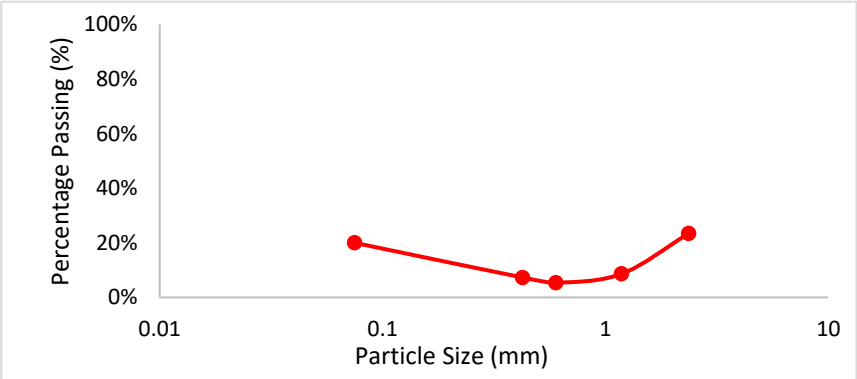

Figure 3.7 Grain size analysis for filter media

3.5.1 Result analysis

The metal retention behavior of mixed metals under different initial metal concentrations and pH in a fixed-bed column study was shown as a breakthrough curve analysis from adsorption isotherm. The adsorption isotherms adopted is the Thomas model, which is an extensively used model to understand column adsorption data. Additionally, the Thomas model can predict the characteristics of the breakthrough curve in column study. It was built on assumptions such as the kinetics of adsorption fitting the Langmuir model, no axial dispersion, and the rate of force fits second-order kinetics (Prabhu et al., 2021).

The total adsorbed amount of metals at different times and equilibrium adsorption capacity are expressed as Equations 6 and 7, respectively, while the Thomas model is expressed in Equation 8

Adsorption capacity, $q_{c}=\frac{QA}{100}=\frac{QC_O}{100}\int_{t=t_o}^{t=t}[1-f\ (t)]\ dt$ (6)

Adsorption capacity, $q_{e}=\frac{q_c}{m}=\frac{QC_O}{100m}\int_{t=t_o}^{t=t}[1-f\ (t)]\ dt$ (7)

Where Q is the inflow rate (ml/min), A is the area below the breakthrough curve, f(t) is the function breakthrough curve, and m is the mass of SMC biochar (g).

Thomas model, (8)

$$\frac{C}{C_O} = \frac{1}{1 + \exp\left(\frac{K_{TH}}{F}\left(q_o M - C_O V_{eff}\right)\right)}$$

Where K_{TH} is the Thomas rate constant (mL/mg min) and q_o is the maximum adsorption capacity for heavy metal ions (mg/g).

3.6 Stage 4 Biochar modeling in predicting adsorption capacity of SMC biochar

3.6.1 ANFIS model development

This research adopted the ANFIS modeling technique to develop a superior predictive model for adsorption capacity prediction. Work of literature shows that all adsorption behavior is conventionally discussed using empirical adsorption kinetics and isotherm models. However, these models are fixed under a given set of operational conditions; hence it is difficult to simulate adsorption performance under different operating conditions (Tulun et al., 2021). Therefore, there is a need for advanced models that can accommodate the multi-dimensional nature of adsorption for actual life applications.

Hence, the ANFIS model was chosen in this study as it has the potential to solve complex and nonlinear systems. Moreover, this model shows higher accuracy than other models (Hanumanthu et al., 2021). The ANFIS editor of MATLAB was used to develop the ANFIS models for predicting the adsorption capacity. To

model the predictive adsorption capacity of SMC biochar, the primary process is to develop and structure the ANFIS model. The process includes selecting inputs and the type and number of membership functions (MF) for inputs. The proposed algorithm in this study can be divided into three sections: (i) pre-processing data input, (ii) modeling; and (iii) accuracy evaluation. Figure 3.8 shows the flowchart of biochar modeling.

After data collection, data normalization is a pre-processing technique performed before data input into the model. Data normalization is crucial to scale the data features between 0 and 1. This step prevents the dominance of more immense values that override the smaller ones. After the normalization process, data were divided randomly into two parts, training and testing datasets. This division is for learning and fitting classifier variables and assessing the performance of a fully specified classifier. A total of 749 datasets were sampled, where 80 % (599) were used as training and 20 % (150) being testing datasets.

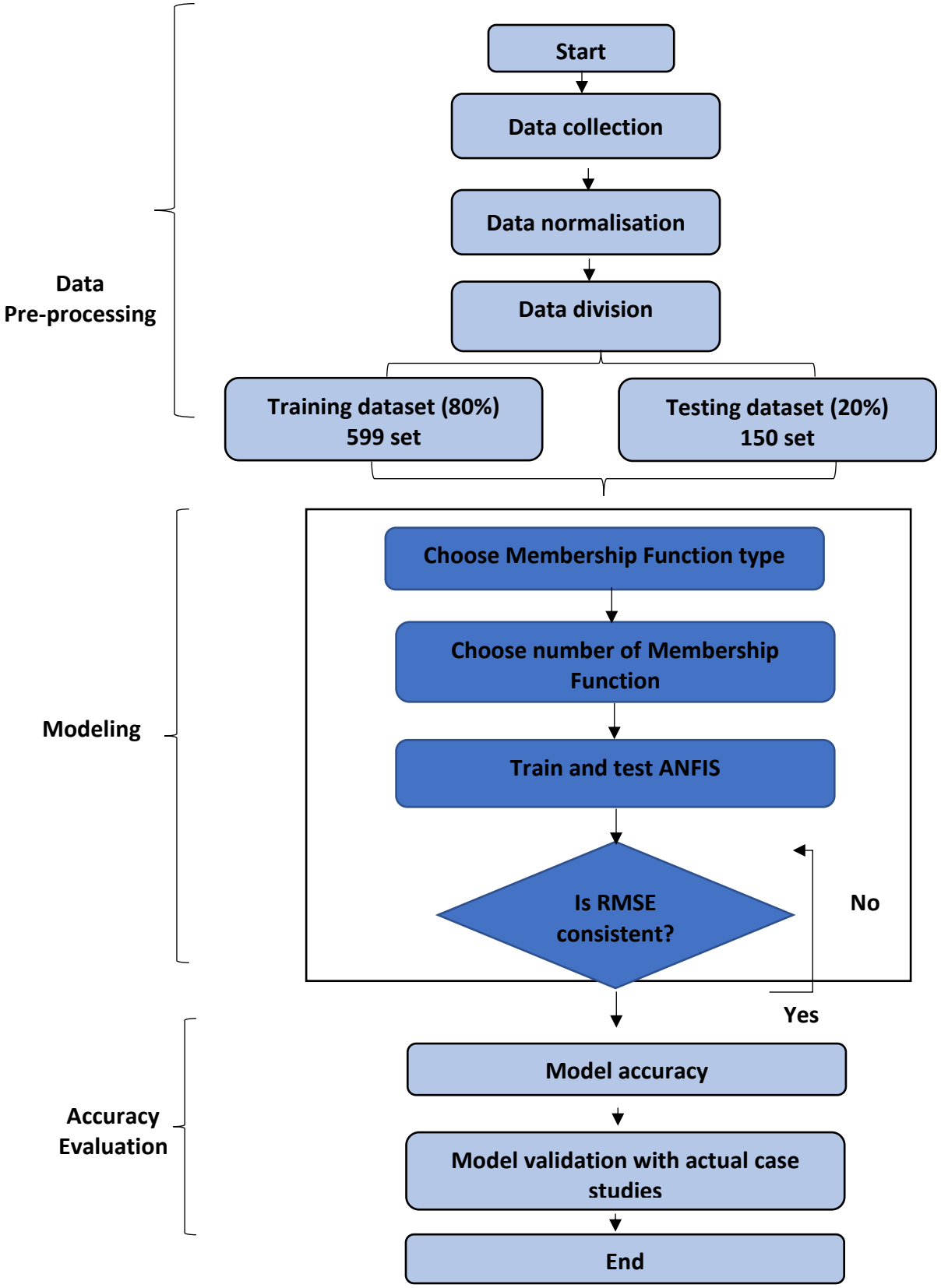

Figure 3.8 Flowchart for biochar modeling

Next is to discover the input and output layers. The input parameter of the model is the initial metal concentrations and pH, while the output layer is the adsorption capacity. Table 3.7 shows the ranges of input and output variables of the model.

Table 3.7 The ranges of input and output variables of ANFIS

Variable	Range of the parameter value
Input layer	
Initial metal concentration (mg/L)	1-300
Influent pH	2.0–10.0
Output layer	
Adsorption capacity (mg/g)	0–50

3.6.2 Multilinear regression (MLR)

MLR is a preliminary statistical procedure for modeling the linear relationship between a dependent variable and a collection of independent variables using the least square method (Agbaogun et al., 2021). In this study, MLR was done using regression function in Matlab software. Notably, the outcome value y is the weighted sum of influences from multiple independent variables *x1, x2, x3…* the following represents a generalized MLR equation in Equation 9.

$$y = \beta_0 + \beta_1 x_1 + \beta_2 x_2 + \ldots . \beta_i x_i \quad (9)$$

Where *y* is the dependent variable, β_0 is the regression constant, x_i is the coefficient of the independent variable, and *x* is the independent variable. Like ANFIS, MLR can model the relationship between the input variables and the output; however, it depends on the correlated linear relationships. Thus, it may lead to inaccurate results for a nonlinear and more complex relationship like adsorption (Agbaogun et al., 2022). Hence it is essential to compare the performance of ANFIS with this linear predictive model, which gives a higher precision, and overcomes the undermining statistical significance of an independent variable and overfitting.

3.6.3 Accuracy evaluation

In order to evaluate the accuracy of the model, correlation coefficient (R), root means squared error (RMSE), and mean absolute error (MAE) were used to support the algorithm. RMSE is a measure of the variation between the actual and predicted data and is an indicator of the absolute fit of the model. Lower values of RMSE indicate better fitting. Predicting is one of the most critical evaluation criteria to get a low value RMSE in Equation 10.

$$RMSE = \sqrt{\frac{1}{N}\sum_{i=1}^{N}(A_i - F_i)x^2} \quad (10)$$

On the other hand, MAE is the absolute value of difference between the actual and predicted data, reducing sensitivity to the outliers as shown in Equation 11.

$$MAE = \frac{1}{N}\sum_{i=1}^{N}|A_i - F_i| \quad (11)$$

3.6.4 Model validation

Simulation using machine learning tools was carried out to predict the adsorption performance of SMC biochar to remove multi-metals in a heavy metal retention system. Then, design charts were developed in reference to pH and initial metal concentrations. Correspondingly, three case studies have been considered as model validation to validate this study's adsorption capacity design charts. The case study chosen for this study was an abandoned mine pond in Puchong, Selangor. Figure 3.9 shows the location of case study sites. The Puchong abandoned mine is at Taman Putra Perdana, Puchong, Selangor. Sampling was taken at a few sampling points, namely station 1 (S1) is located at 2°57'48.9" N 101°36'10" E , station 2 (S2) located at 2°57'14.5n 101°36'22.5"E, and station 3 (S3) is located at 2°57'35.8"N 101°35'21.1"E.

This site was used as a tin mine landfill and is currently turned into a flood retention pond. Table 3.8 shows the sampled water heavy metal concentrations from S1, S2, and S3 at Puchong abandoned mine ponds. Correspondingly, these validation sites were polluted with heavy metals, with a mean water quality index (WQI) of 448.55. Indeed, this is supported with a recent study that showed an extortionate level of Cu (82.9 x 10^4 mg/L), Fe (41.5 x 10^4 mg/L), and Pb (1.1 x10^4 mg/L) found in the water samples from this site (Teow et al., 2018).

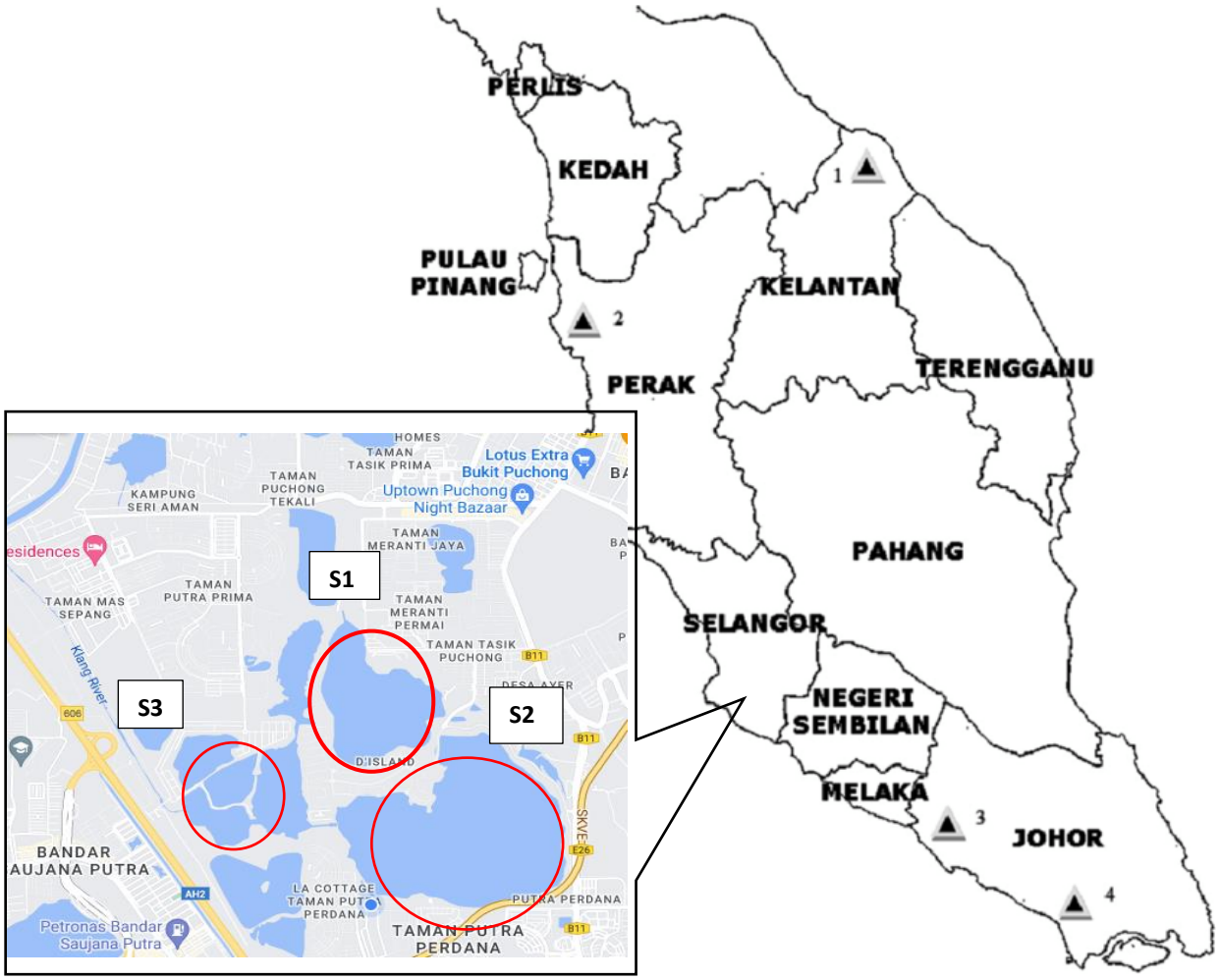

Figure 3.9 Case studies sites for model validation

Additionally, the location of this abandoned mine is adjacent to the Klang River; hence it has an excellent potential to be selected as the case study site for further work. The mine water was sampled and analysed using ICP-OES for Cu, Pb, Mn, and Fe; common metals found in tin mines (Hashim et al., 2018). Then, 20 L of actual mine water were used as influents in the same column studies with SMC biochar as filter media. Water samples were collected from the effluent point at a designated interval (every 15minutes for the first 2 hours and 60minutes until finish) to measure heavy metal concentrations. The actual field data results are then validated with the model for adsorption performance from the metal retention model and verified. Finally, a solid framework containing a detailed design chart for optimal adsorption performance of SMC biochar through machine learning will be developed.

Table 3.8. Heavy metal concentrations at 3 case studies in Puchong abandoned mine ponds

Stations	pH	Heavy metals concentrations (mg/L)			
		Pb	Mn	Cu	Fe
Station 1, S1	2.7	21.563	15.003	69.214	51.662
Station 2, S2	4.5	15.23	13.471	33.665	23.771
Station 3, S3	5.4	3.77	6.288	3.771	7.669

3.7 Summary

In this chapter, the materials' sampling and preparations have been presented. Then, this is followed by a detailed description of research methodology performed in four stages of research as follows.

- Stage 1 – Production and characterisation of SMC biochar at multiple pyrolysis temperatures
- Stage 2 – Batch adsorption study
- Stage 3 – Lab scale metal retention column study
- Stage 4 – Biochar modeling and detailed design charts

Chapter 4 presents research findings where it discusses the results obtained from Stage 1 of the research. This chapter will focus on the production and assessment on the SMC biochar properties at multiple pyrolysis temperatures in terms of physical, chemical and geotechnical aspects.

Chapter 4 Characterisation of SMC biochars and batch adsorption study

4.1 Introduction

This chapter presents the findings of Stage 1 and Stage 2 of the research which satisfies objective 1 of this study which is to determine the most promising pyrolytic temperature of SMC biochar that gives the highest performance in heavy metal removal in a batch study. This chapter starts with a discussion of Stage 1, the physical and chemical characterisations of SMC as biochar produced in multiple pyrolysis temperatures of 300^{o}C, 500^{o}C and 700^{o}C in Section 4.2. The discussion is followed by the results from Stage 2, the batch adsorption study in a multimetal solution in Section 4.3. The results of batch study were discussed according to the adsorption efficiency performance of SMC biochar from multiple pyrolysis temperatures heavy metal removal relative to the values of pH, initial metal concentrations, and time. Next, the adsorption isotherms and kinetics were discussed in detail as well as the mechanism of metal ion adsorption. Finally, the pyrolysis temperature that gives the highest metal adsorption performance was chosen as filter media in column study is discussed in the summary.

4.2 Stage 1 Biochar characterisation with effect of pyrolysis temperature

Characterisation is an essential step in studying biochar properties, as it provides detailed information on the physical and chemical composition of biochar and its correlation with experimental factors such as pyrolysis temperature, pH, time, and initial metal concentration. Limited studies have been conducted to investigate the properties of SMC biochar at different pyrolytic temperatures with the effect of pH and initial metal concentrations. For example, Abdallah et al. (2019a) used SMC biochar prepared at 500°C to remove metal ions in batch and continuous column tests. Meanwhile, corn-cob based biochar prepared at 350^{o}C showed the highest adsorption capacity of Cd from wastewater (Luo et al., 2018b). Consequently, different feedstock and different pyrolysis conditions result in different properties (Li et al., 2019a), hence, in-depth analysis is limited and need to be explored. Therefore, this study provides new insight into the physicochemical evaluation of SMC biochar at different pyrolytic temperatures and investigates which temperature has the highest efficiency in removing heavy metals.

4.2.1 Chemical properties

Chemical properties considered in this study include pH, redox potential, elemental analysis, and biochar yield. Table 4.1 shows the characteristics of SMC biochar from different temperatures (300°C, 500°C, and 700°C) namely B300, B500 and B700 and raw SMC (RS). From the table, it can be observed that the increase in pyrolysis temperatures result in increased pH values of the biochar. For example, B300 is slightly alkaline (8.34) compared to B700, which gives much higher pH values (10.10). Thus, increasing pH values with rising pyrolysis temperatures reflect the abundance of weak bonds within the raw material and its vulnerability to thermal decomposition (Li et al., 2019b). The higher pH is due to the decomposition

of biochar's acidic functional groups (e.g., carboxyl and phenol) and the formation of biochar ash containing alkaline minerals (Zhao et al., 2018). High pH contributes to better heavy metal adsorption by biochar (Mohan et al., 2019). Samsuri et al. (2014) found that a low pH creates a higher hydrogen ion condition which competes with cationic heavy metals for the sorption sites. Besides that, high pH adsorbent can act as an alkalinity generator to increase the acidic pH in acid mine drainage, facilitating the condition for metal removal related to mining water (Muhammad et al., 2017b).

Subsequently, the pH increment is supported by the increasing carbon contents observed from B300 to B500 and B700, with B700 showing the highest (85.69 %) followed by B500 (75.60 %) and B300 showed the lowest with 73.47 %. This shows that the pyrolysis process aids carbon content during heating and decreases O content, decreasing acidity and increasing aromaticity and hydrophobicity. On the other hand, redox potential is a voltage differential that measures a solution's oxidation and reduction potential. The samples above show that all samples have relatively high positive redox measurements, averaging 400 mV to 446 mV. This indicates an oxidation state (the ability to accept electrons from reducing agents such as Fe and Cu) (Hatar et al., 2013) that will promote the ion exchange in heavy metal removal in this study.

The table also shows the yield percentage of biochar, and as temperature increases, the percentage of yield decreases, due to the loss of volatile compounds, which is in good comparison with the previous studies (Oliveira et al., 2017; Pellera et al., 2012).

Table 4.1 Characterisation of SMC biochar in multiple pyrolytic temperatures along with raw SMC (RS)

Sample	pH	Eh (mV)	S_{BET} (m^2g^{-1})	PV (cm^3g^{-1})	Pore size (nm)	Elemental analysis (%)		Yield (%)
						C	O	
B300	8.34	446.20	0.925	0.003	14.86	73.47	16.66	58.22
B500	9.91	443.20	23.95	0.032	5.34	75.60	19.69	28.39
B700	10.10	442.30	247.75	0.139	2.18	85.69	-	25.06
RS	9.48	400.20	0.32	0.003	30.73	70.10	25.08	-

4.2.1.1 FTIR – Active functional groups

One common feature in carbon-rich adsorbents is that they all contain rich surface functional groups crucial for heavy metals adsorption. FTIR spectra that show active functional groups for all pyrolytic temperature biochars are shown in Table 4.2 and Figure 4.1. As observed in Figure 4.2, the functional group decreased gradually when the pyrolysis temperature increased. In B300, a wideband at 3400 cm^{-1} is attributed to a hydroxyl group (-O-H); however, it gradually decreased and disappeared in B500 and B700.

This is due to the disintegration of organic fatty hydrocarbons and alteration into aromatic structures with the increasing pyrolysis temperature (Chen et al., 2019). Subsequently, vibration bands at 1614 cm^{-1} correspond to the stretching of C=C and C=O groups, which decreased in B500 and disappeared in B700. However, the peaks between 1500 and 800 cm^{-1} represent aromatic carbon typically found in these biochars. The peaks between 1440 and 1300 cm^{-1} show aromatic structures (C=O and C-H) enhanced as pyrolysis temperature increases. With higher temperatures, these raw materials decomposed and were

replaced with a more active aromatic functional group, resulting in the enhancement of peak at 1440 to 1300 cm^{-1} in B700 compared to B500 (Shen et al., 2019).

The peak at 1080 cm^{-1} shown in all biochars is attributed to the stretching of carboxyl C-O bonds, which originated from cellulose, hemicellulose, and lignin (Wang & Liu, 2017). In summary, at low pyrolysis temperature, B300, hydroxyl functional groups took over however as pyrolysis temperature increases, these hydroxyl functional groups disappear and are replaced with aromatic functional groups available in B500 and B700 as shown in Table 4.2. Literatures stated that as pyrolysis temperature increases, better adsorption of heavy metals took place. The biomass became completely carbonised at higher temperature, surface area greatly improved, thus providing more active sites for metal adsorption and contains active functional groups for metal exchange. These results indicated that SMC derived biochar has the potent adsorption ability to remove heavy metals (Daghbandan et al., 2022).

Table 4.2 Active functional groups available in SMC biochar

SMC biochar	Wavelength (cm^{-1})	Functional group
B300	3400	O-H (hydroxyl)
	1614	C-C C-O (carboxyl)
	1080	C-O (carboxyl)
B500	1080	C-O (carboxyl)
	1500-800	C=O (carboxyl) C=H (aromatic)
B700	1080	C-O (carboxyl)
	1440 - 300	C=O (carboxyl) C=H (aromatic)

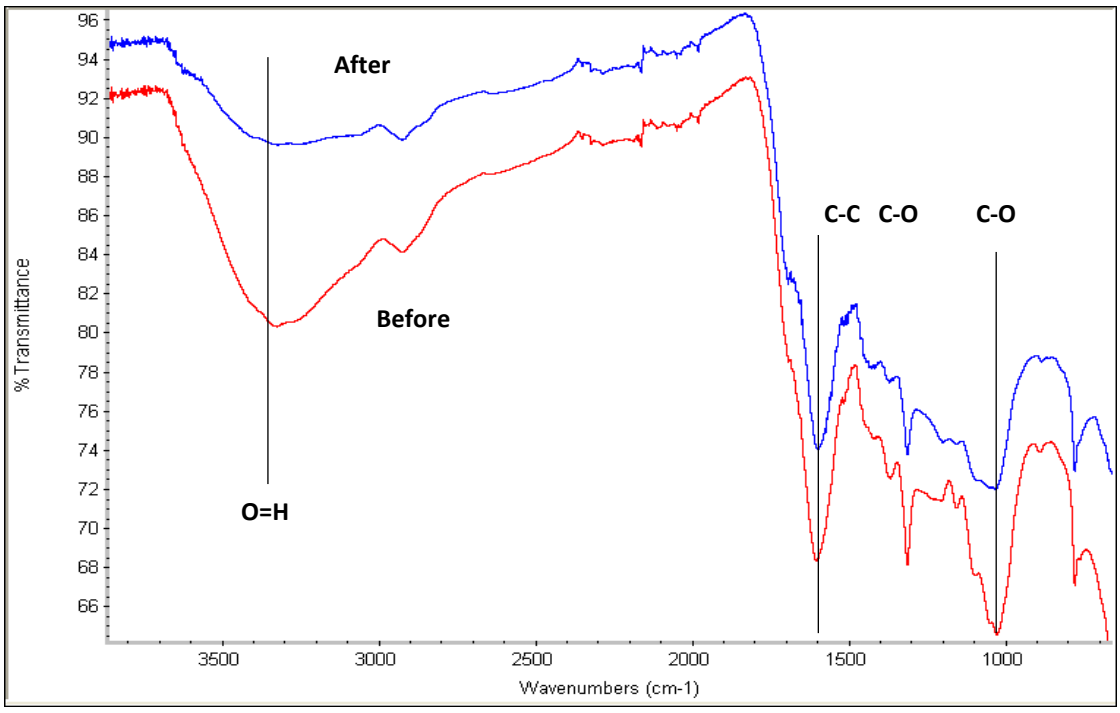
After
Before
O=H
C-C
C-O
C-O
% Transmittance
Wavenumbers (cm-1)

(a)

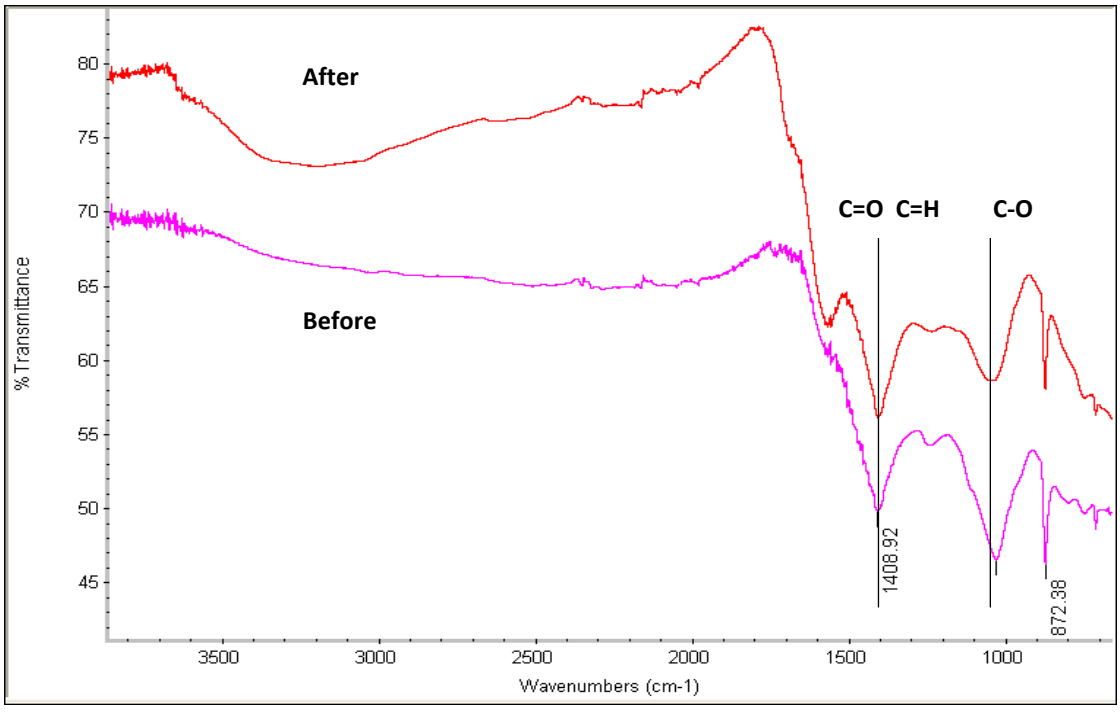
After
Before
C=O
C=H
C-O
1408.92
872.38
% Transmittance
Wavenumbers (cm-1)

(b)

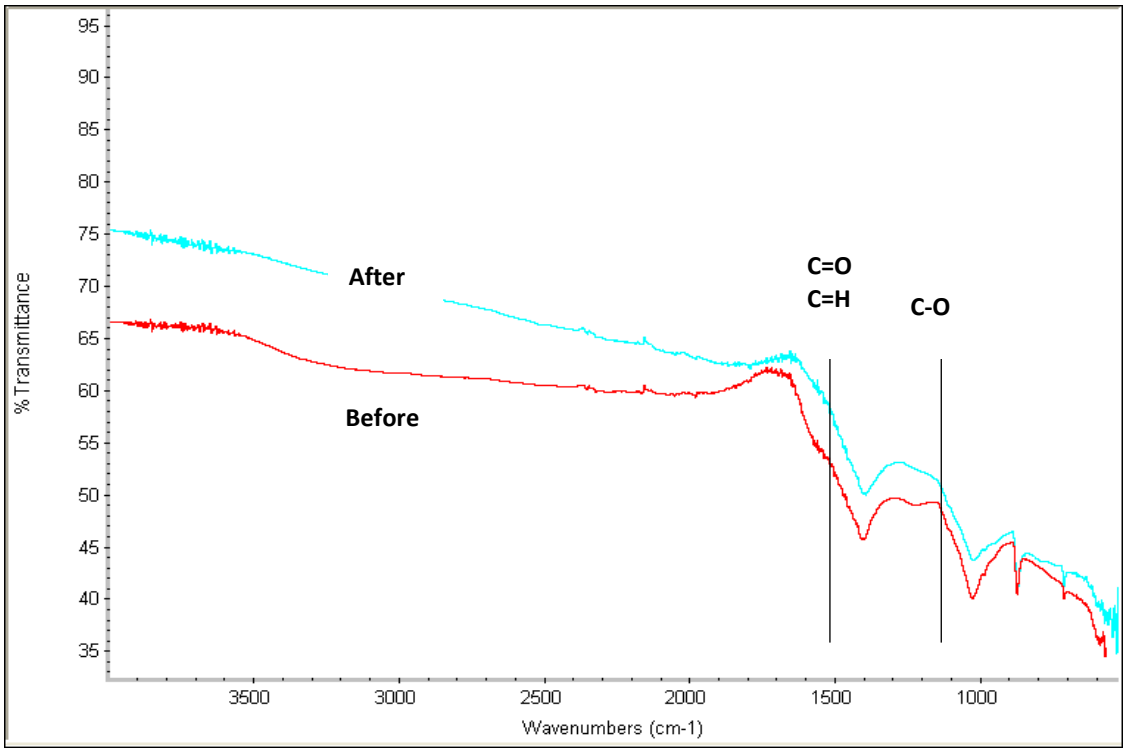

(C)

Figure 4.1 FTIR spectra of (a)B300, (b) B500 and (c) B700 before and after adsorption

4.2.2 Physical properties

4.2.2.1 BET – surface area

Another factor that can be observed in Table 4.1 is the BET surface area of SMC biochars. The surface area was significantly affected by multiple pyrolysis temperatures. As pyrolytic temperature increases, the surface area of samples increases. This condition is similar to previous studies using agricultural waste biochar (Zhang et al., 2011; Shen et al., 2019).

The specific surface area and pore volume are among the most crucial morphological properties for heavy metal removal (Ding et al., 2014) and were measured using the BET method. The surface area of B300 was relatively low, 0.972 m^2/g; however, it climbed to 23.95 m^2/g at B500 and exponentially increased to 247.75 m^2/g for B700. Particularly, the surface area of B700 is reportedly higher than those by modified biochars (Wu et al., 2019a). This increment in the surface area suggests that pores in biochar gradually developed with increased production temperature observed in previous studies for other biochar (Shen et al., 2019). When the pyrolysis temperature rises, lignin decomposition generates significant densities of micropores and a large number of pores, indicating a reasonable possibility of heavy metal adsorption in these pores (Chen et al., 2019). However, it is interesting to note that a significant decrease in pore size occurred with increased production temperature. This shows that the amount of mesopore and macropore volume decreased while the amount of micropore volume increased. Although mesopores and macropores are important to help pollutants to diffuse into the biochar particles, increases in micropores will increase surface area to promote physical adsorption.

4.2.2.2 FESEM – surface morphological structure

The morphological properties of SMC biochars is further strengthened by the FESEM micrographs in Figure 4.2, which shows the morphological structure of macropores a micron scale. The SEM images in all temperatures show that the porous image is available in B300 but not as much in B500 and B700. On the other hand, as the temperature increases, the macropores formation is present in B500 and B700 where the rod like structures and vertical channels contributed towards the BET surface area expansion and the mesopores is transformed into macropores. The difference in porous structure in RS is shown where the porous structure is not as much in the raw materials as in biochar form. These observations are in line with the literature – that the pyrolysis process into biochar result in decomposition of cellulose, hemicellulose and other components hence increasing the porous structure in biochar (Joseph et al., 2019b; Pullammanappallil et al., 2015).

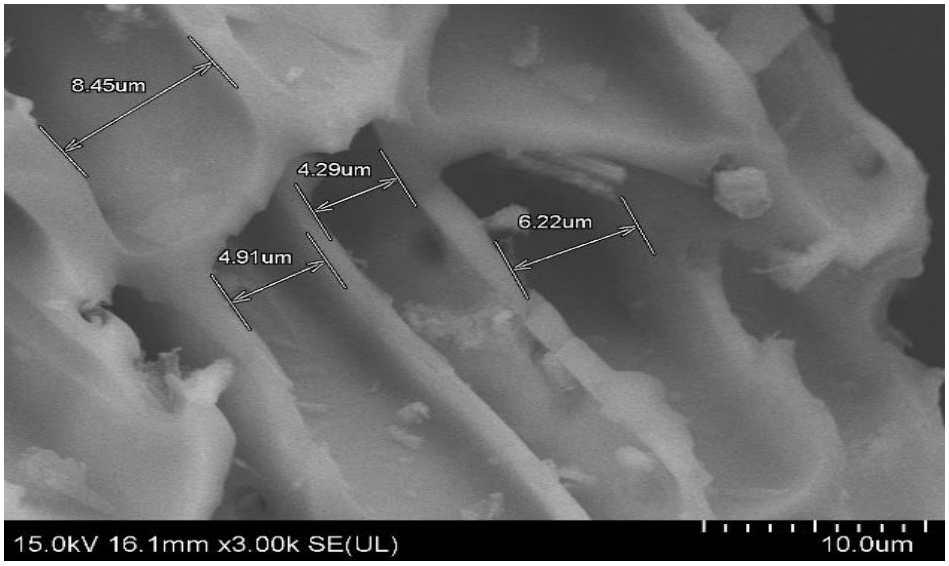

(a)

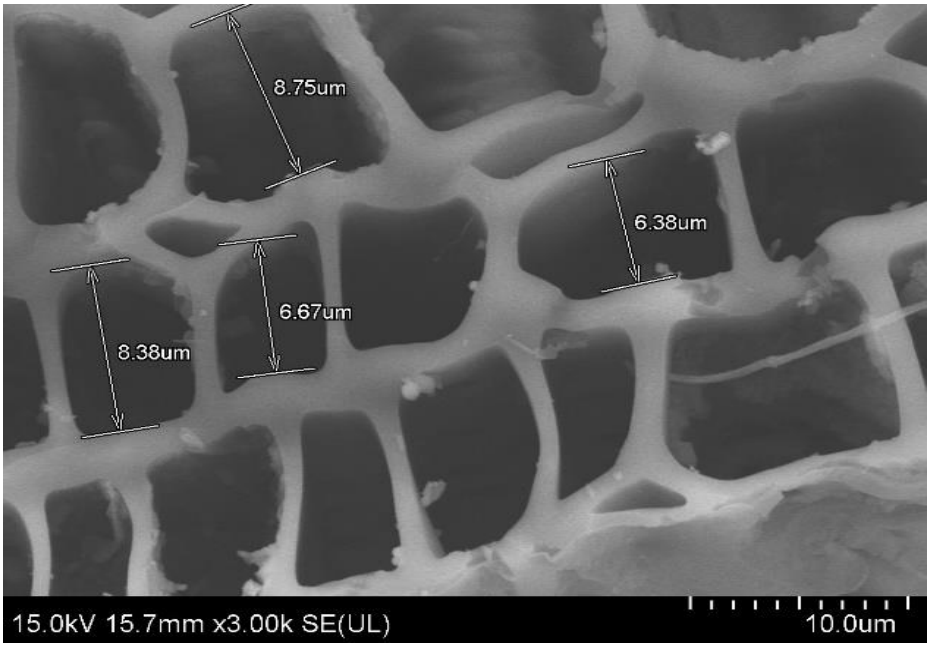
8.75um
6.38um
6.67um
8.38um
15.0kV 15.7mm x3.00k SE(UL)
10.0um

(b)

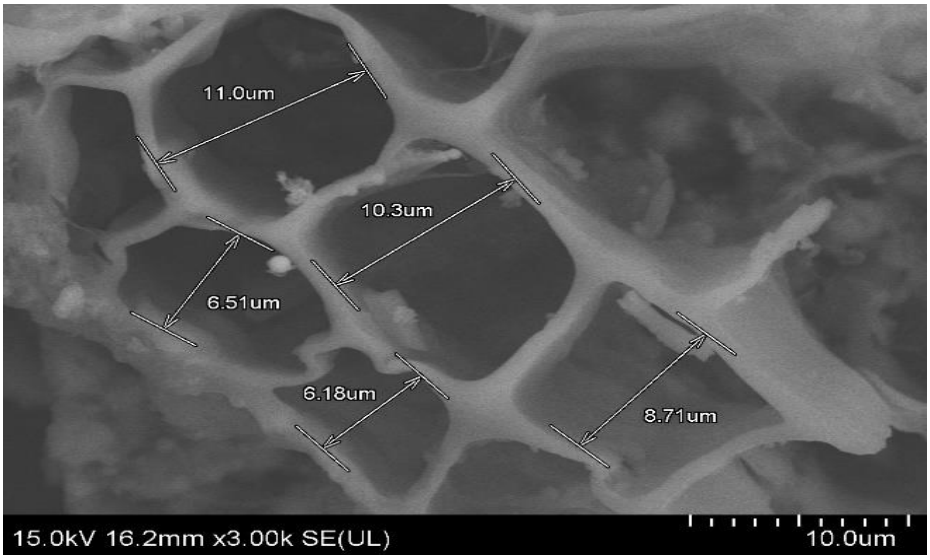
11.0um
10.3um
6.51um
6.18um
8.71um
15.0kV 16.2mm x3.00k SE(UL)
10.0um

(c)

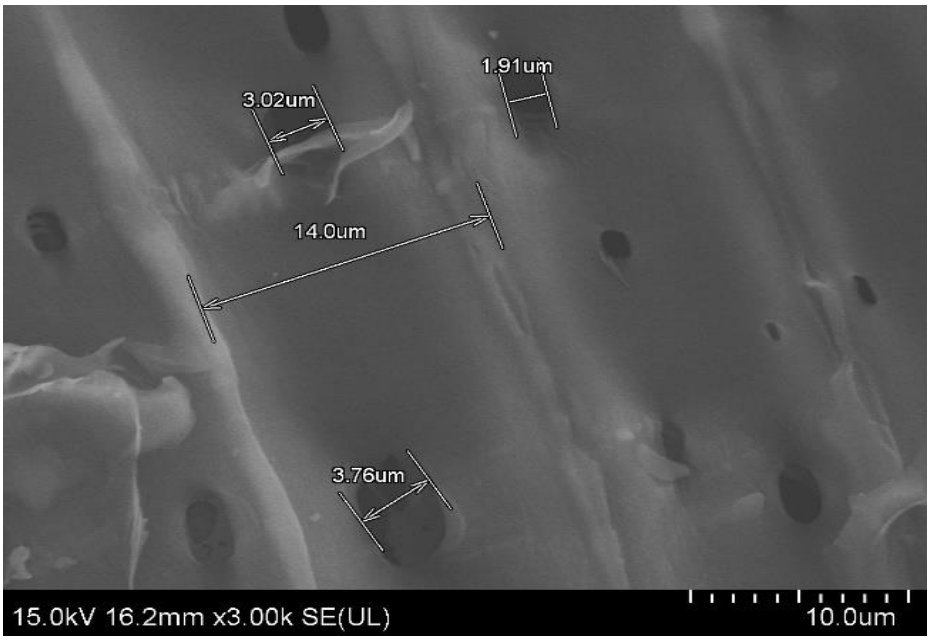

(d)

Figure 4.2 FESEM images of SMC biochars namely (a) B300, (b) B500, (c) B700 and (d) RS

The surface area and pore volume of biochars are essential features affecting the adsorption and retention properties of the materials. Masebinu (2019) found that adsorbate uptake into biochar relies on the accessible volume of micropores and the surface area of the biochar. Hence higher pore volume shown by B500 and B700 showed the potential to increase adsorption performance.

4.3 Stage 2 Batch adsorption study

4.3.1 Adsorption efficiency performance of SMC biochar – percentage removal of heavy metals at different pyrolysis temperature

The feasibility of biochars adsorption pyrolyzed at different pyrolytic temperature was demonstrated in the percentage of removal and FTIR spectra as illustrated in Figure 4.3 and Figure 4.1 respectively. In Figure 4.3, all SMC biochars with raw SMC (RS) as control were assessed in different initial metal concentration, and their removal percentage were calculated. Overall, it is clear that different pyrolytic temperature gives different average removal percentage where the trend for all initial metal concentrations are: B700 > B500 > B300 > RS for all metal ions with average removal percentage of 98.38 %, 97.43 %, 87.11 % and, 66.33 % respectively. Hence the pyrolysis temperature has a vital influence on the metal adsorption behavior of the biochars. Notably, as pyrolysis temperature increased, the BET surface area and pore volume increased, promoting a higher metal removal efficiency (Jin et al., 2020). The specific surface area and pore volume are the most crucial morphological properties for heavy metal removal (Chang et al., 2020b).

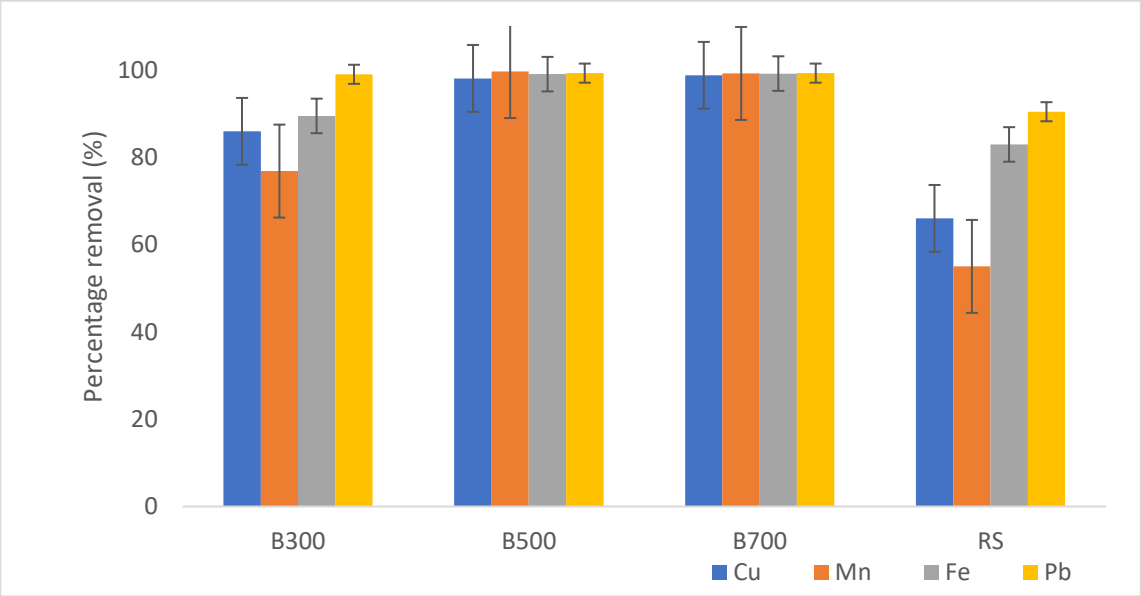
Percentage removal (%)
100
80
60
40
20
0
B300
B500
B700
RS
Cu
Mn
Fe
Pb

(a)

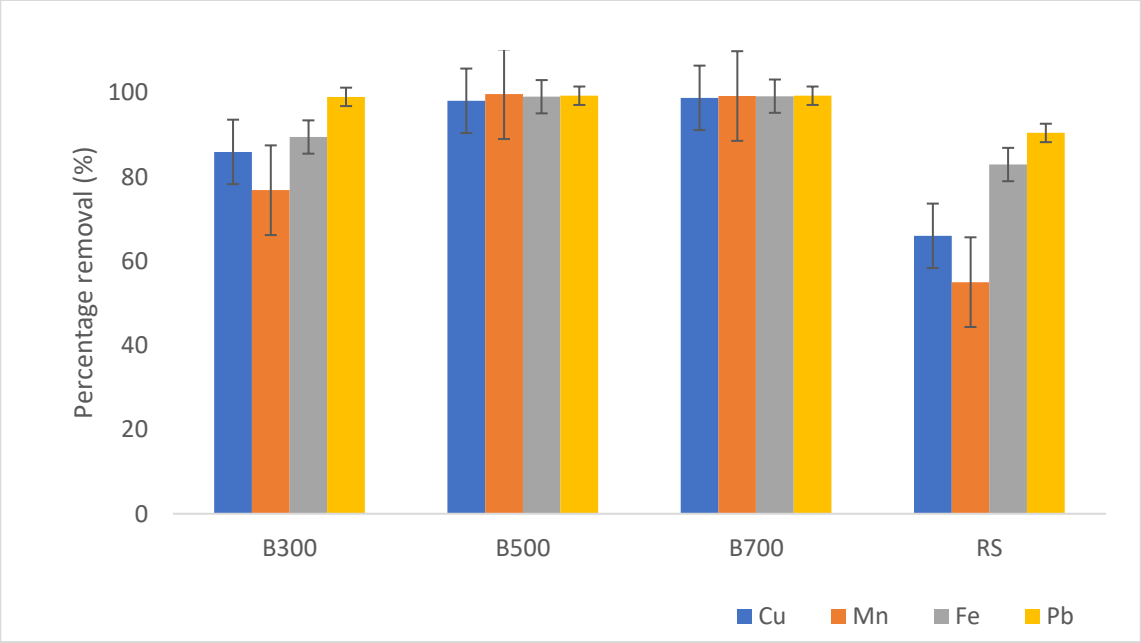
Percentage removal (%)
100
80
60
40
20
0
B300
B500
B700
RS
Cu
Mn
Fe
Pb

(b)

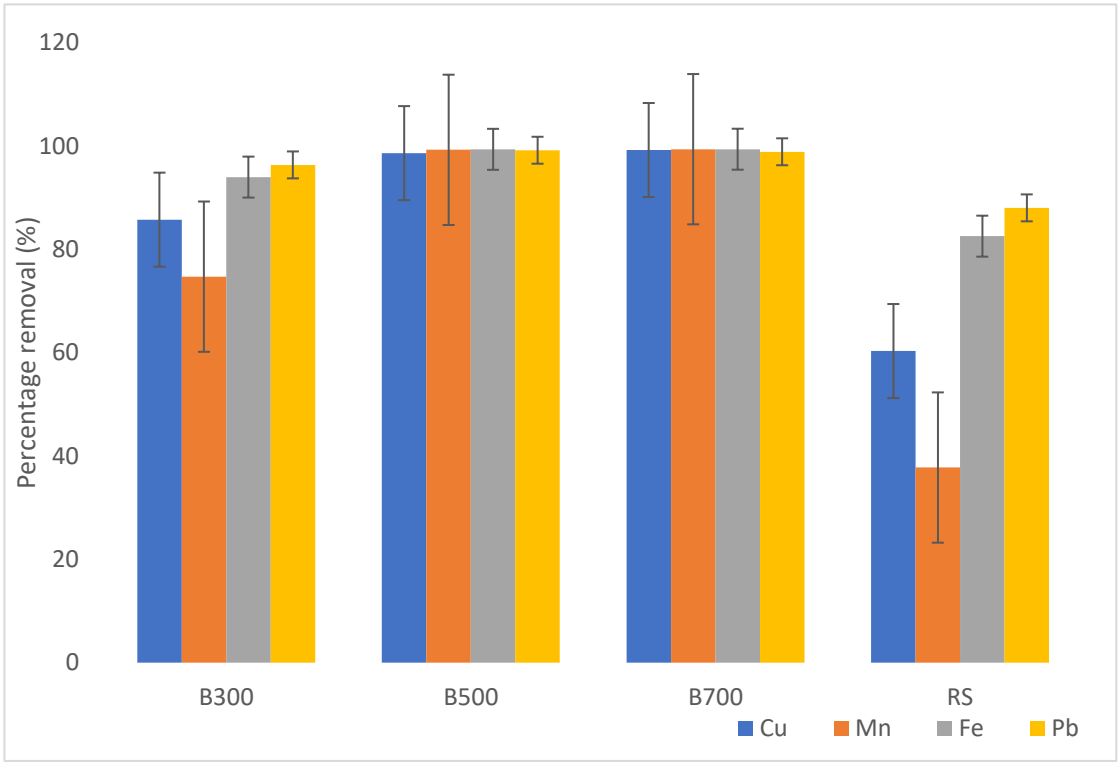
120
100
80
60
40
20
0
Percentage removal (%)
B300
B500
B700
RS
Cu
Mn
Fe
Pb

(c)

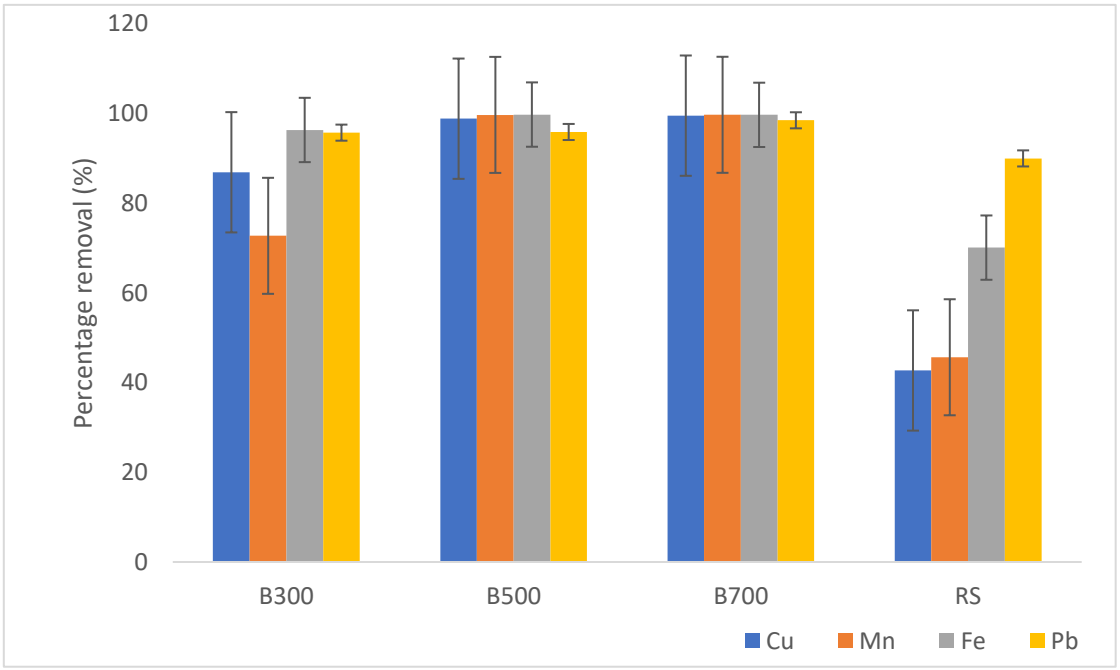
120
100
80
60
40
20
0
Percentage removal (%)
B300
B500
B700
RS
Cu
Mn
Fe
Pb

(d)

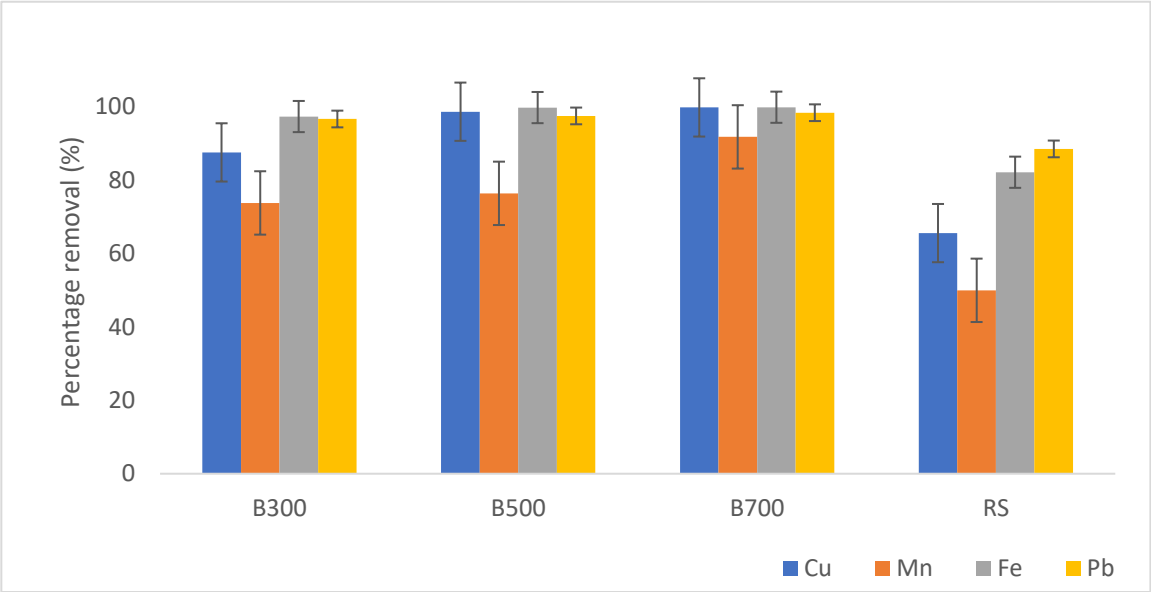

(e)

Figure 4.3. Percentage removal of SMC biochar at different pyrolysis temperature at (a) 1 mg/L, (b) 3 mg/L, (c) 5 mg/L, (d) 10 mg/L and (e) 30 mg/L

Conversely, carbon-rich adsorbents contain rich surface functional groups, which are essential for the surface chemical reaction to take place and the adsorption of heavy metals (Yang et al., 2019). This functional group can be enhanced by chemically and physically modifying the surface of the materials to introduce the desired heteroatoms on surface materials. The surface functional group analysis can be explained through the FTIR spectra in Figure 4.1. Subsequently, it is noticeable that the intensity and wavenumbers have changed before and after batch adsorption. Some peaks shifted and some are weakened or enhanced. From the spectra in Figure 4.1a, the intense heavy metal adsorption bands have weakened the strong hydroxyl band of B300 at 3400 cm^{-1}, and a similar situation occurred at all wavelengths.

This shows that at low temperature biochar, most of the available binding sites were used by metal ions for coordination and ion exchange mechanisms (Abdallah et al., 2019b). It means that the mechanism of metal sorption is consistent with the FTIR analysis, where oxygen-containing groups in B300 aid the ion exchange mechanism. Conversely, higher temperature biochar (B500 and B700), contains more aromatic structure functional groups that provides π-electron and promotes π-complexation mechanism. For example, in B500 and B700, as the C-H stretching became weakened at 1400 cm^{-1}, it shifted into an M-C bond which could be metal-methylidyne (MCH) or methyl-metal (MCH3), depending on the ligand attached to the carbon atom. The disappearance of weakening peak demonstrates a high sorption effect where chemical interactions have taken place between heavy metal ions and the functional group on the surface of the adsorbent during adsorption.

Notably, in this research, B700 showed the highest removal percentage of all metal ions, averaging at 98.38 %. Significantly, at high pyrolysis temperatures, the aromatic structure provides π-electron, which were suggested to create a strong bond with heavy metal cations hence causing the high removal percentage (Chen et al., 2019). However, it is essential to note that B500 showed the second highest removal rate with an average of 97.43 %, very close to B700. It is noteworthy to observe that B500 resulted in high removal percentage even though the BET surface area is much smaller than B700. Significantly, B500 also contains aromatic functional groups that create strong chemical π complexation on the surface of biochar which could be the primary removal mechanism in B500. Subsequently, B300 (average 87.11 %) came third in the percentage of removal. Although B300 has a hydroxyl functional group, it has the smallest surface area compared to B500 and B700. Finally, the raw SMC removed the least with an average of 66.33 %. This is an important discovery to confer that biochar derived from raw material through thermal conversion has proven to be more effective in removing heavy metals than using raw materials adsorbents. This process enhances the surface area of biochar and provides multiple active

functional groups to create active adsorption sites. Therefore, the metal ions adsorption performance of biochar is highly influenced by both physical and chemical properties.

4.3.2 Adsorption efficiency of SMC biochar in the removal of heavy metals – effect of pH

The batch adsorption study involves studying the effect of initial pH on the synthetic mine water to mimic actual events. In this study, 4 ranges of pH from acidic to alkali namely pH 2,4,6,8 and 10 were chosen to emulate the pH of real case studies in Malaysia. A few studies found cases of abandoned mining ponds to be acidic due to high heavy metals deposition in the ponds (Hamzah et al., 2018; Koki et al., 2018; Takaijudin et al., 2012; Wan Yaacob et al., 2009). Hence it is important to establish the influence of pH for the adsorption process as the first step for reference in real-life applications in the future.

Figure 4.4 shows the overall adsorption capacity of Cu, Fe, Mn, and Pb using B300, B500, and B700 biochars from different pH with raw SMC (RS) as control samples. In particular, the adsorption capacity trend was similar for all 4 biochars with increasing pH. pH 2 showed increasing trend, however not so much in Mn. Nonetheless, pH 4 shown improved adsorption process and eventually adsorption increased rapidly in pH 6,8 and 10. Overall, B500 and B700 showed high removal efficiency, with 76-99 % for B500 and 86-99 % for B700, followed by 60-90 % removal by B300. The highest adsorption capacity for Pb (II) is 2.997 mg/g in B500 at pH 6 ($R^2 = 0.894$, $p < 0.05$). While Fe is 2.98 mg/g in B700 at pH 6 ($R^2 = 0.947$, $p < 0.05$), Mn is 1.93 mg/g in B700 at pH 6 ($R^2 = 0.965$, $p < 0.05$) and Cu is 2.95 mg/g in B500 in pH 6 ($R^2 = 0.875$, $p < 0.05$). These values revealed that SMC biochar's removal efficiency increased with pyrolysis temperatures. From this study, it can be concluded that all pH can remove the proposed heavy metals. However, the highest adsorption capacity occurred at pH = 6. When pH is subsided, metal adsorption is

relatively low due to the protonation state of biochar, where hydrogen ions are available and tough competition with positively charged metal ions for an ion exchange mechanism (Abbas et al., 2016).

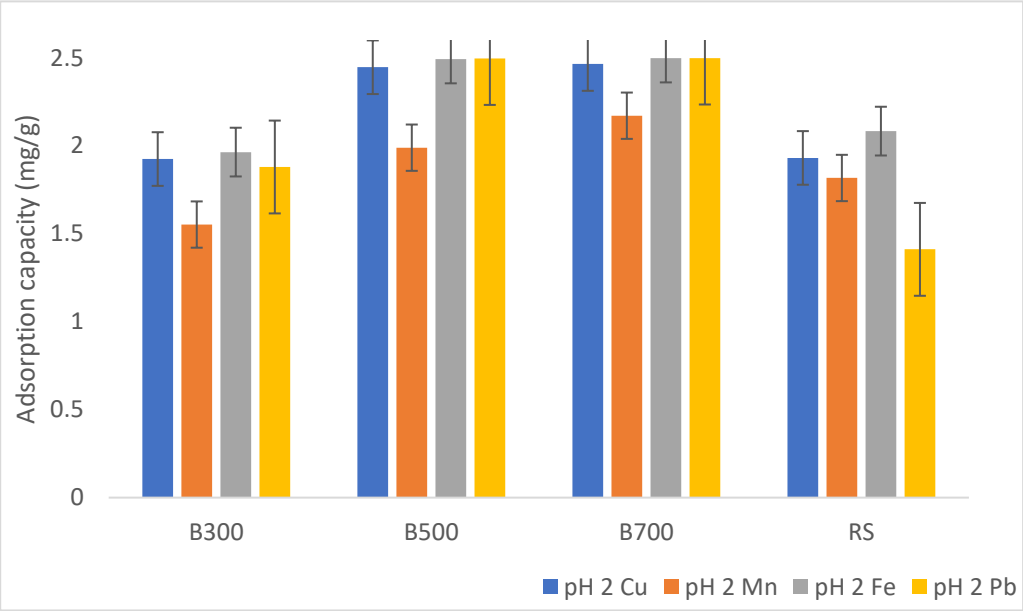

(a)

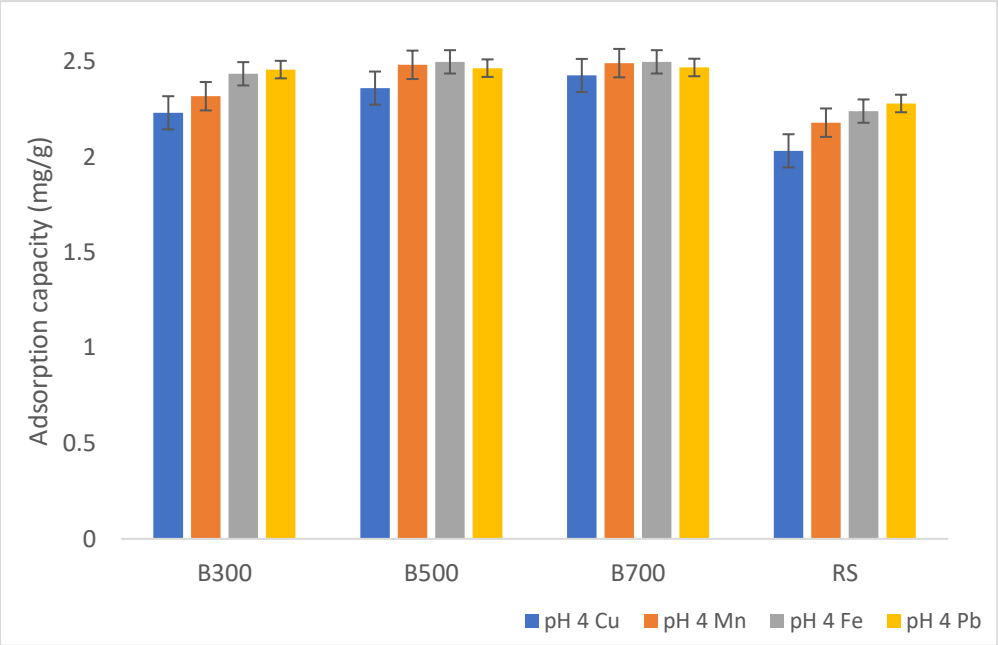
2.5
2
1.5
1
0.5
0
Adsorption capacity (mg/g)
B300
B500
B700
RS
pH 4 Cu
pH 4 Mn
pH 4 Fe
pH 4 Pb

(b)

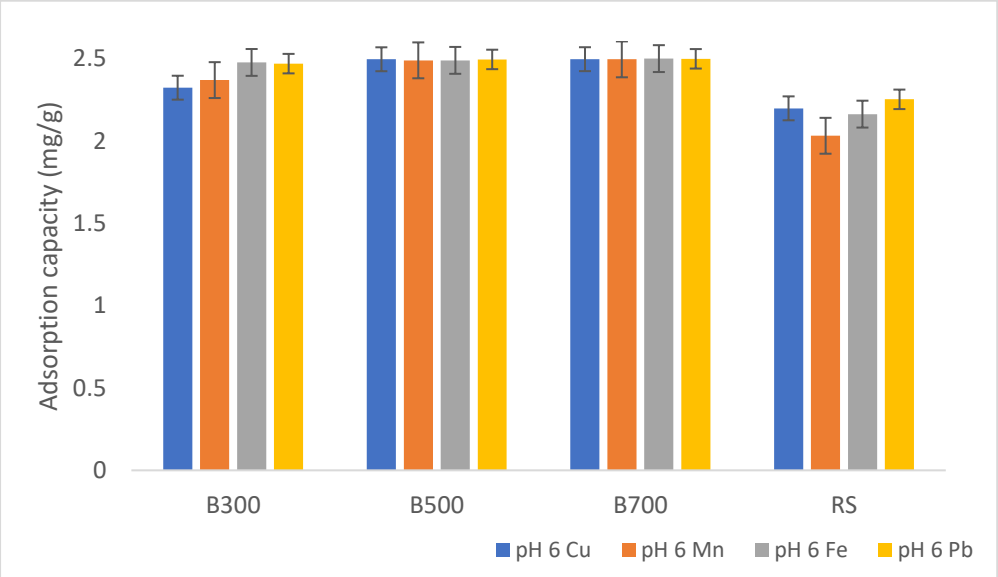
2.5
2
1.5
1
0.5
0
Adsorption capacity (mg/g)
B300
B500
B700
RS
pH 6 Cu
pH 6 Mn
pH 6 Fe
pH 6 Pb

(c)

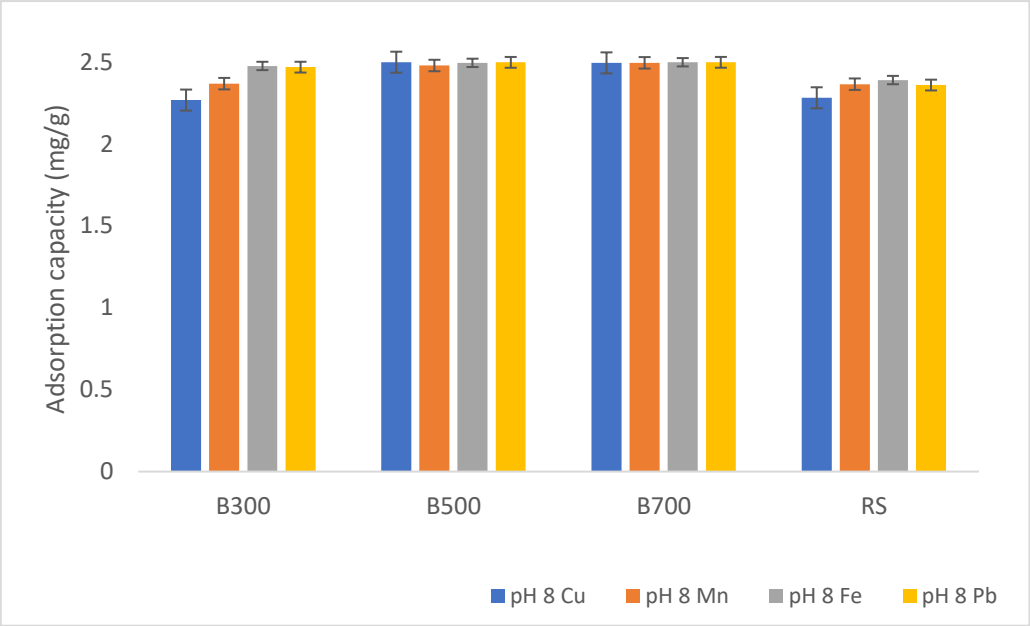

(d)

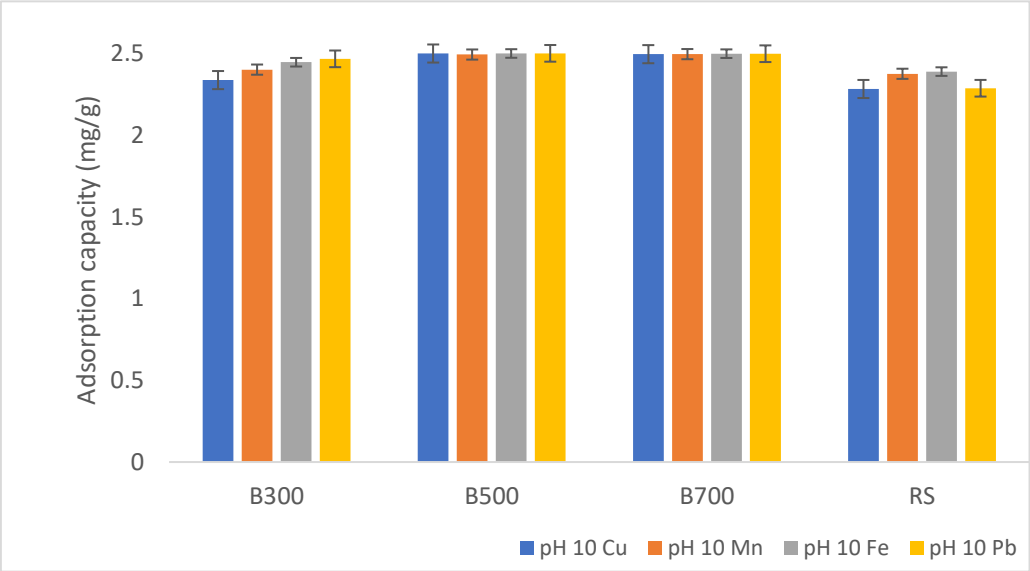

(e)

Figure 4.4 Relationship between adsorption capacity (mg/g) and (a) pH 2, b) pH 4, (c) pH 6, (d) pH 8 and (e) pH 10 for all heavy metals

However, at low initial pH values, metal removal took place through precipitation process where the cation precipitated to form metal hydroxide and slowly increased the pH from 2 to 10.34, an indication that precipitation took place (Abdallah et al., 2019b). Albeit, as precipitation occurs, the metal hydroxide will be the dominant species, which lowers the interactions between cations in the solution and the surface of biochar, decreasing adsorption capacity (Jin et al., 2018b).

Conversely, the escalating in pH is associated with the dissolution of mineral solids in SMC biochar. Hence, SMC biochar can also act as pH generator and remove heavy metals. Subsequently, at rising initial pH, deprotonation takes place, where hydrogen ions are low and liberates more binding sites and solid electrostatic attraction between positive metal ions and biochar surface; and these leads to increased adsorption. According to research, pH 3-6 has been found favourable for adsorption using biochar as the adsorbent charge changed from positive to negative thus enhancing ion exchange ability and favored metal adsorption as proven by the highest adsorption capacity of Fe at pH 6. At pH > 6, negative charges increased, making more negative sites available. This led to increased adsorption as electrostatic attraction increased, and OH- presence encouraged adsorption (Nworie et al., 2019).

In contrast, SMC biochar showed high adsorption capacity of Pb (II), Mn (II), and Cu (II) at pH > 8 as well. This may be due to the formation of metal precipitates, which should be distinguished from adsorption and avoided during experiments as the accumulation of metal hydroxide can lead to the exhaustion of biochar (Jin et al., 2021). Contrarily, precipitation often works with other mechanisms, such as electrostatic interaction (Yang et al., 2019). It is interesting to note that high adsorption could be due to the high surface area of SMC biochar. It promotes electrostatic interactions with the metals (23.95- 345.81 m^2g^{-1}) as compared to other biochar such as mushroom stick biochar 67.89 m^2g^{-1} (Chen et al., 2019),

sugarcane bagasse biochar 17.7 m^2g^{-1} (Inyang et al., 2011) and rice husk biochar at 29.18 m^2g^{-1} (Chen et al., 2019). The high surface area made more binding sites available for adsorption capacity. Raw SMC shows a low adsorption capacity that showed good adsorption capacity but not as high as using SMC biochar as imposed from Figure 4.4a at pH 2 and 4.4e at pH 10.

4.3.3 Adsorption kinetics

A kinetic investigation was carried out to quantify the adsorption rate. The adsorption rate and dynamic behaviour are crucial factors in assessing the rate limiting step and contact time required for the adsorption mechanism in biochar. Biochar prepared from different pyrolysis temperature have different structures and characteristics. The study lasted for 24 hours to assess the adsorption kinetics (Liu, 2018; Luo et al., 2019). Two of the most frequently used models, the pseudo-first-order (PFO) and pseudo-second-order (PSO) kinetic models were applied for the kinetic study. The PFO model is based on assumption that the adsorption rate is controlled by the diffusion of adsorbate (Ighalo et al., 2020). The PSO model is based on the assumption that the rate-limiting step is from chemical adsorption due to adsorption interactions on the surface.

Table 4.3 shows the comparison between adsorption rate constants, the estimated adsorption capacity, q_{max}, and the coefficients of correlation associated with the kinetic models for SMC biochar with the best-fitting model having the highest correlation factor (R^2). From the table shown, it is evident that both models well describe the metal adsorption. The coefficients of correlation (R^2) of the PSO kinetic model were higher than PFO ($R^2 > 0.999$) for all metals and more accurately described the kinetic adsorption process. The PSO model assumes that the sorption is controlled mainly by the chemisorption process,

where chemical reactions (valence forces) that occur as a result of sharing or exchanging electrons between sorbents and sorbates. This is similar to other kinetic studies using other biochar sorbents (Esfandiar et al., 2022).

Table 4.3 Comparison of each metal between PFO and PSO models of B300, B500 and B700

		Pseudo-first-order (PFO)			Pseudo-second-order (PSO)		
Heavy metals	Biochar	k^2 (min^{-1})	qe (mg/g)	R^2	k^2 (g/mg min)	qe (mg/g)	R^2
Cu	B300	0.070	2.171	0.799	2.876	2.478	0.999
	B500	0.020	2.469	0.753	3.869	2.573	0.999
	B700	0.034	2.486	0.998	6.102	2.493	0.999
	RS	0.026	1.067	0.999	5.037	1.334	0.999
Mn	B300	0.056	1.817	0.688	2.322	1.944	0.999
	B500	0.036	2.490	0.734	0.558	1.522	0.999
	B700	0.061	2.491	0.994	2.279	1.494	0.996
	RS	0.051	1.140	0.998	35.177	1.103	0.999
Pb	B300	0.052	2.391	0.732	4.689	2.486	0.995
	B500	0.491	2.395	0.978	10.073	2.490	0.999
	B700	0.083	2.460	0.825	27.318	2.490	0.999
	RS	0.836	2.248	0.987	1.559	1.316	0.999
Fe	B300	0.943	2.406	0.794	7.937	2.398	0.886
	B500	0.641	2.492	0.890	21.798	2.396	0.999
	B700	0.558	2.491	0.795	10.263	2.464	0.999
	RS	0.023	1.751	0.982	3.905	1.874	0.999

The nonlinear forms of PSO kinetic models are represented in Figure 4.5 and Figure 4.6 by plotting q vs t. It can be seen that metal sorption by the biochars varied with time and was affected by pyrolysis temperatures. The trends for the four types of biochars are similar and occurred in two steps. First, at time 0 – 1 hour, the plot shows a sharp increase in the adsorbed amount. At this initial phase, all active

sites were available hence the adsorption rate was high. However, the adsorption rate slowed down and turned into plateau state when equilibrium was reached. All biochar portrayed fast sorption for all metals with equilibrium at approximately 60 minutes. In addition, Figure 4.6 shows the kinetic plots for all biochars in PFO and PSO model and apparently PSO model fit better than the PFO model, hence PSO is favoured.

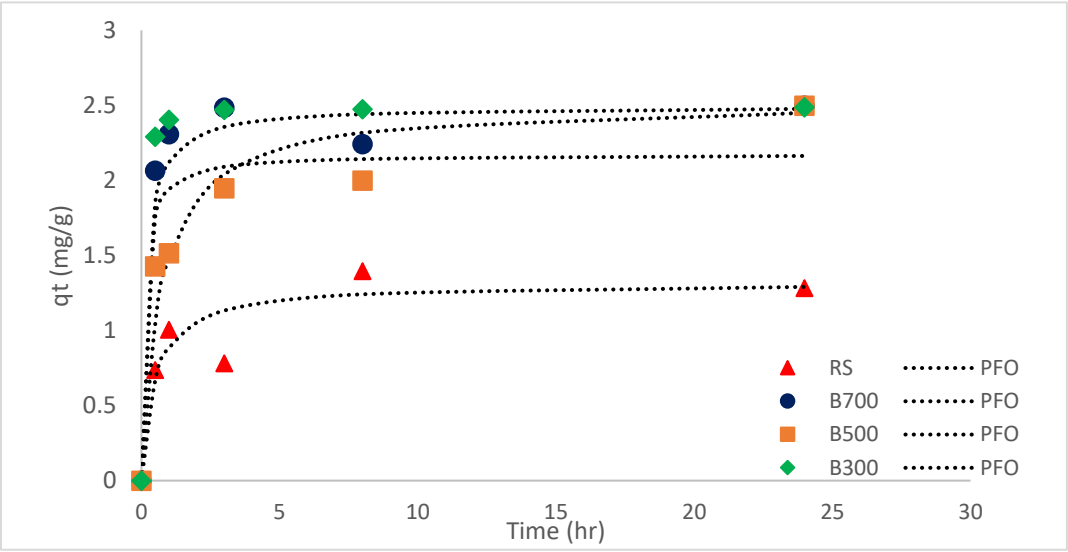

(a)

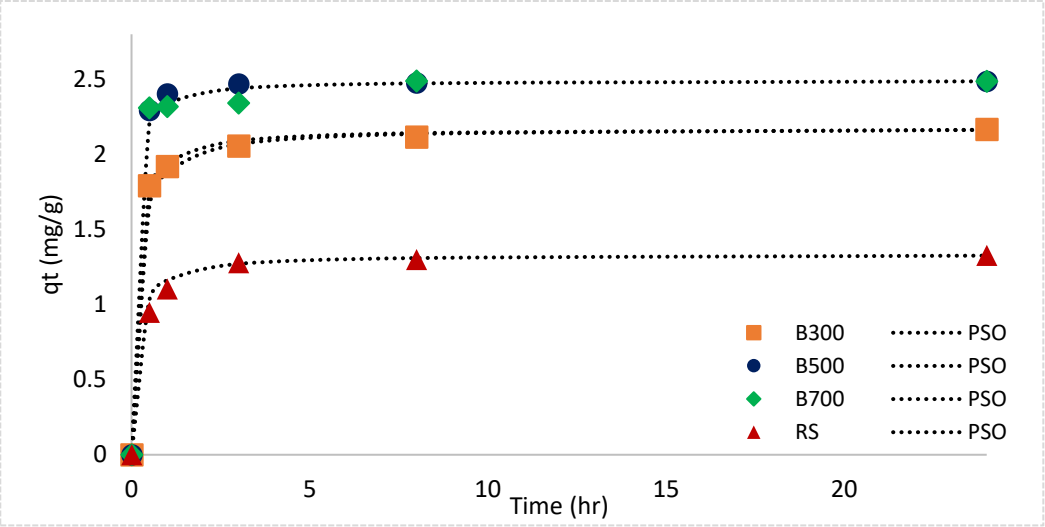

(b)

Figure 4.5 Kinetic models for Cu adsorption onto four type of biochars (a)PFO model, (b) PSO model

This is supported with the high correlation coefficient (R^2) of PSO in Table 4.3. The adsorption capacities of biochar to adsorb all metals are ranked in the following order B700 > B500 > B300 > RS. B700 exhibited the highest adsorption capacities with the highest q_{max} of Pb (2.490 mg/g) and Fe (2.464 mg/g). It is interesting to note that B500 gave a comparative result to B700 despite its small surface area. Therefore, chemical sorption interaction is the dominant factor in the adsorption mechanism. B500 showed the highest adsorption capacity of Cu (2.573 mg/g), Mn (1.522 mg/g) and Pb (2.490 mg/g). Nonetheless, B300 showed competitive result in Mn and Pb with B500 and B700 but not in Cu and Fe. This could be due to the interaction between Mn and Pb ions with the hydroxyl functional groups available in B300. Conversely, RS showed the lowest adsorption capacity for all heavy metals.

This may be due to it having the lowest surface area with no active functional groups available hence it is easily exhausted once the metal ions are adsorbed on the surface. In addition, the experimental removal efficiency is much closer to PSO, suggesting the rate-limiting step of chemisorption (Chen et al., 2021). Thus, the overall mechanism of adsorption was mainly controlled by chemical process than physical processes. This can be proven from the FTIR result before and after adsorption, where surface modification of biochar after adsorption occurred.

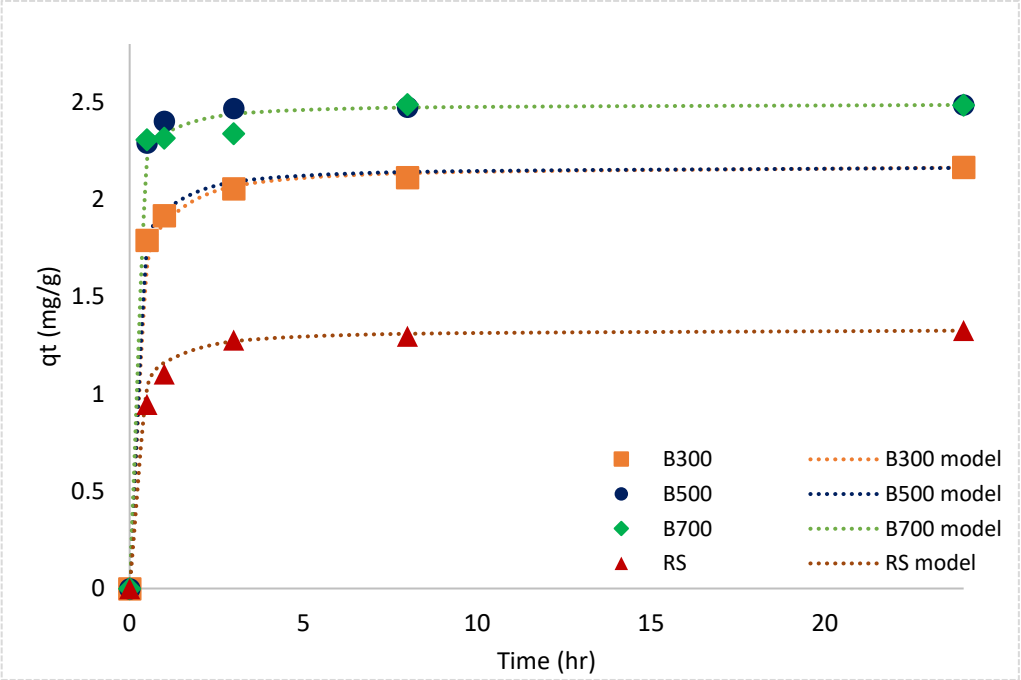

(a)

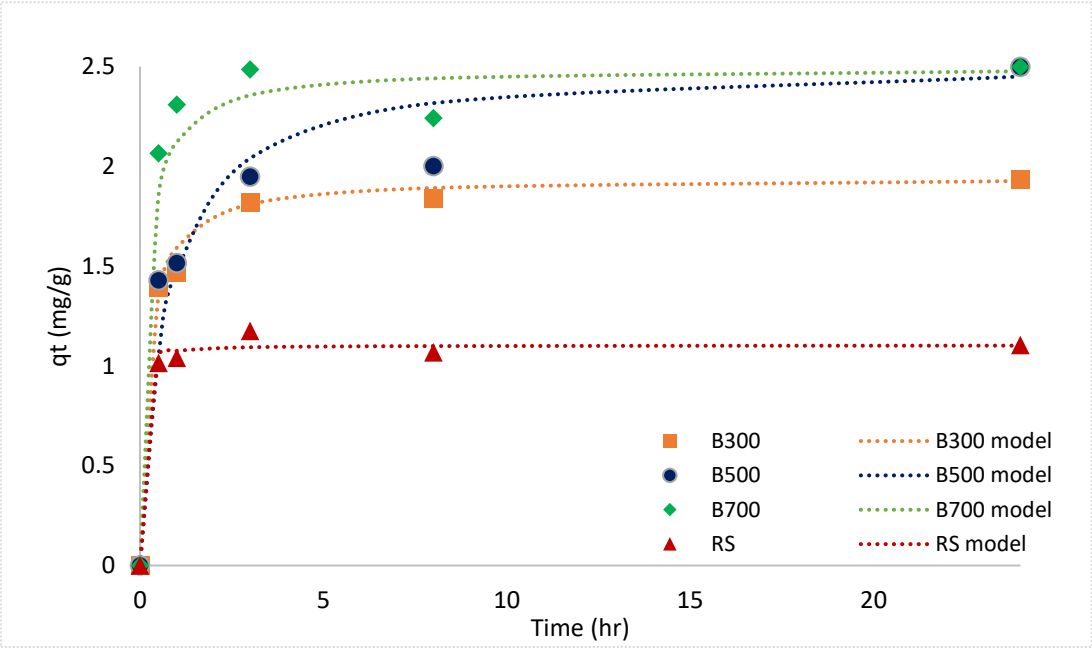
2.5
2
1.5
1
0.5
0
qt (mg/g)
0
5
10
15
20
Time (hr)
B300
B500
B700
RS
B300 model
B500 model
B700 model
RS model

(b)

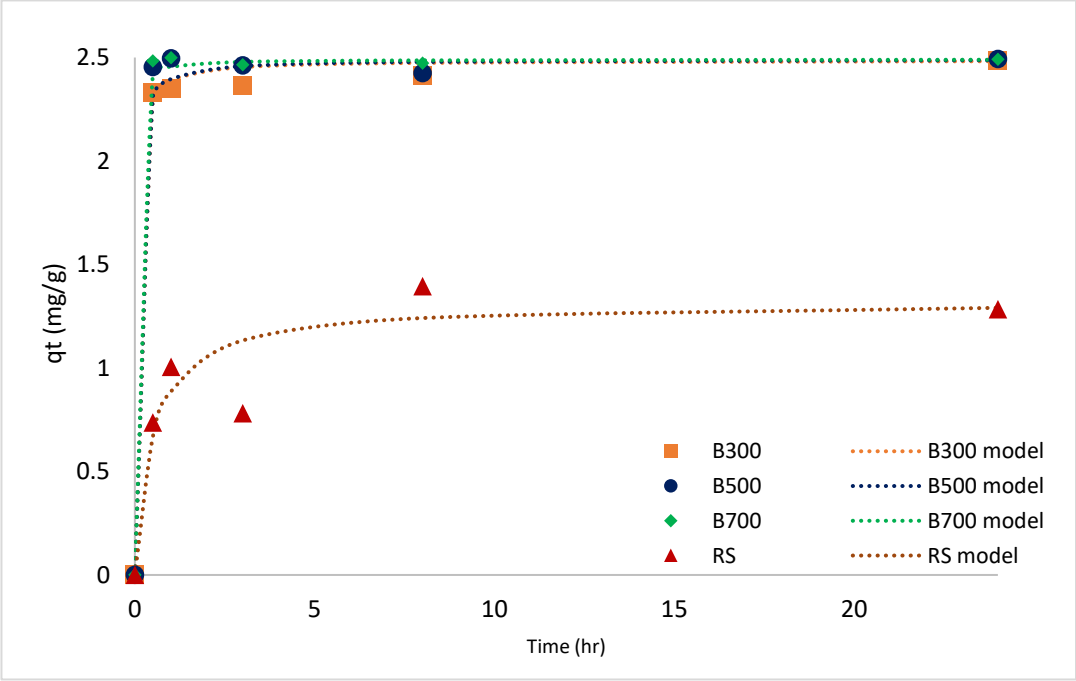
2.5
2
1.5
1
0.5
0
qt (mg/g)
0
5
10
15
20
Time (hr)
B300
B500
B700
RS
B300 model
B500 model
B700 model
RS model

(c)

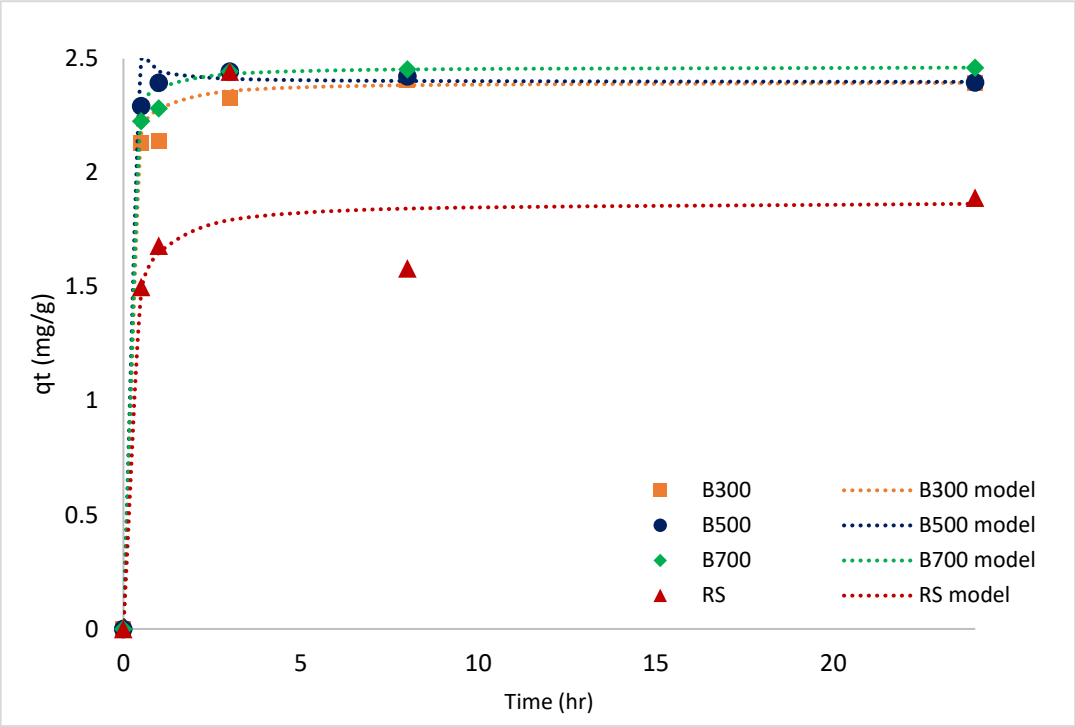

(d)

Figure 4.6 Nonlinear plot of PSO for adsorption capacity of (a) Cu, (b) Fe, (c) Mn and (d) Pb

4.3.4 Adsorption isotherms

Initial metal concentration is vital in adsorption efficiency as it determines the performance of a potential biosorbent and its feasibility in heavy metal adsorption. The initial metal concentrations analyses are better explained through adsorption isotherms. For adsorption isotherms, three types of isotherms adopted were the Langmuir, Freundlich and Temkin models. The Langmuir model promotes monolayer adsorption that assume all adsorption sites have the same adsorption energies with no mutual interactions with the adsorbed ions. The Freundlich model is applicable to heterogenous surface adsorption, and higher concentrations contributes to higher adsorption capacity. The Temkin model

assumes that adsorption decreases with the adsorption coverage due to the interaction between adsorbent and adsorbate. The fitting parameters of all three isotherm models are listed in Table 4.4. Compared to the correlation coefficients, R^2, all biochars had a better line-fitting to Langmuir isotherms (R^2 = 0.957 – 0.996) than Freundlich (R^2 = 0.536 – 0.991). Figure 4.7 shows the linear fit for all isotherms. The results show that the Langmuir model provides a slightly better fit than the other two (R^2 > 0.9). This indicates that monolayer adsorption is favored, where once a site is occupied by metal ions, no more ions will be adsorbed at that site (Jin et al., 2021).

Table 4.4 Adsorption isotherm models and parameters

		Langmuir			**Freundlich**				**Temkin**	
Biochar	Metal	$C_e/Q_e = 1/(Q_m K_{L)}) + C_e/Q_m$			$lnQ_e = lnK_f + (lnC_e)/n$				$Q_e = B\ lnA + B_L\ lnC_t$	
		Q_{max} (mg/g)	K_L (L/g)	R^2	lnK_F (mg/g)	n	R^2	A (L/g)	B (J/mol)	R^2
B300	Cu	0.227	4.040	0.989	0.439	1.133	0.991	3.67	2.058	0.562
	Mn	0.892	3.171	0.993	18.879	3.917	0.982	7.132	6.743	0.894
	Fe	0.107	2.741	0.957	649.673	5.652	0.883	1.771	5.785	0.884
	Pb	1.204	0.777	0.978	7.382	2.226	0.901	4.941	3.603	0.781
B500	Cu	6.508	0.312	0.993	3.47	3.365	0.892	2.194	3.225	0.997
	Mn	1.482	0.918	0.967	12.998	3.339	0.993	0.725	2.551	0.889
	Pb	7.987	1.19	0.993	7.111	8.614	0.981	0.321	4.819	0.994
	Fe	2.228	7.19	0.963	6.667	4.021	0.960	49.341	7.360	0.998
B700	Cu	8.196	0.496	0.996	1.181	4.773	0.536	28.067	11.44	0.971
	Mn	1.907	8.519	0.902	4.999	0.493	0.636	4.521	4.819	0.884
	Fe	2.218	25.463	0.990	3.633	4.933	0.884	7.551	6.891	0.987
	Pb	9.833	0.029	0.993	11.078	0.713	0.945	2.985	1.966	0.876
RS	Cu	1.008	0.039	0.892	1.0891	0.804	0.906	1.609	1.025	0.995
	Mn	0.997	9.876	0.971	9.562	0.992	0.754	2.591	2.736	0.556
	Fe	0.549	3.183	0.989	53.672	4.701	0.729	8.682	1.893	0.692
	Pb	1.338	4.100	0.991	9.798	2.567	0.899	6.263	6.002	0.789

Overall, the highest adsorption capacity is shown at 700°C (B700), with an adsorption capacity of 2.486 mg/g and an adsorption rate removal of 98.38 %. At the same time, B500 is slightly behind with an adsorption capacity of 2.398 mg/g and an adsorption rate of 97.43 % and finally B300 with adsorption capacity of 2.003 mg/g and removal rate of 87.11 %. The characterisation of biochar supports this where at higher temperatures (500°C and 700°C), higher BET surface area is available for adsorption. Nevertheless, higher temperature biochars contain multiple aromatic functional groups, where the aromatic structure could provide π-electron, which is very likely to create a strong bond with heavy metal cations, promoting chemisorption and thus results in the high removal percentages (Xu et al., 2016). This is supported by Chen (2019), the lignocellulosic material in SMC biochar contains an aromatic functional structure that promotes electrical connection with the metal ions at high pyrolysis temperature. This finding is in line with the kinetic finding that SMC biochars with higher pyrolysis temperature tend to have higher adsorption capacities.

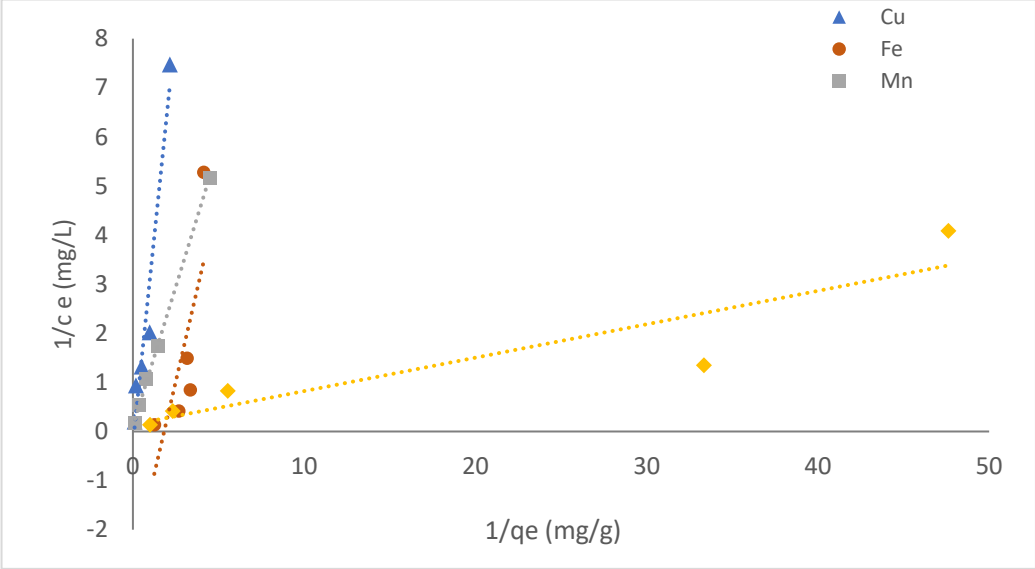

(a)

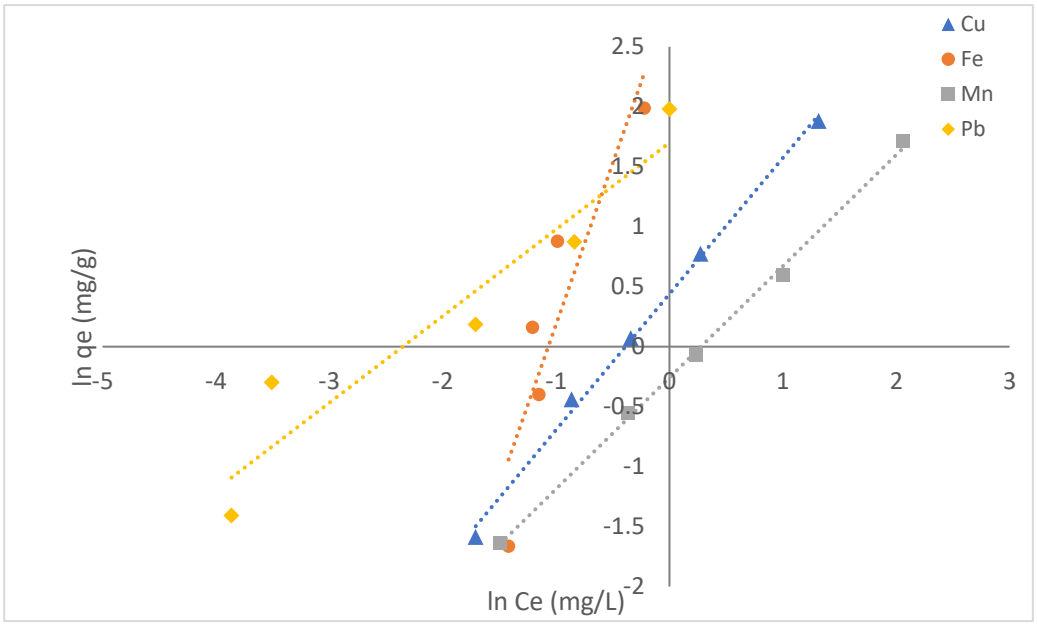

(b)

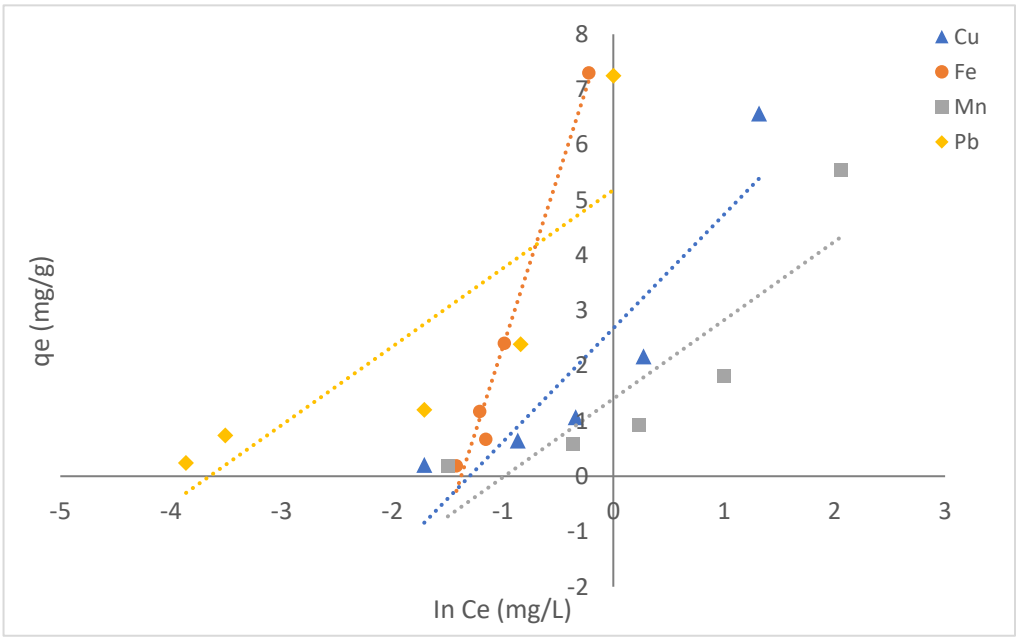

(c)

Figure 4.7 Linear fit for all heavy metals in B500 in (a) Langmuir (b) Freundich and (c) Temkin models

Using the Langmuir isotherm model, the maximum monolayer adsorption capacities (q_{max}) for B300, B500 and B700 were calculated as 8.196 mg/g for Cu (B700), 1.907 mg/g for Mn (B700), 2.228 mg/g (B500) for Fe and 9.883 mg/g for Pb (B700). Notably, the values of maximum adsorption capacities are much smaller than other feedstock biochar due to the low concentrations used in this study to imitate the actual concentrations in abandoned mining ponds. Accordingly, higher adsorption capacities are likely to be achieved using higher metal concentrations. Hence, a higher initial metal solution should be recommended for future reference. Overall, SMC biochar is a potential material as filter media for mine water treatment. Subsequently, the value of the dimensionless constant separation factor RL was calculated to determine whether the adsorption was favourable. The value obtained was ($0 < RL < 1$), indicating adsorption is favourable for all metal ions in SMC biochars. Nevertheless, Mn in B500 is more fitted in the Freundlich isotherm, indicating that metal ions' adsorption is likely to occur in a heterogeneous multilayer adsorption surface.

On the other hand, the Temkin model was adopted in this study to verify whether adsorption is favourable. The Temkin model is relatively different from the other two models as the Temkin model verifies the existence of electrostatic interaction between SMC biochars and heavy metal ions (Chen et al., 2019). It is interesting to note that Fe with B500 fits the Temkin model the best with $R^2 = 0.998$, consequently favouring the chemisorption process as one of the adsorption mechanisms of metal ions using SMC biochar.

4.3.5 Competitive adsorption of heavy metals in batch study

It is interesting to note that based on the initial metal concentrations, Mn gave the lowest adsorption performance than other metals. This is obviously shown in the adsorption isotherms where Mn gave the lowest maximum adsorption capacity for all pyrolysis temperature. This may be due to the competition in adsorption that happens when multimetal solution is used hence creating competition between the heavy metals. To further explore on the competitive adsorption among the heavy metals, a batch study using monometal solution of Pb, Mn, Fe and Cu at initial concentration of 30 mg/L on B300, B500, B700 and RS was done. To compare the percentage removal with multimetal solution at 30mg/L, removal percentage using monometal solution was drafted and shown in Figure 4.8.

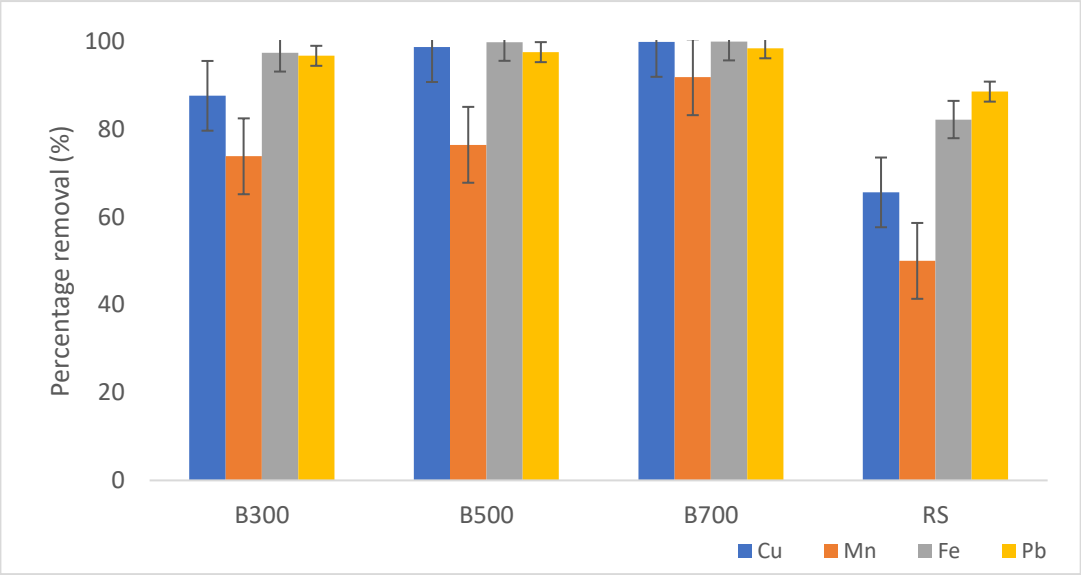

(a)

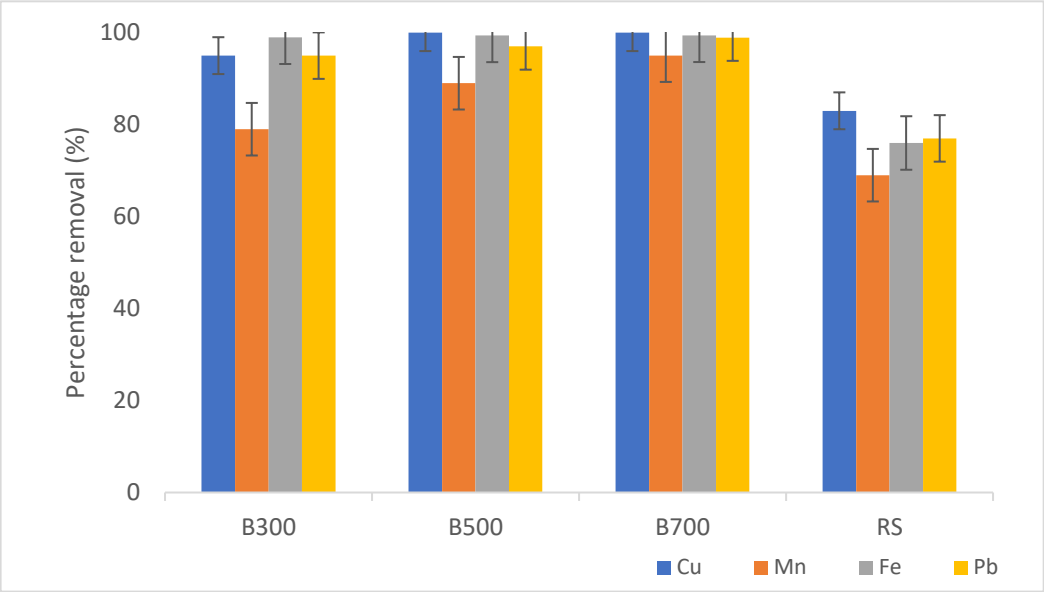

(b)

Figure 4.8 Percentage removal of heavy metals at initial concentration of 30 mg/L in (a) multimetal and (b) monometal solution

The removal percentage of each heavy metals in multimetal solution decreased compared to monometal solution, which confirms the presence of competitive adsorption on the SMC biochars. In the graph, Cu, Mn, Fe and Pb gave an average percentage removal of 87.89 %, 72.98 %, 94.78 % and 95.26 % for multimetal solution while 94.51 %, 83.76 %, 93.45 % and 91.98 % for monometal solution. The different reduction can be due to the saturation of the adsorption site of the biochar (Shan et al., 2020a). It is interesting to note that the adsorption affinity for heavy metals in multimetal solution was in the order of Pb > Fe > Cu > Mn which was different from the single ion adsorption Cu > Fe > Pb > Mn. This indicated that Cu had the strongest affinity than other metal ions, however, the presence of other heavy metal ions obstruct Cu from further adsorption onto biochar.

Nevertheless, Pb showed the highest affinity in multimetal solution which demonstrated that Pb showed the strongest competitiveness for metal adsorption but less competitive in monometal solution. This could be due to the resultant accord for adsorption sites and differences in metal characteristics (Ni et al., 2019). Conversely, Mn showed distinguish low percentage removal for B300, B500, B700 and RS in both monometal and multimetal solutions. This may be due to the initial concentration of multimetal solution that affect the overall sorption. Higher initial concentrations create more metal ions available hence results in higher competitive ions among them (Huang et al., 2021). Therefore, the coexistence of different metals should be considered when assessing the metal performance.

4.4 Mechanism of metal ion adsorption

In order to understand the removal mechanism of metal ions onto the SMC biochar, a batch study with various experimental conditions including pH, adsorption isotherms (initial metal concentrations) and time (adsorption kinetics) was conducted to further understand the adsorption behavior of metals onto the biochars. Generally, there are more than one mechanism that is responsible for the heavy metal adsorption onto biochar surface. Based on the batch study, heavy metal removal mechanisms for SMC biochar may include both physical and chemical adsorption. The physical adsorption involves physical adsorption and precipitation while the underlying chemical mechanisms involved are cation exchange, electrostatic interaction, and π-complexation. These mechanisms are consistent with other biochar-related studies (Chang et al., 2020b; Jin et al., 2018; Luo et al., 2018a; Shan et al., 2020b).

In order to prove physical adsorption occurrence in the batch study, Figure 4.9 shows the SEM-EDX images of B300, B500, and B700 before and after adsorption. From the SEM images, heavy metal salt deposits (white particles) could be observed on the surface of the biochar specimens. The EDX analysis further confirms the precipitation – based on the EDX, the presence of metal ions was distinctly found on the surface of biochar after adsorption. This could represent physical adsorption, where the metal ions were adsorbed on the surface of the biochar.

Additionally, another removal mechanism is chemical adsorption. The availability of other elements, such as Na, Mg, and K in the EDX analysis indicated the ion exchange mechanism involved where SMC biochar exhibits high tendency to adsorb Pb, Mn, Cu and Fe ions by releasing other cations such as Ca, Mg, Na and K from the adsorbent. The ion exchange mechanism before and after adsorption of metal ions onto SMC biochar was studied by measuring the amount of Na, K, Ca and Mg released from adsorbent. After adsorption, the cations available in the biochars were different at different pyrolysis temperatures. At B300, the number of cations released was 0.721 meq/L thus suggesting that ion exchange accounted about 21% of the total adsorption. This result indicated that cation exchange was not dominant at B300. However, for higher temperature B500 and B700, cations availability decreased significantly, resulting to 45 % and 50 % of ion exchange.

In addition, chemical adsorption could be discussed through the role of chemical functional group using FTIR analysis before and after adsorption. FTIR spectra that show active functional groups for all pyrolytic temperature biochars are shown in Figure 4.1. Subsequently, after batch adsorption, it is noticeable that the intensity and wavenumbers changed, some peaks shifts and some became weakened or enhanced. From the spectra in Figure 4.1a, the intense heavy metal adsorption band has weakened the strong

hydroxyl band at 3400 cm^{-1}, and a similar situation occurred at all wavelengths. These bands corresponds to the stretching and bending vibrations which contributed to the heavy metals removal (Jin et al., 2021). This shows that most of the binding sites available were used by metal ions for coordination and ion exchange mechanisms (Abdallah et al., 2019). For example, as the C-H stretching was weakened at 1400 cm^{-1}, it shifted into an M-C bond, which could be metal-methylidyne (MCH) or methyl-metal (MCH_3), depending on the ligand attached to the carbon atom. The disappearance or weakening peak demonstrates a high sorption effect where chemical interactions occur between heavy metal ions and the functional group on the adsorbent surface during adsorption (Mahdi, Hanandeh, et al., 2019). This result is consistent with adsorption kinetics in this study that fits pseudo second order model, which promotes chemisorption.

At low pyrolysis temperature, the hydroxyl functional group aid in metal adsorption through an ion exchange mechanism. These functional groups available on the surface of the adsorbent will be exchanged with metal ions (Xu et al., 2016). At B300, the peak of 1626 cm^{-1} corresponding to C=C O-H bonds shifted to 1580 cm^{-1} after adsorption. These results indicated that O-H took part on the adsorption process. Nevertheless, at high pyrolysis temperatures, more aromatic and aliphatic functional groups are available. These aromatic functional groups could provide π-electron, which were suggested to create a strong bond with heavy metal cations (Chen et al., 2019). The decreased C=C peak manifests that the delocalized π- electron contributes to surface complexation removal mechanism. This explains the highest removal percentage shown in B500 and B700.

As conclusion, more oxygen-containing groups are available at low temperature biochar to aid the ion-exchange mechanism. However, a strong aromatic structure as π-electron donor or acceptor at higher

temperature biochar creates a π-complexation mechanism. As SMC biochar mainly consists of lignin and cellulose, many functional groups such as hydroxyl, carboxyl, and amine from aromatic groups were detected as beneficial to the adsorption of metal ions (Jin et al., 2018c). It is interesting to note that it could be reused in the second pyrolysis to further remove heavy metals, which simultaneously put it to maximum usage and reduce secondary pollution (Liu et al., 2021).

Element	Weight%	Atomic%
C K	46.20	62.35
O K	25.41	25.74
Mg K	2.43	1.62
Al K	0.43	0.26
Si K	0.49	0.28
P K	1.33	0.70
S K	1.90	0.96
Ca K	16.13	6.52
Fe K	3.23	0.94
Cu L	2.46	0.63
Totals	100.00	

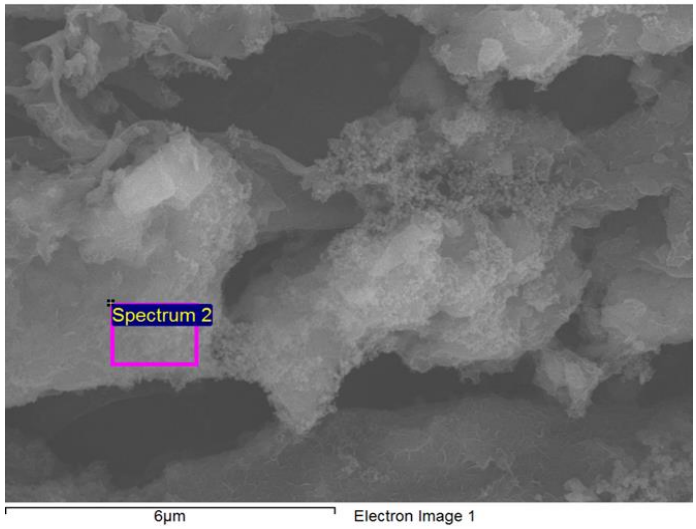

(a)

Element	Weight%	Atomic%
C K	60.33	72.38
O K	25.22	22.71
Mg K	1.68	1.00
K K	0.40	0.15
Ca K	9.56	3.44
Mn K	0.09	0.02
Fe K	0.44	0.11
Cu L	0.12	0.03
Au M	1.82	0.13
Pb M	0.33	0.02
Totals	100.00	

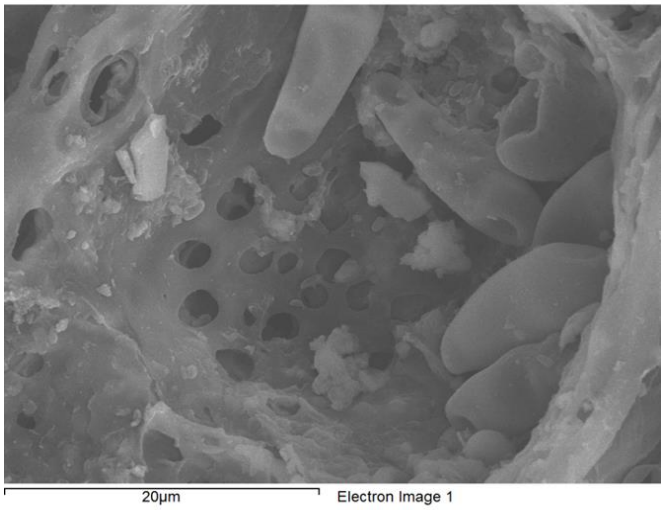

(b)

Element	Weight%	Atomic%
C K	38.92	52.37
O K	37.69	38.07
Mg K	1.92	1.28
Al K	0.24	0.15
P K	1.24	0.65
S K	0.91	0.46
Cl K	0.30	0.14
K K	0.20	0.08
Ca K	13.46	5.43
Mn K	1.12	0.33
Fe K	1.32	0.38
Cu L	2.68	0.68
Totals	100.00	

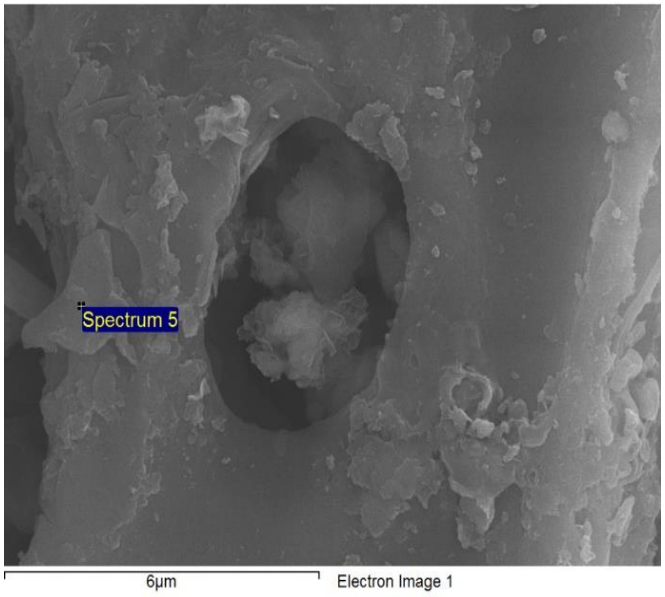

(c)

Figure 4.9 EDX image and elemental composition of mixed metals on the surface of (a) B300, (b) B500 and (c) B700.

4.5 Summary

Based on the batch adsorption study in terms of physicochemical analysis of SMC biochar at multiple pyrolytic temperatures, adsorption isotherms, and adsorption kinetics, it is interesting to conclude that SMC biochar pyrolyzed at 500^{o}C (B500) was selected as the filter media for column study. In summary, although B700 showed the highest metal removal, B500 showed a total removal rate of 97.43 % with an adsorption capacity of 2.398 mg/g while B700 gave 98.38 % removal with an adsorption capacity of 2.486 mg/g. Since the removal rate and adsorption capacity are comparable, the selection of B500 as the filter media for the lab scale metal retention column study is justified by its cost effectiveness and energy efficiency compared to B700. The evidence why B500 was chosen as the filter media is discussed in summary below.

Although the surface area is much lower than B700, the batch study has proved its high removal efficiency similar to B700. This proves that physical sorption is not the primary removal mechanism. B500 is rich in aromatic functional groups that can form metal complexation to the metal pollutants. In addition, as the biochar has plenty of carbon and cations, ion exchange mechanism is also favorable.

Based on adsorption isotherm observed in batch study, the Langmuir model was found to be a suitable fit where the maximum monolayer adsorption capacity of B500 is high for all metals where at this pyrolytic temperature, the aromatic structure could provide π- electron, which creates a strong bond with heavy metals cations. Nevertheless, B500 has high surface area which promotes physical adsorption and precipitations.

This can be supported by the result from adsorption kinetics, where it fits the PSO with $R^2 > 0.999$, which assumes that the chemisorption process mainly controls the sorption. Moreover, B500 showed the highest adsorption capacity of Cu (2.573 mg/g), Mn (1.522 mg/g) and Pb (2.491 mg/g). The PSO graphs from the kinetics model showed that the adsorption capacity plots of B500 and B700 are somewhat highly similar, followed by B300 and RS.

Chapter 5 Lab scale metal retention column study

5.1 Introduction

Next, the study continues with the discussion of Stage 3, the lab scale metal retention column study in Chapter 5. The performance of SMC biochar as filter media to remove heavy metals in column study is discussed with the breakthrough analysis with different pH and initial metal concentration. The study was performed using B500 as filter media (evaluated by batch study). Additionally, the heavy metal removal mechanism and the competitive adsorption among the heavy metals and adsorption isotherms using Thomas model were assessed. This section satisfies objective 2 of this research.

5.2 Breakthrough curve analysis

Conventional filter media using the soil layer alone can provide successful physical-chemical and biological treatments (Wang et al., 2017). However, the performance was varying, and research proved that it has a first flush effect and transient wetting and drying, which could hinder contaminant attenuation and re-immobilises contaminants (Sun et al., 2020). This leads to advanced design using readily available, replaceable, and inexpensive materials, including biochar (Tsang et al., 2019). On the other hand, biochar application as filter media for mining water treatment has not yet been rigorously explored. The selection of an optimum filtration media is crucial as it will influence heavy metal removal. Two common properties of filtration media are (1) high hydraulic conductivity to minimize flooding and (2) high storage volume to

enhance contaminant removals. Hence medium - coarse sand is commonly used to maintain high conductivity. While clay increases the storage volume, it lowers the hydraulic conductivity. In contrast, biochar provides both advantages simultaneously. Biochar has a unique property of extensive internal pore structures that increase storage volume and hydraulic conductivity (Mohanty et al., 2018). Thus, to alleviate the efficiency of water treatment facilities, researchers have attempted to enhance the performance by mixing it with suitable materials, including biochar.

This study discussed further on application of SMC biochar as filter media to remove heavy metals in abandoned mine water through lab scale metal retention column study. SMC biochar pyrolyzed at 500^{o}C was chosen as filter media due to its outstanding adsorption performance in batch study. Seventeen different sets of initial metal concentrations were constructed, and the adsorption performance was assessed from lowest to highest concentration based on the actual mine water data. One of the most critical factors in measuring the feasibility of an adsorbent in an accurate and practical application is the performance of the adsorption process in a continuous fixed bed column, as the batch result only represents the equilibrium and kinetics (Abdolali et al., 2017). The column study will be interpreted through breakthrough analysis and the adsorption capacity with the effect of pH and initial metal concentration conditions.

The breakthrough curve plays an essential role in characterising column experiment and determine the dynamic response of the column. The breakthrough curve showed the relative concentrations (Ct/C_o) on the y-axis versus time on the x-axis. Figure 5.1 shows the adsorption of each metal in the highest initial metal concentration set (B500Q) at pH 7. In the column, the flow of synthetic mine water created a wavefront through the adsorbent bed. The area's wavefront is known as the mass transfer zone (MTZ).

The adsorption process takes place in the MTZ. As the SMC biochar becomes exhausted over time, the MTZ moves forward across the column bed and leaves behind saturated metal contaminants. The breakthrough point is defined when the ratio between the influent concentration and outlet concentration becomes 0.5 to 0.9. According to the literature, the adsorbent is replaced when the ratio of C_t/C_o = 0.5 in the case of industrial-scale application (Chowdhury et al., 2015). The column will be fully exhausted when inlet concentration is almost equal to outlet concentration C_t/C_o = 1.

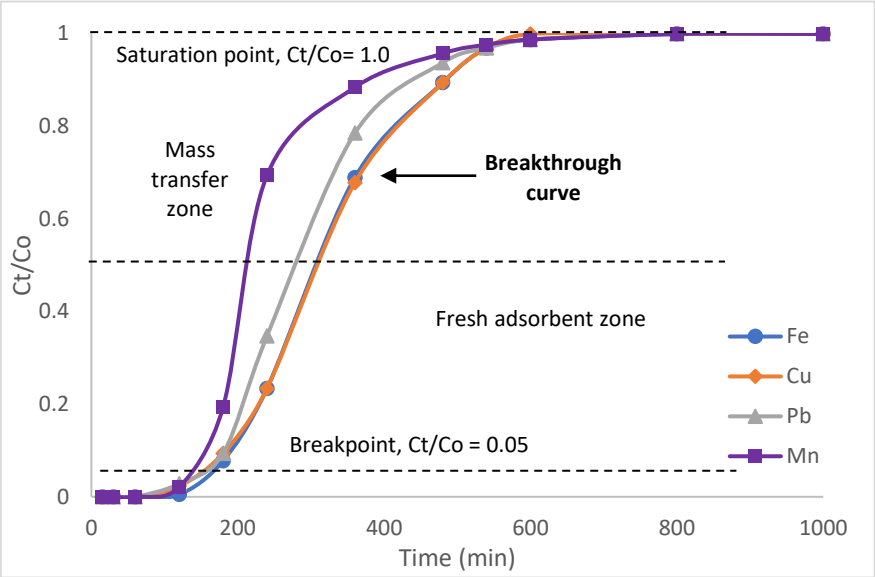

Figure 5.1. Adsorption of heavy metals in B500Q

In this study, Cu showed the highest adsorption capacity of 49.833 mg/g, followed by Fe at 33.186 mg/g, Pb at 16.218 mg/g, and Mn at 6.665 mg/g. This is supported by the breakthrough curve, where Mn showed the earliest saturation point followed by Pb, then Fe and Cu had similar S-shaped performance. All metals showed a similar breakthrough point, which is at 100 min. Initially, each metal ion was rapidly adsorbed

on the B500 mass due to the high availability of active sites. Consequently, the metal ions were captured on the surface or inside the biochar, thus, making the effluent solute free. Nevertheless, as the solution continued to flow at approximately 100 min, the uptake became less effective due to the decreasing number of active sites available. Thus, the outlet concentration increased until a saturation point was reached (>90 % inlet concentration).

5.2.1 Effect of pH

The constant flow rate of 10 ml/min with a 10cm pond depth effectively gives more contact time for SMC biochar adsorption, resulting in a more significant removal of heavy metals from the solution. Breakthrough time and exhaustion time increased intensively with an increase in bed depth due to the more adsorbent-specific surface hence more binding sites and functional groups for more effective adsorption (Abdolali et al., 2017). Next, influent pH is an important factor on the interaction between SMC biochar and solubility heavy metals. The effect of pH is discussed through the breakthrough curves of Cu under different pH and initial metal concentrations. A total of seventeen sets of multimetal solution at different initial metal concentration from the lowest to the highest concentration found in real abandoned mine pond case studies. Figure 5.2 shows the breakthrough curves of Cu under different pH and initial metal concentrations from B500A to B500Q.

Based on the figure, all the experimental breakthrough curves were typically S-shaped, indicating the influence of the column's mass transfer of parameter. The breakthrough and saturation time were prolonged and smoother under weak acid pH and neutral conditions. Cu at pH 2 is the first to leave the column in the effluent, followed by pH 5, pH 7, and pH 10. Notably, as pH increases, adsorption capacity

increases as well. The Cu adsorption capacity at B500Q was increased from 0.115 mg/g at pH 2 to 49.833 mg/g at pH 7. Under acidic conditions, the higher amount of H^+ ions create competition suppressing the accessibility of Cu metal ion with surface functional group available. However, the value decreases to 48.4 mg/g at pH 10. The alkaline conditions lead to precipitation, increasing OH^- ions and hinder adsorption (Daghbandan et al., 2022). Overall, pH 7 showed the shorter mass transfer zone, which represented highly efficient utilisation of adsorbent, hence could be the optimum pH for column adsorption. However, it is interesting to note that as initial metal concentration increases, the S-shaped curves were shortened and reaches saturation point faster. The effect of initial metal concentrations will be further discussed.

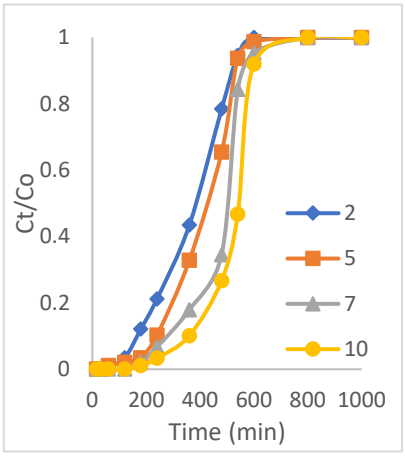

(a) B500A

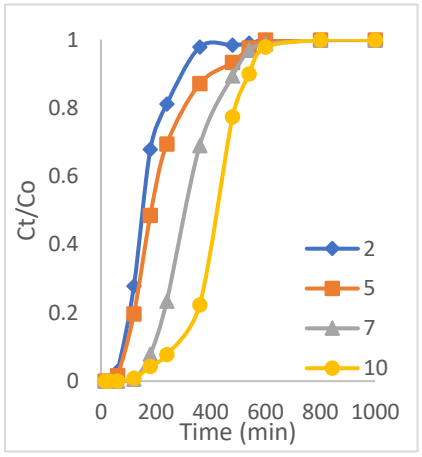

(b) B500B

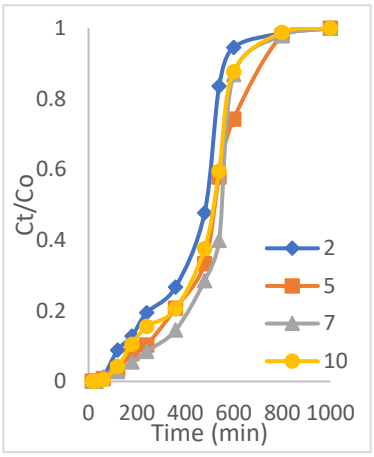

(c) B500C

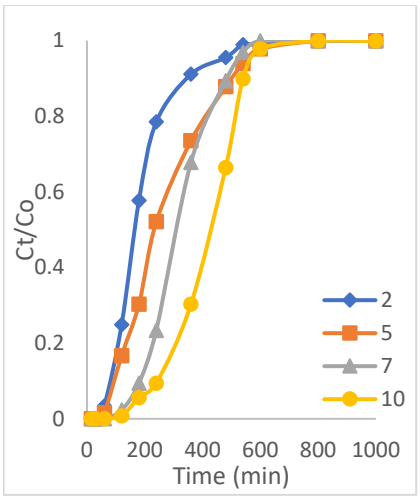

(d) B500D

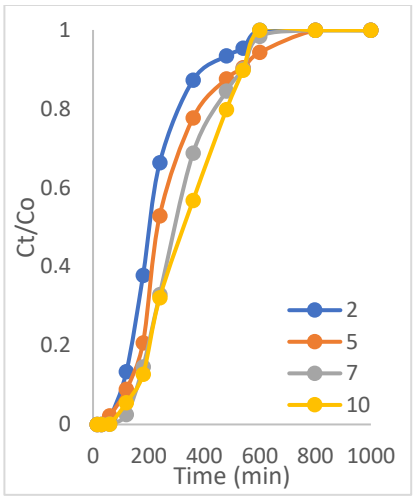

(e) B500E

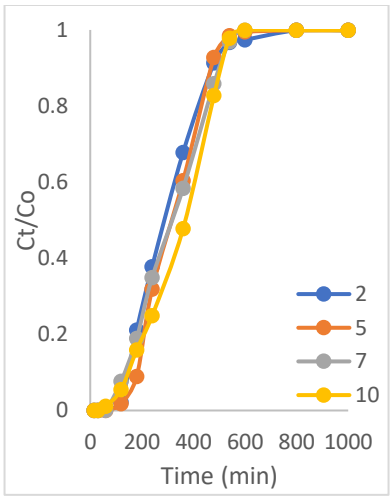

(f) B500F

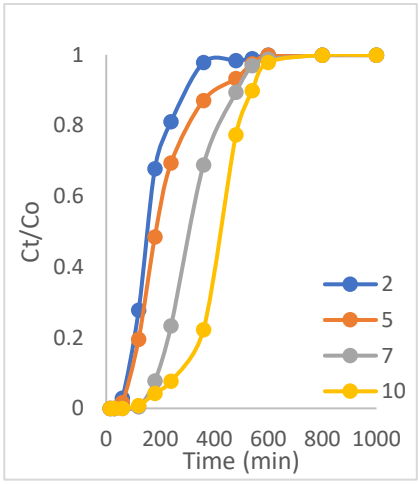

(g) B500G

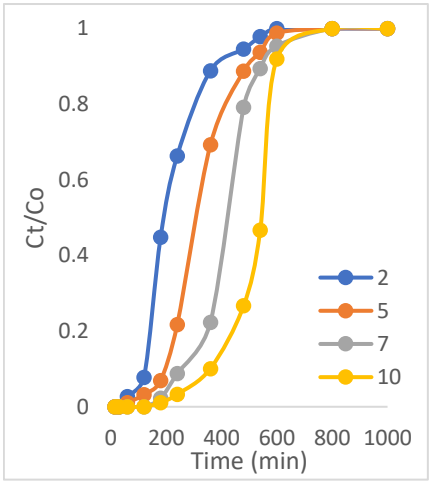

(h) B500H

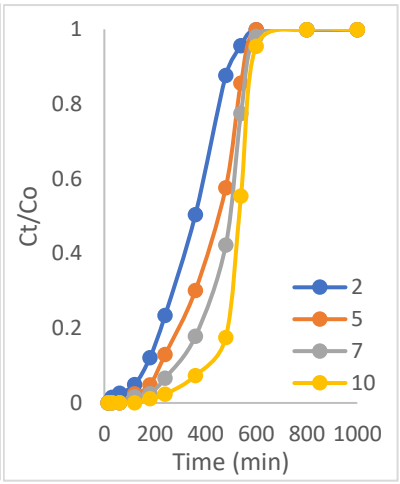

(i) B500I

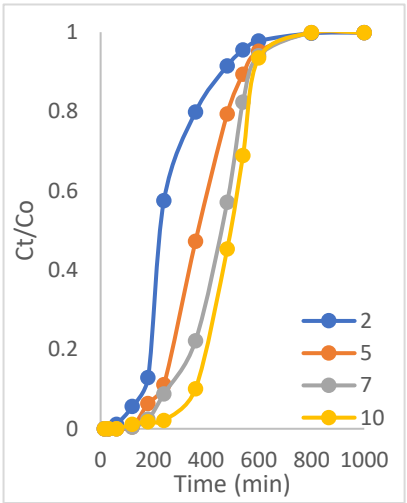

(j) B500J

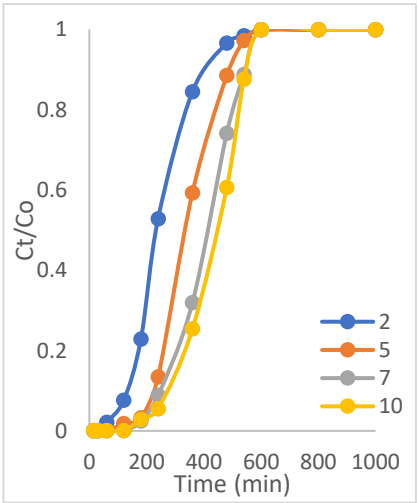

(k) B500K

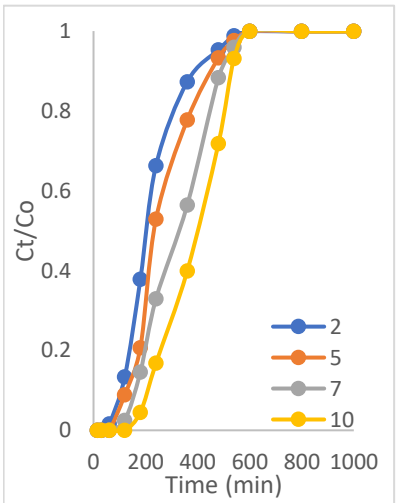

(l) B500L

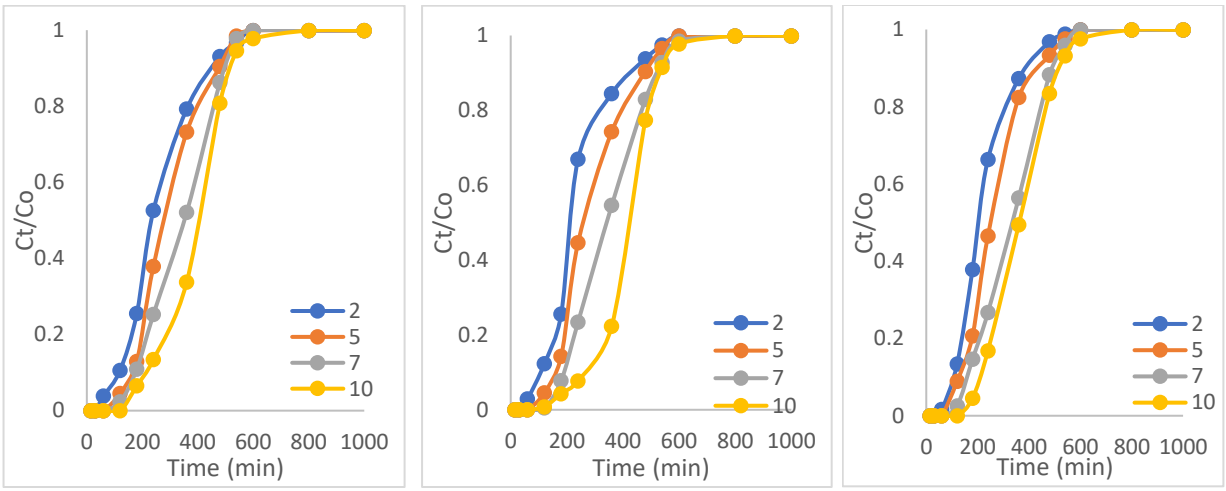

(m) B500M (n) B500N (o) B500O

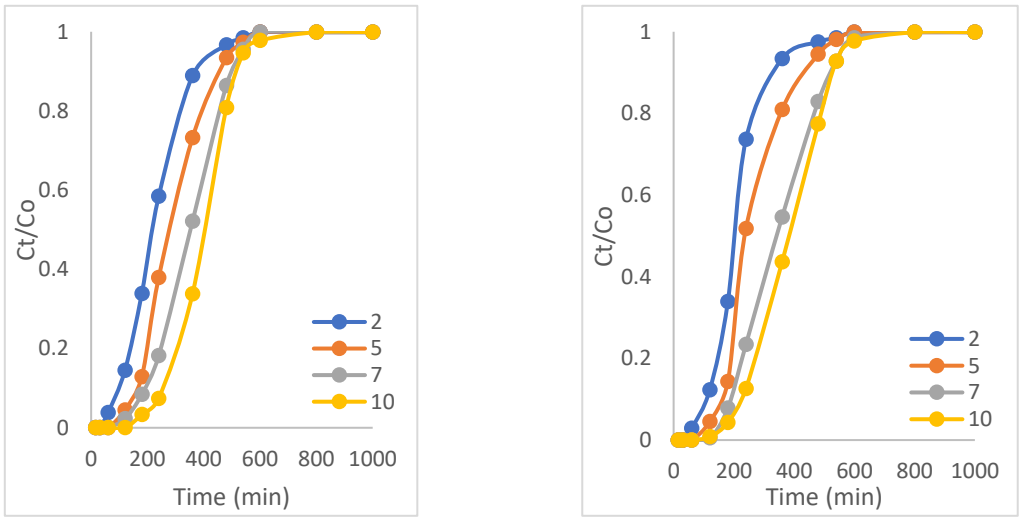

(p) B500P (q) B500Q

Figure 5.2 Breakthrough curve analysis of Cu from (a) B500A to (q) B500Q

5.2.2 Effect of initial metal concentrations

Due to the similar trend for all 17 sets, 7 sets were chosen to further discuss the effect of initial metal concentration in column study. Table 5.1 displayed the initial metal concentrations of Pb, Mn, cu and Fe for these 7 sets. Figure 5.3 is the breakthrough curve of Cu, Fe, Mn and Pb at different metal concentrations namely B500A, B500D, B500G, B500J, B500M, B500P, and B500Q with a bed depth of 30cm and a fixed flow rate of 10 ml/min (HRT = 24 hours). As seen in Figure 9, the shape and gradient of the breakthrough curve changed significantly with an increase in metal concentration. As the influent concentration increased, the breakthrough time was shortened. The highest influent metal concentration B500Q, resulted in the fastest breakthrough and saturation where the curves shifted towards the left.

Table 5.1 Initial metal concentrations of Pb, Mn, Cu and Pb in B500A, B500D, B500G, B500J, B500M, B500P and B500Q

Name of set	Initial metal concentrations (mg/l)			
	Pb	Mn	Cu	Fe
B500A	1	5	1	5
B500D	23	12	30	23
B500G	20	15	70	50
B500J	28	19	87	65
B500M	50	30	150	100
B500P	85	45	215	175
B500Q	100	50	300	200

On the contrary, B500A showed much smoother and longer shapes. These results demonstrated that higher influent concentrations expedited the saturation of adsorbent. The earlier exhaustion might be attributed by two factors; first is the greater concentration gradient; and second is the slower mass

transport of heavy metal ions from the solution to the adsorbent's surface (Abdolali et al., 2017). Due to the higher concentrations, large concentration gradient and higher driving force for mass transfer were predicted. Additionally, it can be observed that the breakthrough curves of Mn for all sets of concentrations are sharper than other metal ions. This could be due to the lowest concentration of Mn in all concentration sets that contributed to the sharp curve. Thus, the accumulation of heavy metals during the adsorption process depends on the initial concentration.

These results demonstrated that heavy metal adsorption is highly dependent on metal concentration. At a lower concentration range, longer contact time between adsorbent and adsorbate is available, and a larger volume of mine water solution can be treated. This is due to the slower transportation of adsorbate cations in low concentration solutions, hence decreasing the mass transfer zone (Z. Z. Chowdhury et al., 2015). Initially, adsorption was rapid because of the availability of many active sites. Subsequently, increasing initial metal concentration results in a more significant force in the mass transfer zone, resulting in the available sites being quickly exhausted, causing the volume of effluent to decrease (Patel, 2019). B500 has a high capacity for adsorption on metallic pollutants due to its physicochemical characteristics, high surface area, and pore volume, which is equivalent to activated carbon (Inyang et al., 2016). The metallic ions can be physically adsorbed into the biochar pores. Correspondingly, the presence of functional groups aids in metal removal in the form of metal complexation or metal precipitation by reactions with hydroxide ions (Biswal et al., 2022).

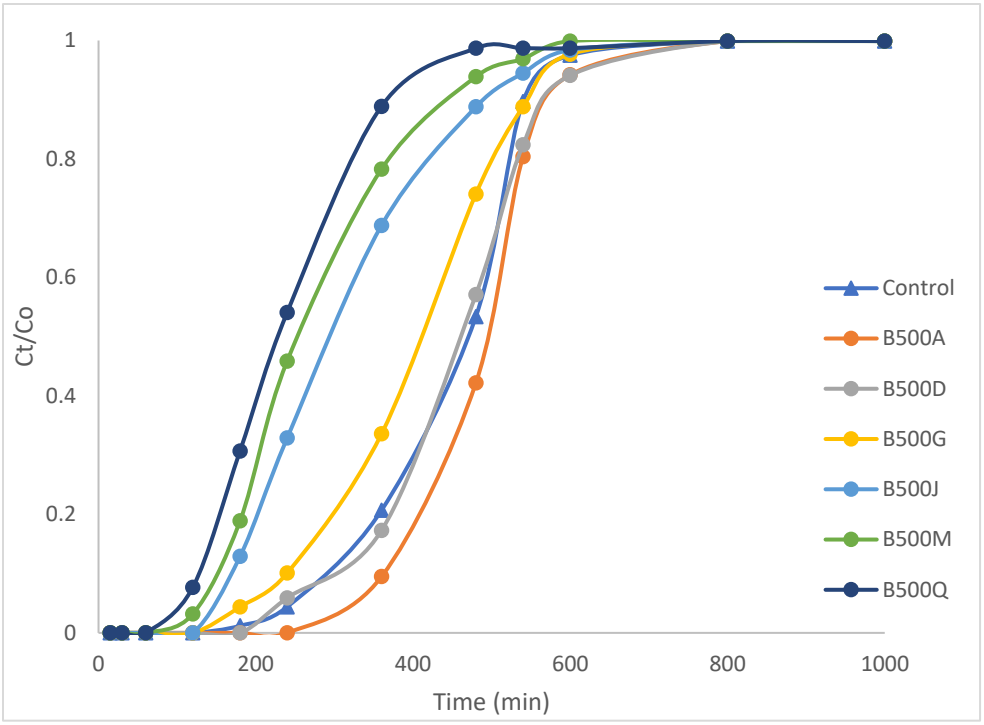
1
0.8
0.6
0.4
0.2
0
Ct/Co
0
200
400
600
800
1000
Time (min)
Control
B500A
B500D
B500G
B500J
B500M
B500Q

(a)

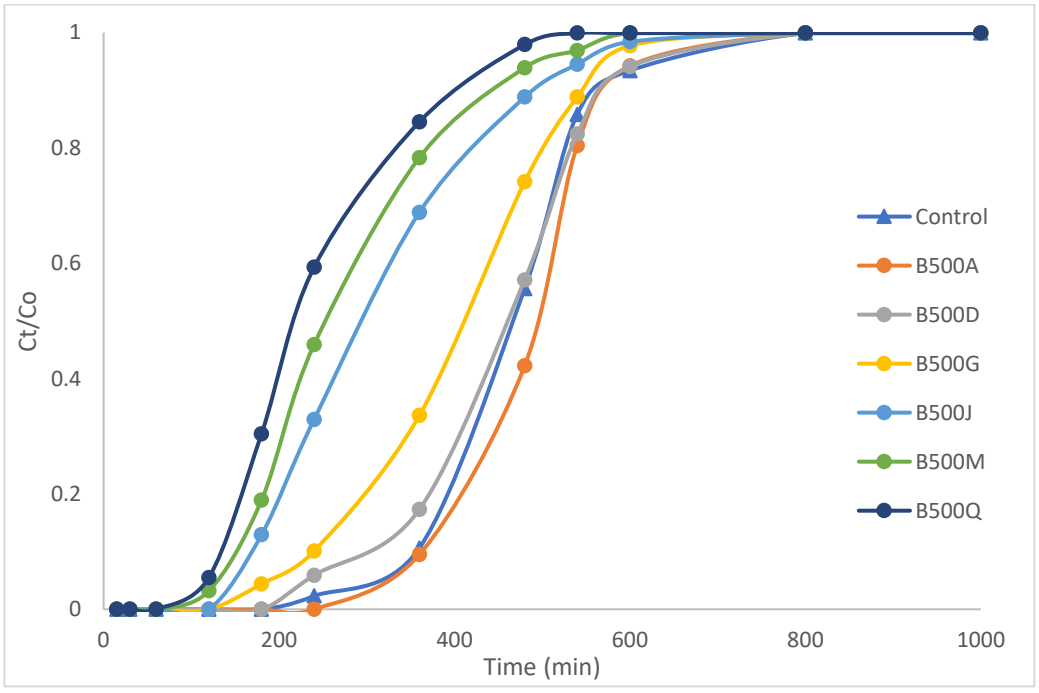
1
0.8
0.6
0.4
0.2
0
Ct/Co
0
200
400
600
800
1000
Time (min)
Control
B500A
B500D
B500G
B500J
B500M
B500Q

(b)

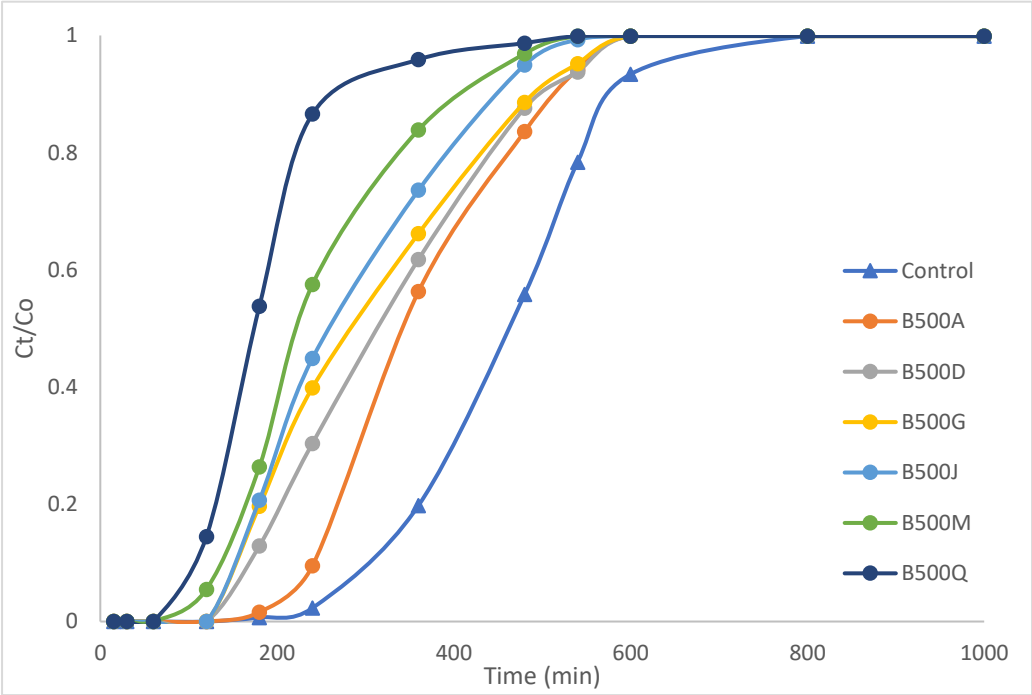

(c)

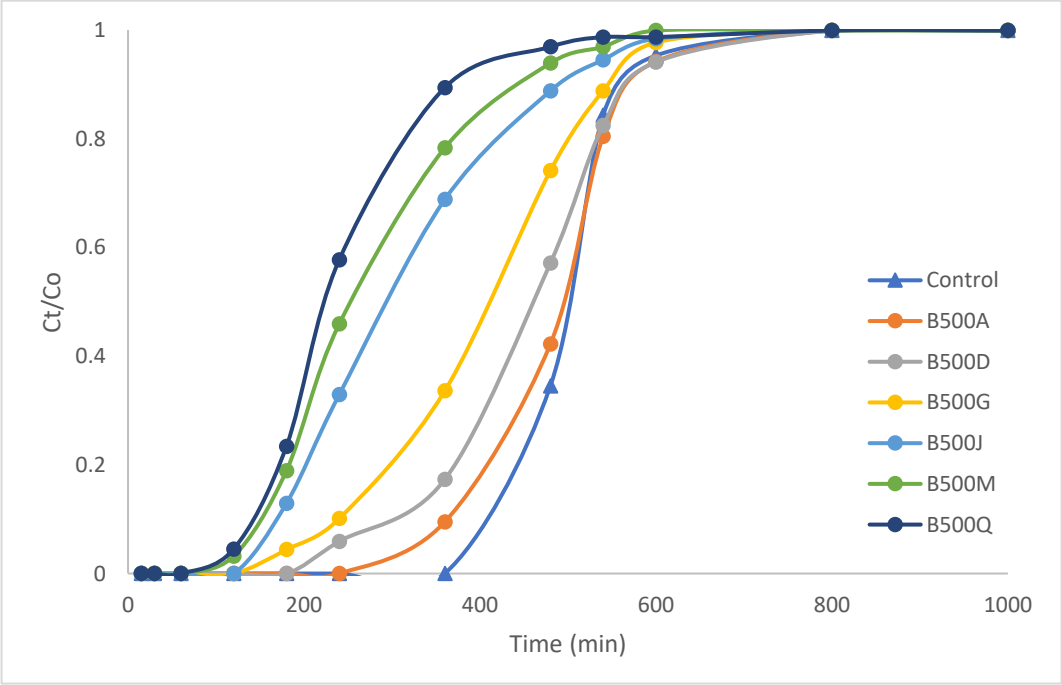

(d)

Figure 5.3. Breakthrough analysis of (a) Cu, (b) Fe, (c) Mn and (d) Pb at various initial metal concentration

As a result, ion exchange and surface complexation are the main mechanisms of metal removal for B500 in this metal retention column study. In consistent with physicochemical analyses, B500 had a highly aromatic structure instead of oxygen functional groups that assist metal complexation. Although the surface area is lower than B700, with high polarity, exchangeable cations and mineral functional groups on their surface are very effective for heavy metal removal. It was more effective in removing metals (Esfandiar et al., 2022).

5.3 Thomas model

An efficient column treatment system design requires a good prediction of the adsorbate and adsorbent behaviour which can be explained through the breakthrough curves. The numerical model validates the laboratory study results by comparing the experimental curves with the numerical ones (Malik et al., 2018). Thomas model was chosen as it follows Langmuir isotherms and obeys pseudo second order kinetics and no axial dispersion, which is the isotherm and kinetic that previously fit the batch study in this research. Furthermore, this model can predict the maximum adsorption capacity of SMC biochar in fixed bed columns. The fitted nonlinear curves for each metal are shown in Figure 5.4. The performance evaluation was assessed in R^2, RMSE, and MSE functions presented in Table 5.1. From the table, it is apparent that the coefficient R^2 values of the Thomas model were all above 0.9. The low MSE values calculated for each metal demonstrate similar suitability of this model. Notably, the predicted maximum capacity for Fe, Cu, Mn and Pb were 31.264 mg/g, 48.763 mg/g, 6.044 mg/g and 16.781 mg/g, respectively. The experimental data and the predicted maximum capacity for Fe, Cu, Mn, and Pb showed good agreement, confirming the Thomas model's suitability for column analysis (Zang et al., 2017).

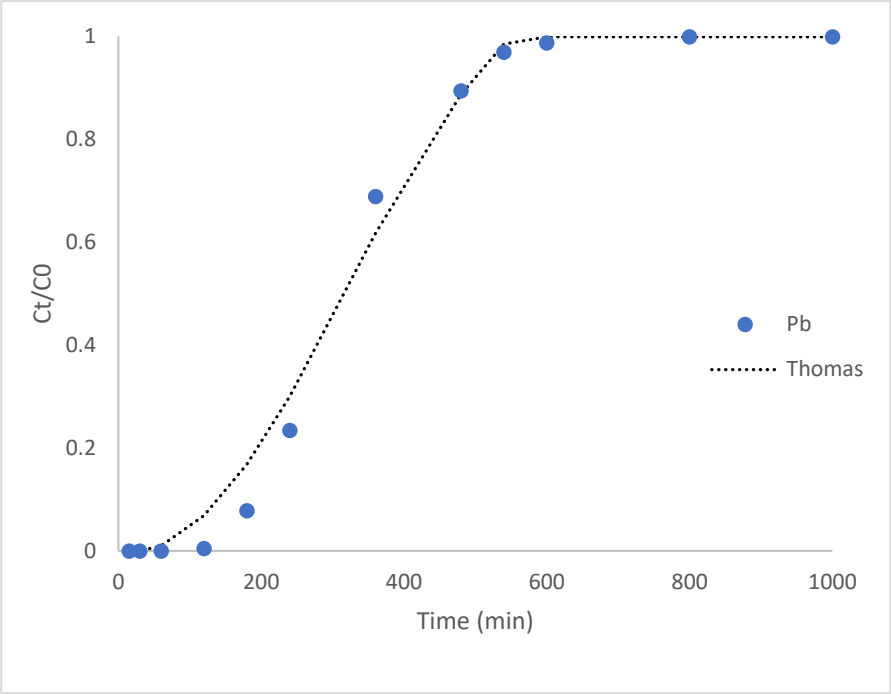
1
0.8
0.6
0.4
0.2
0
Ct/C0
0
200
400
600
800
1000
Time (min)
Pb
Thomas

(a)

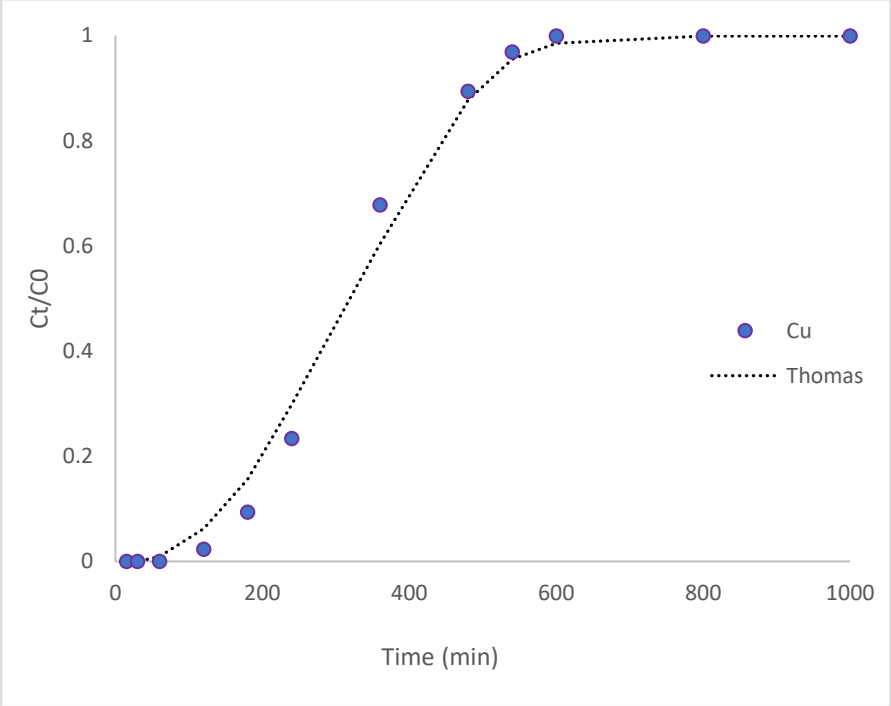
1
0.8
0.6
0.4
0.2
0
Ct/C0
0
200
400
600
800
1000
Time (min)
Cu
Thomas

(b)

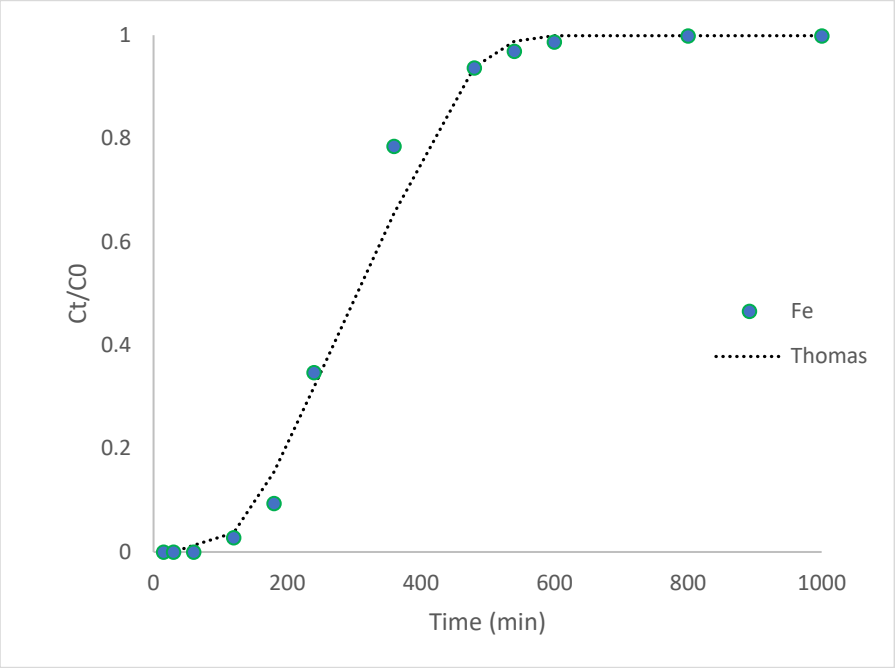

(c)

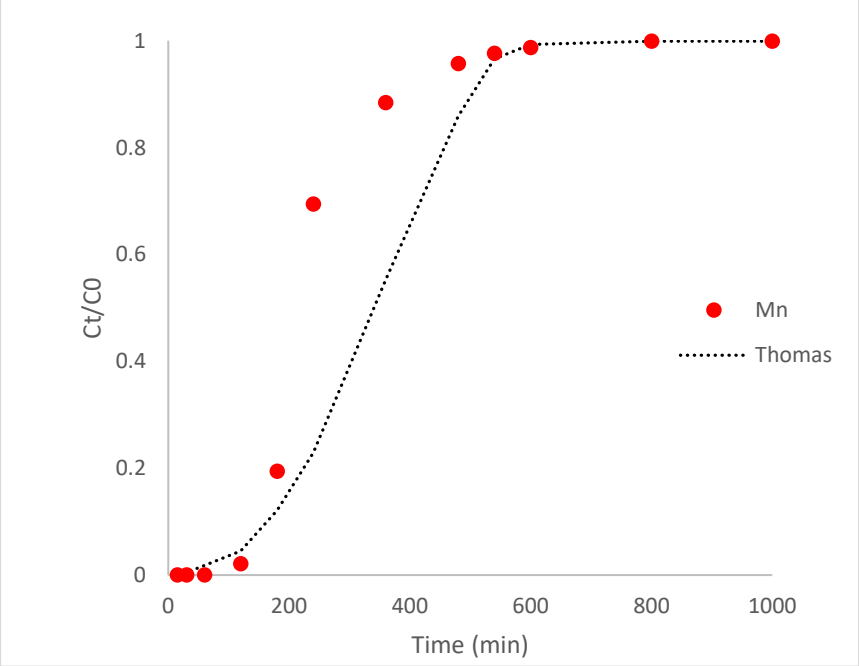

(d)

Figure 5.4 Nonlinear regression analysis for breakthrough curve modeling using Thomas model for (Pb, (b) Cu, (c) Fe and (d) Mn.

Table 5.2 Evaluation performance of Thomas model of each metals

Heavy metal	Actual	Thomas			
	Adsorption capacity (mg/g)	Q_{max} (mg/g)	RMSE	MSE	R2
Cu	49.833	48.763	0.478	1.07	0.986
Mn	6.665	6.044	0.654	1.621	0.917
Pb	16.218	16.781	0.845	0.563	0.998
Fe	33.186	31.264	0.194	0.922	0.995

This indicates that the external and internal diffusion is limitless (Chowdhury et al., 2015). Overall, these results were consistent with the batch study and fully supports the chemisorption mechanism of SMC biochar towards the heavy metals. The characterisation of the biochar showed chemical interactions on the surface which is confirmed by highest fitting in Langmuir models that promotes monolayer adsorption. Furthermore, the study of initial pH implied that precipitation is involved as one of the batch removal mechanisms and this is confirmed by the best fit of pseudo second order in the batch study that promotes chemisorption. Accurate simulation of the breakthrough curve is vital for determining the effectiveness of the SMC biochar and the capacity of the adsorption bed for proper design and process scale-up (Rosales et al., 2017). Therefore, SMC biochar is a potential material as a sustainable filter media in continuous column for large scale heavy metal retention system for abandoned mine water.

5.4 Competitive adsorption among heavy metals

Competitive adsorption between the metals ions in the column study is observed. Referring to Figure 5.3, it is interesting to note that Mn was the first to leave in the effluent, followed by Pb, Cu, and Fe. This may be due to the competitive effect of co-contaminants on the active adsorption sites available in the mixed metal solution. Another example of competitive adsorption can be proven using single and multimetal adsorption in the column. Figure 5.5 shows the breakthrough curve of single metal (Pb, Mn, Cu and Fe) and mixed metal solution with initial concentration of 100 mg/L. The breakthrough points of Pb, Mn, Cu, Fe in single metal column were 400, 180, 250 and 200 min after treatment, respectively. In the mixed metal solution, the breakthrough points of Pb, Mn, Cu, and Fe are 200, 150, 60, and 100 min after treatment, respectively. The complete exhaustion points for Pb, Mn, Cu and Fe in single metal adsorption were at 800, 500, 580 and 600 min after treatment, and those in mixed metal solution were at 600, 500, 500 and 600 min after treatment, respectively. Metal adsorbed in the mixed solution are lower than in single metal solution, promoting competition for surface adsorption sites from other heavy metals in the solution. As the metal sorption favors surface complexation mechanisms with surface functional groups, higher competitions for complex reaction takes place when there are more metal ions available (Park et al., 2015).

Competitive adsorption among the heavy metals contaminants is a critical aspect to look into as this can impact the adsorbent removal performance (Esfandiar et al., 2022). Overall, Mn showed average percentage removal of 75.4 %, followed by Pb with 79.2 %, while Cu presented an average removal performance of 92.6% and Fe with 93.8%. Henceforth, Mn and Pb were highly affected by the coexistence of other metal cations in the solutions while the presence of the competing ions slightly influenced Cu and

Fe. Mn significantly showed the most negligible affinity due to weak adsorption. Mn has been reported as the most challenging metal to remove and competitive to other metals, mainly Fe. It requires oxidation conditions with pH >8 and a higher alkalinity system (Daghbandan et al., 2022). Nevertheless, the removal of Cu and Fe was highly effective.

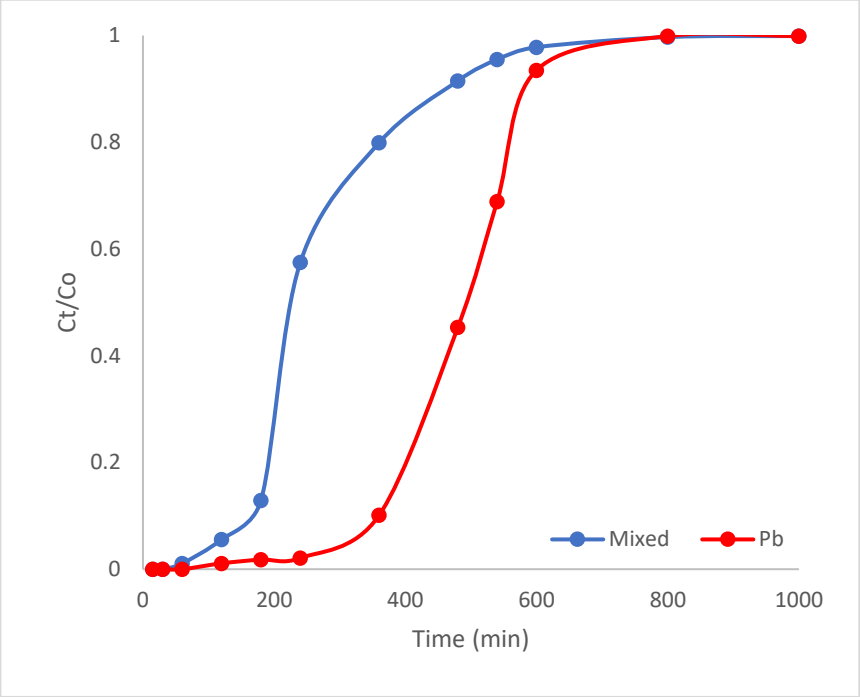

(a)

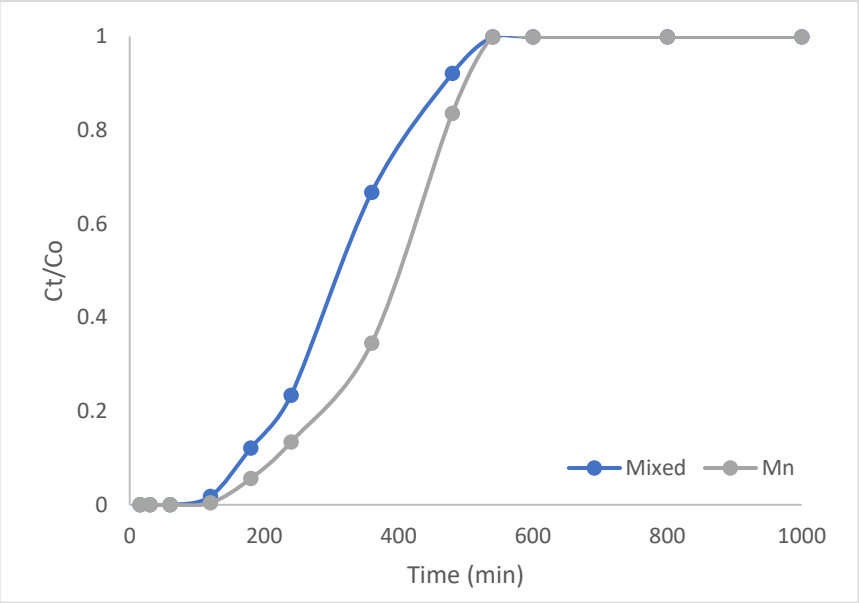
1
0.8
0.6
0.4
0.2
0
Ct/Co
0
200
400
600
800
1000
Time (min)
Mixed
Mn

(b)

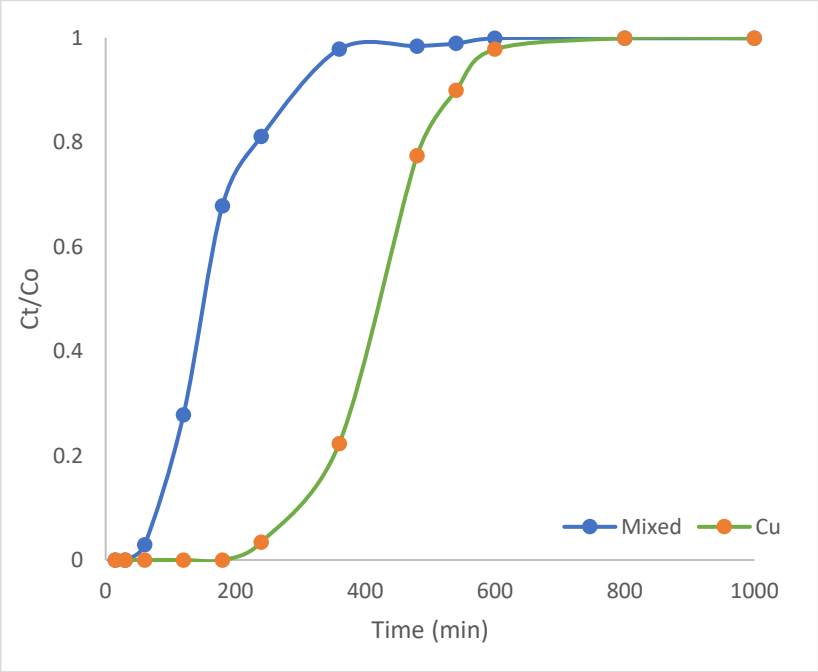
1
0.8
0.6
0.4
0.2
0
Ct/Co
0
200
400
600
800
1000
Time (min)
Mixed
Cu

(c)

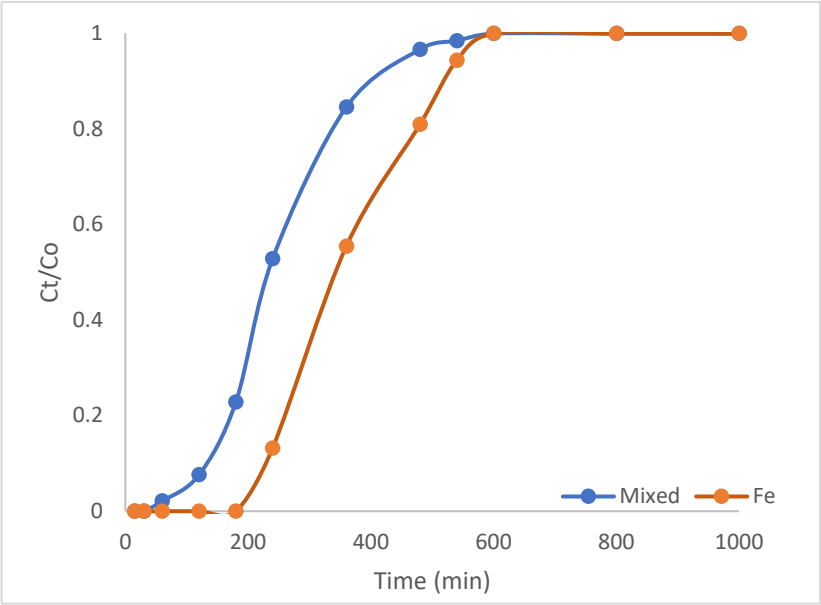

(d)

Figure 5.5 Breakthrough curve of single metal solution (a) Pb, (b) Fe, (c) Cu and (d) Cu and mixed metal solution (Park, J., 2015)

These findings can be attributed to the competitive mechanism, which can be explained by the affinity of the adsorption sites and the variations in the characteristics of the metals (Ni et al., 2019). The parameters that contribute to the adsorption performance are connected to (i) properties of metal ions, (ii) adsorbent characteristics, and its selectivity for each metal ion; (iii) the initial concentration of each metal ion; and (iv) the characteristics of the solution (Esfandiar et al., 2022). Lower hydration energy, higher ionic radius, higher valence, and electronegativity are the metal characteristics associated with increased adsorption. Therefore, the higher selectivity of sorbents for cations such as Cu and Fe in the multi-metal solutions resulted in the adsorption of Mn and Pb being less favorable. On a side note, high selectivity for Fe can be attributed to the low hydration energy in Fe.

Moreover, the initial concentration of competing metal ions in the solution can affect overall sorption. Higher initial concentrations have higher sorption chances due to more competitive ions than to other cations (Medina et al., 2021). In this research, Mn has the lowest initial concentrations of 50 mg/L followed by Pb (100 mg/L), then Fe (200 mg/L), and finally Cu (300 mg/L) presented the highest initial concentrations, which confirmed the above hypothesis. These findings suggest that competitive adsorption is an essential factor affecting metal adsorption, and therefore the coexistence of different metals must be considered when assessing the metal performance of adsorbents.

5.5 Heavy metal removal mechanisms

The potential mechanisms by which SMC biochar adsorbs metal ions includes surface adsorption, precipitation, ion exchange and complexation. Figure 5.6 shows the removal mechanisms for column study. Surface adsorption happens from weak Van-Der-Waals reaction and electrostatic forces. The metal ions adhere energy on the surface of the adsorbent and is governed by covalent bonds between metal ion and the surface structure of adsorbent. Hence, surface area plays an important role in this part. Furthermore, based on the study of initial pH and the surface morphological image of SMC biochar after adsorption, the formation of metal hydroxide confirms precipitation mechanism. The surface precipitation is highly dependent on the pH. At higher pH, redissolution of metal hydroxide takes place (Malik et al., 2018). Other possible mechanism is through ion exchange. This is supported by the abundant of cations available on the SMC biochar through EDX analysis. The cations are exchanged between the metals at the surface of adsorbent.

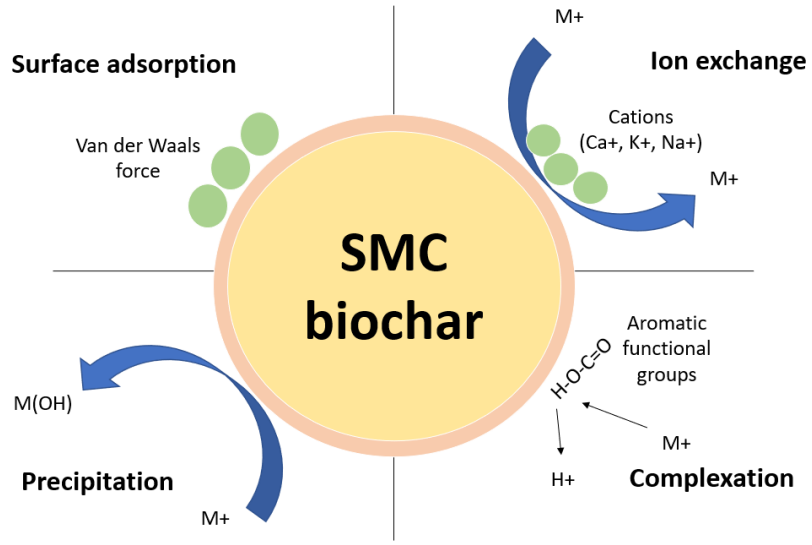

Figure 5.6 Removal mechanism of heavy metals in SMC biochar filter media

This process is aid by negatively charged surface functional groups available, leading to binding affinity with the positively charged metal ions. These results confirm the earlier conclusion from batch studies that although B500 has a much smaller surface area than B700, B500 showed the highest adsorption efficiency. B500 contains exchangeable cation sites for ion exchange and aromatic functional groups for complexation.

The surface functional groups available in all biochars that contributes to surface complexation removal mechanism. Lower pyrolysis biochar contains oxygen functional groups (carboxyl, and hydroxyl groups) that creates strong binding affinity with the metallic ions. In contrast, higher pyrolysis biochar contains aromatic functional groups that act as π-π electron donor acceptor interaction to bind with metal ions and create surface complexation mechanisms. This mechanism can be proven through FTIR analysis before and after adsorption where the surface functional groups were shortened or weakened after

adsorption. this showed that complexation process occurred between metal ions and the functional group. Notably, removal mechanisms by biochar varies depending on the nature of metallic ions. For example, many studies reported that Cu and Pb are usually removed through complex formation and precipitation (Biswal et al., 2022). Thus, SMC biochar has proven to have high capacity for adsorption of metal ions due to its surface heterogeneity characteristics, high surface area and pore volume. This biochar also contains multiple surface functional groups that aids in chemical adsorption.

5.6 Summary

After batch study, a continuous column study was initiated for further application of SMC biochar as filter media in heavy metal adsorption. B500 SMC biochar was chosen as filter media which gave the most effective adsorption capacity in batch study. A total of 17 different concentration sets from the lowest to the highest metal concentration were chosen with effect of pH and initial metal concentrations. The column study was interpreted through breakthrough curves and all breakthrough curves showed S shaped trends. From the column study, the adsorption capacities for Cu, Mn, Pb and Fe were 49.833 mg/g, 6.665 mg/g, 16.218 mg/g and 33.186 mg/g respectively. Predictive maximum adsorption capacity was simulated using Thomas model and the resultant $R^2 > 0.9$ show similar adsorption capacities to the experimental result, thus, Thomas model is strongly correlated with the experiment data. Competitive adsorption among heavy metals were explored and single metal solution gave higher adsorption performance than multimetal solution. The mechanism for these results were attributed to the resultant affinity for adsorption sites and the difference in metal characteristics.

Scaling up

Lab scale column study was assessed to study the relationship between adsorbate (heavy metals) and adsorbent (SMC biochar) in the adsorption system. The performance of the column study is analysed by breakthrough curves, which represent the pollutant-effluent concentration versus time profile. Most adsorption studies were conducted on synthetic solution as adsorbate, in which metal solution is prepared and treated with adsorbent. The effect of various process parameters such as pH and initial metal concentration were performed, and all these parameters are essential in evaluating the efficiency of SMC biochar as an adsorbent in a continuous treatment process of effluents on a pilot or industrial scale. The experimental approach was based on techniques commonly used in wastewater studies, and the column study was chosen according to the literature (Boni et al., (2021), Chittoor et al., (2020) and Patel, (2019)) and Urban Stormwater Management Manual Malaysia (MSMA).

While the columns were small relative to the size of a field-scale filter, a smaller column size was necessary to achieve a breakthrough in a reasonable time frame. This study focused on the removal performance of heavy metals from abandoned mine water using SMC biochar as filter media. According to Hatt (2011), problems with upscaling from laboratory to field conditions occur due to homogenous laboratory conditions compared to heterogenous field conditions. However, given that soil-based filters are engineered systems, they are relatively homogenous at laboratory and field scales. Although the lab scale column study has demonstrated effective results, it is important to check out and implement a larger scale column in order to further understand if the mechanics, breakthrough and adsorption capacities are affected with the scale increment, thereby unleash the true potential of this technology and implement in an industrial scale in the future. In order to scale up the column design, it is vital to recollect

experimental data from lab scale study. The lab scale column study must be able analyze all the experimental conditions available, so that the large scale test should successfully replicate or has high correlation with the lab scale tests (Juela et al., 2022). Consideration of breakthroughs in the design process is critical, especially in high rainfall areas, such as Malaysia, where breakthroughs can occur very quickly if a filter is small relative to its catchment or has a shallow filter media depth. Such a filter would have associated with high maintenance requirements as removing spent filter media regularly would be necessary. On the other hand, a large or deep filter relative to its catchment may give many years until a breakthrough occurs hence a longer exhaustion time.

Heavy metal recovery of SMC biochar

Based on the column study in this research, SMC biochar as filter media has proven to efficiently remove heavy metals from mine water. It is not just promoting sustainability due to reusing waste material as filter media to remove heavy metals, SMC biochar encourages adsorption process which is a very promising method to remove various pollutants. Adsorption process is recognized as better technique compared to other process due to its effective removal of pollutants, feasibility of low cost adsorbents and simplicity in design (Patel, 2021). This water treatment by economical and effective method is vital in the era of development and technological advancements. However, one of the disadvantages of this process is that it leaves behind hazardous spent adsorbent which require special supervision. In the adsorption process, after some time, the adsorbent will get fully saturated due to the occupying of adsorption sites with adsorbent, upon equilibrium. Therefore, adsorbent has become exhausted and need to be replaced. The spent adsorbent is considered as solid hazardous waste and is usually dumped into the landfill site or incinerated, which creates environmental problems (Vakili et al., 2019).

Nevertheless, researchers are working on the solutions and one of the outcomes is through recovery or regeneration process. From the economic and environmental point of view, the recovery process is a vital aspect to focus upon. The disposal of hazardous spent adsorbent creates various environmental implications and recovery method can reduce the problem. Various recovery methods have been utilised with differing degrees of success. These methods include regeneration and desorption process. Various techniques are available to regenerate the exhausted adsorbent, but desorption method is the most preferred technique for its economical and effective regeneration process factors. Desorption process includes thermal, electrochemical, ultrasonic, and chemical methods where the solvents is called eluting agent (Kulkarni & Kaware, 2014). Spent adsorbent is washed with water and then treated with an eluting agent through batch or column treatment. Then, treated adsorbent is flushed with water to remove eluting agent from the adsorbent making it ready for further adsorption.

Feasibility of the desorption process lies on the desorption efficiency and regeneration cycles (Banerjee et al., 2021a) where based on the literature, most of the adsorbents can regenerate to an average of 4-5 cycles with 80 – 85 % removal (Banerjee et al., 2018; Lata et al., 2015). It can be concluded that regeneration, reuse of adsorbent and recovery of solute are vital aspects of the adsorption that need to be considered when applying in industrial scale applications. Subsequently, used SMC biochar can be used for carbonisation in agricultural industry. The reuse of spent biochar as fertilizers is an effective approach to be considered in the future. By burying the spent biochar, it can improve crop yields as the metal ions coated biochar contains all the necessary metals as nutrients to enhance crop productions (Patel, 2021).

Comparison of adsorption capacities of SMC biochar with previously reported adsorbent

The application of SMC as biochar is still relatively new in the research field especially its application as filter media in mining related water. Table 5.3 summarizes the adsorption capacities from other previously reported feedstock biochars. Compared to other feedstock biochar, SMC shows great adsorption capacity. The adsorption capacity for Pb, Cu, Mn and Fe was shown to be 16.218 mg/g, 49.833 mg/g, 6.665 mg/g and 33.186 mg/g respectively which is higher than pinewood, sewage sludge, rice husk and manure biochars. However, the Pb adsorption for SMC biochar was lower than rice husk biochar but were higher than other types of biochars. Additionally, the adsorption capacity of SMC biochar in this study were much higher than other SMC biochars from literature. There are many factors contributing to this predicament from the pyrolysis production and the experimental conditions involved. Henceforth, from this study and Table 5.3, it is concluded that SMC biochar is an ideal adsorbent for removing heavy metals and has the potential to be filter media in a heavy metal retention system for mining water treatment.

Table 5.3 Comparison of the adsorption capacities of SMC biochar towards the heavy metal removal with literature results

Biochar	Heavy metals	Adsorption capacity (mg/g)	References
Rice husk	Cu	37.5	(Samsuri et al., 2014)
	Pb	43.9	
	Zn	34.3	
Orange peel	Cu	27.86	(Abdelhafez & Li, 2016)
Swine and goat manure	Cu	40.64	(D. Wei et al., 2018)
Sewage sludge	Cu	0.19	(Bakshi et al., 2018)
	Pb	0.926	
	Zn	0.2	
Pinewood	Pb	4.91	(L. Wang et al., 2019a)
Spent mushroom compost biochar	Mn	3.341	(Yunus et al., 2020)
	Pb	15.16	(Frutos et al., 2016)
	Cu	36.2	(Frutos et al., 2016)
	Pb	17.344	This study
	Cu	49.833	
	Mn	7.665	
	Fe	32.186	

Chapter 6 Biochar modelling and detailed design charts

6.1 Introduction

This chapter discusses the results obtained from the final stage of the research. This stage involved biochar modeling using machine learning namely Adaptive Neuro Fuzz Inference System (ANFIS) model and Multilinear Regression (MLR) model. This chapter is presented in three sections, which are Sections 6.2 & 6.3, Section 6.4 and Section 6.5. Sections 6.2 and 6.3 demonstrated the biochar modeling structures and designs for both ANFIS and MLR models. These sections discussed the main components of the models as well as the model parameters. All 17 data sets from the lab scale metal retention column were modeled and the results were presented in the form of model evaluation and model performances. Subsequently, both the ANFIS and MLR evaluations are compared and the prediction performances are further discussed. Next, Section 6.4 covered model validation using ANFIS models.

Three abandoned mining ponds were chosen as validation study sites and water sampling was taken to analyse the heavy metal concentration level of these sites. Then, the sample data were simulated with ANFIS model to compare the performance and the validation results are presented. Finally, Section 6.5 demonstrated the result outcomes from the ANFIS and MLR models in the form of detailed design chart. The design charts portrayed the predicted adsorption capacities of Pb, Mn, Cu and Fe using SMC biochar as filter media at a range of initial metal concentrations with different pH of 2,5,7 and 10. In general, the biochar modeling and the assembled prediction design charts satisfied objective 3 of this research.

6.2 Biochar modelling using ANFIS model

Machine learning techniques are based on computer algorithms and models to predict the adsorption property of concern through experience. It is proven to be useful tools for process design, and regression models as it has been widely recognized for its benefits including time savings, and high prediction accuracy. There are a lot of machine learning methods, however, in this study, ANFIS model was chosen as this model can efficiently address and solve complex nonlinear environmental issues. Based on literatures, this model has proven its efficiency in modelling prediction with higher correlation coefficient than other machine learning techniques in heavy metals removal (Chittoo & Sutherland, 2020; Tulun et al., 2021).

After the lab scale metal retention column study, all the 17 sets of experimental data collected were used for biochar modeling using the ANFIS model. A total of 749 data were available for ANFIS model. Each network was trained and tested, and the corresponding correlation coefficient (R^2), root mean square error (RMSE) and mean absolute error (MAE) of all models were calculated and compared. One of the important aspects that need to be solved is the structure and components of the ANFIS model. In this study, ANFIS model was developed with MATLAB to predict the adsorption capacities of heavy metals using SMC biochar as filter media. The input layer was the initial metal concentration (mg/L) and pH range from 2 – 10, while the output layer was the adsorption capacity (mg/g).

ANFIS model performance was analysed through different model parameters such as the number of membership functions (MF), membership function type, and epoch number. After trial and error runs and using default values from MATLAB and literatures, the design and structures were completed. Table 6.1

shows the parameters for the model. The setting parameter is shown in the table where the epoch number of 10, 2 number of MF, and Gaussian type of MF were chosen as the best method for ANFIS in predicting heavy metal adsorption capacity, with maximum R^2 and accuracy and minimum RMSE and MSE values (Wong et al., 2020). The Sugeno system was the most utilised system as it is proven to be compact and efficient (Wong et al., 2020). Hence, Sugeno-type ANFIS was adopted in this study and comprises of five layers: layer 1 is input layer, layer 2 the fuzzification layer, layer 3 the logical rule layer, layer 4 the defuzzification layer, and layer 5 the output layer. In this algorithm, MF defines the degree of the database related to the cluster. It can be observed that the most optimum number of MF was determined to be 2 with Gaussian type MF, where increasing the number yield diminishing results (Chang et al., 2017). Additionally, after trial and error run, epoch number 10 was the result and adopted for the model.

The developed model obtained MAE of 0.000647 at MF of 2. The error obtained was negligible and this stipulated that the predicted adsorption capacities is at best fit with the experimental data. Additionally, correlation coefficient R^2 of 0.9999 was obtained and this indicates that the predicted and experimental adsorption capacities are closely equal. These confirms the great strength of the developed model in predicting adsorption capacities of heavy metals using SMC biochar as filter media and is suitable to be used to model any adsorption capacities related data.

Table 6.1. Model parameters of the ANFIS model

Model parameters	
Fuzzy inferency type	Sugeno
Clustering method	Grid partitioning
No. of membership functioning per variable	2
Input membership function type	Gaussian membership function
Output membership function type	Linear
Epoch number	10

The graphical comparison between the predicted results and experimental data for Cu, Pb, Mn and Fe adsorption using the Gaussian MF by ANFIS is illustrated in Figure 6.1. The plots indicate that ANFIS model was successfully trained since most of the predicted data are close to the experimental datasets. The scattering ranges of predicted values showed great fit towards the linear line and the ability of the developed ANFIS model to represent data in the experimental data set is >97 %. This developed model has similar or better results than many models from literature (Agbaogun et al., 2021; Hafsa et al., 2020; Tulun et al., 2021). For this reason, the ANFIS models were capable in predicting the final adsorption capacity of heavy metals. Nevertheless, it can be observed that Pb and Mn showed slight outliers than Fe and Cu. This statement can be further proven by the evaluation performance for ANFIS model in terms of statistical parameter presented in Table 6.2.

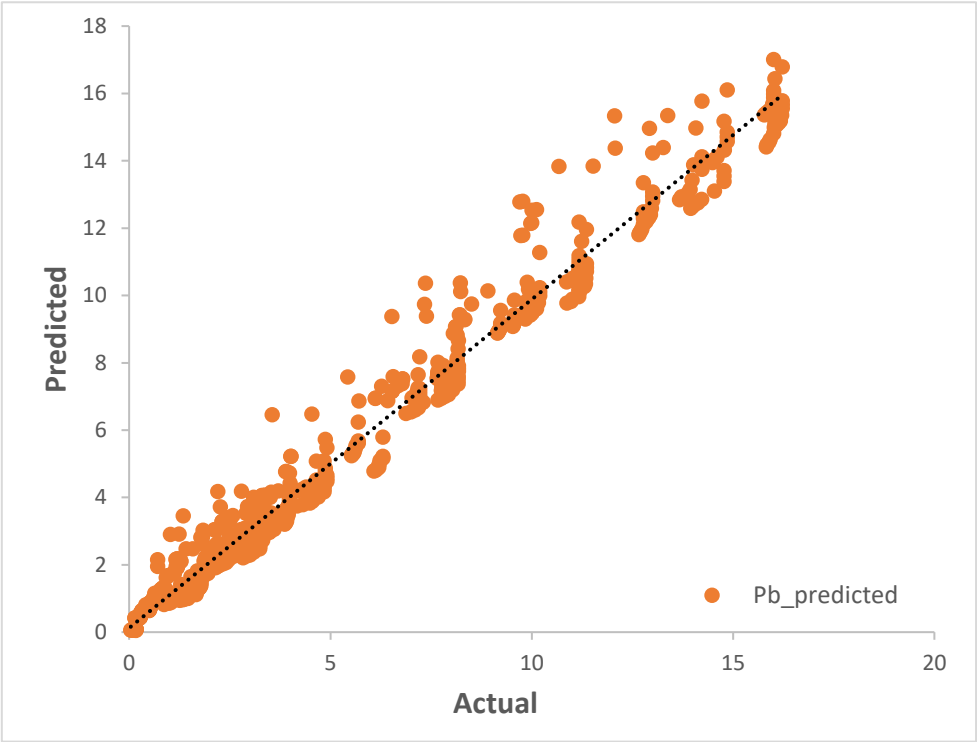
18
16
14
12
10
8
6
4
2
0
Predicted
0
5
10
15
20
Actual
Pb_predicted

(a)

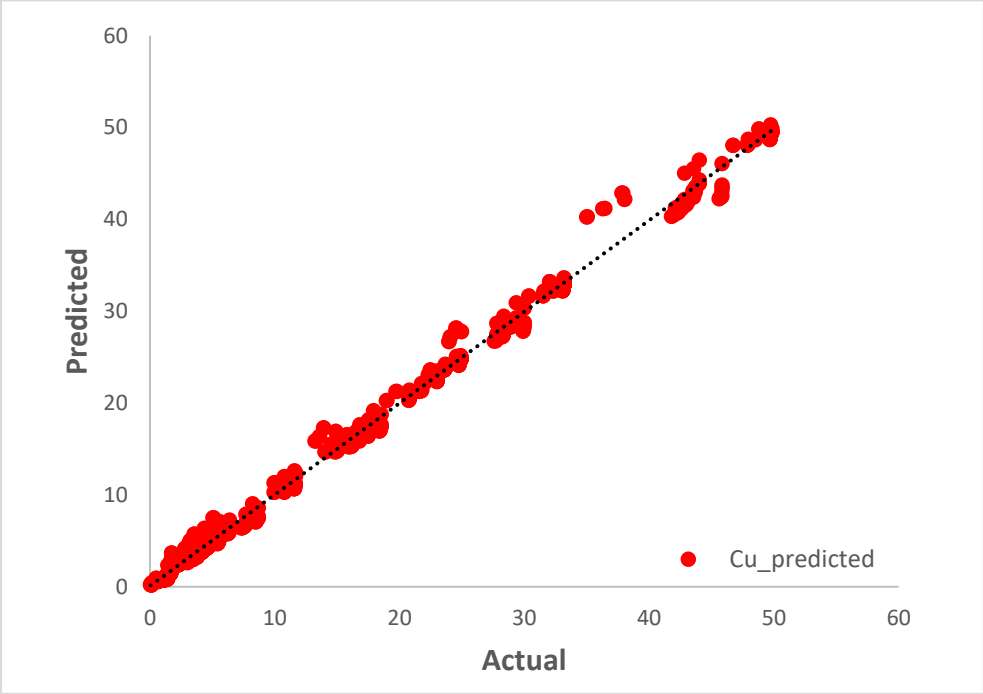
60
50
40
30
20
10
0
Predicted
0
10
20
30
40
50
60
Actual
Cu_predicted

(b)

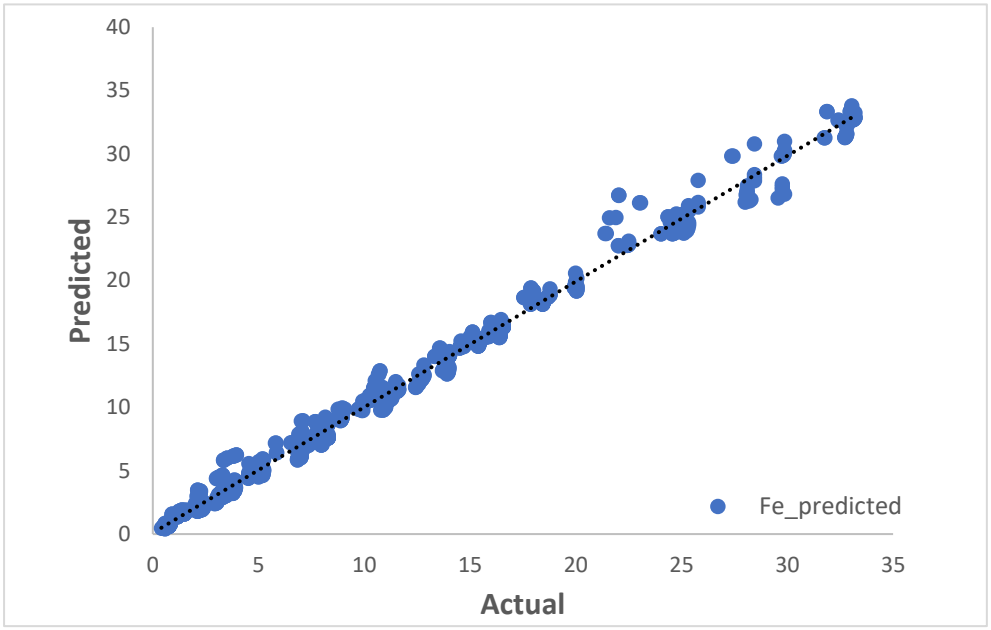

(c)

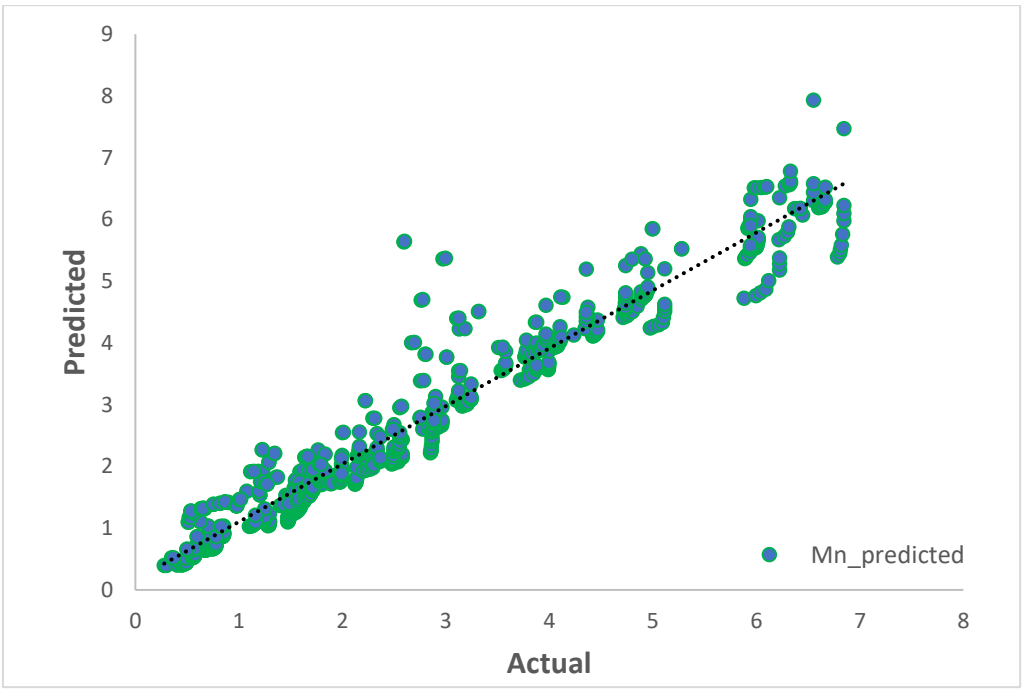

(d)

Figure 6.1 Model calibration results for (a) Pb, (b) Cu, (c) Fe and (d) Mn using ANFIS model

Table 6.2 Performance evaluation of heavy metals using ANFIS model

	ANFIS		
Heavy metals	R^2	RMSE	MAE
Pb	0.979	1.112	0.564
Fe	0.998	1.823	1.023
Cu	0.999	2.315	2.685
Mn	0.983	0.814	0.556

In order to evaluate the accuracy of the model, the model was assessed based on R^2, RMSE and MAE. Generally, ANFIS model showed great performance for all heavy metals with $R^2 > 0.97$. The highest R^2 was demonstrated by Cu (0.9992), followed by Fe (0.9985), and Mn (0.9833), and Pb (0.9799) gave a much lower R^2. This explains why Mn and Pb had outliers and this is expected due to the low adsorption capacity of Pb and Mn in lab scale retention column study. Consequently, low RMSE and MAE values indicates great fitting for all heavy metals except for Cu. Among all heavy metals, Cu had slightly higher RMSE and MAE. This may be due to the nature of biochars that contain more ash and organic matter which complicates the interactions between Cu and SMC biochar (Zhao et al., 2022). This suggests that the ANFIS prediction are consistent with the experimental values. Figure 6.2 shows the plot of the fitting between experimental and simulated data for all heavy metals where Cu, Pb, Mn and Fe presented good fitting effect.

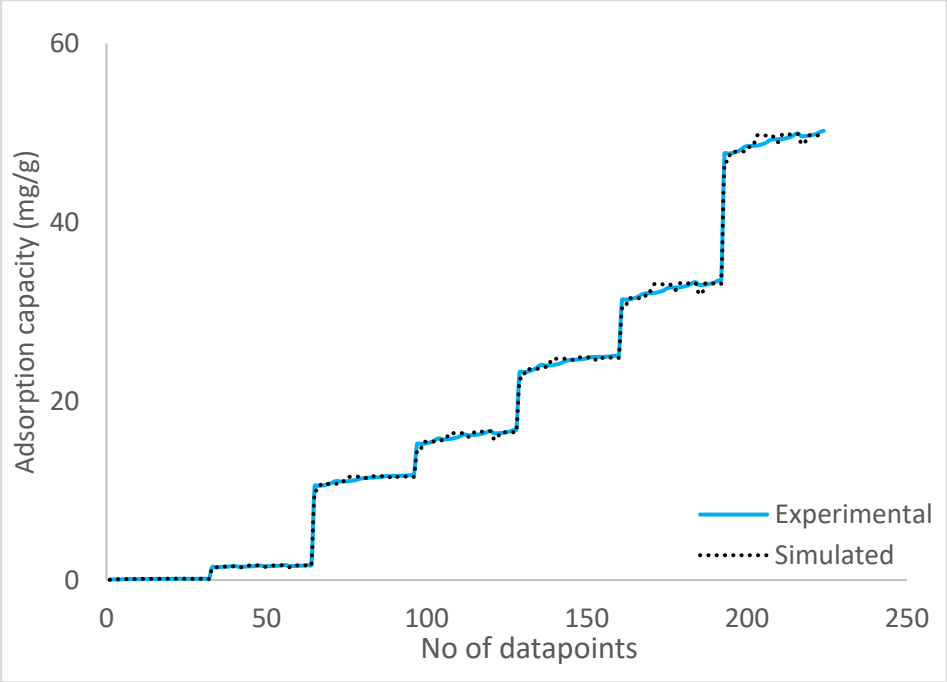
60
40
20
0
Adsorption capacity (mg/g)
0
50
100
150
200
250
No of datapoints
Experimental
Simulated

(a)

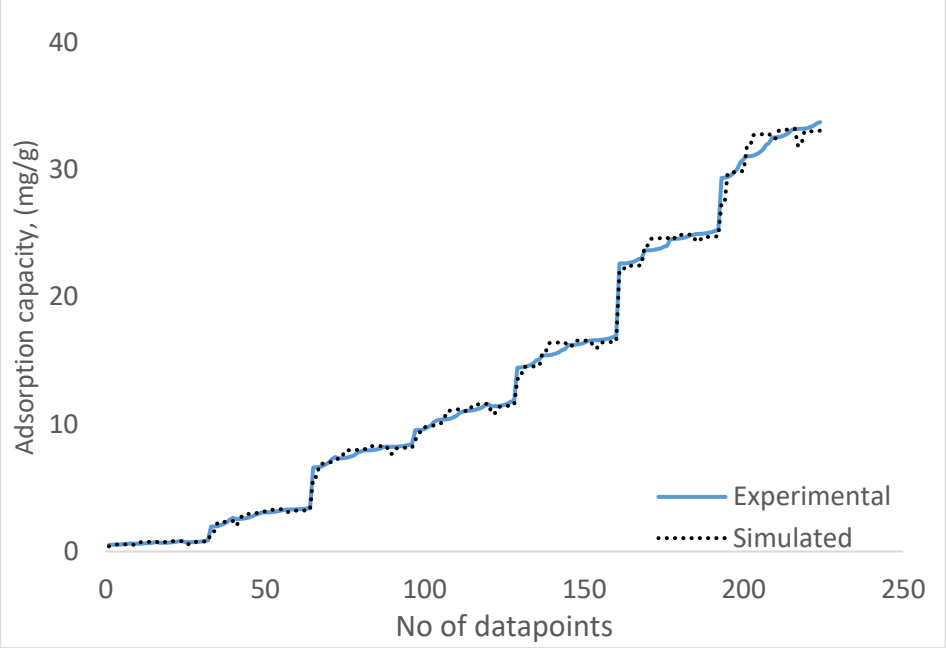
40
30
20
10
0
Adsorption capacity, (mg/g)
0
50
100
150
200
250
No of datapoints
Experimental
Simulated

(b)

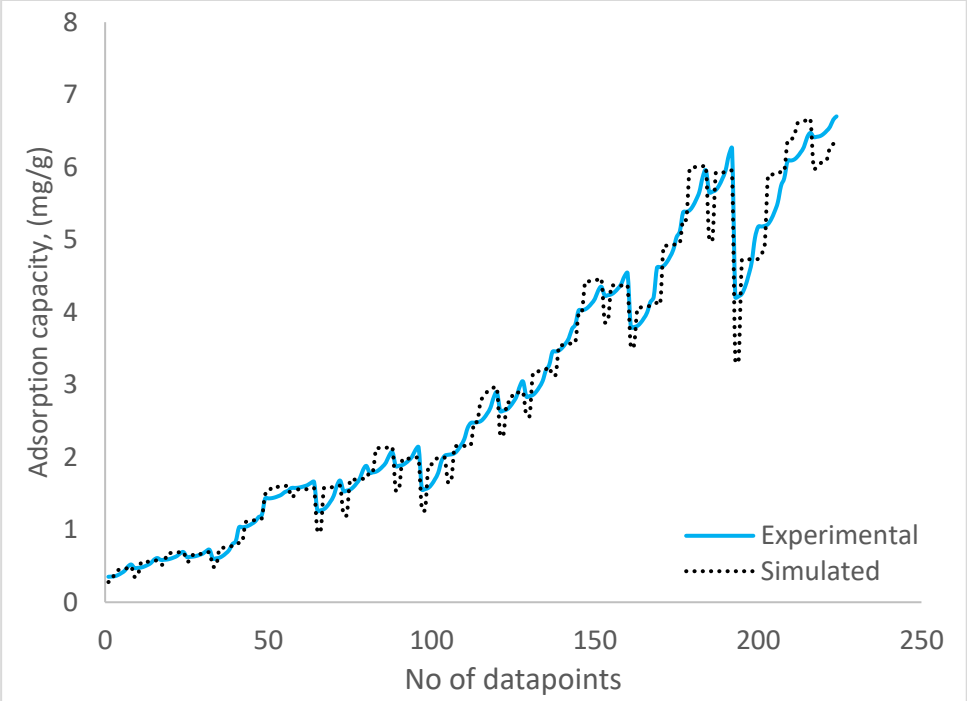

(c)

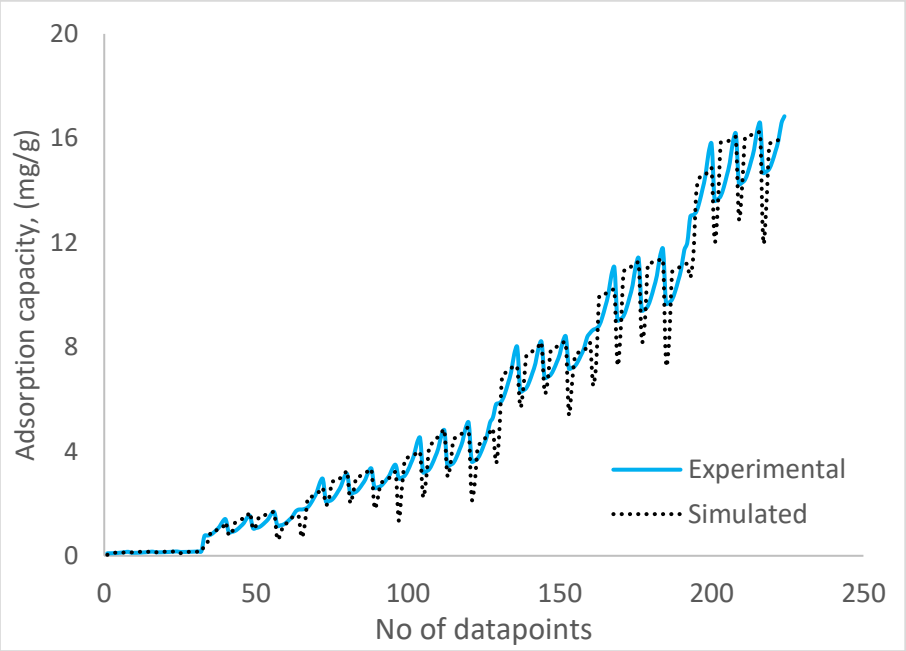

(d)

Figure 6.2 Graph of experimental versus simulated data of (a) Cu, (b) Fe, (c) Mn and (d) Pb generated by ANFIS model

6.3 Biochar modelling using MLR model

For MLR analysis in the column study, the heavy metals (Pb, Fe, Cu and Mn), time and pH were the independent variables. In contrast, the dependent variable is the adsorption capacities (y). MLR model has been a powerful method for exhibiting statistical relationship between dependent and independent variables (Banerjee et al., 2021b). It is a statistical analysis method which is widely used to regulate quantitative relationships between two or more variables using mathematical statistics (Jiang et al., 2019). The relationship between experimental values and model predicted for Cu, Pb, Mn and Fe using MLR model is presented in Figure 6.3. It is observed that the predicted value and experimental data have good fitting effect except for Mn. Notably, with many outliers in Mn, the predicted value in Mn was more scattered in MLR as compared to ANFIS. This statement can be further supported through model evaluation performance in Table 6.3. Based on the coefficient correlation, all heavy metals produced good result with R^2 >0.9 and Cu produced the highest R^2 of 0.9828, followed by Fe (0.9816), Pb (0.9612) and finally Mn (0.9012). Correspondingly, the sequence from highest to lowest heavy metals is similar to ANFIS model.

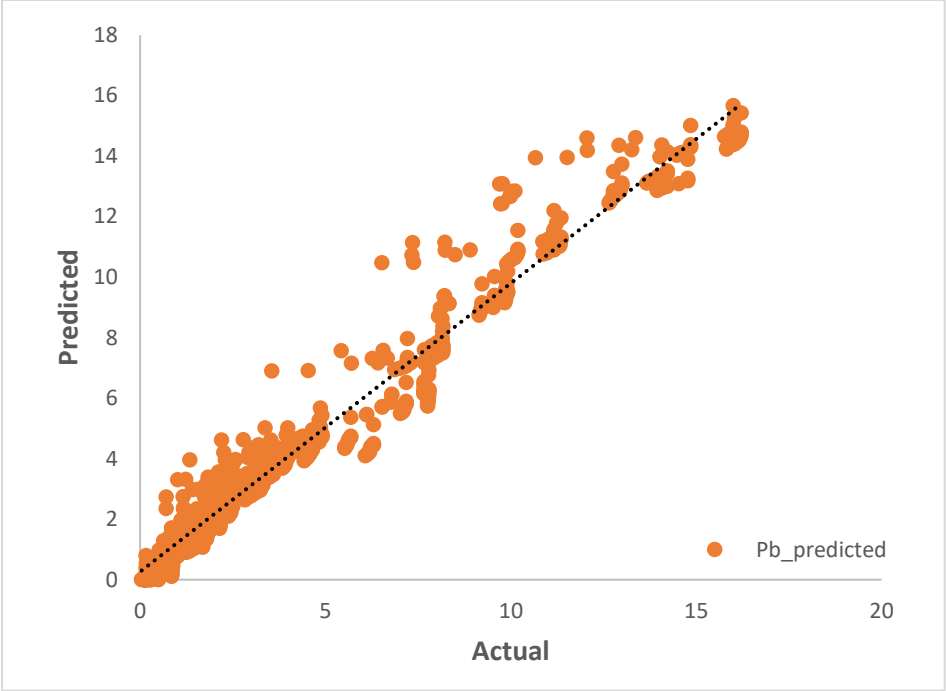
18
16
14
12
10
8
6
4
2
0
Predicted
0
5
10
15
20
Actual
Pb_predicted

(a)

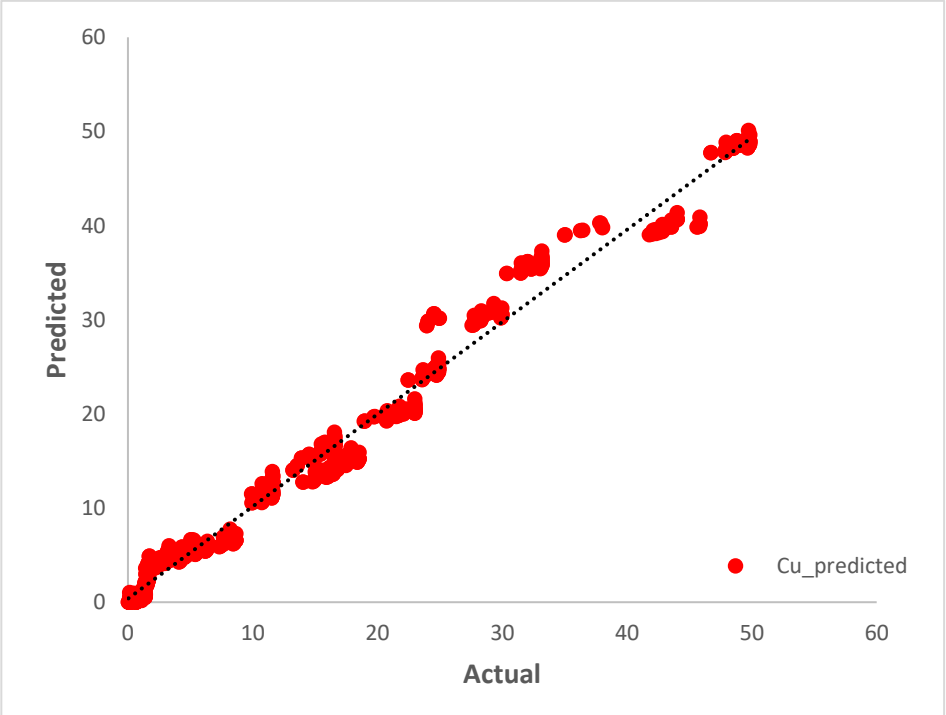
60
50
40
30
20
10
0
Predicted
0
10
20
30
40
50
60
Actual
Cu_predicted

(b)

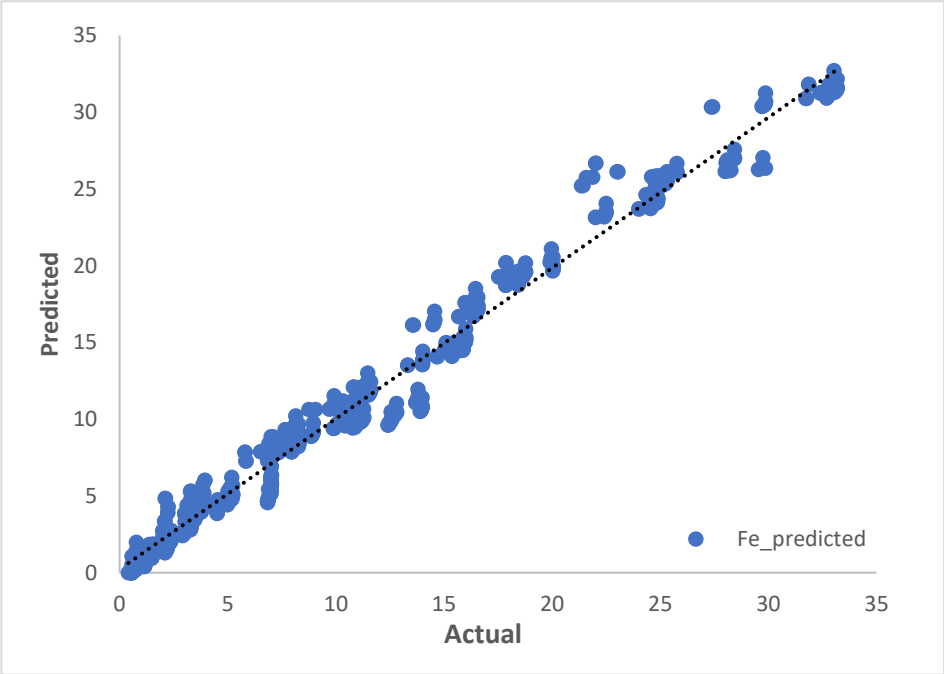

(c)

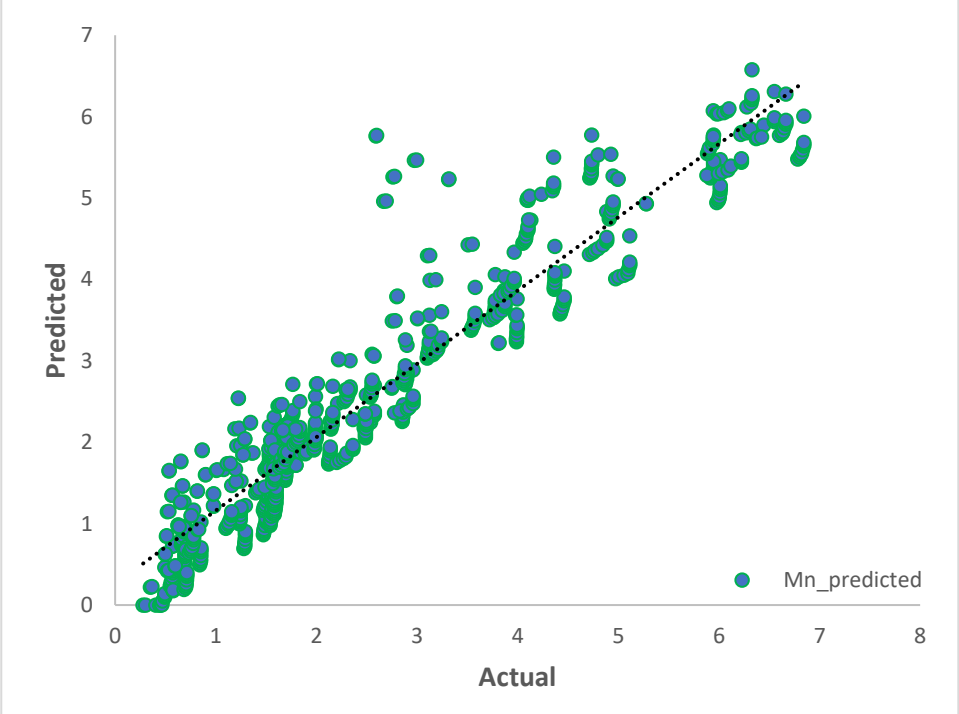

(d)

Figure 6.3 Model calibration results for (a) Pb, (b) Cu, (c) Fe and (d) Mn using MLR model

Table 6.3 Performance evaluation of heavy metals using MLR model

	MLR		
Heavy metals	R^2	RMSE	MAE
Pb	0.961	1.953	0.834
Fe	0.981	2.863	1.876
Cu	0.982	7.121	4.482
Mn	0.901	0.991	0.633

Overall, the MLR model has successfully produced a series of linear equations of adsorption capacities for each heavy metals. The series of linear equations are presented by Equation 10 to 13.

$$Y_{Pb} = \big(Pb(0.534) + Fe(1.811) + Cu(-0.484) + Mn(2.483) + pH(0.239) + time\ (0.293)\big) + 5.140 \quad (10)$$

$$Y_{Fe} = \big(Pb(-0.5666) + Fe(4.361) + Cu(3.557) + Mn(6.590) + pH(0.534) + time(0.250)\big) + 11.831 \quad (11)$$

$$Y_{Cu} = \big(Pb\ (-5.076) + Fe(9.886) + Cu(5.370) + Mn(3.964) + pH(0.461) + +time(0.305)\big) + 16.888 \quad (12)$$

$$Y_{Mn} = \big(Pb(-1.055) + Fe(0.438) + Cu(-0.304) + Mn(2.50) + pH(0.293) + time(0.150)\big) + 2.614$$

. (13)

Conversely, Table 6.4 illustrates the linear coefficients of the equations using MLR. It is interesting to note that the Fe and Cu coefficients are much reduced when high concentrations of Pb are present. These circumstances highlight the competition between heavy metal interactions in the biochar, and this is supported by the competition adsorption discussed in the column study. Fe and Cu removal were highly effective due to higher affinity and the higher selectivity of cations resulting in the inhibition removal of Pb and vice versa.

Table 6.4 Linear coefficients using MLR

Heavy metals	Pb	Fe	Cu	Mn	pH	Time (min)	intercept
Pb	0.534	1.811	-0.484	2.483	0.239	0.292	5.140
Fe	-5.666	4.361	3.557	6.590	0.534	0.250	11.831
Cu	-5.076	9.885	5.370	3.954	0.460	0.305	16.888
Mn	-1.055	0.437	-0.303	2.500	0.292	0.149	2.614

In contrast, it can be observed that Cu adsorption accelerated with greater concentrations of Fe which infers a tremendous mutual relationship between these cations. Despite that, both Cu and Fe have more outstanding hydrolysis content, higher atomic weight, and high ionic radius (Lee & Shin, 2021). Finally, a low concentration of Mn results in high concentrations in other metals, especially Fe, which confirms the negligible weak affinity of Mn. Oxidation of Mn occurs slower than other metals, resulting in lower redox

potential for removal. Additionally, Mn requires higher pH to oxidise, which is 6 to 9 times slower than Fe; thus some removal of Mn will occur as long as Fe is present (Neculita & Rosa, 2019). Generally, through these equations, predictions can be made with a very high reliability and a low margin of error. Equation 14 showed a margin of error of 3.654% with a confidence level of 95%. Thus, it is possible to save cost, time and labor force significantly in predicting removal efficiency in the future. Overall, MLR presented good results in this study, thus, it can be concluded that MLR is capable of predicting the adsorption capacity of heavy metals using SMC biochar as filter media. The adsorption capacity prediction can be simplified in a series of linear equations. This is an excellent outcome in this study, as the predictions can be made without much leverage on complex machine learning.

$$Margin\ of\ error = \frac{100}{\sqrt{749}} = 3.654\ \%$$

(14)

A comparison is made between MLR and the ANFIS model in order to evaluate the prediction performance. The MLR model constructed includes independent variables similar to the ANFIS model. Table 6.5 shows the evaluation performance comparison between ANFIS and MLR models. Based on the results, both ANFIS and MLR models showed $R^2 > 0.9$. Therefore, it can be concluded that the relationship between the predictions and metal adsorptions is linear. Thus, both models could predict the heavy metal's adsorption capacities. However, the ANFIS model showed higher performance than MLR, with R^2 closer to 1.

Table 6.5. Prediction performance comparison between ANFIS and MLR for each metal

	ANFIS			MLR		
Heavy metals	R^2	RMSE	MAE	R^2	RMSE	MAE
Pb	0.9799	1.112	0.564	0.9612	1.953	0.834
Fe	0.9985	1.823	1.023	0.9816	2.863	1.876
Cu	0.9992	2.315	2.685	0.9828	7.121	4.482
Mn	0.9833	0.814	0.556	0.9012	0.991	0.633

Furthermore, the RMSE and MAE values for all metals in ANFIS are much closer to zero than MLR. MLR model is one of the most commonly used regression techniques due to its simplicity and straightforward interpretation compared to ANFIS. However, this model has a significant limit, where nonlinear modeling relationships in the adsorption process can be challenging. On the other hand, the ANFIS model performs better due to the integration of neural network learning capabilities and fuzzy logic principles into one framework, making it capable of establishing a significant relationship between input variables with the final adsorption capacities in the adsorption process. Arising from all these observations, it can be concluded that ANFIS performs better than MLR in predicting adsorption capacities of heavy metals. This is supported by numerous researches that reported the high performance of the ANFIS model in heavy metal adsorption (Jamei et al., 2022; Khalil et al., 2018; Said et al., 2022; Wong et al., 2020).

6.4 Model validation

This section assesses the validation performance of the ANFIS model with actual case studies. It is an important step to identify how the model set would behave on new data. Three sites were chosen as the validation sites, and the abandoned mine water were sampled and injected into the lab column study as influents with SMC biochar as filter media. Next, the effluents results were taken and analysed, and then the results were compared with the ANFIS model. The outcomes were examined for specific measures such as R^2, RMSE, and MAE values. Figure 6.4 shows the model validation result of each heavy metal. Overall, the model fit well in line with the case study for all three sites. When the predicted values are closer to the validation data, the model demonstrated good accuracy and reliability is achieved. Table 6.6 shows the evaluation performance of each heavy metal of the model validation. Overall, the highest R^2 value is Cu (0.9553), followed by Fe (0.8061), Pb (0.7952), and Mn (0.647).

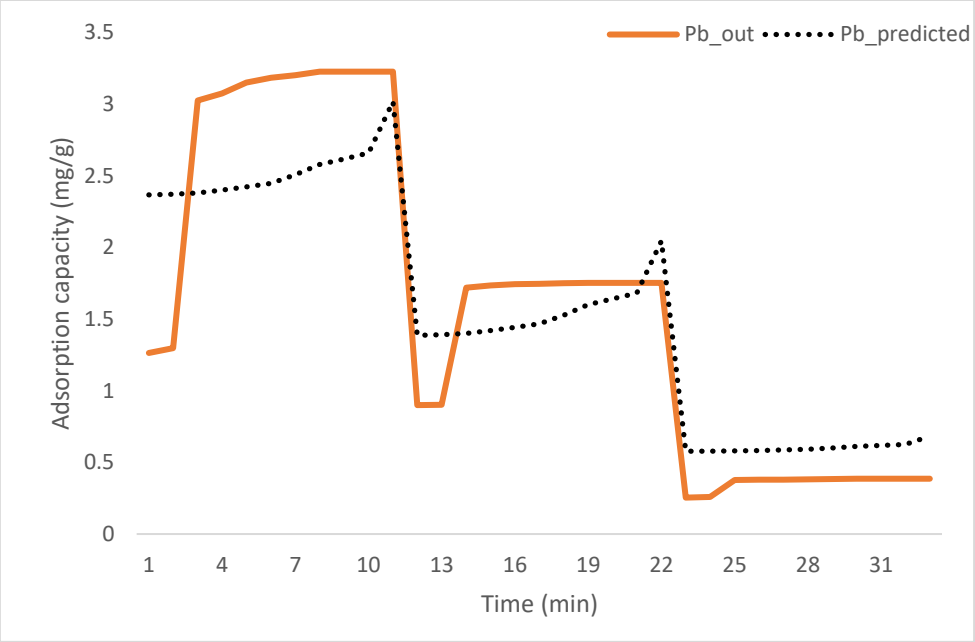
Pb_out
Pb_predicted
Adsorption capacity (mg/g)
3.5
3
2.5
2
1.5
1
0.5
0
1
4
7
10
13
16
19
22
25
28
31
Time (min)

(a)

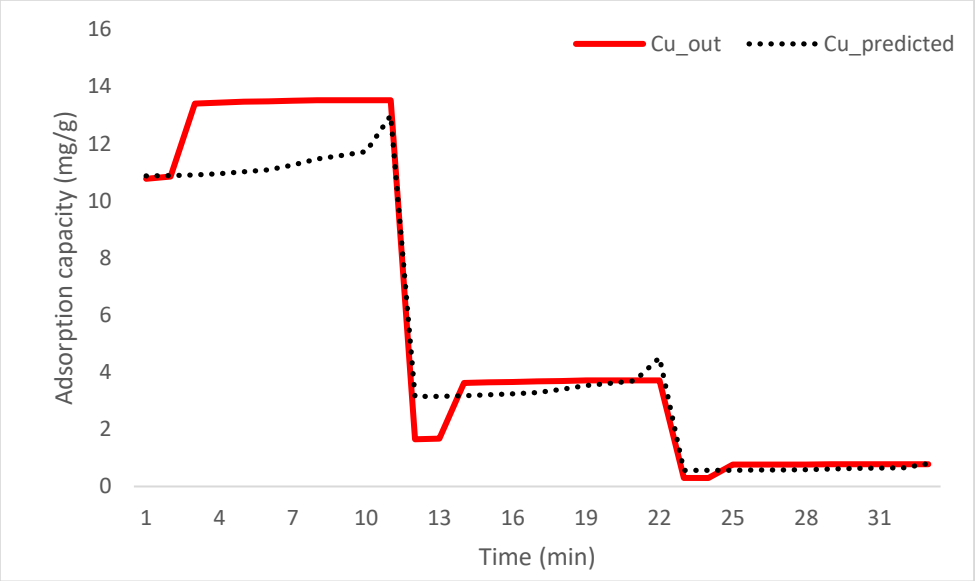
Cu_out
Cu_predicted
Adsorption capacity (mg/g)
16
14
12
10
8
6
4
2
0
1
4
7
10
13
16
19
22
25
28
31
Time (min)

(b)

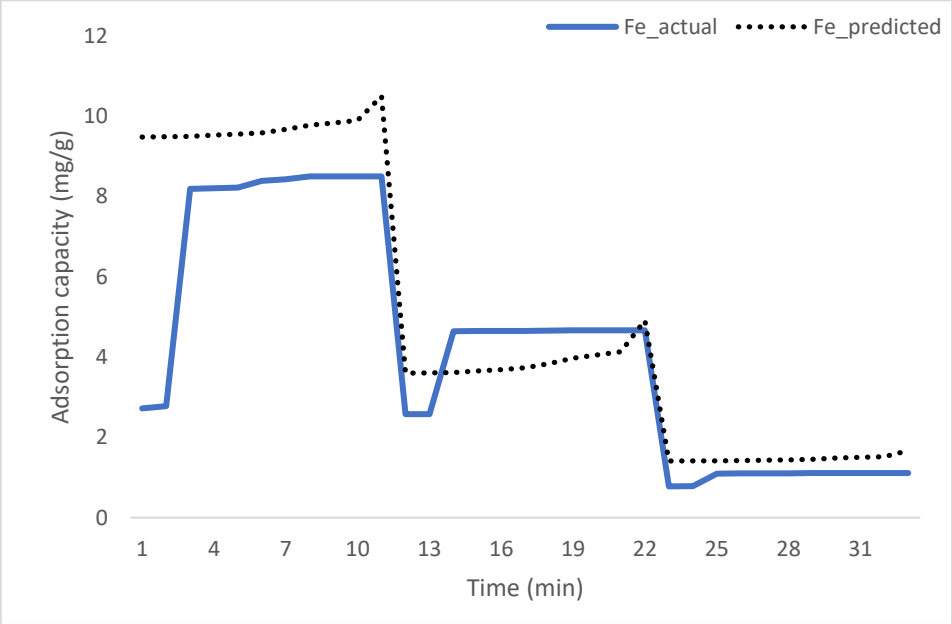

(c)

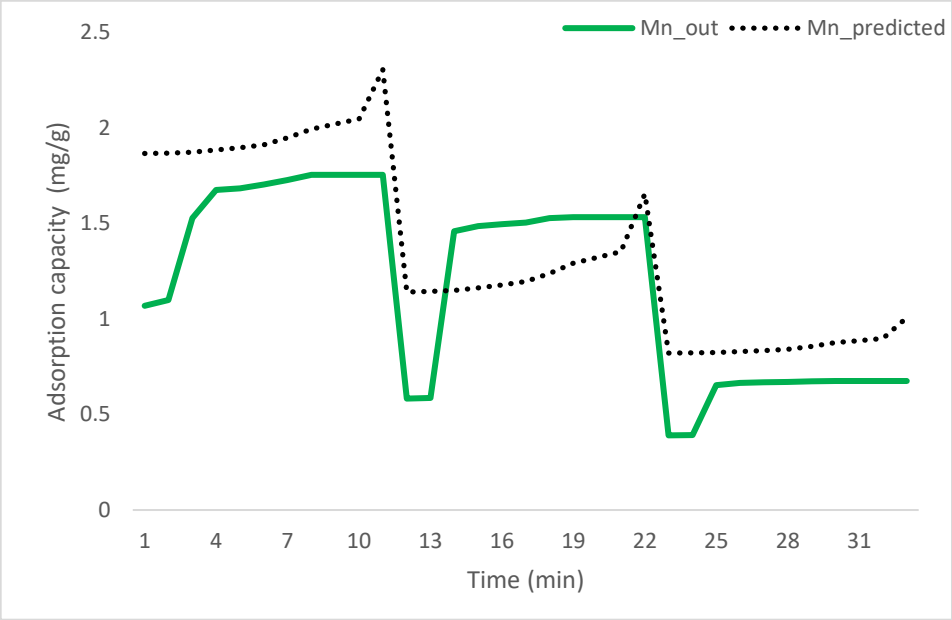

(d)

Figure 6.4 Model validation of (a) Pb, (b) Cu, (c) Fe, and (d) Mn

Table 6.6 Evaluation performance of heavy metals in model validation

	Pb	Cu	Fe	Mn
R^2	0.795	0.955	0.806	0.647
RMSE	1.528	1.120	1.562	2.690
MAE	0.998	0.482	1.476	0.433

Respectively, all developed modes showed good accuracy where the validation and predicted data were close enough to the line (Abdi & Mazloom, 2022). The RMSE values for all metals fluctuations are than 2 except for Cu, while MAE values for all heavy metals were towards zero, indicating the models have been well developed with acceptable accuracy. Hence from the detailed analysis, the developed model for the novel system is accurate with good correlation coefficient. From the developed model, the scale up of the system can be possible in future research work.

6.5 Detailed design charts

In summary, this study assesses the performance of SMC biochar as filter media to remove heavy metals from mining water. In order to evaluate the performance, the first step is the production and characterisation of the SMC biochar. Next, a batch study is performed to distinguish the performance of SMC biochar produced at multiple pyrolysis temperatures and its effect in removing heavy metals with the influence of environmental conditions of pH, initial metal concentrations, time, and adsorbent dosage. The pyrolysis temperature biochar that gave the highest heavy metal removal was chosen as the filter media for the lab metal retention column study. This study is conducted to determine the performance

of biochar as filter media in a continuous system. This phase is essential as the continuous system can imitate the actual water treatment process for future work. In the column study, the research was conducted with the influence of pH and initial metal concentration to discover the adsorption capacities performance of heavy metals onto the filter media. In advance of this study, a total of 749 datasets were analysed and run for biochar modeling using machine learning to predict the adsorption capacities of heavy metals onto the filter media. As a result, detailed design charts of heavy metals are produced to predict the adsorption capacities of heavy metals with the effect of initial metal concentrations and pH.

Figure 6.5 illustrates the design charts of Pb, Fe, Cu, and Mn that portray the predicted adsorption capacities at a range of initial metal concentrations with different pH of 2,5,7 and 10. Based on the graphs, it can be observed that all metals have similar accelerating trends where the increment of initial metal concentration increases the predicted adsorption capacities. All metals showed the same trend except for pH 7 and pH 10 in Mn, where the adsorption capacities decreased when the metal concentrations reached 45 – 50 mg/L. This could be due to the saturation that inhibit other Mn removal. Removal of Mn is less favorable with the existence of other metals (Joseph et al., 2019). Nevertheless, the increasing pH trend for the design chart demonstrated as pH 2 > pH 5 > pH 7 > pH 10 for all heavy metals. Influence of pH towards adsorption capacities have been illustrated in batch and column study where pH does have linear relationship with adsorption capacity. adsorption process favors pH > 6 where ion exchange with cations takes place and aromatic surface functional group available in B500 act as π donor and acceptor for surface complexation removal method. At pH > 10, precipitation method takes over hence promoting the highest adsorption capacity.

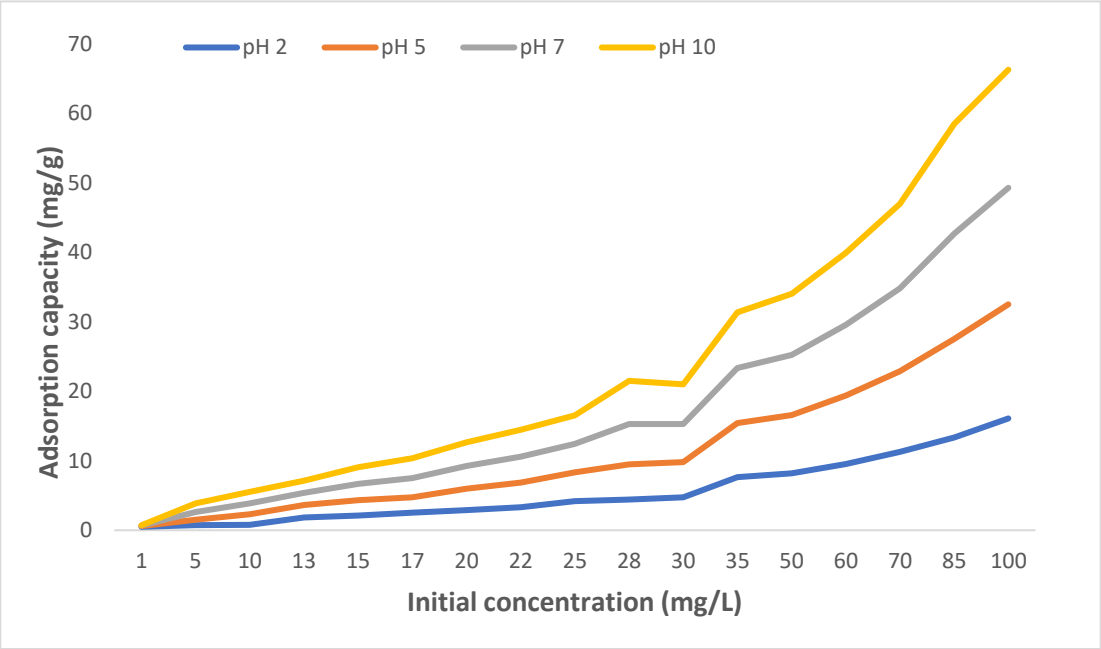
pH 2
pH 5
pH 7
pH 10
Adsorption capacity (mg/g)
0
10
20
30
40
50
60
70
1
5
10
13
15
17
20
22
25
28
30
35
50
60
70
85
100
Initial concentration (mg/L)

(a)

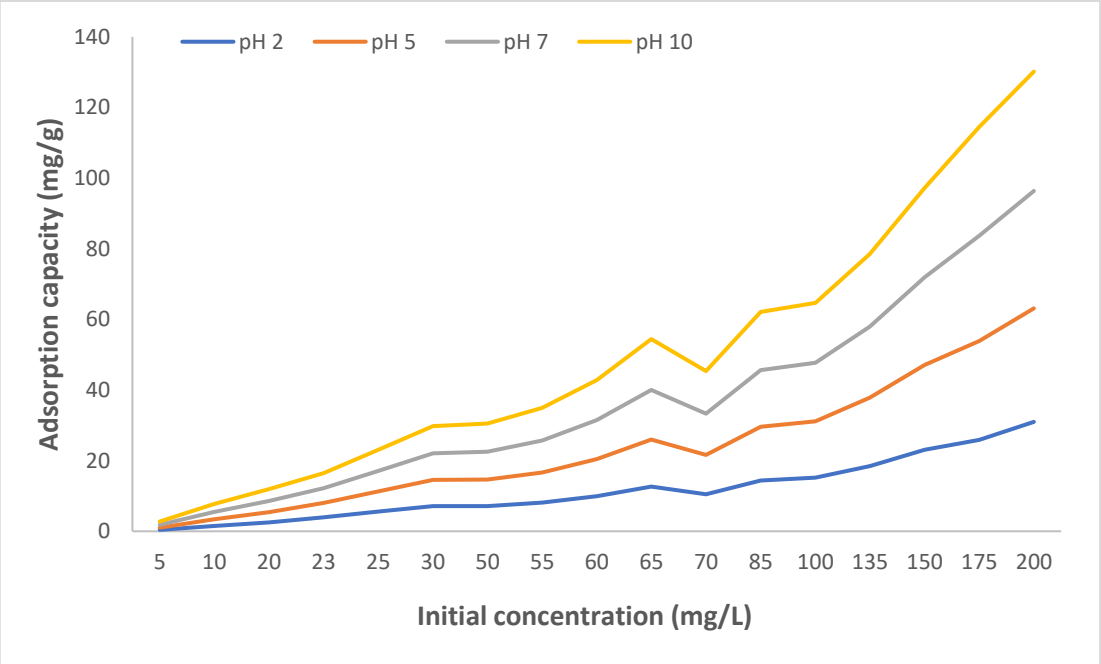
pH 2
pH 5
pH 7
pH 10
Adsorption capacity (mg/g)
0
20
40
60
80
100
120
140
5
10
20
23
25
30
50
55
60
65
70
85
100
135
150
175
200
Initial concentration (mg/L)

(b)

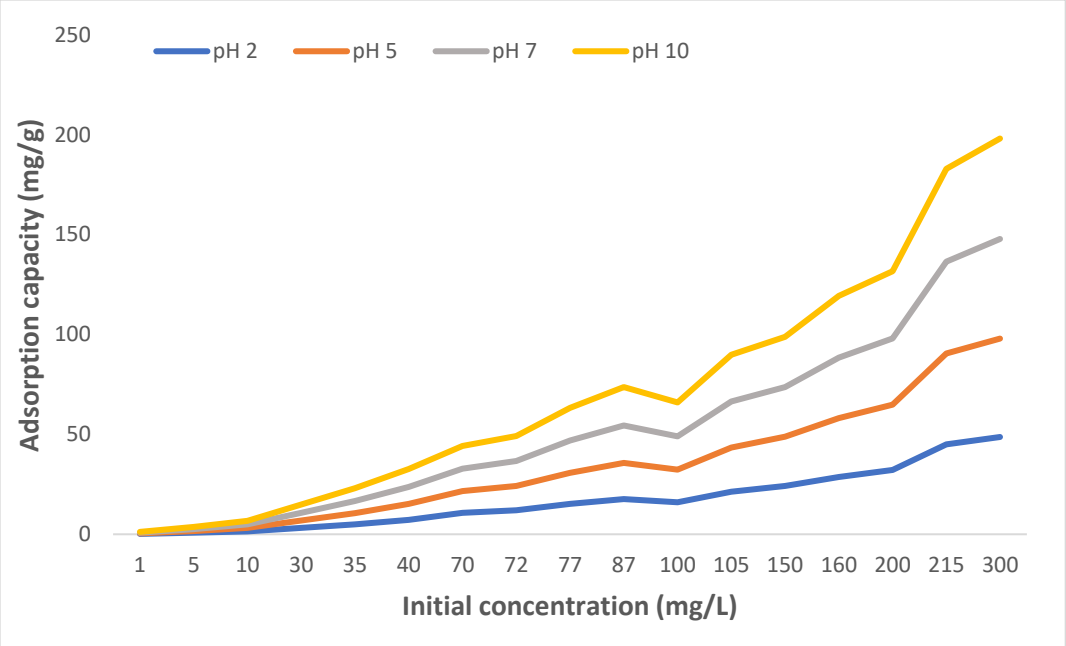

(c)

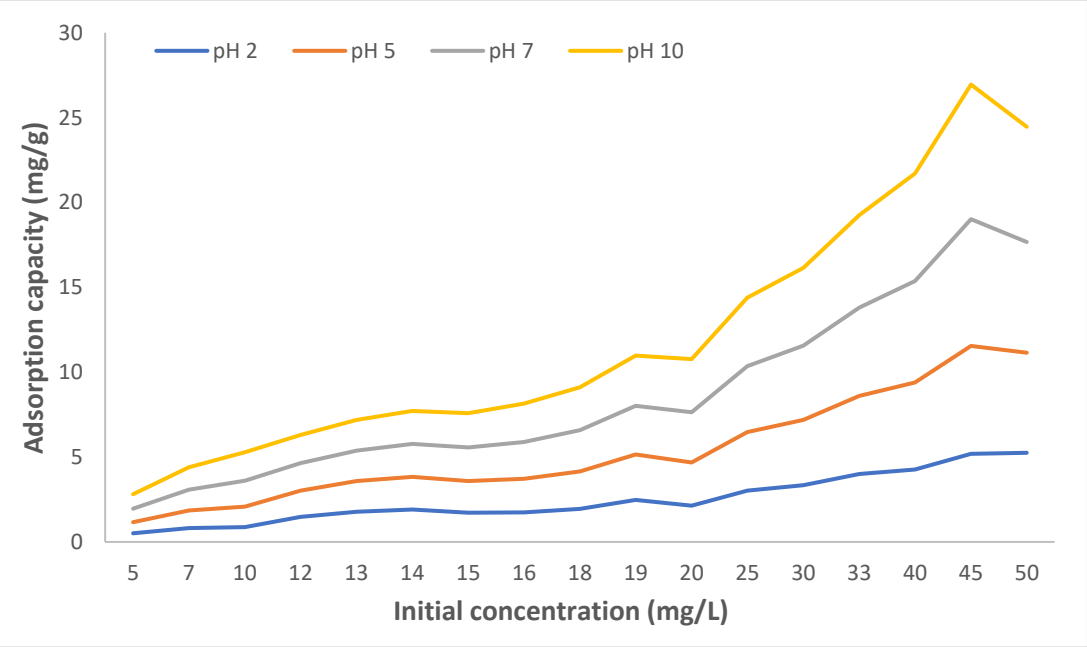

(d)

Figure 6.5 Adsorption capacity VS initial concentration of (a) Pb, (b) Fe, (c) Cu and (d) Mn at pH 2, pH 5, pH 7 and pH 10.

It is interesting to note that at certain point, the plot tends to fluctuate before increasing. This trend is observed at 28 - 30 mg/L for Pb, 65 - 70 mg/L for Fe, 87 - 100 mg/L for Cu and 19 - 20 mg/L for Mn. This may be due to intrusion between the adsorbates and the adsorbents. Conversely, the available adsorption sites for physical adsorption may be saturated with increasing heavy metal concentrations, hence reducing the adsorption capacity. However, as these heavy metals favors chemisorption, as discussed in both batch and column study, increasing metal concentrations results in more significant force in the active binding sites. Regardless, SMC biochar contains multiple functional groups that aids in chemisorption, for example surface complexation and precipitation, hence resulting in the bounce increment of the adsorption (Patel, 2022). These design charts are the outcome of this study; where this chart can be an excellent reference for future research as it can predict the adsorption capacities of Pb, Cu, Fe, and Mn at a different ranges of initial metal concentrations and different pH by using SMC biochar as filter media.

6.7 Summary

In this study, biochar modeling using machine learning was approached to predict the adsorption capacities of heavy metals onto SMC biochar. Machine learning chosen in this study were ANFIS and MLR models. Overall, both models can effectively predict the adsorption capacity of biochar for heavy metal removal in abandoned mine ponds with $R^2 > 0.9$, thus resulting in the feasibility of these models. However, the ANFIS model gives slightly better R^2 than MLR. This model is then adopted to validate with three validation sites from actual case studies as dynamic model validation. All developed models for all heavy metals revealed good accuracy where the validation and predicted data were close enough. The R^2 shows a great value with $0.9 > R^2 < 0.6$. Finally, the design charts of each heavy metal that predict adsorption capacity with the influence of initial metal concentrations and pH were developed. Hence, SMC biochar is proven as feasible filter media to remove heavy metals from mine-related water. Nevertheless, ANFIS provides an excellent modeling approach to predict the adsorption capacities of heavy metals by biochar, as they can capture the effect of interaction between the parameters affecting the adsorption.

Chapter 7 Conclusions and Recommendations

7.1 Conclusions

This report summarizes the general study of SMC biochar adsorption performance in removing heavy metals related to abandoned mine water. This research's main aim is achieved where SMC biochar's performance as filter media is evaluated in batch and column studies. Detailed design charts to predict the adsorption capacities of heavy metals were developed using machine learning, and the performance of SMC biochar to remove heavy metals was successful. The research started with three objectives outlined in Section 1.4, these objectives were re-visited to ensure they have been met:

1. To determine the most promising pyrolytic temperature of SMC biochar that gives the highest performance in heavy metal removal in a batch study

This objective is achieved in Stage 1 and Stage 2 of research. The production and characterisation of SMC biochar at different pyrolytic temperatures significantly affects the overall adsorption efficiency. Low-temperature biochar B300 has the lowest surface area but high pore volume. The FTIR analysis shows that B300 has an oxygen functional group. On the other hand, higher temperature biochar, B500 and B700, showed a high surface area and smaller pore volume with aromatic functional groups.

A batch adsorption study using SMC biochars from different pyrolytic temperatures was conducted, and the overall adsorption performance in removing heavy metals with the effect of experimental conditions of pH, initial concentrations, and contact time was assessed. Overall, SMC biochar can potentially remove heavy metals from abandoned mine water. B300 shows an adsorption capacity of 2.003 mg/g with a removal efficiency of 87.11 %. B500 comes with an adsorption capacity of 2.398 mg/g with a removal efficiency of 97.43 %, and B700 has an overall adsorption capacity of 2.486 mg/g with a removal efficiency of 98.38%. In comparison, RS has an adsorption capacity of 1.798 mg/g with an overall removal efficiency of 66.33 %. Overall, it is clear that different pyrolytic temperature gives different percentage removal where the trend for all initial metal concentrations are: B700 > B500 > B300 > RS for all metal ions.

It is interesting to note that B500 gave a comparative result to B700 despite its low surface area. Henceforth, chemical sorption interaction is the dominant factor of the adsorption mechanism. B500 showed the highest maximum adsorption capacity of Mn (2.522 mg/g) and Pb (2.491 mg/g). Based on the batch adsorption study, SMC biochar pyrolyzed at 500^{o}C (B500) was selected as the filter media for the column study.

2. To evaluate the adsorption performance of SMC biochar as filter media in a lab-scale metal retention column study with effect of pH and initial metal concentration

Objective 2 is achieved in Stage 3 of research. The adsorption performance of SMC biochar is evaluated through the lab scale metal retention column study. This study discussed applying SMC biochar as filter media to remove heavy metals in abandoned mine water through lab scale metal retention continuous column study. SMC biochar pyrolyzed at 500^{o}C was chosen as filter media due to its outstanding

adsorption performance in batch study. Seventeen sets of initial metal concentrations were constructed, and the adsorption performance was assessed from low to highest concentration based on the actual mine water data. The column study was interpreted through breakthrough analysis and the Thomas model. All filer media showed a significant S-shaped breakthrough plot from the breakthrough analysis. Overall, Cu showed the highest adsorption capacity of 49.833 mg/g, followed by Fe at 33.186 mg/g, Pb at 16.218 mg/g, and Mn at 6.665 mg/g. This is supported by the breakthrough curve, where Mn showed the earliest saturation point followed by Pb, then Fe and Cu had similar S-shaped performance. Competitive adsorption among heavy metals were explored and single metal solution gave higher adsorption performance than multimetal solution. The potential mechanisms by which SMC biochar adsorbs metal ions includes surface adsorption, precipitation, ion exchange and complexation.

3. To develop detailed design charts for optimal adsorption capacities of SMC biochar using machine learning with influence of initial metal concentrations and pH and validate the chart with actual case studies.

Objective 3 is achieved in Stage 4 of research. After a series of batch adsorption study and lab scale metal retention column study, this study moved further and adopted biochar modelling using machine learning to develop detailed design charts. In this study, biochar modeling using machine learning was approached to predict the adsorption capacities of heavy metals onto SMC biochar. Machine learning chosen in this study was ANFIS and MLR models. Overall, both models are comparable with $R^2 > 0.9$, thus resulting in the feasibility of these models. However, the ANFIS model gives slightly better R^2 than MLR. This model is then adopted to validate with three validation sites from actual case studies as dynamic model validation. All developed models for all heavy metals revealed good accuracy where the validation and predicted data were close enough. The R^2 shows a great value with $0.9 > R^2 < 0.6$. Finally, the design charts of each

heavy metal that predict adsorption capacity with the influence of initial metal concentrations and pH were developed. Hence, SMC biochar is proven to be a feasible filter media to remove heavy metals from mine-related water. Correspondingly, ANFIS provides an excellent modeling approach to predict the adsorption capacities of heavy metals by biochar, as they can capture the effect of interaction between the parameters affecting the adsorption.

In conclusion, SMC biochar has showed significant potential as filter media to be applied in a metal retention system to remove heavy metals in abandoned mine ponds. Characterization of SMC biochar showed enhanced surface area that provide great adsorption sites for metal adsorption. Pyrolysis of SMC into biochar generated active surface functional groups that promotes chemisorption (ion exchange and surface complexation) which were the dominant removal mechanisms for this study. Batch adsorption study has showed the adsorption performance of SMC biochar with effect of environmental conditions of pH, initial concentrations and time. Next, lab scale metal retention column study was conducted to determine optimal design parameters such as its composition, physic-chemical characteristics, and system configuration. The column is a crucial step in performing continuous adsorption to imitate pH and initial metal concentration for abandoned mining water before releasing it to the river as an alternative raw water source. Overall, SMC biochar showed high adsorption capacity for all heavy metals. The high surface area and multiple active functional groups create strong binding affinity towards the metallic ions. Finally, heavy metal design charts with influence of pH and initial metal concentration where prediction of heavy metal removal by SMC biochar were developed.

Feasibility of SMC biochar as filter media

Access to safe potable water is a significant challenge affecting approximately 600 million people worldwide, necessitating urgent advancements in practical and low-cost solutions to achieve Sustainable Development Goal 6. Biochar, a carbon solid material derived from biomass thermochemical decomposition, has emerged as a promising low cost technology for water treatment. Unlike existing low cost methods, biochar offers advantages such as being readily available, removing a wide range of contaminants, and maintaining the organoleptic properties of water.

However, the application of SMC biochar as filter media in abandoned mine related water is still relatively new and requires further exploration. This study critically assesses and analyses the properties of SMC biochar, including its larger surface area, porous structure, multiple active functional groups, and high mineral content, making it a suitable candidate for removing heavy metal contaminants in abandoned mine water. SMC biochar shows promise as a sustainable and cost effective alternative to conventional activated carbon adsorbents. Activated carbon is a common adsorbent available in the market and biochar shown a great deal to replace activated carbon as sustainable and effective adsorbent due to its much lower production cost and easy production process. Table 7.1 shows the comparison of SMC biochar and activated carbon.

Table 7.1 Comparison of SMC biochar and Activated carbon

SMC biochar	Comparison	Activated carbon	Reference
Simple low oxygen thermochemical process	Production	Char activation using strong acid and expensive oxygen	(Dai et al., 2019)
$ 250/ tonne	Production cost	$ 2 000/ tonne	(Ulrich et al., 2017)
Biomass waste that are low cost and readily available	Material	Produced from non renewable sources and biomass waste	(Wang et al., 2019)

The study also incorporates machine learning techniques to develop detailed design charts predicting the adsorption capacity of SMC biochar as filter media, facilitating potential real-life applications. This research provides a sustainable solution by utilizing SMC biochar to remove heavy metals from abandoned mine water, which can serve as an alternative raw water resource. The study contributes to achieving Sustainable Development Goal 6, addressing water scarcity issues, supporting sustainability, and improving solid waste management by reducing waste buildup.

In summary, this research highlights the potential of SMC biochar as an effective and cost-efficient filter media for removing heavy metals from abandoned mine water. The study offers a novel approach, demonstrates the feasibility of SMC biochar, and provides valuable design charts for practical implementation.

7.2 Limitations and recommendations

The limitations and recommendations of this research can be addressed by considering the limitations and recommendations below:

1. In future research and development sector, for example, in the next five years, this study can be an excellent reference for pilot scale and field study assessment and a real-life application of heavy metal retention filtration system with SMC biochar as filter media. Hence, a scale-up design using real size filter and design can be considered for future topics to perform the pilot test.

2. Future scope should include on the desorption, regeneration and metal recovery of SMC biochar. As for the metal recovery, the metal rich filter media can be proposed as the carbon sequestration of post SMC biochar in the agricultural sector. Biochar contains a lot of nutrients and carbon, and biochar is coated with metal ions, and putting it back to earth is beneficial for agricultural purposes as it improves crop yields. Hence, this study will be beneficial for future applications.

3. This research only focuses on four prominent metals in abandoned mine water (Fe, Cu, Pb, and Mn), other contaminants involved might show different removal trends. Hence, future research could consider a more comprehensive and complete investigation of the effect of other hazardous heavy metals such Arsenic (anion), Nickel, Chromium and other inorganic contaminants. This will give a great insight, especially towards the performance in competitive adsorption in multielement solutions.

4. The design charts can predict adsorption capacities only at the limited metal concentrations range chosen for this research. In the future, more metal concentrations can be added, as well as other parameter conditions to produce a broader design chart for future work.

5. A detailed cost-comparison analysis and economical aspect can be conducted in future studies to review the overall cost analysis from the production of SMC biochar to the construction of the pilot scale metal retention column.

Reference

Abbas, S. H., Ismail, I. M., Mostafa, T. M., & Sulaymon, A. H. (2016). *Biosorption of Heavy Metals : A Review Biosorption of Heavy Metals : A Review*. *January*.

Abdallah, M. M., Ahmad, M. N., Walker, G., Leahy, J. J., & Kwapinski, W. (2019). Batch and Continuous Systems for Zn , Cu , and Pb Metal Ions Adsorption on Spent Mushroom Compost Biochar [Research-article]. *Industrial & Engineering Chemistry Research*, *58*, 7296–7307. https://doi.org/10.1021/acs.iecr.9b00749

Abdel-Fattah, T. M., Mahmoud, M. E., Ahmed, S. B., Huff, M. D., Lee, J. W., & Kumar, S. (2015). Biochar from woody biomass for removing metal contaminants and carbon sequestration. *Journal of Industrial and Engineering Chemistry*, *22*, 103–109. https://doi.org/10.1016/j.jiec.2014.06.030

Abdelhafez, A. A., & Li, J. (2016). *Journal of the Taiwan Institute of Chemical Engineers Removal of Pb (II) from aqueous solution by using biochars derived from sugar cane bagasse and orange peel*. *61*, 367–375. https://doi.org/10.1016/j.jtice.2016.01.005

Abdi, J., & Mazloom, G. (2022). Machine learning approaches for predicting arsenic adsorption from water using porous metal–organic frameworks. *Scientific Reports*, *12*(1), 1–13. https://doi.org/10.1038/s41598-022-20762-y

Abdolali, A., Ngo, H. H., Guo, W., Zhou, J. L., Zhang, J., Liang, S., Chang, S. W., Nguyen, D. D., & Liu, Y. (2017). Application of a breakthrough biosorbent for removing heavy metals from synthetic and real wastewaters in a lab-scale continuous fixed-bed column. *Bioresource Technology*, *229*, 78–87. https://doi.org/10.1016/j.biortech.2017.01.016

Abdullah, N., Tajuddin, M. H., & Yusof, N. (2019). Forward Osmosis (FO) for Removal of Heavy Metals. In

Nanotechnology in Water and Wastewater Treatment. Elsevier Inc. https://doi.org/10.1016/b978-0-12-813902-8.00010-1

Abu Hasan, H., Muhammad, M. H., & Ismail, N. I. (2020). A review of biological drinking water treatment technologies for contaminants removal from polluted water resources. *Journal of Water Process Engineering*, *33*(May 2019), 101035. https://doi.org/10.1016/j.jwpe.2019.101035

Agaricus, M. (2021). *Efficient Removal of Cu (II), Zn (II), and Cd (II) from Aqueous Solutions by a Mineral-Rich Biochar Derived from a Spent*. *Ii*.

Agbaogun, B. K., Alonso, J. M., Buddenbaum, H., & Fischer, K. (2021). Modelling of the adsorption of urea herbicides by tropical soils with an Adaptive-Neural-based Fuzzy Inference System. *Journal of Chemometrics*, *35*(5), 1–17. https://doi.org/10.1002/cem.3335

Agbaogun, B. K., Olu-Owolabi, B. I., Buddenbaum, H., & Fischer, K. (2022). Adaptive neuro-fuzzy inference system (ANFIS) and multiple linear regression (MLR) modelling of Cu, Cd, and Pb adsorption onto tropical soils. *Environmental Science and Pollution Research*, *0123456789*. https://doi.org/10.1007/s11356-022-24296-8

Agustiono, T., Chan, G. Y. S., Lo, W., & Babel, S. (2006). *Physico – chemical treatment techniques for wastewater laden with heavy metals*. *118*, 83–98. https://doi.org/10.1016/j.cej.2006.01.015

Ahmad, A., Khan, N., Giri, B. S., Chowdhary, P., & Chaturvedi, P. (2020). Removal of methylene blue dye using rice husk, cow dung and sludge biochar: Characterization, application, and kinetic studies. *Bioresource Technology*, *306*(January), 1–5. https://doi.org/10.1016/j.biortech.2020.123202

Al-Yaari, M., Aldhyani, T. H. H., & Rushd, S. (2022). Prediction of Arsenic Removal from Contaminated Water Using Artificial Neural Network Model. *Applied Sciences (Switzerland)*, *12*(3). https://doi.org/10.3390/app12030999

Alias, N., Rosli, S. A., Sazalli, N. A. H., Hamid, H. A., Arivalakan, S., Umar, S. N. H., Khim, B. K., Taib, B. N., Keat, Y. K., Razak, K. A., Yee, Y. F., Hussain, Z., Bakar, E. A., Kamaruddin, N. F., Manaf, A. A., Uchiyama, N., Kian, T. W., Matsuda, A., Kawamura, G., … Lockman, Z. (2020). Metal oxide for heavy metal detection and removal. In *Metal Oxide Powder Technologies*. https://doi.org/10.1016/b978-0-12-817505-7.00015-4

Anticó, E., Cot, S., Ribó, A., Rodríguez-Roda, I., & Fontàs, C. (2017). Survey of heavy metal contamination in water sources in the municipality of Torola, El Salvador, through in situ sorbent extraction. *Water (Switzerland)*, *9*(11). https://doi.org/10.3390/w9110877

Ashraf, M. A., Maah, M. J., & Yusoff, I. (2011). Analysis of physio-chemical parameters and distribution of heavy metals in soil and water of ex-mining area of Bestari Jaya, Peninsular Malaysia. *Asian Journal of Chemistry*, *23*(8), 3493–3499.

Aziz, H. A., Adlan, M. N., & Ariffin, K. S. (2008). Heavy metals (Cd, Pb, Zn, Ni, Cu and Cr(III)) removal from water in Malaysia: Post treatment by high quality limestone. *Bioresource Technology*, *99*(6), 1578–1583. https://doi.org/10.1016/j.biortech.2007.04.007

Bakshi, S., Banik, C., Rathke, S. J., & Laird, D. A. (2018). Arsenic sorption on zero-valent iron-biochar complexes. *Water Research*, *137*, 153–163. https://doi.org/10.1016/j.watres.2018.03.021

Banerjee, M., Bar, N., & Das, S. K. (2021a). Cu(II) Removal From Aqueous Solution Using The Walnut Shell: Adsorption Study, Regeneration Study, Plant Scale-Up Design, Economic Feasibility, Statistical, and GA-ANN Modeling. *International Journal of Environmental Research*, *15*(5), 875–891. https://doi.org/10.1007/s41742-021-00362-w

Banerjee, M., Bar, N., & Das, S. K. (2021b). Cu(II) Removal From Aqueous Solution Using The Walnut Shell: Adsorption Study, Regeneration Study, Plant Scale-Up Design, Economic Feasibility, Statistical, and

GA-ANN Modeling. *International Journal of Environmental Research*, *15*(5), 875–891. https://doi.org/10.1007/s41742-021-00362-w

Banerjee, M., Basu, R. K., & Das, S. K. (2018). Cr(VI) adsorption by a green adsorbent walnut shell: Adsorption studies, regeneration studies, scale-up design and economic feasibility. In *Process Safety and Environmental Protection* (Vol. 116, pp. 693–702). https://doi.org/10.1016/j.psep.2018.03.037

Banerjee, S., Mukherjee, S., LaminKa-ot, A., Joshi, S. R., Mandal, T., & Halder, G. (2016). Biosorptive uptake of Fe2+, Cu2+and As5+by activated biochar derived from Colocasia esculenta: Isotherm, kinetics, thermodynamics, and cost estimation. *Journal of Advanced Research*, *7*(5), 597–610. https://doi.org/10.1016/j.jare.2016.06.002

Barakat, M. A. (2011). New trends in removing heavy metals from industrial wastewater. *Arabian Journal of Chemistry*, *4*(4), 361–377. https://doi.org/10.1016/j.arabjc.2010.07.019

Blagojev, N., Kukić, D., Vasić, V., Šćiban, M., Prodanović, J., & Bera, O. (2019). A new approach for modelling and optimization of Cu(II) biosorption from aqueous solutions using sugar beet shreds in a fixed-bed column. In *Journal of Hazardous Materials* (Vol. 363, pp. 366–375). https://doi.org/10.1016/j.jhazmat.2018.09.068

Bora, A. J., & Dutta, R. K. (2019). Removal of metals (Pb, Cd, Cu, Cr, Ni, and Co)from drinking water by oxidation-coagulation-absorption at optimized pH. *Journal of Water Process Engineering*, *31*(May), 100839. https://doi.org/10.1016/j.jwpe.2019.100839

Brewer, G. J. (2010). Risks of copper and iron toxicity during aging in humans. *Chemical Research in Toxicology*, *23*(2), 319–326. https://doi.org/10.1021/tx900338d

Burakov, A. E., Galunin, E. V., Burakova, I. V., Kucherova, A. E., Agarwal, S., Tkachev, A. G., & Gupta, V. K. (2018). Adsorption of heavy metals on conventional and nanostructured materials for wastewater

treatment purposes: A review. *Ecotoxicology and Environmental Safety*, *148*(August 2017), 702–712. https://doi.org/10.1016/j.ecoenv.2017.11.034

Chang, J., Zhang, H., Cheng, H., Yan, Y., Chang, M., Cao, Y., Huang, F., Zhang, G., & Yan, M. (2020a). Spent Ganoderma lucidum substrate derived biochar as a new bio-adsorbent for Pb2+/Cd2+ removal in water. *Chemosphere*, *241*, 1–10. https://doi.org/10.1016/j.chemosphere.2019.125121

Chang, J., Zhang, H., Cheng, H., Yan, Y., Chang, M., Cao, Y., Huang, F., Zhang, G., & Yan, M. (2020b). Spent Ganoderma lucidum substrate derived biochar as a new bio-adsorbent for Pb2+/Cd2+ removal in water. In *Chemosphere* (Vol. 241). https://doi.org/10.1016/j.chemosphere.2019.125121

Chang, T. K., Talei, A., Alaghmand, S., & Ooi, M. P. L. (2017). Choice of rainfall inputs for event-based rainfall-runoff modeling in a catchment with multiple rainfall stations using data-driven techniques. *Journal of Hydrology*, *545*, 100–108. https://doi.org/10.1016/j.jhydrol.2016.12.024

Chen, C., Chen, Z., Shen, J., Kang, J., Zhao, S., Wang, B., Chen, Q., & Li, X. (2021). Dynamic adsorption models and artificial neural network prediction of mercury adsorption by a dendrimer-grafted polyacrylonitrile fiber in fixed-bed column. In *Journal of Cleaner Production* (Vol. 310). https://doi.org/10.1016/j.jclepro.2021.127511

Chen, C., Liu, G., Zhao, Y., Gu, Y., Li, X., Li, G., He, Y., Liu, X., & Wang, X. (2019). Mixed heavy metals removal from wastewater by discarded mushroom-stick biochar: adsorption properties and mechanisms. *Environmental Science: Processes & Impacts*. https://doi.org/10.1039/c8em00457a

Chen, S., Qin, C., Wang, T., Chen, F., Li, X., Hou, H., & Zhou, M. (2019). Study on the adsorption of dyestuffs with different properties by sludge-rice husk biochar: Adsorption capacity, isotherm, kinetic, thermodynamics and mechanism. *Journal of Molecular Liquids*, *285*, 62–74. https://doi.org/10.1016/j.molliq.2019.04.035

Cheng, S., Chen, T., Xu, W., Huang, J., Jiang, S., & Yan, B. (2020). Application research of biochar for the remediation of soil heavy metals contamination: A review. *Molecules*, *25*(14), 1–21. https://doi.org/10.3390/molecules25143167

Cheong, Y. W., Das, B. K., Roy, A., & Bhattacharya, J. (2010). *Performance of a SAPS-Based Chemo-Bioreactor Treating Acid Mine Drainage Using Low-DOC Spent Mushroom Compost , and Limestone as Substrate*. 217–224. https://doi.org/10.1007/s10230-010-0104-6

Chittoo, B. S., & Sutherland, C. (2020). Column breakthrough studies for the removal and recovery of phosphate by lime-iron sludge: Modeling and optimization using artificial neural network and adaptive neuro-fuzzy inference system. In *Chinese Journal of Chemical Engineering* (Vol. 28, Issue 7, pp. 1847–1859). https://doi.org/10.1016/j.cjche.2020.02.022

Chowdhury, S., Mazumder, M. A. J., Al-attas, O., & Husain, T. (2016). *Science of the Total Environment Heavy metals in drinking water : Occurrences , implications , and future needs in developing countries*. *570*, 476–488.

Chowdhury, Z. Z., Abd Hamid, S. B., & Zain, S. M. (2015). Evaluating design parameters for breakthrough curve analysis and kinetics of fixed bed columns for Cu(II) cations using lignocellulosic wastes. *BioResources*, *10*(1), 732–749. https://doi.org/10.15376/biores.10.1.732-749

Corral-Bobadilla, M., González-Marcos, A., Vergara-González, E. P., & Alba-Elías, F. (2019). Bioremediation of waste water to remove heavy metals using the spent mushroom substrate of Agaricus bisporus. *Water (Switzerland)*, *11*(3). https://doi.org/10.3390/w11030454

Daghbandan, A., Souraki, B. A., & Zadeh, M. A. (2022). A comprehensive study on the applicability of tea leaves and rice straw as novel sorbents for iron and manganese removal from running water in a fixed-bed column. *Korean Journal of Chemical Engineering*, *39*(3), 628–637.

https://doi.org/10.1007/s11814-021-0910-5

Dai, Y., Zhang, N., Xing, C., Cui, Q., & Sun, Q. (2019). The adsorption, regeneration and engineering applications of biochar for removal organic pollutants: A review. *Chemosphere*, *223*, 12–27. https://doi.org/10.1016/j.chemosphere.2019.01.161

Daneshfozoun, S., Abdullah, B., & Abdullah, M. A. (2016). The Effects of Oil Palm Empty Fruit Bunch Sorbent Sizes on Plumbum (II) Ion Sorption. *Advanced Materials Research*, *1133*(Ii), 542–546. https://doi.org/10.4028/www.scientific.net/AMR.1133.542

Dawodu, F. A., & Akpomie, K. G. (2014). Simultaneous adsorption of Ni(II) and Mn(II) ions from aqueous solution unto a Nigerian kaolinite clay. *Journal of Materials Research and Technology*, *3*(2), 129–141. https://doi.org/10.1016/j.jmrt.2014.03.002

Dimpe, K. M., Ngila, J. C., & Nomngongo, P. N. (2018). Preparation and application of a tyre-based activated carbon solid phase extraction of heavy metals in wastewater samples. *Physics and Chemistry of the Earth*, *105*(February), 161–169. https://doi.org/10.1016/j.pce.2018.02.005

Ding, Z., Wan, Y., Hu, X., Wang, S., Zimmerman, A. R., & Gao, B. (2016). Journal of Industrial and Engineering Chemistry Sorption of lead and methylene blue onto hickory biochars from different pyrolysis temperatures : Importance of physicochemical properties. *Journal of Industrial and Engineering Chemistry*, *37*, 261–267. https://doi.org/10.1016/j.jiec.2016.03.035

Dong, L., Liang, J., Li, Y., Hunang, S., Wei, Y., Bai, X., Jin, Z., Zhang, M., & Qu, J. (2018). Effect of coexisting ions on Cr(VI) adsorption onto surfactant modified Auricularia auricula spent substrate in aqueous solution. *Ecotoxicology and Environmental Safety*, *166*(June), 390–400. https://doi.org/10.1016/j.ecoenv.2018.09.097

El Hanandeh, A., Mahdi, Z., & Imtiaz, M. S. (2021). Modelling of the adsorption of Pb, Cu and Ni ions from

single and multi-component aqueous solutions by date seed derived biochar: Comparison of six machine learning approaches. *Environmental Research*, *192*(July 2020). https://doi.org/10.1016/j.envres.2020.110338

Eltaweil, A. S., Ali Mohamed, H., Abd El-Monaem, E. M., & El-Subruiti, G. M. (2020). Mesoporous magnetic biochar composite for enhanced adsorption of malachite green dye: Characterization, adsorption kinetics, thermodynamics and isotherms. *Advanced Powder Technology*, *31*(3), 1253–1263. https://doi.org/10.1016/j.apt.2020.01.005

Esfandiar, N., Suri, R., & McKenzie, E. R. (2022). Competitive sorption of Cd, Cr, Cu, Ni, Pb and Zn from stormwater runoff by five low-cost sorbents; Effects of co-contaminants, humic acid, salinity and pH. *Journal of Hazardous Materials*, *423*. https://doi.org/10.1016/j.jhazmat.2021.126938

Evans, a, & Ko, S. (2013). *Metal Removal in Sulphate-Reducing Bioreactors Treating Acid Mine Drainage*.

Fakhre, N. A., & Ibrahim, B. M. (2018). The use of new chemically modified cellulose for heavy metal ion adsorption. *Journal of Hazardous Materials*, *343*, 324–331. https://doi.org/10.1016/j.jhazmat.2017.08.043

Fernández-Real, J. M., & Manco, M. (2014). Effects of iron overload on chronic metabolic diseases. In *The Lancet Diabetes and Endocrinology* (Vol. 2, Issue 6, pp. 513–526). https://doi.org/10.1016/S2213-8587(13)70174-8

Fishbane, S., Mathew, A., & Vaziri, N. D. (2014). Iron toxicity: Relevance for dialysis patients. *Nephrology Dialysis Transplantation*, *29*(2), 255–259. https://doi.org/10.1093/ndt/gft269

Frutos, I., García-Delgado, C., Gárate, A., & Eymar, E. (2016). Biosorption of heavy metals by organic carbon from spent mushroom substrates and their raw materials. *International Journal of Environmental Science and Technology*, *13*(11), 2713–2720. https://doi.org/10.1007/s13762-016-1100-6

Fseha, Y. H., Sizirici, B., & Yildiz, I. (2022). Manganese and nitrate removal from groundwater using date palm biochar: Application for drinking water. In *Environmental Advances* (Vol. 8). https://doi.org/10.1016/j.envadv.2022.100237

Fu, F., & Wang, Q. (2011). Removal of heavy metal ions from wastewaters: A review. *Journal of Environmental Management*, *92*(3), 407–418. https://doi.org/10.1016/j.jenvman.2010.11.011

Gai, X., Wang, H., Liu, J., Zhai, L., Liu, S., Ren, T., & Liu, H. (2014). Effects of feedstock and pyrolysis temperature on biochar adsorption of ammonium and nitrate. *PLoS ONE*, *9*(12), 1–10. https://doi.org/10.1371/journal.pone.0113888

Ganguly, P., Sarkhel, R., & Das, P. (2020). Synthesis of pyrolyzed biochar and its application for dye removal: Batch, kinetic and isotherm with linear and non-linear mathematical analysis. *Surfaces and Interfaces*, *20*(July). https://doi.org/10.1016/j.surfin.2020.100616

Giachini, A. J., Sulzbach, T. S., Pinto, A. L., Armas, R. D., Cortez, D. H., Silva, E. P., Buzanello, E. B., Soares, Á. G., Soares, C. R. F. S., & Rossi, M. J. (2018). Microbially-enriched poultry litter-derived biochar for the treatment of acid mine drainage. *Archives of Microbiology*, *200*(8), 1227–1237. https://doi.org/10.1007/s00203-018-1534-y

Goh, H. W., Lem, K. S., Azizan, N. A., Chang, C. K., Talei, A., Leow, C. S., & Zakaria, N. A. (2019). A review of bioretention components and nutrient removal under different climates—future directions for tropics. *Environmental Science and Pollution Research*, *26*(15), 14904–14919. https://doi.org/10.1007/s11356-019-05041-0

Hafsa, N., Rushd, S., Al-Yaari, M., & Rahman, M. (2020). A generalized method for modeling the adsorption of heavy metals with machine learning algorithms. *Water (Switzerland)*, *12*(12), 1–22. https://doi.org/10.3390/w12123490

Hamzah, N., Diman, C. P., Ahmad, M. A. N., Lazim, M. I. H. M., Zakaria, M. F., & Bashar, N. M. (2018). Water quality assessment of abandoned mines in Selangor. *AIP Conference Proceedings*, *2020*(October 2018). https://doi.org/10.1063/1.5062672

Han, E. S., & goleman, daniel; boyatzis, Richard; Mckee, A. (2019). 済無No Title No Title. *Journal of Chemical Information and Modeling*, *53*(9), 1689–1699.

Hanumanthu, J. R., Ravindiran, G., Subramanian, R., & Saravanan, P. (2021). Optimization of process conditions using RSM and ANFIS for the removal of Remazol Brilliant Orange 3R in a packed bed column. In *Journal of the Indian Chemical Society* (Vol. 98, Issue 6). https://doi.org/10.1016/j.jics.2021.100086

Hashim, M., Shiang, W. F., Said, Z. M., Nayan, N., Mahat, H., & Saleh, Y. (2018). An Analysis of Heavy Metals in Lakes of Former Tin Mining Sites in the City of Ipoh, Perak, Malaysia. *International Journal of Academic Research in Business and Social Sciences*, *8*(2), 673–683. https://doi.org/10.6007/ijarbss/v8-i2/3977

Hassan, M., Liu, Y., Naidu, R., Parikh, S. J., Du, J., Qi, F., & Willett, I. R. (2020). Influences of feedstock sources and pyrolysis temperature on the properties of biochar and functionality as adsorbents: A meta-analysis. *Science of the Total Environment*, *744*, 1–15. https://doi.org/10.1016/j.scitotenv.2020.140714

Hatar, H., Rahim, S. A., Razi, W. M., & Sahrani, F. K. (2013). Heavy metals content in acid mine drainage at abandoned and active mining area. *AIP Conference Proceedings*, *1571*(December 2013), 641–646. https://doi.org/10.1063/1.4858727

Huang, H., Reddy, N. G., Huang, X., Chen, P., Wang, P., Zhang, Y., Huang, Y., Lin, P., & Garg, A. (2021). Effects of pyrolysis temperature, feedstock type and compaction on water retention of biochar

amended soil. *Scientific Reports*, *11*(1), 1–19. https://doi.org/10.1038/s41598-021-86701-5

Hussain, A., & Qazi, J. I. (2016). Application of sugarcane bagasse for passive anaerobic biotreatment of sulphate rich wastewaters. *Applied Water Science*, *6*(2), 205–211. https://doi.org/10.1007/s13201-014-0226-2

Ighalo, J. O., Adeniyi, A. G., Eletta, O. A. A., & Arowoyele, L. T. (2020). Competitive adsorption of Pb(II), Cu(II), Fe(II) and Zn(II) from aqueous media using biochar from oil palm (Elaeis guineensis) fibers: a kinetic and equilibrium study. *Indian Chemical Engineer*, *Ii*, 1–11. https://doi.org/10.1080/00194506.2020.1787870

Inyang, M., Gao, B., Ding, W., Pullammanappallil, P., Zimmerman, A. R., Cao, X., Inyang, M., Gao, B., Ding, W., Pullammanappallil, P., Zimmerman, A. R., & Cao, X. (2011). *Enhanced Lead Sorption by Biochar Derived from Anaerobically Digested Sugarcane Bagasse Enhanced Lead Sorption by Biochar Derived from Anaerobically Digested Sugarcane Bagasse*. *6395*. https://doi.org/10.1080/01496395.2011.584604

Jamei, M., Karbasi, M., Malik, A., Abualigah, L., Islam, A. R. M. T., & Yaseen, Z. M. (2022). Computational assessment of groundwater salinity distribution within coastal multi-aquifers of Bangladesh. *Scientific Reports*, *12*(1), 11165. https://doi.org/10.1038/s41598-022-15104-x

Jan, A. T., Azam, M., Siddiqui, K., Ali, A., Choi, I., & Haq, Q. M. R. (2015). Heavy metals and human health: Mechanistic insight into toxicity and counter defense system of antioxidants. *International Journal of Molecular Sciences*, *16*(12), 29592–29630. https://doi.org/10.3390/ijms161226183

Jiang, W., Xing, X., Li, S., Zhang, X., & Wang, W. (2019). Synthesis, characterization and machine learning based performance prediction of straw activated carbon. *Journal of Cleaner Production*, *212*(x), 1210–1223. https://doi.org/10.1016/j.jclepro.2018.12.093

Jin, Y., Teng, C., Yu, S., Song, T., Dong, L., Liang, J., Bai, X., Liu, X., Hu, X., & Qu, J. (2018). Batch and fixed-bed biosorption of Cd(II) from aqueous solution using immobilized Pleurotus ostreatus spent substrate. *Chemosphere*, *191*, 799–808. https://doi.org/10.1016/j.chemosphere.2017.08.154

Jin, Y., Zhang, M., Jin, Z., Wang, G., Li, R., Zhang, X., Liu, X., Qu, J., & Wang, H. (2020). Characterization of biochars derived from various spent mushroom substrates and evaluation of their adsorption performance of Cu(II) ions from aqueous solution. *Environmental Research*, *February*. https://doi.org/10.1016/j.envres.2020.110323

Jin, Y., Zhang, M., Jin, Z., Wang, G., Li, R., Zhang, X., Liu, X., Qu, J., & Wang, H. (2021). Characterization of biochars derived from various spent mushroom substrates and evaluation of their adsorption performance of Cu(II) ions from aqueous solution. In *Environmental Research* (Vol. 196). https://doi.org/10.1016/j.envres.2020.110323

Jopony, M., & Tongkul, F. (2009). Acid Mine Drainages at Mamut Copper Mine, Sabah, Malaysia. *Borneo Science*, *March*, 83–94.

Joseph, L., Jun, B. M., Flora, J. R. V., Park, C. M., & Yoon, Y. (2019). Removal of heavy metals from water sources in the developing world using low-cost materials: A review. *Chemosphere*, *229*, 142–159. https://doi.org/10.1016/j.chemosphere.2019.04.198

Juela, D., Vera, M., Cruzat, C., Astudillo, A., & Vanegas, E. (2022). A new approach for scaling up fixed-bed adsorption columns for aqueous systems: A case of antibiotic removal on natural adsorbent. In *Process Safety and Environmental Protection* (Vol. 159, pp. 953–963). https://doi.org/10.1016/j.psep.2022.01.046

Kamarudzaman, A. N., Chay, T. C., Amir, A., & Talib, S. A. (2015). Biosorption of Mn(II) ions from Aqueous Solution by Pleurotus Spent Mushroom Compost in a Fixed-Bed Column. *Procedia - Social and*

Behavioral Sciences, *195*(Ii), 2709–2716. https://doi.org/10.1016/j.sbspro.2015.06.379

Ke, B., Nguyen, H., Bui, X. N., Bui, H. B., & Nguyen-Thoi, T. (2021). Prediction of the sorption efficiency of heavy metal onto biochar using a robust combination of fuzzy C-means clustering and back-propagation neural network. *Journal of Environmental Management*, *293*. https://doi.org/10.1016/j.jenvman.2021.112808

Kefeni, K. K., Msagati, T. A. M., & Mamba, B. B. (2017). Acid mine drainage: Prevention, treatment options, and resource recovery: A review. *Journal of Cleaner Production*, *151*, 475–493. https://doi.org/10.1016/j.jclepro.2017.03.082

Khalil, A. S., Starovoytov, S. V., & Serpokrylov, N. S. (2018). The adaptive neuro-fuzzy inference system (ANFIS) application for the ammonium removal from aqueous solution predicting by biochar. *Materials Science Forum*, *931 MSF*, 985–990. https://doi.org/10.4028/www.scientific.net/MSF.931.985

Kiliç, M., Kirbiyik, Ç., Çepelioğullar, Ö., & Pütün, A. E. (2013). Adsorption of heavy metal ions from aqueous solutions by bio-char, a by-product of pyrolysis. *Applied Surface Science*, *283*, 856–862. https://doi.org/10.1016/j.apsusc.2013.07.033

Koki, I. B., Low, K. H., Juahir, H., Abdul Zali, M., Azid, A., & Zain, S. M. (2018a). Consumption of water from ex-mining ponds in Klang Valley and Melaka, Malaysia: A health risk study. *Chemosphere*, *195*, 641–652. https://doi.org/10.1016/j.chemosphere.2017.12.112

Koki, I. B., Low, K. H., Juahir, H., Abdul Zali, M., Azid, A., & Zain, S. M. (2018b). Consumption of water from ex-mining ponds in Klang Valley and Melaka, Malaysia: A health risk study. *Chemosphere*, *195*, 641–652. https://doi.org/10.1016/j.chemosphere.2017.12.112

Komnitsas, K., Zaharaki, D., & Pyliotis, I. (2015). Assessment of Pistachio Shell Biochar Quality and Its

Potential for Adsorption of Heavy Metals. *Waste and Biomass Valorization*, 805–816. https://doi.org/10.1007/s12649-015-9364-5

Kulkarni, N. P., Gangopadhyay, S., & Bharshankar, J. (2022). Medical Geology in Mining. In *Medical Geology in Mining*. https://link.springer.com/chapter/10.1007/978-3-030-99495-2_10

Kulkarni, S., & Kaware, J. (2014). Regeneration and Recovery in Adsorption- a Review. *International Journal of Innovative Science, Engineering & Technology(IJISET)*, *1*(8), 61–64.

Kulshreshtha, S. (2019). Removal of pollutants using spent mushrooms substrates. *Environmental Chemistry Letters*, *17*(2), 833–847. https://doi.org/10.1007/s10311-018-00840-2

Kura, N. U., Ramli, M. F., Sulaiman, W. N. A., Ibrahim, S., & Aris, A. Z. (2015). An overview of groundwater chemistry studies in Malaysia. *Environmental Science and Pollution Research*, 1–19. https://doi.org/10.1007/s11356-015-5957-6

Kusin, F. M., Muhammad, S. N., Zahar, M. S. M., & Madzin, Z. (2016). Integrated River Basin Management: incorporating the use of abandoned mining pool and implication on water quality status. *Desalination and Water Treatment*, *57*(60), 29126–29136. https://doi.org/10.1080/19443994.2016.1168132

Kusin, F. M., Sulong, N. A., Affandi, F. N. A., Molahid, V. L. M., & Jusop, S. (2021). Prospect of abandoned metal mining sites from a hydrogeochemical perspective. *Environmental Science and Pollution Research*, *28*(3), 2678–2695. https://doi.org/10.1007/s11356-020-10626-1

Kusin, F. M., Zahar, M. S. M., Muhammad, S. N., Mohamad, N. D., Zin, Z. M., & Sharif, S. M. (2016). Hybrid off-river augmentation system as an alternative raw water resource: the hydrogeochemistry of abandoned mining ponds. *Environmental Earth Sciences*, *75*(3), 1–15. https://doi.org/10.1007/s12665-015-4981-7

Lata, S., Singh, P. K., & Samadder, S. R. (2015). Regeneration of adsorbents and recovery of heavy metals: a review. *International Journal of Environmental Science and Technology*, *12*(4), 1461–1478. https://doi.org/10.1007/s13762-014-0714-9

Lau, A. Y. T., Tsang, D. C. W., Graham, N. J. D., Ok, Y. S., Yang, X., & Li, X. dong. (2017). Surface-modified biochar in a bioretention system for Escherichia coli removal from stormwater. *Chemosphere*, *169*, 89–98. https://doi.org/10.1016/j.chemosphere.2016.11.048

Lee, H. S., & Shin, H. S. (2021). Competitive adsorption of heavy metals onto modified biochars: Comparison of biochar properties and modification methods. In *Journal of Environmental Management* (Vol. 299). https://doi.org/10.1016/j.jenvman.2021.113651

Lee, M. E., Park, J. H., & Chung, J. W. (2019). Comparison of the lead and copper adsorption capacities of plant source materials and their biochars. *Journal of Environmental Management*, *236*(January), 118–124. https://doi.org/10.1016/j.jenvman.2019.01.100

Li, H., Dong, X., da Silva, E. B., de Oliveira, L. M., Chen, Y., & Ma, L. Q. (2017). Mechanisms of metal sorption by biochars: Biochar characteristics and modifications. *Chemosphere*, *178*, 466–478. https://doi.org/10.1016/j.chemosphere.2017.03.072

Li, S., Harris, S., Anandhi, A., & Chen, G. (2019a). *Predicting biochar properties and functions based on feedstock and pyrolysis temperature : A review and data syntheses*. *215*, 890–902.

Li, S., Harris, S., Anandhi, A., & Chen, G. (2019b). Predicting biochar properties and functions based on feedstock and pyrolysis temperature: A review and data syntheses. *Journal of Cleaner Production*, *215*, 890–902. https://doi.org/10.1016/j.jclepro.2019.01.106

Li, X., Song, Y., Wang, F., Bian, Y., & Jiang, X. (2019). Combined effects of maize straw biochar and oxalic acid on the dissipation of polycyclic aromatic hydrocarbons and microbial community structures in

soil: A mechanistic study. *Journal of Hazardous Materials*, *364*(October 2018), 325–331. https://doi.org/10.1016/j.jhazmat.2018.10.041

Lim, C. S., Shaharuddin, M. S., & Sam, W. Y. (2012). Risk Assessment of Exposure to Lead in Tap Water among Residents of Seri Kembangan, Selangor state, Malaysia. *Global Journal of Health Science*, *5*(2), 1–12. https://doi.org/10.5539/gjhs.v5n2p1

Liu, S.-H. (2018). Waste-Derived Biochar for CO2 Sequestration. In *Biochar from Biomass and Waste*. Elsevier Inc. https://doi.org/10.1016/b978-0-12-811729-3.00016-9

Liu, X., Bai, X., Dong, L., Liang, J., Jin, Y., Wei, Y., Li, Y., Huang, S., & Qu, J. (2018). Composting enhances the removal of lead ions in aqueous solution by spent mushroom substrate: Biosorption and precipitation. *Journal of Cleaner Production*, *200*, 1–11. https://doi.org/10.1016/j.jclepro.2018.07.182

Liu, Z., Singer, S., Tong, Y., Kimbell, L., Anderson, E., Hughes, M., Zitomer, D., & McNamara, P. (2018). Characteristics and applications of biochars derived from wastewater solids. *Renewable and Sustainable Energy Reviews*, *90*(February), 650–664. https://doi.org/10.1016/j.rser.2018.02.040

Lu, L., & Chen, B. (2018). Enhanced bisphenol A removal from stormwater in biochar-amended biofilters: Combined with batch sorption and fixed-bed column studies. *Environmental Pollution*, *243*, 1539–1549. https://doi.org/10.1016/j.envpol.2018.09.097

Luo, L., Wang, G., Shi, G., Zhang, M., Zhang, J., & He, J. (2019). The characterization of biochars derived from rice straw and swine manure , and their potential and risk in N and P removal from water. *Journal of Environmental Management*, *245*(May), 1–7. https://doi.org/10.1016/j.jenvman.2019.05.072

Luo, M., Lin, H., Li, B., Dong, Y., He, Y., & Wang, L. (2018a). A novel modification of lignin on corncob-based

biochar to enhance removal of cadmium from water. *Bioresource Technology*, *259*(January), 312–318. https://doi.org/10.1016/j.biortech.2018.03.075

Luo, M., Lin, H., Li, B., Dong, Y., He, Y., & Wang, L. (2018b). Bioresource Technology A novel modi fi cation of lignin on corncob-based biochar to enhance removal of cadmium from water. *Bioresource Technology*, *259*(January), 312–318. https://doi.org/10.1016/j.biortech.2018.03.075

Mahdi, Z., Hanandeh, A. El, & Yu, Q. J. (2019). Journal of Environmental Chemical Engineering Preparation , characterization and application of surface modi fi ed biochar from date seed for improved lead , copper , and nickel removal from aqueous solutions. *Journal of Environmental Chemical Engineering*, *7*(5), 103379. https://doi.org/10.1016/j.jece.2019.103379

Mahdi, Z., Yu, Q. J., & El Hanandeh, A. (2018). Investigation of the kinetics and mechanisms of nickel and copper ions adsorption from aqueous solutions by date seed derived biochar. In *Journal of Environmental Chemical Engineering* (Vol. 6, Issue 1, pp. 1171–1181). https://doi.org/10.1016/j.jece.2018.01.021

Mahdi, Z., Yu, Q. J., & El Hanandeh, A. (2019). Competitive adsorption of heavy metal ions (Pb 2+ , Cu 2+ , and Ni 2+) onto date seed biochar: batch and fixed bed experiments. *Separation Science and Technology (Philadelphia)*, *54*(6), 888–901. https://doi.org/10.1080/01496395.2018.1523192

Malik, D. S., Jain, C. K., & Yadav, A. K. (2018). Heavy Metal Removal by Fixed-Bed Column – A Review. In *ChemBioEng Reviews* (Vol. 5, Issue 3, pp. 173–179). Wiley-Blackwell. https://doi.org/10.1002/cben.201700018

Mattos, R. C., Hemsi, P. S., Kawachi, E. Y., & Silva, F. T. (2015). Use of sugarcane bagasse as carbon substrate in permeable reactive barriers: Laboratory batch tests and mathematical modeling. *Soils and Rocks*, *38*(3), 219–229.

Mohamed, N. B., Ngadi, N., Lani, N. S., & Rahman, R. A. (2017). Polyethylenimine modified sugarcane bagasse adsorbent for methyl orange dye removal. *Chemical Engineering Transactions*, *56*, 103–108. https://doi.org/10.3303/CET1756018

Mohan, D., Sarswat, A., Ok, Y. S., & Pittman, C. U. (2014). Organic and inorganic contaminants removal from water with biochar, a renewable, low cost and sustainable adsorbent - A critical review. *Bioresource Technology*, *160*, 191–202. https://doi.org/10.1016/j.biortech.2014.01.120

Mohanty, S. K., Valenca, R., Berger, A. W., Yu, I. K. M., Xiong, X., Saunders, T. M., & Tsang, D. C. W. (2018a). Plenty of room for carbon on the ground: Potential applications of biochar for stormwater treatment. *Science of the Total Environment*, *625*, 1644–1658. https://doi.org/10.1016/j.scitotenv.2018.01.037

Mohanty, S. K., Valenca, R., Berger, A. W., Yu, I. K. M., Xiong, X., Saunders, T. M., & Tsang, D. C. W. (2018b). Science of the Total Environment Plenty of room for carbon on the ground : Potential applications of biochar for stormwater treatment. *Science of the Total Environment*, *625*, 1644–1658. https://doi.org/10.1016/j.scitotenv.2018.01.037

Mohd Salleh, I. S., Mustazar, N. A., & Yussof, H. W. (2018). Mercury Removal from Wastewater Using Palm Oil Fuel Ash. *MATEC Web of Conferences*, *150*, 10–14. https://doi.org/10.1051/matecconf/201815002007

Molahid, V. L. M., Mohd Kusin, F., & Madzin, Z. (2018). Role of multiple substrates (spent mushroom compost, ochre, steel slag, and limestone) in passive remediation of metal-containing acid mine drainage. *Environmental Technology (United Kingdom)*, *0*(0), 1–14. https://doi.org/10.1080/09593330.2017.1422546

Montoya-Suarez, S., Colpas-Castillo, F., Meza-Fuentes, E., Rodríguez-Ruiz, J., & Fernandez-Maestre, R.

(2016). Activated carbons from waste of oil-palm kernel shells, sawdust and tannery leather scraps and application to chromium(VI), phenol, and methylene blue dye adsorption. *Water Science and Technology*, *73*(1), 21–27. https://doi.org/10.2166/wst.2015.293

Muhammad, S. N., Kusin, F. M., Md Zahar, M. S., Mohamat Yusuff, F., & Halimoon, N. (2017a). Passive bioremediation technology incorporating lignocellulosic spent mushroom compost and limestone for metal- and sulfate-rich acid mine drainage. *Environmental Technology (United Kingdom)*, *38*(16), 2003–2012. https://doi.org/10.1080/09593330.2016.1244568

Muhammad, S. N., Kusin, F. M., Md Zahar, M. S., Mohamat Yusuff, F., & Halimoon, N. (2017b). Passive bioremediation technology incorporating lignocellulosic spent mushroom compost and limestone for metal- and sulfate-rich acid mine drainage. *Environmental Technology (United Kingdom)*, *38*(16), 2003–2012. https://doi.org/10.1080/09593330.2016.1244568

Nasir, A. M., Goh, P. S., Abdullah, M. S., Ng, B. C., & Ismail, A. F. (2019). Adsorptive nanocomposite membranes for heavy metal remediation: Recent progresses and challenges. *Chemosphere*, *232*, 96–112. https://doi.org/10.1016/j.chemosphere.2019.05.174

Neculita, C. M., & Rosa, E. (2019). A review of the implications and challenges of manganese removal from mine drainage. *Chemosphere*, *214*, 491–510. https://doi.org/10.1016/j.chemosphere.2018.09.106

Neculita, C. M., Zagury, G. J., & Kulnieks, V. (2007). Short-term and long-term bioreactors for acid mine drainage treatment. *Association for Environmental Health and Sciences - 22nd Annual International Conference on Contaminated Soils, Sediments and Water 2006*, *12*(2007), 1–10. http://www.scopus.com/inward/record.url?eid=2-s2.0-58349115629&partnerID=tZOtx3y1

Ni, B. J., Huang, Q. S., Wang, C., Ni, T. Y., Sun, J., & Wei, W. (2019). Competitive adsorption of heavy metals in aqueous solution onto biochar derived from anaerobically digested sludge. In *Chemosphere* (Vol.

219, pp. 351–357). https://doi.org/10.1016/j.chemosphere.2018.12.053

Niazi, N. K., Murtaza, B., Bibi, I., Shahid, M., White, J. C., Nawaz, M. F., Bashir, S., Shakoor, M. B., Choppala, G., Murtaza, G., & Wang, H. (2016). Removal and Recovery of Metals by Biosorbents and Biochars Derived From Biowastes. In *Environmental Materials and Waste: Resource Recovery and Pollution Prevention*. Elsevier Inc. https://doi.org/10.1016/B978-0-12-803837-6.00007-X

Noor Syuhadah, S., & Rohasliney, H. (2012). Rice Husk as bioabsorbent: Areview. *Health and the Environment Journal*, *3*(1), 89–95.

Nworie, F. S., Nwabue, F. I., Oti, W., Mbam, E., & Nwali, B. U. (2019). Removal of methylene blue from aqueous solution using activated rice husk biochar: Adsorption isotherms, kinetics and error analysis. *Journal of the Chilean Chemical Society*, *64*(1), 4365–4376. https://doi.org/10.4067/s0717-97072019000104365

O'Connor, D., Peng, T., Zhang, J., Tsang, D. C. W., Alessi, D. S., Shen, Z., Bolan, N. S., & Hou, D. (2018). Biochar application for the remediation of heavy metal polluted land: A review of in situ field trials. *Science of the Total Environment*, *619–620*, 815–826. https://doi.org/10.1016/j.scitotenv.2017.11.132

Onaga Medina, F. M., Aguiar, M. B., Parolo, M. E., & Avena, M. J. (2021). Insights of competitive adsorption on activated carbon of binary caffeine and diclofenac solutions. In *Journal of Environmental Management* (Vol. 278). https://doi.org/10.1016/j.jenvman.2020.111523

Pal, D. B., Singh, A., Jha, J. M., Srivastava, N., Hashem, A., Alakeel, M. A., Abd_Allah, E. F., & Gupta, V. K. (2021). Low-cost biochar adsorbents prepared from date and delonix regia seeds for heavy metal sorption. In *Bioresource Technology* (Vol. 339). https://doi.org/10.1016/j.biortech.2021.125606

Pan, J., Ma, J., Zhai, L., Luo, T., Mei, Z., & Liu, H. (2019). Achievements of biochar application for enhanced

anaerobic digestion: A review. *Bioresource Technology*, 122058. https://doi.org/10.1016/j.biortech.2019.122058

Pan, X., Gu, Z., Chen, W., & Li, Q. (2021). Preparation of biochar and biochar composites and their application in a Fenton-like process for wastewater decontamination: A review. *Science of the Total Environment*, *754*. https://doi.org/10.1016/j.scitotenv.2020.142104

Paranavithana, G. N., Kawamoto, K., Inoue, Y., & Saito, T. (2016). Adsorption of Cd 2 + and Pb 2 + onto coconut shell biochar and biochar-mixed soil. *Environmental Earth Sciences*, *75*(6), 1–12. https://doi.org/10.1007/s12665-015-5167-z

Park, J. H., Cho, J. S., Ok, Y. S., Kim, S. H., Kang, S. W., Choi, I. W., Heo, J. S., Delaune, R. D., & Seo, D. C. (2015). Competitive adsorption and selectivity sequence of heavy metals by chicken bone-derived biochar: Batch and column experiment. *Journal of Environmental Science and Health - Part A Toxic/Hazardous Substances and Environmental Engineering*, *50*(11), 1194–1204. https://doi.org/10.1080/10934529.2015.1047680

Patel, H. (2019). Fixed-bed column adsorption study: a comprehensive review. *Applied Water Science*, *9*(3). https://doi.org/10.1007/s13201-019-0927-7

Patel, H. (2021). Review on solvent desorption study from exhausted adsorbent. In *Journal of Saudi Chemical Society* (Vol. 25, Issue 8). https://doi.org/10.1016/j.jscs.2021.101302

Patel, H. (2022). Comparison of batch and fixed bed column adsorption: a critical review. *International Journal of Environmental Science and Technology*, *19*(10), 10409–10426. https://doi.org/10.1007/s13762-021-03492-y

Phing, A., Ahmad, L., & Aris, Z. (2014). *A review on economically adsorbents on heavy metals removal in water and wastewater*. 163–181. https://doi.org/10.1007/s11157-013-9330-2

Prabhu, A. A., Chityala, S., Jayachandran, D., Deshavath, N. N., & Veeranki, V. D. (2021). A two step optimization approach for maximizing biosorption of hexavalent chromium ions (Cr (VI)) using alginate immobilized Sargassum sp in a packed bed column. *Separation Science and Technology (Philadelphia)*, *56*(1), 90–106. https://doi.org/10.1080/01496395.2019.1708933

Qambrani, N. A., Rahman, M. M., Won, S., Shim, S., & Ra, C. (2017). Biochar properties and eco-friendly applications for climate change mitigation, waste management, and wastewater treatment: A review. *Renewable and Sustainable Energy Reviews*, *79*(May), 255–273. https://doi.org/10.1016/j.rser.2017.05.057

Qiu, B., Tao, X., Wang, H., Li, W., Ding, X., & Chu, H. (2021). Biochar as a low-cost adsorbent for aqueous heavy metal removal: A review. In *Journal of Analytical and Applied Pyrolysis* (Vol. 155). https://doi.org/10.1016/j.jaap.2021.105081

Rashidi, N. A., & Yusup, S. (2019). *Biochar as potential precursors for activated carbon production : parametric analysis and multi-response optimization*.

Rosales, E., Meijide, J., Pazos, M., & Sanromán, M. A. (2017). Challenges and recent advances in biochar as low-cost biosorbent: From batch assays to continuous-flow systems. *Bioresource Technology*, *246*, 176–192. https://doi.org/10.1016/j.biortech.2017.06.084

Roychowdhury, A., Sarkar, D., & Datta, R. (2015). *Remediation of Acid Mine Drainage-Impacted Water*. 131–141. https://doi.org/10.1007/s40726-015-0011-3

S, R., & P, B. (2019). The potential of lignocellulosic biomass precursors for biochar production: Performance, mechanism and wastewater application—A review. *Industrial Crops and Products*, *128*(November 2018), 405–423. https://doi.org/10.1016/j.indcrop.2018.11.041

Said, Z., Nguyen, T. H., Sharma, P., Li, C., Ali, H. M., Nguyen, V. N., Pham, V. V., Ahmed, S. F., Van, D. N., &

Truong, T. H. (2022). Multi-attribute optimization of sustainable aviation fuel production-process from microalgae source. In *Fuel* (Vol. 324). https://doi.org/10.1016/j.fuel.2022.124759

Samsuri, A. W., Sadegh-Zadeh, F., & Seh-Bardan, B. J. (2014). Characterization of biochars produced from oil palm and rice husks and their adsorption capacities for heavy metals. *International Journal of Environmental Science and Technology*, *11*(4), 967–976. https://doi.org/10.1007/s13762-013-0291-3

Sarker, T. C., Azam, S. M. G. G., El-Gawad, A. M. A., Gaglione, S. A., & Bonanomi, G. (2017). Sugarcane bagasse: a potential low-cost biosorbent for the removal of hazardous materials. *Clean Technologies and Environmental Policy*, *19*(10), 2343–2362. https://doi.org/10.1007/s10098-017-1429-7

Sewu, D. D., Boakye, P., & Woo, S. H. (2017). Highly efficient adsorption of cationic dye by biochar produced with Korean cabbage waste. *Bioresource Technology*, *224*, 206–213. https://doi.org/10.1016/j.biortech.2016.11.009

Shaheen, S. M., Niazi, N. K., Hassan, N. E. E., Bibi, I., Wang, H., Tsang, D. C. W., Ok, Y. S., Bolan, N., & Rinklebe, J. (2018). Wood-based biochar for the removal of potentially toxic elements in water and wastewater: a critical review. *International Materials Reviews*, *6608*, 1–32. https://doi.org/10.1080/09506608.2018.1473096

Shamsollahi, Z., & Partovinia, A. (2019). Recent advances on pollutants removal by rice husk as a bio-based adsorbent : A critical review. *Journal of Environmental Management*, *246*(February), 314–323. https://doi.org/10.1016/j.jenvman.2019.05.145

Shan, R., Shi, Y., Gu, J., Wang, Y., & Yuan, H. (2020a). Single and competitive adsorption affinity of heavy metals toward peanut shell-derived biochar and its mechanisms in aqueous systems. *Chinese Journal of Chemical Engineering*, *28*(5), 1375–1383. https://doi.org/10.1016/j.cjche.2020.02.012

Shan, R., Shi, Y., Gu, J., Wang, Y., & Yuan, H. (2020b). Single and competitive adsorption affinity of heavy metals toward peanut shell-derived biochar and its mechanisms in aqueous systems. *Chinese Journal of Chemical Engineering*, *28*(5), 1375–1383. https://doi.org/10.1016/j.cjche.2020.02.012

Shen, Z., Hou, D., Jin, F., Shi, J., Fan, X., Tsang, D. C. W., & Alessi, D. S. (2019). Effect of production temperature on lead removal mechanisms by rice straw biochars. *Science of the Total Environment*, *655*, 751–758. https://doi.org/10.1016/j.scitotenv.2018.11.282

Shi, Y., Hu, H., & Ren, H. (2019). Dissolved organic matter (DOM) removal from biotreated coking wastewater by chitosan-modified biochar: Adsorption fractions and mechanisms. *Bioresource Technology*, 122281. https://doi.org/10.1016/j.biortech.2019.122281

Spokas, K., Wang, C., Xie, T., Yargicoglu, E., & Reddy, K. R. (2014). Characteristics and Applications of Biochar for Environmental Remediation: A Review. *Critical Reviews in Environmental Science and Technology*, *45*(9), 939–969. https://doi.org/10.1080/10643389.2014.924180

Subratti, A., Vidal, J. L., Lalgee, L. J., Kerton, F. M., & Jalsa, N. K. (2021). Preparation and characterization of biochar derived from the fruit seed of Cedrela odorata L and evaluation of its adsorption capacity with methylene blue. *Sustainable Chemistry and Pharmacy*, *21*. https://doi.org/10.1016/j.scp.2021.100421

Sulyman, M., Namiesnik, J., & Gierak, A. (2017). *Low-cost Adsorbents Derived from Agricultural By-products / Wastes for Enhancing Contaminant Uptakes from Wastewater : A Review*. *26*(2), 479–510. https://doi.org/10.15244/pjoes/66769

Sun, Y., Chen, S. S., Lau, A. Y. T., Tsang, D. C. W., Mohanty, S. K., Bhatnagar, A., Rinklebe, J., Lin, K. Y. A., & Ok, Y. S. (2020). Waste-derived compost and biochar amendments for stormwater treatment in bioretention column: Co-transport of metals and colloids. *Journal of Hazardous Materials*,

383(August 2019). https://doi.org/10.1016/j.jhazmat.2019.121243

Sun, Y., Shah, K. J., Sun, W., & Zheng, H. (2019). Performance evaluation of chitosan-based flocculants with good pH resistance and high heavy metals removal capacity. *Separation and Purification Technology*, *215*(January), 208–216. https://doi.org/10.1016/j.seppur.2019.01.017

Tay, C. C., Liew, H. H., Redzwan, G., Yong, S. K., Surif, S., & Abdul-Talib, S. (2011). Pleurotus ostreatus spent mushroom compost as green biosorbent for nickel (II) biosorption. *Water Science and Technology*, *64*(12), 2425–2432. https://doi.org/10.2166/wst.2011.805

Teow, Y. H., Mohammad, A. W., Ramli, S., Sajab, M. S., & Mohamad Mazuki, N. I. (2018). Potential of Membrane Technology for Treatment and Reuse of Water from Old Mining Lakes. *Sains Malaysiana*, *47*(11), 2887–2897. https://doi.org/10.17576/jsm-2018-4711-32

Tsai, W. T., Bai, Y. C., Lin, Y. Q., Lai, Y. C., & Tsai, C. H. (2020). Porous and adsorption properties of activated carbon prepared from cocoa pod husk by chemical activation. *Biomass Conversion and Biorefinery*, *10*(1), 35–43. https://doi.org/10.1007/s13399-019-00403-7

Tsang, D. C. W., Yu, I. K. M., & Xiong, X. (2019). Novel Application of Biochar in Stormwater Harvesting. *Biochar from Biomass and Waste*, 319–347. https://doi.org/10.1016/b978-0-12-811729-3.00018-2

Tulun, Ş., Akgül, G., Alver, A., & Çelebi, H. (2021). Adaptive neuro-fuzzy interference system modelling for chlorpyrifos removal with walnut shell biochar. In *Arabian Journal of Chemistry* (Vol. 14, Issue 12). https://doi.org/10.1016/j.arabjc.2021.103443

Ulrich, B. A., Loehnert, M., & Higgins, C. P. (2017). Improved contaminant removal in vegetated stormwater biofilters amended with biochar. *Environmental Science: Water Research and Technology*, *3*(4), 726–734. https://doi.org/10.1039/c7ew00070g

Vakili, M., Deng, S., Cagnetta, G., Wang, W., Meng, P., Liu, D., & Yu, G. (2019). Regeneration of chitosan-

based adsorbents used in heavy metal adsorption: A review. In *Separation and Purification Technology* (Vol. 224, pp. 373–387). https://doi.org/10.1016/j.seppur.2019.05.040

Vareda, J. P., Valente, A. J. M., & Durães, L. (2019). Assessment of heavy metal pollution from anthropogenic activities and remediation strategies : A review. *Journal of Environmental Management*, *246*(May), 101–118. https://doi.org/10.1016/j.jenvman.2019.05.126

Vítková, M., Sylva, C., Trakal, L., Veselská, V., & Šafar, I. (2016). *Bioresource Technology Lead and cadmium sorption mechanisms on magnetically modified biochars*. *203*, 318–324. https://doi.org/10.1016/j.biortech.2015.12.056

Walker, J., & Walker, S. M. (2000). Review: Effects of iron overload on the immune system. *Annals of Clinical and Laboratory Science*, *30*(4), 354–365.

Wan Yaacob, W. Z., Mohd Pauzi, N. S., & Abdul Mutalib, H. (2009). Acid mine drainage and heavy metals contamination at abandoned and active mine sites in Pahang. *Bulletin of the Geological Society of Malaysia*, *55*(November 2009), 15–20. https://doi.org/10.7186/bgsm2009003

Wang, H., Gao, B., Wang, S., Fang, J., Xue, Y., & Yang, K. (2015). Bioresource Technology Removal of Pb (II), Cu (II), and Cd (II) from aqueous solutions by biochar derived from KMnO 4 treated hickory wood. *BIORESOURCE TECHNOLOGY*, *197*, 356–362. https://doi.org/10.1016/j.biortech.2015.08.132

Wang, J., & Wang, S. (2019). Preparation, modification and environmental application of biochar: A review. *Journal of Cleaner Production*, *227*, 1002–1022. https://doi.org/10.1016/j.jclepro.2019.04.282

Wang, L., Wang, Y., Ma, F., Tankpa, V., Bai, S., Guo, X., & Wang, X. (2019a). Mechanisms and reutilization of modified biochar used for removal of heavy metals from wastewater: A review. *Science of the Total Environment*, *668*, 1298–1309. https://doi.org/10.1016/j.scitotenv.2019.03.011

Wang, L., Wang, Y., Ma, F., Tankpa, V., Bai, S., Guo, X., & Wang, X. (2019b). *Science of the Total Environment Mechanisms and reutilization of modi fi ed biochar used for removal of heavy metals from wastewater : A review*. *668*, 1298–1309.

Wang, R., Huang, D., Liu, Y., Zhang, C., & Lai, C. (2019). Recent advances in biochar-based catalysts : Properties , applications and mechanisms for pollution remediation. *Chemical Engineering Journal*, *371*(April), 380–403. https://doi.org/10.1016/j.cej.2019.04.071

Wei, D., Li, B., Huang, H., Luo, L., Zhang, J., Yang, Y., Guo, J., Tang, L., Zeng, G., & Zhou, Y. (2018). Biochar-based functional materials in the purification of agricultural wastewater: Fabrication, application and future research needs. *Chemosphere*, *197*, 165–180. https://doi.org/10.1016/j.chemosphere.2017.12.193

Wei, Y., Jin, Z., Zhang, M., Li, Y., Huang, S., Liu, X., Jin, Y., Wang, H., & Qu, J. (2020). Impact of spent mushroom substrate on Cd immobilization and soil property. *Environmental Science and Pollution Research*, *27*(3), 3007–3022. https://doi.org/10.1007/s11356-019-07138-y

Wong, Y. J., Arumugasamy, S. K., Chung, C. H., Selvarajoo, A., & Sethu, V. (2020). Comparative study of artificial neural network (ANN), adaptive neuro-fuzzy inference system (ANFIS) and multiple linear regression (MLR) for modeling of Cu (II) adsorption from aqueous solution using biochar derived from rambutan (Nephelium lappaceum) peel. *Environmental Monitoring and Assessment*, *192*(7). https://doi.org/10.1007/s10661-020-08268-4

Wu, Q., Xian, Y., He, Z., Zhang, Q., Wu, J., Yang, G., Zhang, X., Qi, H., Ma, J., Xiao, Y., & Long, L. (2019a). Adsorption characteristics of Pb(II) using biochar derived from spent mushroom substrate. *Scientific Reports*, *9*(1), 1–11. https://doi.org/10.1038/s41598-019-52554-2

Wu, Q., Xian, Y., He, Z., Zhang, Q., Wu, J., Yang, G., Zhang, X., Qi, H., Ma, J., Xiao, Y., & Long, L. (2019b).

Adsorption characteristics of Pb(II) using biochar derived from spent mushroom substrate. *Scientific Reports*, *9*(1), 1–11. https://doi.org/10.1038/s41598-019-52554-2

Xiao-jing, H., Hai-dong, G., Ting-ting, Z., Yu, J., & Juan-juan, Q. (2014). Biosorption mechanism of Cu2+ by innovative immobilized spent substrate of fragrant mushroom biomass. *Ecological Engineering*, *73*, 509–513. https://doi.org/10.1016/j.ecoleng.2014.09.067

Xu, D., Lee, L. Y., Lim, F. Y., Lyu, Z., Zhu, H., Ong, S. L., & Hu, J. (2019). Water treatment residual: A critical review of its applications on pollutant removal from stormwater runoff and future perspectives. *Journal of Environmental Management*, *September*. https://doi.org/10.1016/j.jenvman.2019.109649

Yadav, V. B., Gadi, R., & Kalra, S. (2019). Clay based nanocomposites for removal of heavy metals from water: A review. *Journal of Environmental Management*, *232*(October 2018), 803–817. https://doi.org/10.1016/j.jenvman.2018.11.120

Yang, X., Wan, Y., Zheng, Y., He, F., Yu, Z., Huang, J., Wang, H., Ok, Y. S., Jiang, Y., & Gao, B. (2019). Surface functional groups of carbon-based adsorbents and their roles in the removal of heavy metals from aqueous solutions: A critical review. *Chemical Engineering Journal*, *366*(February), 608–621. https://doi.org/10.1016/j.cej.2019.02.119

Yunus, K., Zuraidah, M. A., & John, A. (2020). A review on the accumulation of heavy metals in coastal sediment of Peninsular Malaysia. *Ecofeminism and Climate Change*, *1*(1), 21–35. https://doi.org/10.1108/efcc-03-2020-0003

Zang, T., Cheng, Z., Lu, L., Jin, Y., Xu, X., Ding, W., & Qu, J. (2017). Removal of Cr(VI) by modified and immobilized Auricularia auricula spent substrate in a fixed-bed column. *Ecological Engineering*, *99*, 358–365. https://doi.org/10.1016/j.ecoleng.2016.11.070

Zhang, S., Zhu, C., Xia, S., & Li, M. (2019). Impact of different running conditions on performance of biofilters treating secondary effluent during start-up. *Bioresource Technology*, *281*(122), 168–178. https://doi.org/10.1016/j.biortech.2019.02.094

Zhao, Y., Fan, D., Li, Y., & Yang, F. (2022). Application of machine learning in predicting the adsorption capacity of organic compounds onto biochar and resin. In *Environmental Research* (Vol. 208). https://doi.org/10.1016/j.envres.2022.112694

Zhu, X., Wang, X., & Ok, Y. S. (2019). The application of machine learning methods for prediction of metal sorption onto biochars. In *Journal of Hazardous Materials* (Vol. 378). https://doi.org/10.1016/j.jhazmat.2019.06.004

Appendices

Matlab calibration codes using ANFIS

```
%%% ANFIS %%%%%%%%%%%%%%%%%%%%%%%%%%%%%%%%%%%%%%%%%%%%
%%%%%%%%%%%%%%%%%%%%%%%%%%%%%%%%%%%%%%%%%%%%%%%%%%%%%%
clear; addpath('Functions'); tic;

% Directory
train_filename = 'Biochar_adsorptioncap_c1.csv';
test_filename = 'Biochar_adsorptioncap_validation.csv';

%%%%%%%%%%%%%%%%%%%%%%%%%%%%%%%%%%%%%%%%%%%%%%%%%%%%%%
% Import training data %%%%%%%%%%%%%%%%%%%%%%%%%%%%%%%
data = importdataX(train_filename).data{:};
x1 = data(:, 1:4);
ph1 = data(:, 5);
t1 = data(:, 6);
y1 = data(:, 7:end);

interval = [0.1 0.9];
[x2,c_x] = normX(x1,interval,'normalize');
[ph2,c_ph] = normX(ph1,interval,'normalize');
[t2,c_t] = normX(t1,interval,'normalize');
[y2,c_y] = normX(y1,interval,'normalize');
```

```
%%%%%%%%%%%%%%%%%%%%%%%%%%%%%%%%%%%%%%%%%%%%%%%%%%%%%%%%%%%%%%%%%%%%%%%
% Import testing data %%%%%%%%%%%%%%%%%%%%%%%%%%%%%%%%
data = importdataX(test_filename).data{:};
t_x1 = data(:, 1:4);
t_ph1 = data(:, 5);
t_t1 = data(:, 6);
t_y1 = data(:, 7:end);

t_x2 = normX(t_x1,interval,'normalize', c_x);
t_ph2 = normX(t_ph1,interval,'normalize', c_ph);
t_t2 = normX(t_t1,interval,'normalize', c_t);
t_y2 = normX(t_y1,interval,'normalize', c_y);

%%%%%%%%%%%%%%%%%%%%%%%%%%%%%%%%%%%%%%%%%%%%%%%%%%%%%%%%%%%%%%%%%%%%%%%
% Running ANFIS %%%%%%%%%%%%%%%%%%%%%%%%%%%%%%%%%%%%%%%%
opt = genfisOptions('GridPartition');
opt.NumMembershipFunctions = 2;
opt.InputMembershipFunctionType = 'gaussmf';
opt.OutputMembershipFunctionType = 'constant';
epoch_n = 10;

% figure
label = {'Cu' 'Fe' 'Mn' 'Pb'};
for i = 1:4
   fis = genfis([x2 ph2 t2], y2(:,i), opt);
   an_opt = anfisOptions('InitialFIS', fis, 'EpochNumber', epoch_n);
   an_opt.DisplayANFISInformation = 0;
   an_opt.DisplayErrorValues = 0;
```

```
    an_opt.DisplayStepSize = 0;
    an_opt.DisplayFinalResults = 0;
    model = anfis([x2 ph2 t2 y2(:,i)],an_opt);

    % Calibration results
%     modelOut = evalfis(model, [x2 ph2 t2]);
%     out = normX(modelOut,interval,'denormalize',c_y(:,i));
%     out(out < 0) = 0;
%     y_out(:,i) = out;
%     [~,RS(i),RMSE(i),MAE(i)] = validation(y1(:,i),out);
%     subplot(4,1,i)
%     plot(y1(:,i))
%     hold on
%     plot(out)
%     ylabel(label{i})

    % Testing results
    modelOut = evalfis(model, [t_x2 t_ph2 t_t2]);
    out = normX(modelOut,interval,'denormalize',c_y(:,i));
    out(out < 0) = 0;
    y_out(:,i) = out;
    [~,RS(i),RMSE(i),MAE(i)] = validation(t_y1(:,i),out);
    subplot(4,1,i)
    plot(t_y1(:,i))
    hold on
    plot(out)
    ylabel(label{i})
end
```

```
summary = array2table([RS; RMSE; MAE], 'RowNames', {'Rsquared', 'RMSE', 'MAE'}, 'VariableNames', label)

data = array2table([t_x1, t_ph1, t_t1, y_out], 'VariableNames', [label, 'pH', 't', strcat(label, '_out')]);
writetable(summary, strcat('Results\Stats_', test_filename), 'WriteRowNames', true)
writetable(data, strcat('Results\ANFISData_', test_filename))
```

Matlab validation performance code using ANFIS

```
%VALIDATION Calculates CE, RS, RMSE, MAE, and RPE between observed and simulated data.
%   [CE,RS,RMSE,MAE,RPE] = VALIDATION(OBS_DATA,SIM_DATA) calculates the 5
%   criteria from the data inputs. RPE is calculated from the largest
%   observed value/peak.
%
%   [CE,RS,RMSE,MAE,RPE] = VALIDATION(DATA1,DATA2,RPE_THRESHOLD) calculates
%   RPE for multiple observed values/peaks above the RPE_THRESHOLD value
%   against simulated values. Empty RPE_THRESHOLD value returns result for
%   only the highest value/peak, same as default case.
%
%

function [CE,RS,RMSE,MAE,RPE,rpeThresh] = validation(Obs_OUT,Sim_OUT,varargin)
narginchk(2,3)

% CE
v = mean(Obs_OUT);
```

```
e = mean((Obs_OUT-v).^2);

f = mean((Sim_OUT-Obs_OUT).^2);

CE = 1-(f/e);


% RMSE

RMSE = sqrt(f);


% Rsquared

R2 = corrcoef(Obs_OUT,Sim_OUT);

RS = (R2(1,2).^2);


% MAE

MAE = mean(abs(Sim_OUT-Obs_OUT));


% RPE

if nargin == 3 && ~isempty(varargin{1}) % If 3rd input present
   if ischar(varargin{1}) % If percentile, else observed value
      percStr = varargin{1};
      if percStr(end) == '%'
         rpePerc = str2double(percStr(1:end-1));
         rpeThresh = prctile(Obs_OUT,100-rpePerc);
      else
         error('Unknown expression for RPE parameter')
      end
   else
       rpeThresh = varargin{1};
   end
   threshIdx = Obs_OUT > rpeThresh;
```

```
    obsPeaks = Obs_OUT(threshIdx);
    simPeaks = Sim_OUT(threshIdx);
    RPE = mean(abs(simPeaks - obsPeaks)./obsPeaks);
else
    RPE = abs(max(Sim_OUT)-max(Obs_OUT))/max(Obs_OUT);
end
```

Seventeen sets of lab scale metal retention column data calibration results using ANFIS model

		Pb	Fe	Cu	Mn
Pb		0.063364	0.47192	0.194969	0.397847
	1	0.06383	0.471588	0.194979	0.39844
	1	0.064815	0.470879	0.195001	0.399701
	1	0.067011	0.469273	0.195049	0.402547
	1	0.069533	0.467393	0.195107	0.405866
	1	0.072404	0.46521	0.195173	0.409701
	1	0.07923	0.45986	0.195336	0.419041
	1	0.087405	0.453195	0.19554	0.430585
	1	0.091887	0.449434	0.195656	0.437066
	1	0.096529	0.445461	0.195778	0.443888
	1	0.137539	0.406737	0.196981	0.509733
	1	0.075352	0.618677	0.244826	0.518904
	1	0.075539	0.618671	0.244941	0.519623
	1	0.075933	0.618657	0.245186	0.521151
	1	0.076813	0.618625	0.245743	0.524602
	1	0.077824	0.618589	0.246396	0.528625
	1	0.078975	0.618546	0.247156	0.533276
	1	0.081711	0.618442	0.249025	0.544599
	1	0.084988	0.618311	0.251364	0.558596
	1	0.086784	0.618238	0.252688	0.566454
	1	0.088645	0.61816	0.254089	0.574725
	1	0.105082	0.617404	0.267855	0.654559
	1	0.088235	0.758925	0.299839	0.635567
	1	0.088122	0.75923	0.30007	0.636407
	1	0.087882	0.759881	0.300562	0.638194
	1	0.087348	0.761354	0.301678	0.642227
	1	0.086735	0.763079	0.302989	0.64693

1	0.086037	0.765082	0.304514	0.652366
1	0.084378	0.76999	0.308265	0.665601
1	0.08239	0.776104	0.31296	0.681962
1	0.0813	0.779555	0.315617	0.691146
1	0.080172	0.7832	0.318429	0.700814
1	0.070201	0.818728	0.346057	0.794128
1	0.096403	0.828044	0.337284	0.683784
1	0.096099	0.828503	0.337593	0.684674
1	0.095458	0.829481	0.338253	0.686568
1	0.094027	0.831695	0.339751	0.690842
1	0.092384	0.834289	0.341509	0.695826
1	0.090514	0.8373	0.343556	0.701586
1	0.086068	0.844678	0.348588	0.715612
1	0.080743	0.85387	0.354886	0.732949
1	0.077823	0.859058	0.35845	0.742682
1	0.0748	0.864537	0.362222	0.752927
1	0.048086	0.917947	0.399287	0.851812
1	0.416302	1.358268	0.568812	0.682685
5	0.417237	1.359253	0.569611	0.683441
5	0.419215	1.361351	0.571317	0.685049
5	0.423628	1.366103	0.575186	0.688677
5	0.428696	1.371669	0.579731	0.692908
5	0.434464	1.37813	0.585019	0.697798
5	0.448179	1.393962	0.598024	0.709705
5	0.464605	1.413688	0.614298	0.724424
5	0.47361	1.42482	0.623511	0.732686
5	0.482937	1.436577	0.633258	0.741384
5	0.565336	1.551187	0.729041	0.825333
5	0.637047	1.582182	0.683641	0.861125
5	0.638167	1.583504	0.68458	0.862028
5	0.640535	1.586319	0.686584	0.86395
5	0.645818	1.592696	0.691129	0.868288
5	0.651885	1.600165	0.696467	0.873346
5	0.65879	1.608835	0.702679	0.879192
5	0.675209	1.630081	0.717956	0.893426
5	0.694874	1.656551	0.737073	0.911021
5	0.705654	1.67149	0.747894	0.920898
5	0.71682	1.687267	0.759345	0.931296
5	0.815466	1.841066	0.871859	1.031651
5	0.87428	1.796165	0.810344	1.033089
5	0.875598	1.797808	0.811438	1.034135
5	0.878385	1.80131	0.81377	1.036359
5	0.884603	1.809239	0.819062	1.04138

5	0.891744	1.818526	0.825275	1.047235
5	0.899871	1.829308	0.832506	1.054002
5	0.919196	1.855728	0.85029	1.070479
5	0.942342	1.888643	0.872543	1.090846
5	0.95503	1.90722	0.885141	1.10228
5	0.968172	1.926838	0.898469	1.114316
5	1.084277	2.118088	1.029445	1.230482
5	1.024687	1.901623	0.896587	1.104162
5	1.026131	1.903425	0.897785	1.105267
5	1.029184	1.907264	0.900341	1.107616
5	1.035995	1.915958	0.90614	1.11292
5	1.043816	1.926142	0.91295	1.119104
5	1.052719	1.937964	0.920875	1.126252
5	1.073886	1.966934	0.940364	1.143655
5	1.099238	2.003026	0.964753	1.165168
5	1.113136	2.023395	0.978559	1.177245
5	1.127531	2.044907	0.993166	1.189958
5	1.254706	2.254614	1.136707	1.312659
5	0.806296	1.886329	1.301721	0.656583
10	0.810146	1.889647	1.30273	0.657684
10	0.818288	1.896717	1.304883	0.660025
10	0.836449	1.912729	1.309767	0.665309
10	0.857307	1.931483	1.315503	0.671471
10	0.881046	1.953255	1.322177	0.678593
10	0.937491	2.006605	1.338592	0.695933
10	1.005097	2.073071	1.359133	0.717367
10	1.042157	2.110583	1.37076	0.7294
10	1.080542	2.150199	1.383063	0.742067
10	1.41967	2.536392	1.503958	0.864321
10	0.931658	2.39559	1.396601	1.025804
10	0.935246	2.398006	1.397771	1.026773
10	0.942834	2.403154	1.400267	1.028835
10	0.95976	2.414813	1.405929	1.033487
10	0.979199	2.428469	1.412578	1.038912
10	1.001324	2.444322	1.420316	1.045183
10	1.053929	2.483168	1.439345	1.06045
10	1.116937	2.531565	1.463158	1.079323
10	1.151476	2.558879	1.476638	1.089917
10	1.18725	2.587725	1.490901	1.10107
10	1.503311	2.868929	1.631053	1.208712
10	1.066383	2.882264	1.501292	1.381625
10	1.06969	2.883818	1.50264	1.382467
10	1.076683	2.88713	1.505514	1.384259

10	1.092281	2.894628	1.512034	1.388302
10	1.110195	2.903412	1.519692	1.393018
10	1.130585	2.913608	1.528603	1.398468
10	1.179064	2.938595	1.550517	1.411739
10	1.23713	2.969724	1.57794	1.428142
10	1.268961	2.987292	1.593464	1.437351
10	1.301929	3.005846	1.609889	1.447044
10	1.5932	3.186717	1.771291	1.540604
10	1.1518	3.122114	1.572552	1.528686
10	1.154928	3.123243	1.57402	1.529476
10	1.161544	3.125649	1.577151	1.531157
10	1.176301	3.131098	1.584256	1.534949
10	1.193248	3.13748	1.5926	1.539371
10	1.212537	3.144889	1.602309	1.544482
10	1.258401	3.163044	1.626188	1.556927
10	1.313334	3.185663	1.656068	1.57231
10	1.343446	3.198429	1.672983	1.580946
10	1.374635	3.21191	1.69088	1.590036
10	1.65019	3.343334	1.866745	1.677776
10	1.305228	2.985025	2.32332	1.095835
13	1.30843	2.989898	2.327982	1.097843
13	1.315203	3.000283	2.337926	1.102114
13	1.330309	3.023799	2.360489	1.111754
13	1.347658	3.051345	2.386985	1.122996
13	1.367404	3.08332	2.417818	1.13599
13	1.414354	3.161677	2.493648	1.167626
13	1.470587	3.259298	2.588536	1.206732
13	1.501413	3.314393	2.642251	1.228685
13	1.533341	3.372577	2.699085	1.251795
13	1.815421	3.939787	3.257564	1.474842
13	1.28396	3.186355	2.611952	1.171967
13	1.287181	3.1909	2.616737	1.173965
13	1.293994	3.200585	2.626942	1.178214
13	1.309191	3.222517	2.650097	1.187805
13	1.326644	3.248207	2.677288	1.198989
13	1.346509	3.278029	2.708929	1.211916
13	1.39374	3.351107	2.786747	1.24339
13	1.450312	3.442151	2.884125	1.282294
13	1.481323	3.493534	2.939248	1.304135
13	1.513442	3.547799	2.997572	1.327126
13	1.797216	4.076798	3.570698	1.549026
13	1.261102	3.378756	2.930432	1.245337
13	1.264344	3.382987	2.935351	1.247324

13	1.271201	3.392004	2.945844	1.251553
13	1.286496	3.412422	2.969652	1.261096
13	1.304061	3.436338	2.997609	1.272224
13	1.324053	3.464101	3.030143	1.285086
13	1.371587	3.532134	3.110156	1.316403
13	1.428522	3.616894	3.210279	1.355114
13	1.459731	3.66473	3.266956	1.376846
13	1.492057	3.715249	3.326926	1.399723
13	1.777652	4.207731	3.916213	1.620518
13	1.246611	3.473577	3.147208	1.27566
13	1.249866	3.477654	3.152219	1.277644
13	1.25675	3.486341	3.162908	1.281864
13	1.272107	3.506013	3.18716	1.291387
13	1.289743	3.529055	3.21564	1.302492
13	1.309815	3.555804	3.248781	1.315328
13	1.357542	3.621351	3.330287	1.34658
13	1.414706	3.703013	3.432279	1.385211
13	1.446043	3.749101	3.490015	1.406898
13	1.478499	3.797774	3.551104	1.429728
13	1.765247	4.272259	4.151392	1.650066
13	1.622669	4.384506	3.660067	1.3146
15	1.625729	4.390473	3.666846	1.317086
15	1.632201	4.403189	3.681304	1.322375
15	1.646637	4.431983	3.714111	1.334312
15	1.663216	4.465712	3.752635	1.348231
15	1.682086	4.504865	3.797466	1.36432
15	1.726953	4.600809	3.90772	1.403492
15	1.780692	4.720342	4.045686	1.451912
15	1.81015	4.787802	4.123785	1.479095
15	1.840661	4.859047	4.20642	1.50771
15	2.110227	5.553571	5.018436	1.783884
15	1.676055	4.492267	4.137135	1.315993
15	1.679443	4.498479	4.144013	1.31853
15	1.686607	4.511714	4.158685	1.323926
15	1.702588	4.541686	4.191975	1.336103
15	1.72094	4.576792	4.231067	1.350304
15	1.741829	4.617546	4.276558	1.366718
15	1.791496	4.717412	4.388437	1.406681
15	1.850984	4.841831	4.528436	1.45608
15	1.883594	4.912049	4.607686	1.483811
15	1.917369	4.986206	4.691539	1.513004
15	2.215774	5.70912	5.51552	1.794759
15	1.733429	4.595249	4.663534	1.317336

15	1.737169	4.601694	4.670523	1.319921
15	1.745077	4.615426	4.68543	1.32542
15	1.762717	4.646522	4.719253	1.33783
15	1.782976	4.682946	4.758972	1.352302
15	1.806035	4.725229	4.805192	1.369028
15	1.86086	4.828843	4.918863	1.409755
15	1.926527	4.957931	5.061105	1.460096
15	1.962523	5.030785	5.141625	1.488357
15	1.999807	5.107725	5.226822	1.518107
15	2.329205	5.857769	6.064006	1.805238
15	1.769805	4.646002	5.021834	1.317891
15	1.773767	4.652562	5.028898	1.320496
15	1.782147	4.666538	5.043965	1.326038
15	1.80084	4.698189	5.078151	1.338544
15	1.822307	4.735263	5.118296	1.353127
15	1.846741	4.778299	5.165012	1.369984
15	1.904837	4.883761	5.279904	1.411025
15	1.974421	5.01515	5.423673	1.461756
15	2.012565	5.089302	5.505057	1.490236
15	2.052073	5.167614	5.591169	1.520216
15	2.401121	5.931029	6.43734	1.809569
15	1.904569	5.826256	5.712764	1.383481
17	1.908353	5.832992	5.720501	1.386291
17	1.916354	5.847346	5.737005	1.392267
17	1.934201	5.879849	5.774451	1.405755
17	1.954698	5.917922	5.818424	1.421484
17	1.978027	5.962119	5.869595	1.439663
17	2.033496	6.070422	5.995442	1.483927
17	2.099933	6.205352	6.152921	1.53864
17	2.136352	6.281503	6.242066	1.569356
17	2.174073	6.361925	6.336389	1.60169
17	2.507337	7.145913	7.26325	1.91376
17	2.001131	5.993577	6.335801	1.400205
17	2.005104	6.000599	6.343535	1.402985
17	2.013507	6.015562	6.360032	1.408898
17	2.03225	6.049445	6.397463	1.422244
17	2.053774	6.089134	6.441417	1.437807
17	2.078274	6.135207	6.492567	1.455795
17	2.136525	6.248109	6.618362	1.499591
17	2.206295	6.388767	6.775775	1.553729
17	2.244541	6.468151	6.864883	1.58412
17	2.284154	6.551987	6.959166	1.616113
17	2.634135	7.36926	7.88564	1.924894

17	2.104906	6.153476	7.023265	1.416322
17	2.109083	6.160772	7.030996	1.419073
17	2.117916	6.176317	7.047485	1.424926
17	2.137621	6.211519	7.084898	1.438134
17	2.160251	6.252753	7.128833	1.453538
17	2.186008	6.300619	7.179959	1.471341
17	2.247249	6.417914	7.305696	1.514688
17	2.320601	6.564047	7.463036	1.568269
17	2.360811	6.646521	7.552103	1.598349
17	2.402457	6.73362	7.646343	1.630013
17	2.770405	7.5827	8.572389	1.935623
17	2.170699	6.23228	7.491195	1.422983
17	2.175005	6.23971	7.498923	1.425723
17	2.184113	6.255543	7.515407	1.43155
17	2.204428	6.291395	7.552809	1.444702
17	2.227758	6.33339	7.59673	1.460039
17	2.254312	6.38214	7.64784	1.477766
17	2.31745	6.5016	7.773537	1.520927
17	2.393072	6.650431	7.930828	1.574279
17	2.434526	6.734427	8.019867	1.604229
17	2.477462	6.823134	8.114077	1.635758
17	2.8568	7.687891	9.039833	1.940058
17	1.946633	6.428399	10.2823	1.362976
20	1.952569	6.432085	10.2843	1.364894
20	1.965123	6.43994	10.28856	1.368976
20	1.993126	6.457727	10.29824	1.378187
20	2.025285	6.478561	10.30961	1.388929
20	2.061888	6.502747	10.32283	1.401344
20	2.148919	6.562014	10.35537	1.431573
20	2.253159	6.635852	10.39607	1.46894
20	2.310301	6.677524	10.41912	1.489916
20	2.369486	6.721534	10.4435	1.511998
20	2.892378	7.150557	10.68308	1.725123
20	2.187338	7.006352	10.65924	1.537995
20	2.192957	7.008885	10.66061	1.539676
20	2.204839	7.014282	10.66352	1.543253
20	2.231345	7.026504	10.67012	1.551325
20	2.261785	7.04082	10.67788	1.560738
20	2.296432	7.057439	10.6869	1.571618
20	2.37881	7.098163	10.7091	1.598109
20	2.477479	7.148899	10.73688	1.630854
20	2.531566	7.177534	10.7526	1.649237
20	2.587587	7.207774	10.76924	1.668588

20	3.082528	7.502569	10.93271	1.855355
20	2.446021	7.558671	11.07517	1.706662
20	2.451299	7.560102	11.07583	1.708115
20	2.46246	7.563151	11.07725	1.711205
20	2.487357	7.570055	11.08046	1.718179
20	2.51595	7.578141	11.08423	1.726312
20	2.548494	7.587529	11.08862	1.735713
20	2.625873	7.610532	11.09942	1.758601
20	2.718553	7.639192	11.11292	1.786892
20	2.769358	7.655366	11.12057	1.802775
20	2.821978	7.672448	11.12866	1.819494
20	3.28688	7.838968	11.20816	1.980862
20	2.610028	7.830873	11.35828	1.776372
20	2.615089	7.831761	11.35846	1.777731
20	2.625794	7.833652	11.35886	1.78062
20	2.649671	7.837935	11.35976	1.78714
20	2.677093	7.842951	11.36082	1.794744
20	2.708303	7.848775	11.36206	1.803533
20	2.782512	7.863045	11.36509	1.824932
20	2.871395	7.880824	11.36888	1.851383
20	2.920119	7.890858	11.37103	1.866233
20	2.970584	7.901455	11.37331	1.881864
20	3.416441	8.004757	11.39565	2.032734
20	2.154217	7.181693	11.30399	1.358947
22	2.161529	7.186398	11.30745	1.361014
22	2.176993	7.196421	11.31481	1.36541
22	2.211487	7.21912	11.33152	1.375333
22	2.251102	7.245708	11.35115	1.386904
22	2.29619	7.276572	11.37399	1.400279
22	2.403396	7.352205	11.43015	1.432842
22	2.531801	7.446433	11.50044	1.473094
22	2.602189	7.499613	11.54023	1.495691
22	2.675094	7.555775	11.58232	1.519478
22	3.319201	8.103269	11.99599	1.749062
22	2.471669	7.879096	11.5941	1.595849
22	2.478292	7.882615	11.59716	1.597816
22	2.4923	7.890114	11.6037	1.602001
22	2.523548	7.907096	11.61852	1.611446
22	2.559433	7.926987	11.63593	1.62246
22	2.600277	7.950078	11.65618	1.63519
22	2.69739	8.006661	11.706	1.666185
22	2.813708	8.077156	11.76834	1.704498
22	2.87747	8.116942	11.80363	1.726006

22	2.943511	8.158958	11.84096	1.748647
22	3.526983	8.568557	12.20786	1.967171
22	2.812831	8.545567	11.91421	1.824154
22	2.818715	8.547954	11.91684	1.826025
22	2.831159	8.55304	11.92246	1.830006
22	2.858916	8.564558	11.93519	1.83899
22	2.890794	8.57805	11.95015	1.849467
22	2.927076	8.593712	11.96756	1.861576
22	3.013344	8.632091	12.01037	1.891059
22	3.11667	8.679905	12.06394	1.927503
22	3.173311	8.706891	12.09426	1.947962
22	3.231977	8.735389	12.12635	1.969499
22	3.750285	9.013208	12.44164	2.177364
22	3.029131	8.874026	12.1321	1.918513
22	3.034546	8.875855	12.13443	1.920344
22	3.045998	8.879753	12.13942	1.924241
22	3.071543	8.888578	12.15074	1.933034
22	3.100879	8.898916	12.16403	1.943289
22	3.134269	8.910916	12.1795	1.955142
22	3.21366	8.940324	12.21754	1.984
22	3.308751	8.976961	12.26514	2.019672
22	3.360877	8.997638	12.29209	2.039697
22	3.414866	9.019474	12.3206	2.060778
22	3.89186	9.232348	12.60076	2.264238
22	2.898366	8.930061	14.67516	1.463918
25	2.906518	8.935247	14.67773	1.466496
25	2.923759	8.9463	14.6832	1.471981
25	2.962218	8.971327	14.69563	1.484358
25	3.006385	9.000643	14.71021	1.498793
25	3.056656	9.034674	14.72719	1.515476
25	3.176183	9.118068	14.76894	1.556096
25	3.319345	9.221963	14.82118	1.606307
25	3.397823	9.280599	14.85075	1.634494
25	3.479107	9.342524	14.88204	1.664167
25	4.197241	9.946193	15.18951	1.950553
25	3.037515	9.758868	15.22361	1.752864
25	3.044506	9.762683	15.22556	1.755217
25	3.059292	9.770813	15.22974	1.760222
25	3.092275	9.789223	15.23921	1.771517
25	3.130153	9.810787	15.25033	1.784689
25	3.173265	9.83582	15.26327	1.799914
25	3.275772	9.897162	15.29509	1.836982
25	3.39855	9.973586	15.33491	1.882803

25	3.465853	10.01672	15.35745	1.908525
25	3.535562	10.06227	15.3813	1.935603
25	4.151438	10.50631	15.61567	2.196947
25	3.187057	10.55092	15.82877	2.031324
25	3.192801	10.55342	15.83005	2.03346
25	3.204948	10.55876	15.83279	2.038002
25	3.232046	10.57084	15.839	2.048255
25	3.263165	10.585	15.84629	2.06021
25	3.298584	10.60143	15.85478	2.074029
25	3.3828	10.6417	15.87565	2.107675
25	3.483669	10.69187	15.90177	2.149264
25	3.538963	10.72019	15.91655	2.172611
25	3.596234	10.75009	15.93219	2.197189
25	4.102215	11.04159	16.08591	2.4344
25	3.281867	10.94126	16.24068	2.146412
25	3.28682	10.94312	16.2415	2.148458
25	3.297295	10.94708	16.24326	2.15281
25	3.320661	10.95605	16.24725	2.162631
25	3.347495	10.96656	16.25194	2.174084
25	3.378037	10.97875	16.2574	2.187322
25	3.450657	11.00864	16.27081	2.219552
25	3.537636	11.04587	16.2876	2.259393
25	3.585316	11.06688	16.29711	2.281758
25	3.6347	11.08907	16.30716	2.305303
25	4.071007	11.3054	16.40598	2.532539
25	3.391675	11.54406	15.84139	1.915519
28	3.398146	11.54966	15.85031	1.918469
28	3.411832	11.5616	15.86934	1.924744
28	3.44236	11.58863	15.91251	1.938906
28	3.477419	11.62028	15.9632	1.955422
28	3.517322	11.65704	16.02219	1.974511
28	3.6122	11.7471	16.16726	2.020988
28	3.72584	11.8593	16.3488	2.078438
28	3.788134	11.92262	16.45156	2.11069
28	3.852655	11.98949	16.5603	2.144641
28	4.422694	12.64142	17.62877	2.47232
28	4.053509	12.09031	16.34088	2.064186
28	4.059966	12.09673	16.34996	2.067424
28	4.07362	12.11043	16.36934	2.07431
28	4.104079	12.14144	16.41329	2.089852
28	4.139059	12.17776	16.46491	2.107976
28	4.178873	12.21993	16.52498	2.128925
28	4.273536	12.32326	16.6727	2.179929

28	4.386919	12.45199	16.85755	2.242975
28	4.449073	12.52464	16.9622	2.278369
28	4.513448	12.60137	17.07292	2.315627
28	5.082201	13.34935	18.1609	2.675224
28	4.764776	12.61233	16.89202	2.207458
28	4.771217	12.61954	16.90128	2.210973
28	4.784839	12.63492	16.92104	2.218448
28	4.815224	12.66973	16.96586	2.23532
28	4.850118	12.71051	17.0185	2.254994
28	4.889835	12.75785	17.07976	2.277734
28	4.984269	12.87386	17.23041	2.333102
28	5.097376	13.01839	17.41892	2.401541
28	5.159379	13.09996	17.52563	2.439962
28	5.223597	13.18611	17.63854	2.480407
28	5.790967	14.02588	18.74806	2.870764
28	5.215725	12.86959	17.26716	2.266673
28	5.222156	12.8772	17.27654	2.270302
28	5.235756	12.8934	17.29656	2.278021
28	5.266094	12.93009	17.34198	2.295442
28	5.300935	12.97307	17.39531	2.315757
28	5.34059	13.02296	17.45738	2.339238
28	5.434878	13.14522	17.61001	2.396408
28	5.547811	13.29754	17.80102	2.467077
28	5.609717	13.3835	17.90914	2.506749
28	5.673837	13.47429	18.02354	2.548511
28	6.24033	14.35929	19.14771	2.951581
28	3.456525	9.847534	15.50076	1.711298
30	3.464495	9.85085	15.50337	1.713519
30	3.481348	9.857916	15.50895	1.718245
30	3.518943	9.873916	15.52162	1.728911
30	3.562118	9.892658	15.53649	1.741349
30	3.611259	9.914414	15.55379	1.755725
30	3.728101	9.967727	15.59634	1.790727
30	3.868047	10.03415	15.64959	1.833994
30	3.944762	10.07163	15.67974	1.858283
30	4.024219	10.11122	15.71163	1.883852
30	4.726219	10.49715	16.02504	2.130629
30	3.718062	10.55888	15.86199	2.163027
30	3.726664	10.56176	15.86439	2.1651
30	3.744857	10.56788	15.8695	2.16951
30	3.78544	10.58176	15.88111	2.179462
30	3.832045	10.59801	15.89473	2.191067
30	3.885092	10.61688	15.91059	2.204481

30	4.011218	10.66311	15.94959	2.237141
30	4.162285	10.72071	15.99839	2.277511
30	4.245096	10.75322	16.02601	2.300175
30	4.330867	10.78755	16.05524	2.324032
30	5.088651	11.12221	16.34246	2.554293
30	3.999132	11.23868	16.26058	2.598362
30	4.008416	11.24113	16.26274	2.600292
30	4.028048	11.24636	16.26734	2.604397
30	4.071841	11.25821	16.27777	2.613661
30	4.122134	11.27208	16.29003	2.624464
30	4.179377	11.28819	16.30429	2.636951
30	4.315481	11.32765	16.33936	2.667353
30	4.4785	11.37682	16.38325	2.704933
30	4.567862	11.40457	16.4081	2.72603
30	4.660419	11.43387	16.43439	2.748238
30	5.478154	11.71955	16.69271	2.962582
30	4.177333	11.57371	16.53188	2.778288
30	4.187048	11.57595	16.53388	2.780158
30	4.207593	11.58074	16.53812	2.784137
30	4.253421	11.59158	16.54777	2.793116
30	4.306052	11.60429	16.55909	2.803588
30	4.365955	11.61903	16.57226	2.815691
30	4.508386	11.65516	16.60467	2.84516
30	4.678982	11.70017	16.64522	2.881587
30	4.772498	11.72557	16.66817	2.902036
30	4.869357	11.7524	16.69246	2.923563
30	5.725102	12.01394	16.93111	3.131329
30	6.942543	14.02857	20.25764	2.547488
35	6.946951	14.03042	20.26323	2.550016
35	6.956272	14.03434	20.27516	2.555393
35	6.977065	14.04323	20.30221	2.567529
35	7.000945	14.05364	20.33399	2.581682
35	7.028124	14.06573	20.37096	2.59804
35	7.092746	14.09535	20.4619	2.637868
35	7.170148	14.13225	20.57569	2.687099
35	7.212578	14.15308	20.64011	2.714737
35	7.256524	14.17507	20.70826	2.743831
35	7.644786	14.38948	21.378	3.024631
35	7.152277	14.814	21.23716	3.06389
35	7.156212	14.81612	21.24155	3.065963
35	7.164534	14.82065	21.25091	3.070373
35	7.183099	14.83091	21.27215	3.080325
35	7.204418	14.84292	21.29709	3.09193

35	7.228684	14.85686	21.32611	3.105344
35	7.28638	14.89103	21.39749	3.138005
35	7.355485	14.93361	21.48681	3.178376
35	7.393366	14.95763	21.53737	3.20104
35	7.432602	14.98301	21.59087	3.224898
35	7.779247	15.23037	22.11655	3.455163
35	7.377676	15.56458	22.31798	3.56155
35	7.381103	15.56698	22.32104	3.563185
35	7.388352	15.57208	22.32757	3.566662
35	7.404521	15.58364	22.34239	3.574509
35	7.423089	15.59719	22.35979	3.583661
35	7.444224	15.61291	22.38003	3.594237
35	7.494476	15.65143	22.42983	3.61999
35	7.554664	15.69942	22.49214	3.651823
35	7.587658	15.7265	22.52742	3.669694
35	7.621831	15.75511	22.56474	3.688506
35	7.92375	16.03395	22.93148	3.87007
35	7.52058	15.9345	23.05365	3.767235
35	7.523686	15.93703	23.05581	3.768688
35	7.530253	15.94242	23.06041	3.77178
35	7.544904	15.95462	23.07086	3.778757
35	7.561729	15.96891	23.08312	3.786894
35	7.580878	15.98551	23.0974	3.796298
35	7.62641	16.02617	23.1325	3.819196
35	7.680946	16.07684	23.17643	3.8475
35	7.71084	16.10543	23.2013	3.863389
35	7.741804	16.13562	23.22761	3.880116
35	8.015365	16.42999	23.48617	4.041552
35	6.459645	14.67627	23.57225	2.971103
50	6.470445	14.67906	23.57554	2.973038
50	6.493284	14.685	23.58256	2.977153
50	6.54423	14.69847	23.59848	2.986441
50	6.602738	14.71424	23.61717	2.997272
50	6.669332	14.73255	23.63892	3.009791
50	6.827668	14.77743	23.69242	3.040273
50	7.017315	14.83333	23.75936	3.07795
50	7.121274	14.86488	23.79726	3.099102
50	7.22895	14.8982	23.83736	3.121368
50	8.180259	15.22301	24.23136	3.33627
50	6.866512	15.50507	24.08614	3.548268
50	6.876216	15.50724	24.0885	3.549929
50	6.896739	15.51185	24.09354	3.553462
50	6.942519	15.5223	24.10495	3.561435

50	6.995094	15.53453	24.11836	3.570733
50	7.054935	15.54874	24.13396	3.58148
50	7.197215	15.58355	24.17234	3.607646
50	7.367631	15.62691	24.22035	3.639989
50	7.461049	15.65139	24.24754	3.658146
50	7.557805	15.67723	24.2763	3.67726
50	8.412647	15.9292	24.55891	3.861738
50	7.303767	16.29712	24.65318	4.104487
50	7.312295	16.29869	24.65451	4.105884
50	7.330329	16.30203	24.65735	4.108855
50	7.370557	16.30959	24.6638	4.115561
50	7.416756	16.31844	24.67138	4.123382
50	7.469339	16.32872	24.6802	4.13242
50	7.594364	16.35391	24.70188	4.154427
50	7.744113	16.3853	24.72902	4.18163
50	7.826201	16.40301	24.74438	4.196902
50	7.911223	16.42172	24.76063	4.212978
50	8.662393	16.60408	24.92033	4.368136
50	7.58099	16.68747	25.03913	4.334374
50	7.588772	16.68874	25.03977	4.335662
50	7.605228	16.69145	25.04112	4.338401
50	7.641936	16.69759	25.04419	4.344583
50	7.684092	16.70478	25.0478	4.351793
50	7.732074	16.71313	25.052	4.360125
50	7.84616	16.73358	25.06232	4.380414
50	7.982805	16.75906	25.07524	4.405492
50	8.05771	16.77344	25.08256	4.419571
50	8.135293	16.78863	25.09029	4.434391
50	8.820733	16.93668	25.16633	4.577431
50	8.86885	18.12893	26.6757	3.386682
60	8.87313	18.13064	26.68561	3.389913
60	8.882182	18.13427	26.70674	3.396786
60	8.902373	18.1425	26.75469	3.412297
60	8.925561	18.15214	26.81099	3.430385
60	8.951953	18.16333	26.87652	3.451291
60	9.014706	18.19075	27.03765	3.502194
60	9.089867	18.22492	27.23929	3.565115
60	9.131069	18.2442	27.35344	3.600437
60	9.173743	18.26456	27.47421	3.637621
60	9.550769	18.46307	28.66098	3.996501
60	9.068163	18.65729	27.19025	3.813513
60	9.0731	18.66076	27.20153	3.81773
60	9.083541	18.66815	27.22558	3.8267

60	9.10683	18.6849	27.28017	3.846943
60	9.133577	18.70451	27.34426	3.87055
60	9.164019	18.72728	27.41885	3.897835
60	9.2364	18.78307	27.60228	3.964268
60	9.323095	18.85258	27.83182	4.046386
60	9.370619	18.8918	27.96176	4.092486
60	9.419842	18.93323	28.09924	4.141015
60	9.854721	19.33709	29.45023	4.609391
60	9.282363	19.16221	27.758	4.224854
60	9.288006	19.16737	27.77079	4.23002
60	9.299939	19.17836	27.79808	4.241011
60	9.326559	19.20324	27.85998	4.265815
60	9.357129	19.23238	27.93267	4.29474
60	9.391923	19.26621	28.01726	4.328172
60	9.474653	19.34911	28.2253	4.409573
60	9.573743	19.4524	28.48562	4.510192
60	9.628061	19.51069	28.63298	4.566678
60	9.684321	19.57224	28.78891	4.62614
60	10.18138	20.17235	30.32109	5.200038
60	9.418168	19.41106	28.14445	4.394862
60	9.424258	19.41705	28.15827	4.400421
60	9.437138	19.4298	28.18775	4.412247
60	9.465868	19.45869	28.25463	4.438935
60	9.498863	19.49253	28.33318	4.470059
60	9.536417	19.53182	28.42458	4.506032
60	9.625708	19.62808	28.64936	4.593618
60	9.732656	19.74801	28.93064	4.701884
60	9.791282	19.81569	29.08986	4.762662
60	9.852003	19.88717	29.25834	4.826643
60	10.38848	20.584	30.91385	5.444154
60	9.373291	22.76693	31.65039	3.926194
70	9.385243	22.76864	31.65295	3.92798
70	9.410521	22.77228	31.65842	3.931779
70	9.466908	22.78052	31.67083	3.940352
70	9.531663	22.79017	31.6854	3.95035
70	9.605367	22.80137	31.70236	3.961906
70	9.78061	22.82881	31.74406	3.990043
70	9.990507	22.86301	31.79624	4.024823
70	10.10557	22.88231	31.82577	4.044347
70	10.22474	22.90269	31.85703	4.064901
70	11.27763	23.10137	32.16414	4.263272
70	9.732149	23.7006	32.19307	4.739238
70	9.743901	23.70207	32.1955	4.741337

70	9.768756	23.70521	32.20069	4.745803
70	9.824199	23.71231	32.21245	4.755881
70	9.887871	23.72063	32.22627	4.767633
70	9.960341	23.73028	32.24235	4.781217
70	10.13265	23.75394	32.28189	4.814291
70	10.33904	23.78342	32.33138	4.855174
70	10.45217	23.80006	32.35939	4.878125
70	10.56935	23.81763	32.38902	4.902285
70	11.60462	23.9889	32.68026	5.135466
70	10.11781	24.59285	32.79187	5.522775
70	10.12935	24.5941	32.79415	5.525176
70	10.15375	24.59676	32.79903	5.530284
70	10.20818	24.60277	32.81008	5.541812
70	10.27068	24.60982	32.82307	5.555255
70	10.34183	24.618	32.83818	5.570793
70	10.51099	24.63804	32.87535	5.608625
70	10.7136	24.66301	32.92185	5.655389
70	10.82466	24.6771	32.94818	5.681642
70	10.9397	24.69198	32.97603	5.709278
70	11.95603	24.83707	33.24975	5.976005
70	10.36232	25.03259	33.19944	5.846612
70	10.37372	25.03372	33.20163	5.849139
70	10.39784	25.03614	33.20629	5.854512
70	10.45162	25.04162	33.21687	5.866639
70	10.51339	25.04804	33.22929	5.880781
70	10.58369	25.05549	33.24374	5.897127
70	10.75086	25.07375	33.27929	5.936926
70	10.95107	25.0965	33.32377	5.986121
70	11.06083	25.10934	33.34895	6.013738
70	11.1745	25.1229	33.37559	6.04281
70	12.17883	25.25507	33.63738	6.323402
70	11.77731	23.71972	40.23631	4.003378
85	11.78717	23.73089	40.26008	4.009688
85	11.80802	23.75468	40.31077	4.023108
85	11.85454	23.80856	40.4258	4.053396
85	11.90797	23.87166	40.56088	4.088716
85	11.96878	23.94492	40.71807	4.12954
85	12.11336	24.12444	41.10465	4.228938
85	12.28653	24.34809	41.5884	4.351803
85	12.38145	24.47431	41.86223	4.420777
85	12.47977	24.60761	42.15198	4.493386
85	13.34843	25.9071	44.99913	5.194169
85	12.14128	24.95423	41.15083	4.693516

85	12.15437	24.96938	41.17254	4.702306
85	12.18204	25.00166	41.21884	4.721004
85	12.24376	25.07478	41.32391	4.763201
85	12.31464	25.16042	41.44728	4.81241
85	12.39532	25.25983	41.59085	4.869286
85	12.58715	25.50345	41.94393	5.007767
85	12.81691	25.80696	42.38576	5.178944
85	12.94286	25.97825	42.63587	5.27504
85	13.07331	26.15915	42.90051	5.3762
85	14.22584	27.92264	45.50095	6.352537
85	12.53244	26.13397	42.15992	5.358607
85	12.54899	26.15294	42.17936	5.369788
85	12.58398	26.19334	42.22082	5.393571
85	12.66204	26.28484	42.31488	5.447245
85	12.75169	26.39201	42.42534	5.509839
85	12.85372	26.51642	42.55388	5.582185
85	13.09633	26.8213	42.87	5.758332
85	13.38691	27.20112	43.26558	5.976067
85	13.5462	27.41548	43.48951	6.0983
85	13.71118	27.64187	43.72644	6.226974
85	15.16878	29.84878	46.05467	7.468865
85	12.78044	26.71539	42.84677	5.633491
85	12.79918	26.73623	42.86466	5.64566
85	12.83882	26.78064	42.90282	5.671545
85	12.92724	26.8812	42.9894	5.729963
85	13.02878	26.99898	43.09107	5.798088
85	13.14436	27.13572	43.20937	5.876827
85	13.41915	27.47078	43.50034	6.068542
85	13.74829	27.88821	43.86444	6.30552
85	13.92872	28.1238	44.07054	6.438555
85	14.11559	28.3726	44.28862	6.578601
85	15.76661	30.79805	46.43157	7.930246
85	13.83028	29.82002	48.0461	4.506385
100	13.84456	29.82594	48.04939	4.510337
100	13.87476	29.83856	48.05642	4.518744
100	13.94211	29.86713	48.07237	4.537717
100	14.01947	29.90059	48.09109	4.559843
100	14.10751	29.93943	48.11289	4.585416
100	14.31685	30.03462	48.16648	4.647681
100	14.56758	30.15321	48.23355	4.724647
100	14.70503	30.22014	48.27152	4.767854
100	14.84739	30.29083	48.31169	4.813338
100	16.10512	30.97988	48.70642	5.252326

100	14.37394	31.27149	48.67294	5.355214
100	14.38687	31.2759	48.67587	5.358092
100	14.4142	31.2853	48.68213	5.364214
100	14.47516	31.30658	48.69632	5.37803
100	14.54517	31.3315	48.71299	5.394141
100	14.62486	31.36043	48.73239	5.412763
100	14.81433	31.43133	48.78009	5.458104
100	15.04126	31.51966	48.83978	5.514149
100	15.16566	31.56951	48.87357	5.545612
100	15.29451	31.62216	48.90932	5.578733
100	16.43286	32.13539	49.26064	5.898398
100	14.95821	32.65859	49.36461	6.173237
100	14.96968	32.66155	49.36714	6.175079
100	14.99393	32.66787	49.37254	6.178999
100	15.04802	32.68218	49.3848	6.187845
100	15.11014	32.69895	49.39919	6.198161
100	15.18085	32.71841	49.41595	6.210084
100	15.34896	32.7661	49.45714	6.239114
100	15.55032	32.82551	49.50869	6.274998
100	15.6607	32.85904	49.53788	6.295143
100	15.77502	32.89445	49.56875	6.31635
100	16.78508	33.23965	49.87217	6.521023
100	15.32864	33.34219	49.8354	6.511327
100	15.33919	33.34445	49.83766	6.512742
100	15.36148	33.34925	49.84248	6.515752
100	15.41122	33.36013	49.85342	6.522544
100	15.46834	33.37287	49.86627	6.530464
100	15.53335	33.38766	49.88122	6.539618
100	15.68792	33.42391	49.91799	6.561908
100	15.87307	33.46907	49.964	6.589459
100	15.97456	33.49456	49.99005	6.604927
100	16.07967	33.52147	50.0176	6.621209
100	17.00838	33.78386	50.28841	6.778355

Validation results using ANFIS model

Pb	Fe	Cu	Mn
2.368549	9.480554	10.87109	1.86507
2.372632	9.485722	10.88166	1.867399
2.381266	9.496735	10.90421	1.872353
2.400524	9.521674	10.95536	1.883533
2.422642	9.550885	11.01543	1.896572
2.447816	9.584795	11.08534	1.911641
2.50767	9.667892	11.25726	1.948332
2.579361	9.771418	11.47239	1.993686
2.61866	9.829845	11.59418	2.019147
2.659364	9.89155	11.72303	2.045949
3.018981	10.49307	12.98923	2.304632
3.222742	10.09495	15.10661	1.656518
3.230623	10.10103	15.11316	1.659377
3.247289	10.11398	15.12715	1.665457
3.284466	10.14331	15.15889	1.679179
3.327161	10.17767	15.19616	1.695182
3.375756	10.21756	15.23953	1.713678
3.491299	10.3153	15.34619	1.758711
3.62969	10.43708	15.47967	1.814377
3.705552	10.5058	15.55523	1.845627
3.784126	10.57838	15.63517	1.878523
4.478323	11.28593	16.42075	2.196023
1.387548	3.595378	3.152062	1.140719
1.391679	3.602107	3.158857	1.143442
1.400416	3.616445	3.173348	1.149235
1.419907	3.648914	3.20623	1.162307
1.44229	3.686946	3.244842	1.177552
1.467766	3.731096	3.289775	1.195172
1.528339	3.839284	3.400281	1.238073
1.600891	3.97407	3.538563	1.291103

1.640661	4.05014	3.616841	1.320873
1.681854	4.130476	3.699665	1.352212
2.045788	4.913631	4.513537	1.654677
0.578262	1.410312	0.563631	0.821277
0.578927	1.411614	0.564808	0.822261
0.580333	1.414387	0.567318	0.824354
0.583469	1.420668	0.573014	0.829077
0.58707	1.428024	0.579702	0.834585
0.591169	1.436564	0.587485	0.840951
0.600915	1.457491	0.606627	0.856451
0.612587	1.483563	0.63058	0.875611
0.618986	1.498277	0.644139	0.886368
0.625614	1.513817	0.658486	0.89769
0.684168	1.665303	0.799463	1.006972

Seventeen sets lab scale metal retention column study calibration results using MLR model

Pb	Fe	Cu	Mn
0	0	0	0
0	0	0	0
0	0	0	0
0	0	0	0
0	0	0	0
0	0	0	0.004705
0	0	0	0.050515
0	0	0	0.096326
0	0	0	0.119232
0	0	0	0.142137
0.136025	0.507096	0	0.462812
0	0.147166	0	0.220019
0	0.156739	0	0.225745
0	0.175885	0	0.237198
0	0.214178	0	0.260103
0	0.25247	0	0.283009
0	0.290762	0	0.305914
0	0.367347	0	0.351725
0	0.443932	0	0.397536
0	0.482224	0	0.420441
0	0.520517	0	0.443346
0.382677	1.05661	0.23582	0.764022
0	0.513509	0	0.420825

0	0.523082	0	0.426552
0	0.542228	0	0.438004
0	0.58052	0	0.46091
0	0.618813	0	0.483815
0	0.657105	0	0.50672
0	0.73369	0	0.552531
0	0.810275	0	0.598342
0	0.848567	0	0.621247
0	0.886859	0	0.644153
0.547111	1.422952	0.552	0.964828
0	1.063023	0	0.722035
0	1.072596	0	0.727761
0	1.091742	0	0.739214
0	1.130034	0	0.762119
0	1.168327	0.04494	0.785025
0	1.206619	0.09167	0.80793
0	1.283204	0.18513	0.853741
0.0777	1.359788	0.27859	0.899551
0.122453	1.398081	0.32532	0.922457
0.167207	1.436373	0.37205	0.945362
0.793763	1.972466	1.02627	1.266037
0	0.359033	0	0.176984
0	0.368606	0	0.18271
0	0.387752	0	0.194163
0	0.426044	0	0.217068
0	0.464337	0	0.239974
0	0.502629	0	0.262879
0	0.579214	0	0.30869
0.013692	0.655798	0.02207	0.354501
0.058446	0.694091	0.0688	0.377406
0.1032	0.732383	0.11553	0.400311
0.729755	1.268476	0.76976	0.720986
0	0.908547	0.13419	0.478193
0	0.91812	0.14587	0.48392
0	0.937266	0.16924	0.495372
0	0.975558	0.21597	0.518278
0.036574	1.013851	0.2627	0.541183
0.081328	1.052143	0.30943	0.564088
0.170836	1.128728	0.40289	0.609899
0.260344	1.205312	0.49635	0.65571
0.305098	1.243605	0.54308	0.678615
0.349852	1.281897	0.58981	0.701521
0.976407	1.81799	1.24403	1.022196

0.077935	1.274889	0.45037	0.679
0.089124	1.284462	0.46205	0.684726
0.111501	1.303609	0.48542	0.696179
0.156255	1.341901	0.53215	0.719084
0.201009	1.380193	0.57888	0.741989
0.245763	1.418486	0.62561	0.764895
0.33527	1.49507	0.71907	0.810706
0.424778	1.571655	0.81253	0.856516
0.469532	1.609947	0.85926	0.879422
0.514286	1.64824	0.90599	0.902327
1.140842	2.184333	1.56021	1.223002
0.324587	1.824403	0.92465	0.980209
0.335775	1.833976	0.93633	0.985935
0.358152	1.853122	0.95969	0.997388
0.402906	1.891415	1.00642	1.020293
0.44766	1.929707	1.05315	1.043199
0.492414	1.968	1.09988	1.066104
0.581922	2.044584	1.19334	1.111915
0.67143	2.121169	1.2868	1.157726
0.716184	2.159461	1.33354	1.180631
0.760938	2.197754	1.38027	1.203536
1.387494	2.733847	2.03449	1.524212
0.622961	1.849529	1.7171	0.624803
0.63415	1.859102	1.72878	0.630529
0.656527	1.878248	1.75214	0.641982
0.701281	1.916541	1.79887	0.664887
0.746035	1.954833	1.8456	0.687792
0.790789	1.993126	1.89233	0.710698
0.880297	2.06971	1.98579	0.756509
0.969804	2.146295	2.07925	0.802319
1.014558	2.184587	2.12599	0.825225
1.059312	2.22288	2.17272	0.84813
1.685868	2.758973	2.82694	1.168805
0.869613	2.399043	2.19137	0.926012
0.880802	2.408616	2.20305	0.931738
0.903179	2.427762	2.22642	0.943191
0.947932	2.466055	2.27315	0.966097
0.992686	2.504347	2.31988	0.989002
1.03744	2.542639	2.36661	1.011907
1.126948	2.619224	2.46007	1.057718
1.216456	2.695809	2.55353	1.103529
1.26121	2.734101	2.60026	1.126434
1.305964	2.772394	2.64699	1.149339

1.93252	3.308487	3.30121	1.470015
1.034048	2.765386	2.50755	1.126818
1.045236	2.774959	2.51923	1.132545
1.067613	2.794105	2.5426	1.143997
1.112367	2.832397	2.58933	1.166903
1.157121	2.87069	2.63606	1.189808
1.201875	2.908982	2.68279	1.212714
1.291383	2.985567	2.77625	1.258524
1.380891	3.062151	2.86971	1.304335
1.425645	3.100444	2.91644	1.32724
1.470399	3.138736	2.96317	1.350146
2.096954	3.674829	3.6174	1.670821
1.280699	3.3149	2.98183	1.428028
1.291888	3.324473	2.99351	1.433754
1.314265	3.343619	3.01687	1.445207
1.359019	3.381911	3.0636	1.468112
1.403773	3.420204	3.11033	1.491018
1.448527	3.458496	3.15706	1.513923
1.538035	3.535081	3.25053	1.559734
1.627543	3.611665	3.34399	1.605544
1.672297	3.649958	3.39072	1.62845
1.71705	3.68825	3.43745	1.651355
2.343606	4.224343	4.09167	1.97203
1.038859	3.365908	3.62563	0.84546
1.050047	3.375481	3.63731	0.851186
1.072424	3.394627	3.66068	0.862639
1.117178	3.43292	3.70741	0.885544
1.161932	3.471212	3.75414	0.90845
1.206686	3.509505	3.80087	0.931355
1.296194	3.586089	3.89433	0.977166
1.385702	3.662674	3.98779	1.022976
1.430456	3.700966	4.03452	1.045882
1.47521	3.739259	4.08125	1.068787
2.101765	4.275352	4.73547	1.389462
1.285511	3.915422	4.0999	1.146669
1.296699	3.924995	4.11159	1.152396
1.319076	3.944141	4.13495	1.163848
1.36383	3.982434	4.18168	1.186754
1.408584	4.020726	4.22841	1.209659
1.453338	4.059018	4.27514	1.232564
1.542846	4.135603	4.3686	1.278375
1.632354	4.212188	4.46206	1.324186
1.677108	4.25048	4.50879	1.347091

1.721862	4.288773	4.55552	1.369997
2.348417	4.824866	5.20975	1.690672
1.449945	4.281765	4.41609	1.347476
1.461134	4.291338	4.42777	1.353202
1.483511	4.310484	4.45113	1.364655
1.528265	4.348776	4.49786	1.38756
1.573019	4.387069	4.5446	1.410465
1.617773	4.425361	4.59133	1.433371
1.70728	4.501946	4.68479	1.479181
1.796788	4.57853	4.77825	1.524992
1.841542	4.616823	4.82498	1.547897
1.886296	4.655115	4.87171	1.570803
2.512852	5.191208	5.52593	1.891478
1.696597	4.831279	4.89036	1.648685
1.707786	4.840852	4.90204	1.654411
1.730162	4.859998	4.92541	1.665864
1.774916	4.89829	4.97214	1.688769
1.81967	4.936583	5.01887	1.711675
1.864424	4.974875	5.0656	1.73458
1.953932	5.05146	5.15906	1.780391
2.04344	5.128044	5.25252	1.826202
2.088194	5.166337	5.29925	1.849107
2.132948	5.204629	5.34598	1.872012
2.759504	5.740722	6.0002	2.192687
1.302035	3.840635	4.24299	0.959476
1.313223	3.850208	4.25467	0.965202
1.3356	3.869354	4.27803	0.976655
1.380354	3.907647	4.32476	0.99956
1.425108	3.945939	4.37149	1.022466
1.469862	3.984231	4.41822	1.045371
1.55937	4.060816	4.51168	1.091182
1.648878	4.137401	4.60515	1.136993
1.693632	4.175693	4.65188	1.159898
1.738386	4.213985	4.69861	1.182803
2.364941	4.750078	5.35283	1.503479
1.548687	4.390149	4.71726	1.260686
1.559875	4.399722	4.72894	1.266412
1.582252	4.418868	4.75231	1.277865
1.627006	4.457161	4.79904	1.30077
1.67176	4.495453	4.84577	1.323675
1.716514	4.533745	4.8925	1.346581
1.806022	4.61033	4.98596	1.392391
1.89553	4.686915	5.07942	1.438202

1.940284	4.725207	5.12615	1.461107
1.985038	4.763499	5.17288	1.484013
2.611593	5.299592	5.8271	1.804688
1.713121	4.756492	5.03344	1.461492
1.72431	4.766065	5.04513	1.467218
1.746687	4.785211	5.06849	1.478671
1.791441	4.823503	5.11522	1.501576
1.836195	4.861796	5.16195	1.524482
1.880949	4.900088	5.20868	1.547387
1.970457	4.976673	5.30214	1.593198
2.059964	5.053257	5.3956	1.639008
2.104718	5.09155	5.44233	1.661914
2.149472	5.129842	5.48906	1.684819
2.776028	5.665935	6.14329	2.005494
1.959773	5.306006	5.50772	1.762701
1.970962	5.315579	5.5194	1.768428
1.993339	5.334725	5.54276	1.77988
2.038092	5.373017	5.58949	1.802786
2.082846	5.411309	5.63622	1.825691
2.1276	5.449602	5.68295	1.848596
2.217108	5.526187	5.77642	1.894407
2.306616	5.602771	5.86988	1.940218
2.35137	5.641064	5.91661	1.963123
2.396124	5.679356	5.96334	1.986029
3.02268	6.215449	6.61756	2.306704
1.659609	4.542704	5.37564	1.096304
1.670798	4.552277	5.38733	1.10203
1.693175	4.571424	5.41069	1.113483
1.737929	4.609716	5.45742	1.136388
1.782683	4.648008	5.50415	1.159293
1.827437	4.686301	5.55088	1.182199
1.916945	4.762885	5.64434	1.228009
2.006453	4.83947	5.7378	1.27382
2.051207	4.877762	5.78453	1.296725
2.095961	4.916055	5.83126	1.319631
2.722516	5.452148	6.48549	1.640306
1.906261	5.092218	5.84992	1.397513
1.91745	5.101791	5.8616	1.403239
1.939827	5.120938	5.88497	1.414692
1.984581	5.15923	5.9317	1.437597
2.029335	5.197522	5.97843	1.460503
2.074089	5.235815	6.02516	1.483408
2.163597	5.312399	6.11862	1.529219

2.253104	5.388984	6.21208	1.57503
2.297858	5.427276	6.25881	1.597935
2.342612	5.465569	6.30554	1.62084
2.969168	6.001662	6.95976	1.941515
2.070696	5.458561	6.1661	1.598319
2.081884	5.468134	6.17778	1.604046
2.104261	5.48728	6.20115	1.615498
2.149015	5.525573	6.24788	1.638404
2.193769	5.563865	6.29461	1.661309
2.238523	5.602157	6.34134	1.684214
2.328031	5.678742	6.4348	1.730025
2.417539	5.755327	6.52826	1.775836
2.462293	5.793619	6.57499	1.798741
2.507047	5.831911	6.62172	1.821647
3.133602	6.368004	7.27594	2.142322
2.317348	6.008075	6.64038	1.899529
2.328536	6.017648	6.65206	1.905255
2.350913	6.036794	6.67542	1.916708
2.395667	6.075086	6.72215	1.939613
2.440421	6.113379	6.76888	1.962518
2.485175	6.151671	6.81561	1.985424
2.574683	6.228256	6.90907	2.031235
2.664191	6.304841	7.00253	2.077045
2.708945	6.343133	7.04926	2.099951
2.753699	6.381425	7.09599	2.122856
3.380254	6.917518	7.75022	2.443531
2.358676	7.277929	10.5624	1.215487
2.369864	7.287502	10.5741	1.221213
2.392241	7.306648	10.5975	1.232666
2.436995	7.34494	10.6442	1.255571
2.481749	7.383233	10.6909	1.278476
2.526503	7.421525	10.7377	1.301382
2.616011	7.49811	10.8311	1.347193
2.705519	7.574695	10.9246	1.393003
2.750273	7.612987	10.9713	1.415909
2.795027	7.651279	11.0181	1.438814
3.421583	8.187372	11.6723	1.759489
2.605328	7.827443	11.0367	1.516696
2.616516	7.837016	11.0484	1.522423
2.638893	7.856162	11.0718	1.533875
2.683647	7.894454	11.1185	1.556781
2.728401	7.932747	11.1652	1.579686
2.773155	7.971039	11.2119	1.602591

2.862663	8.047624	11.3054	1.648402
2.952171	8.124208	11.3989	1.694213
2.996925	8.162501	11.4456	1.717118
3.041679	8.200793	11.4923	1.740024
3.668234	8.736886	12.1466	2.060699
2.769762	8.193785	11.3529	1.717502
2.780951	8.203358	11.3646	1.723229
2.803328	8.222505	11.3879	1.734681
2.848082	8.260797	11.4347	1.757587
2.892836	8.299089	11.4814	1.780492
2.93759	8.337382	11.5281	1.803398
3.027098	8.413966	11.6216	1.849208
3.116605	8.490551	11.7151	1.895019
3.161359	8.528843	11.7618	1.917924
3.206113	8.567136	11.8085	1.94083
3.832669	9.103229	12.4627	2.261505
3.016414	8.743299	11.8272	2.018712
3.027603	8.752872	11.8389	2.024438
3.04998	8.772019	11.8622	2.035891
3.094734	8.810311	11.9089	2.058796
3.139487	8.848603	11.9557	2.081702
3.184241	8.886896	12.0024	2.104607
3.273749	8.96348	12.0959	2.150418
3.363257	9.040065	12.1893	2.196229
3.408011	9.078357	12.2361	2.219134
3.452765	9.11665	12.2828	2.242039
4.079321	9.652743	12.937	2.562714
2.734207	7.848071	11.496	1.363583
2.745395	7.857644	11.5076	1.36931
2.767772	7.87679	11.531	1.380762
2.812526	7.915083	11.5777	1.403668
2.85728	7.953375	11.6245	1.426573
2.902034	7.991667	11.6712	1.449478
2.991542	8.068252	11.7647	1.495289
3.08105	8.144837	11.8581	1.5411
3.125804	8.183129	11.9049	1.564005
3.170558	8.221422	11.9516	1.586911
3.797113	8.757515	12.6058	1.907586
2.980858	8.397585	11.9702	1.664793
2.992047	8.407158	11.9819	1.670519
3.014424	8.426304	12.0053	1.681972
3.059178	8.464597	12.052	1.704877
3.103932	8.502889	12.0987	1.727782

3.148686	8.541181	12.1455	1.750688
3.238194	8.617766	12.2389	1.796499
3.327702	8.694351	12.3324	1.842309
3.372456	8.732643	12.3791	1.865215
3.41721	8.770936	12.4259	1.88812
4.043765	9.307028	13.0801	2.208795
3.145293	8.763928	12.2864	1.865599
3.156482	8.773501	12.2981	1.871325
3.178858	8.792647	12.3215	1.882778
3.223612	8.830939	12.3682	1.905683
3.268366	8.869232	12.4149	1.928589
3.31312	8.907524	12.4617	1.951494
3.402628	8.984109	12.5551	1.997305
3.492136	9.060693	12.6486	2.043116
3.53689	9.098986	12.6953	2.066021
3.581644	9.137278	12.742	2.088926
4.2082	9.673371	13.3963	2.409601
3.391945	9.313442	12.7607	2.166808
3.403133	9.323015	12.7724	2.172535
3.42551	9.342161	12.7957	2.183987
3.470264	9.380453	12.8425	2.206893
3.515018	9.418746	12.8892	2.229798
3.559772	9.457038	12.9359	2.252704
3.64928	9.533623	13.0294	2.298514
3.738788	9.610207	13.1229	2.344325
3.783542	9.6485	13.1696	2.36723
3.828296	9.686792	13.2163	2.390136
4.454851	10.22289	13.8705	2.710811
3.302818	8.856377	12.7524	1.655793
3.314006	8.86595	12.7641	1.661519
3.336383	8.885096	12.7874	1.672972
3.381137	8.923388	12.8342	1.695877
3.425891	8.961681	12.8809	1.718783
3.470645	8.999973	12.9276	1.741688
3.560153	9.076558	13.0211	1.787499
3.649661	9.153142	13.1145	1.833309
3.694415	9.191435	13.1613	1.856215
3.739169	9.229727	13.208	1.87912
4.365724	9.76582	13.8622	2.199795
3.549469	9.405891	13.2266	1.957002
3.560658	9.415464	13.2383	1.962729
3.583035	9.43461	13.2617	1.974181
3.627789	9.472902	13.3084	1.997087

3.672543	9.511195	13.3552	2.019992
3.717297	9.549487	13.4019	2.042897
3.806805	9.626072	13.4953	2.088708
3.896313	9.702656	13.5888	2.134519
3.941067	9.740949	13.6355	2.157424
3.98582	9.779241	13.6823	2.18033
4.612376	10.31533	14.3365	2.501005
3.713904	9.772233	13.5428	2.157809
3.725092	9.781806	13.5545	2.163535
3.747469	9.800952	13.5779	2.174988
3.792223	9.839245	13.6246	2.197893
3.836977	9.877537	13.6713	2.220798
3.881731	9.91583	13.7181	2.243704
3.971239	9.992414	13.8115	2.289514
4.060747	10.069	13.905	2.335325
4.105501	10.10729	13.9517	2.358231
4.150255	10.14558	13.9984	2.381136
4.77681	10.68168	14.6527	2.701811
3.960556	10.32175	14.0171	2.459018
3.971744	10.33132	14.0288	2.464744
3.994121	10.35047	14.0522	2.476197
4.038875	10.38876	14.0989	2.499102
4.083629	10.42705	14.1456	2.522008
4.128383	10.46534	14.1923	2.544913
4.217891	10.54193	14.2858	2.590724
4.307399	10.61851	14.3793	2.636535
4.352153	10.65681	14.426	2.65944
4.396907	10.6951	14.4727	2.682345
5.023462	11.23119	15.1269	3.00302
3.649599	9.575375	14.0351	1.736047
3.660788	9.584948	14.0468	1.741773
3.683165	9.604094	14.0701	1.753226
3.727919	9.642387	14.1169	1.776131
3.772673	9.680679	14.1636	1.799037
3.817427	9.718971	14.2103	1.821942
3.906935	9.795556	14.3038	1.867753
3.996443	9.872141	14.3973	1.913564
4.041197	9.910433	14.444	1.936469
4.085951	9.948725	14.4907	1.959374
4.712506	10.48482	15.1449	2.280049
3.896251	10.12489	14.5094	2.037256
3.90744	10.13446	14.5211	2.042983
3.929817	10.15361	14.5444	2.054435

3.974571	10.1919	14.5912	2.077341
4.019325	10.23019	14.6379	2.100246
4.064079	10.26849	14.6846	2.123152
4.153587	10.34507	14.7781	2.168962
4.243094	10.42165	14.8715	2.214773
4.287848	10.45995	14.9183	2.237678
4.332602	10.49824	14.965	2.260584
4.959158	11.03433	15.6192	2.581259
4.060686	10.49123	14.8256	2.238063
4.071874	10.5008	14.8372	2.243789
4.094251	10.51995	14.8606	2.255242
4.139005	10.55824	14.9073	2.278147
4.183759	10.59654	14.9541	2.301052
4.228513	10.63483	15.0008	2.323958
4.318021	10.71141	15.0943	2.369769
4.407529	10.788	15.1877	2.415579
4.452283	10.82629	15.2344	2.438485
4.497037	10.86458	15.2812	2.46139
5.123592	11.40067	15.9354	2.782065
4.307338	11.04075	15.2998	2.539272
4.318526	11.05032	15.3115	2.544999
4.340903	11.06946	15.3349	2.556451
4.385657	11.10776	15.3816	2.579357
4.430411	11.14605	15.4283	2.602262
4.475165	11.18434	15.4751	2.625167
4.564673	11.26093	15.5685	2.670978
4.654181	11.33751	15.662	2.716789
4.698935	11.3758	15.7087	2.739694
4.743689	11.4141	15.7555	2.7626
5.370244	11.95019	16.4097	3.083275
3.959291	10.62925	15.6988	1.842824
3.970479	10.63882	15.7105	1.84855
3.992856	10.65797	15.7338	1.860003
4.03761	10.69626	15.7806	1.882908
4.082364	10.73455	15.8273	1.905813
4.127118	10.77285	15.874	1.928719
4.216626	10.84943	15.9675	1.97453
4.306134	10.92602	16.0609	2.02034
4.350888	10.96431	16.1077	2.043246
4.395642	11.0026	16.1544	2.066151
5.022197	11.53869	16.8086	2.386826
4.205943	11.17876	16.1731	2.144033
4.217131	11.18834	16.1847	2.14976

4.239508	11.20748	16.2081	2.161212
4.284262	11.24578	16.2548	2.184118
4.329016	11.28407	16.3016	2.207023
4.37377	11.32236	16.3483	2.229928
4.463278	11.39894	16.4418	2.275739
4.552786	11.47553	16.5352	2.32155
4.59754	11.51382	16.5819	2.344455
4.642294	11.55211	16.6287	2.367361
5.268849	12.08821	17.2829	2.688036
4.370377	11.54511	16.4892	2.344839
4.381566	11.55468	16.5009	2.350566
4.403943	11.57383	16.5243	2.362018
4.448697	11.61212	16.571	2.384924
4.493451	11.65041	16.6177	2.407829
4.538205	11.6887	16.6645	2.430735
4.627712	11.76529	16.7579	2.476545
4.71722	11.84187	16.8514	2.522356
4.761974	11.88016	16.8981	2.545261
4.806728	11.91846	16.9449	2.568167
5.433284	12.45455	17.5991	2.888842
4.617029	12.09462	16.9635	2.646049
4.628217	12.10419	16.9752	2.651775
4.650594	12.12334	16.9986	2.663228
4.695348	12.16163	17.0453	2.686133
4.740102	12.19992	17.092	2.709039
4.784856	12.23822	17.1387	2.731944
4.874364	12.3148	17.2322	2.777755
4.963872	12.39139	17.3257	2.823566
5.008626	12.42968	17.3724	2.846471
5.05338	12.46797	17.4191	2.869376
5.679936	13.00406	18.0734	3.190051
5.456538	13.51702	19.2259	2.715009
5.467727	13.52659	19.2376	2.720735
5.490104	13.54574	19.261	2.732188
5.534858	13.58403	19.3077	2.755093
5.579612	13.62233	19.3544	2.777998
5.624366	13.66062	19.4012	2.800904
5.713873	13.7372	19.4946	2.846714
5.803381	13.81379	19.5881	2.892525
5.848135	13.85208	19.6348	2.915431
5.892889	13.89037	19.6816	2.938336
6.519445	14.42646	20.3358	3.259011
5.70319	14.06654	19.7002	3.016218

5.714378	14.07611	19.7119	3.021944
5.736755	14.09525	19.7353	3.033397
5.781509	14.13355	19.782	3.056302
5.826263	14.17184	19.8287	3.079208
5.871017	14.21013	19.8754	3.102113
5.960525	14.28672	19.9689	3.147924
6.050033	14.3633	20.0624	3.193735
6.094787	14.40159	20.1091	3.21664
6.139541	14.43989	20.1558	3.239545
6.766097	14.97598	20.81	3.560221
5.867624	14.43288	20.0164	3.217024
5.878813	14.44245	20.0281	3.222751
5.90119	14.4616	20.0514	3.234203
5.945944	14.49989	20.0982	3.257109
5.990698	14.53818	20.1449	3.280014
6.035452	14.57647	20.1916	3.302919
6.12496	14.65306	20.2851	3.34873
6.214468	14.72964	20.3785	3.394541
6.259222	14.76794	20.4253	3.417446
6.303976	14.80623	20.472	3.440352
6.930531	15.34232	21.1262	3.761027
6.114276	14.98239	20.4907	3.518234
6.125465	14.99197	20.5023	3.52396
6.147842	15.01111	20.5257	3.535413
6.192596	15.0494	20.5724	3.558318
6.23735	15.0877	20.6192	3.581224
6.282104	15.12599	20.6659	3.604129
6.371612	15.20257	20.7594	3.64994
6.461119	15.27916	20.8528	3.69575
6.505873	15.31745	20.8996	3.718656
6.550627	15.35574	20.9463	3.741561
7.177183	15.89184	21.6005	4.062236
6.905713	16.13433	23.59	3.059024
6.916901	16.1439	23.6017	3.06475
6.939278	16.16305	23.6251	3.076203
6.984032	16.20134	23.6718	3.099108
7.028786	16.23963	23.7185	3.122014
7.07354	16.27792	23.7653	3.144919
7.163048	16.35451	23.8587	3.19073
7.252556	16.43109	23.9522	3.236541
7.29731	16.46938	23.9989	3.259446
7.342064	16.50768	24.0456	3.282351
7.968619	17.04377	24.6999	3.603026

7.152365	16.68384	24.0643	3.360233
7.163553	16.69341	24.076	3.36596
7.18593	16.71256	24.0993	3.377412
7.230684	16.75085	24.1461	3.400318
7.275438	16.78914	24.1928	3.423223
7.320192	16.82744	24.2395	3.446129
7.4097	16.90402	24.333	3.491939
7.499208	16.98061	24.4264	3.53775
7.543962	17.0189	24.4732	3.560655
7.588716	17.05719	24.5199	3.583561
8.215271	17.59328	25.1741	3.904236
7.316799	17.05018	24.3805	3.56104
7.327988	17.05976	24.3922	3.566766
7.350365	17.0789	24.4155	3.578219
7.395119	17.11719	24.4622	3.601124
7.439873	17.15549	24.509	3.624029
7.484627	17.19378	24.5557	3.646935
7.574135	17.27036	24.6492	3.692746
7.663642	17.34695	24.7426	3.738556
7.708396	17.38524	24.7894	3.761462
7.75315	17.42353	24.8361	3.784367
8.379706	17.95963	25.4903	4.105042
7.563451	17.5997	24.8547	3.862249
7.57464	17.60927	24.8664	3.867975
7.597017	17.62842	24.8898	3.879428
7.641771	17.66671	24.9365	3.902334
7.686524	17.705	24.9833	3.925239
7.731278	17.74329	25.03	3.948144
7.820786	17.81988	25.1234	3.993955
7.910294	17.89646	25.2169	4.039766
7.955048	17.93476	25.2636	4.062671
7.999802	17.97305	25.3104	4.085576
8.626358	18.50914	25.9646	4.406252
8.714224	18.72448	29.3642	3.489196
8.725413	18.73405	29.3759	3.494922
8.74779	18.75319	29.3992	3.506375
8.792544	18.79149	29.446	3.52928
8.837298	18.82978	29.4927	3.552186
8.882052	18.86807	29.5394	3.575091
8.97156	18.94466	29.6329	3.620902
9.061067	19.02124	29.7263	3.666713
9.105821	19.05953	29.7731	3.689618
9.150575	19.09783	29.8198	3.712523

9.777131	19.63392	30.474	4.033198
8.960876	19.27399	29.8385	3.790405
8.972065	19.28356	29.8501	3.796132
8.994442	19.30271	29.8735	3.807584
9.039195	19.341	29.9202	3.83049
9.083949	19.37929	29.967	3.853395
9.128703	19.41759	30.0137	3.876301
9.218211	19.49417	30.1072	3.922111
9.307719	19.57076	30.2006	3.967922
9.352473	19.60905	30.2474	3.990827
9.397227	19.64734	30.2941	4.013733
10.02378	20.18343	30.9483	4.334408
9.125311	19.64033	30.1546	3.991212
9.136499	19.64991	30.1663	3.996938
9.158876	19.66905	30.1897	4.008391
9.20363	19.70734	30.2364	4.031296
9.248384	19.74564	30.2832	4.054201
9.293138	19.78393	30.3299	4.077107
9.382646	19.86051	30.4233	4.122918
9.472154	19.9371	30.5168	4.168728
9.516908	19.97539	30.5635	4.191634
9.561662	20.01368	30.6103	4.214539
10.18822	20.54978	31.2645	4.535214
9.371962	20.18985	30.6289	4.292421
9.383151	20.19942	30.6406	4.298147
9.405528	20.21857	30.664	4.3096
9.450282	20.25686	30.7107	4.332506
9.495036	20.29515	30.7574	4.355411
9.53979	20.33344	30.8042	4.378316
9.629298	20.41003	30.8976	4.424127
9.718806	20.48661	30.9911	4.469938
9.76356	20.5249	31.0378	4.492843
9.808313	20.5632	31.0845	4.515748
10.43487	21.09929	31.7388	4.836424
10.48146	23.15502	34.9166	4.427298
10.49265	23.16459	34.9283	4.433025
10.51502	23.18374	34.9516	4.444478
10.55978	23.22203	34.9984	4.467383
10.60453	23.26032	35.0451	4.490288
10.64929	23.29862	35.0918	4.513194
10.73879	23.3752	35.1853	4.559004
10.8283	23.45179	35.2788	4.604815
10.87306	23.49008	35.3255	4.62772

10.91781	23.52837	35.3722	4.650626
11.54436	24.06446	36.0264	4.971301
10.72811	23.70453	35.3909	4.728508
10.7393	23.71411	35.4026	4.734234
10.76168	23.73325	35.4259	4.745687
10.80643	23.77155	35.4727	4.768592
10.85118	23.80984	35.5194	4.791498
10.89594	23.84813	35.5661	4.814403
10.98545	23.92472	35.6596	4.860214
11.07495	24.0013	35.753	4.906025
11.11971	24.03959	35.7998	4.92893
11.16446	24.07788	35.8465	4.951835
11.79102	24.61398	36.5007	5.27251
10.89254	24.07088	35.7071	4.929314
10.90373	24.08045	35.7187	4.935041
10.92611	24.0996	35.7421	4.946493
10.97086	24.13789	35.7888	4.969399
11.01562	24.17618	35.8356	4.992304
11.06037	24.21447	35.8823	5.015209
11.14988	24.29106	35.9758	5.06102
11.23939	24.36764	36.0692	5.106831
11.28414	24.40593	36.1159	5.129736
11.3289	24.44423	36.1627	5.152642
11.95545	24.98032	36.8169	5.473317
11.1392	24.62039	36.1813	5.230524
11.15039	24.62996	36.193	5.23625
11.17276	24.64911	36.2164	5.247703
11.21752	24.6874	36.2631	5.270608
11.26227	24.72569	36.3098	5.293513
11.30702	24.76399	36.3566	5.316419
11.39653	24.84057	36.45	5.36223
11.48604	24.91716	36.5435	5.40804
11.53079	24.95545	36.5902	5.430946
11.57555	24.99374	36.6369	5.453851
12.2021	25.52983	37.2912	5.774526
12.42486	25.21086	39.007	4.960041
12.43605	25.22044	39.0187	4.965767
12.45842	25.23958	39.0421	4.97722
12.50318	25.27787	39.0888	5.000126
12.54793	25.31617	39.1355	5.023031
12.59268	25.35446	39.1823	5.045936
12.68219	25.43104	39.2757	5.091747
12.7717	25.50763	39.3692	5.137558

12.81645	25.54592	39.4159	5.160463
12.86121	25.58421	39.4627	5.183368
13.48776	26.12031	40.1169	5.504044
12.67151	25.76038	39.4813	5.261251
12.6827	25.76995	39.493	5.266977
12.70507	25.7891	39.5164	5.27843
12.74983	25.82739	39.5631	5.301335
12.79458	25.86568	39.6098	5.32424
12.83934	25.90397	39.6565	5.347146
12.92884	25.98056	39.75	5.392956
13.01835	26.05714	39.8435	5.438767
13.06311	26.09544	39.8902	5.461673
13.10786	26.13373	39.9369	5.484578
13.73442	26.66982	40.5911	5.805253
12.83594	26.12672	39.7975	5.462057
12.84713	26.13629	39.8092	5.467783
12.86951	26.15544	39.8325	5.479236
12.91426	26.19373	39.8793	5.502141
12.95902	26.23202	39.926	5.525047
13.00377	26.27032	39.9727	5.547952
13.09328	26.3469	40.0662	5.593763
13.18279	26.42349	40.1596	5.639574
13.22754	26.46178	40.2064	5.662479
13.27229	26.50007	40.2531	5.685384
13.89885	27.03616	40.9073	6.006059
13.08259	26.67623	40.2718	5.763266
13.09378	26.68581	40.2834	5.768993
13.11616	26.70495	40.3068	5.780445
13.16091	26.74325	40.3535	5.803351
13.20567	26.78154	40.4003	5.826256
13.25042	26.81983	40.447	5.849161
13.33993	26.89641	40.5405	5.894972
13.42944	26.973	40.6339	5.940783
13.47419	27.01129	40.6807	5.963688
13.51895	27.04958	40.7274	5.986594
14.1455	27.58568	41.3816	6.307269
13.94928	30.345	47.7439	5.22984
13.96047	30.35458	47.7556	5.235567
13.98284	30.37372	47.7789	5.247019
14.0276	30.41202	47.8257	5.269925
14.07235	30.45031	47.8724	5.29283
14.1171	30.4886	47.9191	5.315735
14.20661	30.56518	48.0126	5.361546

14.29612	30.64177	48.106	5.407357
14.34087	30.68006	48.1528	5.430262
14.38563	30.71835	48.1995	5.453168
15.01218	31.25445	48.8537	5.773843
14.19593	30.89452	48.2182	5.53105
14.20712	30.90409	48.2298	5.536776
14.22949	30.92324	48.2532	5.548229
14.27425	30.96153	48.2999	5.571134
14.319	30.99982	48.3467	5.594039
14.36376	31.03811	48.3934	5.616945
14.45326	31.1147	48.4869	5.662755
14.54277	31.19128	48.5803	5.708566
14.58753	31.22958	48.627	5.731472
14.63228	31.26787	48.6738	5.754377
15.25884	31.80396	49.328	6.075052
14.36036	31.26086	48.5343	5.731856
14.37155	31.27043	48.546	5.737582
14.39393	31.28958	48.5694	5.749035
14.43868	31.32787	48.6161	5.77194
14.48344	31.36616	48.6629	5.794846
14.52819	31.40446	48.7096	5.817751
14.6177	31.48104	48.803	5.863562
14.70721	31.55763	48.8965	5.909373
14.75196	31.59592	48.9432	5.932278
14.79671	31.63421	48.99	5.955183
15.42327	32.1703	49.6442	6.275858
14.60702	31.81037	49.0086	6.033065
14.6182	31.81995	49.0203	6.038792
14.64058	31.83909	49.0437	6.050244
14.68533	31.87739	49.0904	6.07315
14.73009	31.91568	49.1371	6.096055
14.77484	31.95397	49.1839	6.118961
14.86435	32.03056	49.2773	6.164771
14.95386	32.10714	49.3708	6.210582
14.99861	32.14543	49.4175	6.233487
15.04337	32.18372	49.4642	6.256393
15.66992	32.71982	50.1185	6.577068

Validation results using MLR model

Pb	Fe	Cu	Mn
2.503789	7.182049	10.62326	1.242948
2.514978	7.191622	10.63494	1.248674
2.537355	7.210768	10.65831	1.260127
2.582109	7.24906	10.70504	1.283032
2.626863	7.287353	10.75177	1.305937
2.671617	7.325645	10.7985	1.328843
2.761125	7.40223	10.89196	1.374654
2.850633	7.478814	10.98542	1.420464
2.895387	7.517107	11.03215	1.44337
2.94014	7.555399	11.07888	1.466275
3.566696	8.091492	11.7331	1.78695
3.646205	9.467021	13.61636	1.859041
3.657394	9.476595	13.62804	1.864768
3.679771	9.495741	13.65141	1.87622
3.724525	9.534033	13.69814	1.899126
3.769279	9.572325	13.74487	1.922031
3.814033	9.610618	13.7916	1.944936
3.903541	9.687203	13.88506	1.990747
3.993049	9.763787	13.97852	2.036558
4.037803	9.80208	14.02525	2.059463
4.082557	9.840372	14.07198	2.082369
4.709112	10.37646	14.7262	2.403044
1.571779	4.338854	4.439693	1.288257
1.582968	4.348427	4.451376	1.293984
1.605345	4.367574	4.474741	1.305437
1.650099	4.405866	4.521471	1.328342
1.694852	4.444158	4.568201	1.351247
1.739606	4.482451	4.614931	1.374153
1.829114	4.559035	4.708392	1.419963
1.918622	4.63562	4.801852	1.465774
1.963376	4.673913	4.848582	1.488679
2.00813	4.712205	4.895313	1.511585

2.634686	5.248298	5.549536	1.83226
0	0.639226	0	0.41438
0	0.648799	0	0.420106
0	0.667946	0	0.431559
0	0.706238	0	0.454464
0	0.74453	0	0.47737
0	0.782823	0	0.500275
0	0.859407	0	0.546086
0.066974	0.935992	0.084597	0.591896
0.111728	0.974284	0.131327	0.614802
0.156482	1.012577	0.178057	0.637707
0.783037	1.54867	0.83228	0.958382